*Cotutelle Agreement for Joint Doctoral Supervision between*

**CHARLES UNIVERSITY IN PRAGUE, CZECH REPUBLIC**

Faculty of Science - Institute of Hydrogeology, Engineering Geology and Applied Geophysics

*and*

**UNIVERSITY BORDEAUX-1, FRANCE**

GHYMAC Géosciences, Hydrosciences

Study program: Hydrogeology

**Mgr. Hana Jiráková**

# ISOTOPE HYDROGEOLOGY AND GEOTHERMAL APPLICATIONS TO CLARIFY THE ORIGIN, THE SUSTAINABILITY AND THE CHARACTER OF GROUNDWATER FLOW

*Examples of the Bohemian and the Aquitaine sedimentary basins*

## Ph.D. Thesis

Supervisors:
Dr. Zbyněk Hrkal, Charles University, Prague
Dr. Frédéric Huneau, University Bordeaux-1
Dr. Philippe Le Coustumer, University Bordeaux-1

Prague, 2011

# Declaration

I hereby declare that I have developed this Ph.D. Thesis entirely on my own. All the resources and any other used previously published results are properly cited and included in the list of references. I permit the lending of the thesis to anyone to whom it may be of interest. I confirm that this work or any of its significant portions was not used to acquire any academic degree elsewhere.

In Prague, February 2011

Mgr. Hana Jiráková

# Acknowledgements

The entire research effort presented in this thesis was carried out in the co-direction of the Institute of Hydrogeology, Geophysics and Engineering Geology, Charles University, Prague, Czech Republic and GHYMAC- Géosciences, Hydrosciences, Université Bordeaux 1, France.

I would not have been able to complete the Ph.D. studies without the aid and support of countless people over the past four years.

First and foremost, I would like to thank my supervisor Frédéric Huneau for his expert monitoring and guidance throughout the whole of my Ph.D. Thesis. I appreciate his vast knowledge and skill in the area of isotopic hydrogeology and geochemistry, his assistance in writing scientific papers by giving me important advice how to optimize my work and giving me the opportunity to participate in many international scientific meetings.

Many thanks also to my other supervisors Philippe Le Coustumer and Zbyněk Hrkal who agreed with this university co-direction and made the friendly and supportive atmosphere. They were always open for scientific discussions and help with administrative matters.

I am particularly grateful to Hélène Celle-Jeanton for many productive hints in the field of isotopic hydrogeology and geochemistry and for her assistance in writing scientific papers, and leading scientific discussions.

I must also acknowledge Martin Procházka for taking time out from his busy schedule to provide me data and to share his valuable practical experience, knowledge and observations from the field well-logging measurements.

Furthemore, thanks to Miroslav Kobr and Petr Dědeček for their kind cooperation towards sharing knowledge regarding geothermal applications.

I would like to sincerely thank my family for the never ending support and for instilling in me confidence and motivation.

Very special thanks go to my wonderful friends and colleagues in Bordeaux for making me feel home with their warm hospitality and care. I can never forget numerous leisure time and sport activities that significantly enriched my life.

Certainly, I would like to thank my Czech friends as well, because they did not forget about me during my long six-months absences and always cared about my success.

This Ph.D. studies would not have been possible without support and guidance of so many people. I would like to thank them all once again.

In conclusion, I recognize that this research would not have been possible without the financial assistance of the French Ministry of Foreign Affairs, the Ministry of Education, Youth and Sports of the Czech Republic and the Grant Agency of the Czech Republic in the scope of the following project: GACR 205/07/0691 „Optimalization of the use and protection of thermal waters in the Benešov - Ústí aquifer system".

# Abstract

Isotopic investigations combined with geothermal applications represent powerful tools for the exploration of groundwater potential as a drinking or geothermal resource. This Ph.D. Thesis combines both approaches, environmental and radioactive isotopes together with temperature data in deep aquifers, in order to enrich and update the knowledge concerning the aquifer recharge processes in the Aquitaine Basin (France) and the aquifer recharge processes and geothermal potential in the Bohemian Cretaceous Basin (Czech Republic).
Stable isotopes ($^{18}O$, $^{2}H$, $^{13}C$) combined with radioisotope data ($^{14}C$, $^{3}H$) are used to estimate the recharge timing and climatic conditions prevailing during the infiltration from the Late Pleistocene up to modern time. The character of groundwater recharge and regime are necessary to generate relevant source data for the accurate modelling of complex groundwater systems. Three groups of groundwater recharge types can be distinguished throughout Europe – (i) continuous recharge and (ii) interrupted recharge during Last Glacial Maximum and (iii) a group corresponding to particular recharge conditions.
The contrasted geographic and climate conditions at both study sites in France and the Czech Republic have entailed a great heterogeneity of the recharge conditions and processes. Southern France, with generally mild climatic conditions during the last 40 ka BP, did not experienced considerable hiatus in groundwater recharge. The residence time of groundwater in the Bohemian aquifers is estimated about 11 ka BP at the maximum but the depletion in the stable isotopes suggests that this groundwater originates in the melting of the north European ice sheets after the Last Glacial Maximum period, i.e. 18-20 ka BP. Further investigations on both stable and radioactive carbon isotopes indicated numerous groundwater interactions within the reservoir that were used to delineate the carbon origin within the Bohemian aquifers.
Information on groundwater geochemistry was supplemented in the Czech case study by geothermal data in order to improve our knowledge of groundwater flow and dynamics. More than one hundred of temperature records from well-logging measurements were used to assess the geothermal gradient in the Bohemian Cretaceous Basin which is the most promising heat accumulation within the country. Many phenomena can affect the thermal field in the region. Vertical groundwater flow and variations in the lithology and the topography lead to a complicated areal distribution of the geothermal gradient and the heat flux which is dominantly controlled by groundwater. Shallow tectonic structures and numerous volcanic rocks exercise an influence on groundwater flow and therefore exert a secondary effect on the thermal field. The geothermal investigation provided useful information on the geothermal resources within the region but also represents an important tool for understanding groundwater flow, and for constructing realistic hydrogeological models in such a complex geological, tectonic and geothermal context.

*Key words: deep aquifers, isotopic hydrogeology, residence time, geothermal potential, heat flux*

# Résumé

Les études isotopiques couplées avec des informations géothermiques peuvent constituer des outils pertinents pour l'exploration des eaux souterraines en tant que ressources en eau potable ou géothermiques. Ce travail combine les deux approches, isotopes de l'environnement et radioactifs associés à des données de température sur des aquifères profonds, dans l'objectif d'enrichir et d'améliorer la connaissance des mécanismes de recharge (Bassin d'Aquitaine, France) ainsi que des mécanismes de recharge et du potentiel géothermique (Bassin Crétacé de Bohème, République Tchèque).

Les isotopes stables ($^{18}$O, $^{2}$H, $^{13}$C) utilisés conjointement avec des radioisotopes ($^{14}$C, $^{3}$H) sont utilisés pour estimer l'époque de la recharge ainsi que les conditions climatiques qui prévalaient lors de l'infiltration depuis la fin de Pléistocène jusqu'à nos jours. Définir le type de recharge et les conditions d'écoulement est nécessaire pour parvenir à modéliser de façon satisfaisante et fiable les grands systèmes aquifères profonds. Trois types de recharge ont été définis en Europe - (i) continue, (ii) interrompue lors du dernier maximum glaciaire (LGM) – un troisième type (iii) correspond à des situations particulières de recharge.

Les conditions géographiques et climatiques très différentes rencontrées en France et en République Tchèque ont engendrées une importante hétérogénéité des conditions et processus de recharge. Le sud de la France, avec un climat relativement doux depuis les derniers 40 ka BP, n'a pas enregistré d'interruption de la recharge. Le temps de séjour des eaux souterraines en Bohème est estimé à environ 11 ka BP au maximum. Cependant, l'appauvrissement des teneurs en isotopes stables enregistré suggère une recharge liée à la fonte de la calotte glaciaire Nord Européenne après le dernier maximum glaciaire (LGM), autour de 18-20 ka BP. Des investigations sur les isotopes du carbone minéral dissous des eaux souterraines du bassin de Bohème ont montrées d'importantes interactions avec différentes sources de carbone qui ont été identifiées.

Pour le site d'étude tchèque, les informations apportées par la géochimie ont été complétées par des données géothermiques afin d'améliorer la connaissance des flux et de la dynamique des eaux souterraines. Plus d'une centaine d'enregistrements diagraphiques de température ont été utilisés pour estimer le gradient géothermique. Plusieurs phénomènes viennent perturber le gradient géothermique de la région. Les flux d'eau souterraine verticaux et les variations lithologiques et topographiques sont à l'origine d'une distribution complexe du flux de chaleur, étant majoritairement conditionné par les écoulements souterraines. Les discontinuités peu profondes et les nombreux pointements volcaniques exercent aussi une influence importante sur l'écoulement souterrain et donc aussi sur le potentiel géothermique du réservoir. Les investigations sur la géothermie ont ainsi fourni des informations fondamentales sur le potentiel géothermique mais aussi sur les conditions d'écoulement des eaux souterraines. La prise en compte de ces informations s'avère nécessaire afin de proposer des modèles mathématiques d'écoulement réalistes.

*Mots clés : aquifère profond, hydrogéologie isotopique, temps de séjour, potentiel géothermique, flux de chaleur*

# Shrnutí

Kombinace metod izotopové hydrogeologie a geotermiky je významným nástrojem pro průzkum podzemních zdrojů k získávání pitné vody i geotermální energie. Tento postup byl v předkládané práci použit pro splnění hlavního cíle - zpřesnění a obohacení dosavadních znalostí o procesech napájení hluboko uložených kolektorů v Akvitánské pánvi (Francie) a o infiltračních a geotermálních dějích v České křídové pánvi (ČR) s využitím přírodních a radioaktivních izotopů a teplotních údajů.

Stabilní izotopy ($^{18}$O, $^{2}$H, $^{13}$C) se spolu s radioaizotopy ($^{14}$C, $^{3}$H) používají k odhadům střední doby zdržení podzemní vody a k objasnění klimatických podmínek v době infiltrace v časovém úseku od konce Pleistocenu do dnešní doby. Pro vytvoření věrohodných hydrogeologických modelů rozsáhlých kolektorových systémů je nezbytné správné pochopení režimu proudění podzemních vod a charakteru doplňování podzemních zdrojů. V Evropě byly rozpoznány tři způsoby dotace srážkových vod do kolektorů – (i) průběžné doplňování, (ii) přerušené doplňování během posledního glaciálního maxima (LGM) a (iii) doplňování kolektorů podléhající specifickým podmínkám.

Rozdílné geografické a klimatické podmínky ve Francii a České republice vedou k odlišnému charakteru napájení kolektorů podzemních vod. V jižní Francii, kde panují relativně mírné klimatické podmínky, nedošlo za posledních 40 tisíc let k významnějšímu přerušení napájení kolektorů. V České křídové pánvi byly z důvodu blízkosti severoevropského ledovce podmínky infiltrace komplikovanější. Maximální doba zdržení podzemních vod dosahuje 11 tisíc let. Tento odhad doby zdržení se však vztahuje k době infiltrace do horninového prostředí a nikoliv k období, ve kterém došlo ke srážkové činnosti. Nízký obsah stabilních izotopů totiž naznačuje, že infiltrovaná voda pochází z tání ledovců pokrývajících severní Evropu, ke kterému došlo po posledním glaciálním maximu, před 18 – 20 tisíci lety. Studium izotopů uhlíku obsažených v podzemních vodách České křídové pánve pomohlo popsat probíhající chemické procesy v kolektorech, a tím přispět k objasnění původu rozpuštěného uhlíku v podzemních vodách.

V České křídové pánvi bylo kromě geochemických dat vyhodnoceno více než teplotních záznamů z karotážních měření, které byly využity k výpočtu geotermálního gradientu. Teplotní pole je v této geotermálně významné oblasti narušeno vertikálním prouděním podzemních vod, různorodou petrografií a topografií. To vede ke složitému plošnému rozložení tepelného toku řízeného prouděním podzemních vod, které odráží tektonickou stavbu území a četnost výskytu vulkanitů. Popsaný výzkum přinesl nové informace o geotermálním poli, ale také údaje důležité pro konstrukci realistických hydrogeologických modelů.

*Klíčová slova: hluboké kolektory, izotopová hydrogeologie, doba zdržení, geotermální potenciál, tepelný tok*

# Foreword

This study initiated in October 2007 was carried out in the framework of the Co-tutelle Ph.D. program both at Charles University in Prague (Institute of Hydrogeology Engineering Geology and Applied Geophysics), and at the Université Bordeaux 1 (GHYMAC Géosciences Hydrosciences), assuming 6-months intervals to alternate between both institutions.

The idea of this project was initiated when the Grant Agency of the Czech Republic attributed to Charles University a financial grant designated to optimize the sustainable development of groundwater resources in the Bohemian Cretaceous Basin. The emerging project needed several independent studies requiring an extensive team consisting of experts from various scientific fields such as geology, tectonics, geochemistry, hydrogeology, hydrogeophysics, etc. This thesis covering the field of hydrogeophysics and hydrogeochemistry clarifies conditions of heat distribution and groundwater flow conditions in the concerned area in the Czech Republic.

The study was extended to France and particularly to the Aquitaine Basin thanks to the financial support of the French Ministry of Foreign Affairs, through the French Embassy in Prague, who granted this project and attributed to Hana Jiráková a joint supervision Ph.D. allowance.

# Collaboration team

Considering the Czech-French conception of the proposed work, the collaboration of different institutes in both countries formed an international team. English was assigned as the common language to facilitate the communication within the team members from both France and the Czech Republic and is also being used for the thesis manuscript elaboration.

The whole team consists of experts in various fields of study and positively contributed to new conclusions in the issue of groundwater resources sustainability for drinking and geothermal purposes. The entire working team is introduced here below:

- Mgr. Hana Jiráková – Ph.D. student
- Dr. Philippe Le Coustumer – consultation on geology and hydrogeology in Aquitaine Basin
- Dr. Frédéric Huneau – consultation on geochemistry and application of environmental isotopes and groundwater dating in deep sedimentary formations
- Dr. Hélène Celle-Jeanton – consultation on application of environmental isotopes and groundwater dating
- Doc. RNDr. Zbyněk Hrkal, CSc. – consultation on hydrogeology of the Bohemian Cretaceous Basin
- RNDr. Martin Procházka – provision of temperature data and consultation on hydrogeology, field conditions and geothermal assessment of the Bohemian Cretaceous Basin
- Mgr. Petr Dědeček – correction on the effect of topography and consultation on geothermal gradient and heat flux of the Bohemian Cretaceous Basin
- RNDr. Miroslav Kobr – consultation on lithology within the Bohemian Cretaceous Basin

# List of publications originating from this work

PAPER 1

Jiráková, H., Huneau, F., Celle-Jeanton, H., Hrkal, Z., Le Coustumer, .P., 2009. Palaeorecharge conditions of the deep aquifers of the Northern Aquitaine region (France). Journal of Hydrology, 368, 1-16. [doi:10.1016/j.jhydrol.2009.01.017]

PAPER 2

Jiráková, H., Huneau, F., Hrkal, Z., Le Coustumer, .P., Celle-Jeanton, H., 2010. Carbon isotopes to constrain the origin and residence time of groundwater in the Cretaceous Basin of Bohemia (Czech Republic). Applied Geochemistry [doi:10.1016/j.apgeochem.2010.05.012]

PAPER 3

Jiráková, H., Procházka, M., Dědeček, P., Kobr, M., Hrkal, Z., Huneau, F., Le Coustumer, P., *in press*. Geothermal assessment of the deep aquifers of the northwestern part of the Bohemian Basin, Czech Republic. Geothermics.

PAPER 4

Jiráková, H., Huneau, F., Celle-Jeanton, H., Hrkal, Z., Le Coustumer, P., *accepted for publication.* Insight into palaeorecharge conditions of European deep aquifers. Hydrogeology Journal.

# List of conferences

Jiráková, H., Huneau, F., Hrkal, Z., Le Coustumer, .P., Celle-Jeanton, H., 2008. Paleo-hydrogeology of the deep aquifers of the Northern Aquitaine Region (France). 36th International Association of Hydrogeologists Congress, Toyama, Japan, 26 October -1 November 2008 (poster)

Jiráková, H., Huneau, F., Hrkal, Z., Celle-Jeanton, H., Le Coustumer, P., 2009. Carbon isotopes and groundwater dating in the north-western part of the Bohemian Cretaceous Basin (Czech Republic). 37th International Association of Hydrogeologists Congress, Hyderabad, India, 6-12 September 2009 (oral)

Jiráková, H., Procházka, M., Datel, J., Kobr, M., Hrkal, Z., 2009. Geothermal conditions in the western part of the Bohemian Cretaceous Basin (Czech Republic) deduced from the well-logging measurements. 10th Czech-Slovakian international congress in hydrogeology, Ostrava, Czech Republic, 31 August – 3 September 2009 (oral)

Jiráková, H., Huneau, F., Celle-Jeanton, H., Le Coustumer, P., Hrkal, Z., 2010. Deep aquifers as archives of palaeorecharge conditions in Europe. 23ème Réunion des Sciences de la Terre Bordeaux, 25 - 29 October 2010 (oral)

Jiráková, H., Huneau, F., Celle-Jeanton, H., Hrkal, Z., Le Coustumer, P., 2010. Insight into the Pleistocene palaeorecharge conditions of confined aquifers throughout Europe. Hydrology Conference 2010, San Diego, CA, USA, 11 - 13 October 2010 (oral)

# Table of content

# List of Figures

# List of Tables

# List of Annexes

# Abbreviation list

| | |
|---|---|
| AB | Aquitaine Basin |
| BCB | Bohemian Cretaceous Basin |
| BUAS | Benešov-Ústí aquifer system |
| bu | Balance unit |
| DIC | Dissolved inorganic carbon |
| DRIRE | Direction Régionale de l'Industrie, de la Recherche et de l'Environnement (Regional Directive for Industry, Research and Environment) |
| GMWL | Global Meteoric Water Line |
| ka | Thousand of years |
| LGM | Last Glacial Maximum |
| PDB | Pee Dee Belemnite standard for carbon-13 |
| pmC | Percent of modern carbon |
| RPDE | Réseau Partenarial des Données sur l'Eau (Water Data Partnership Network) |
| SMOW | Standard Mean of Ocean Water |
| SDAGE | Schéma d'Aménagement et de Gestion des Eaux (Land use Planning and Water Management) |
| TOE | Tonne of Oil Equivalent |

# 1 INTRODUCTION

The quest for a sustainable development is a key concept in water resource management and is the strongest driving force of the water industry. The consensus definition of sustainable development is the process that "meets present needs without compromising our ability to meet those of the future" (Environmental and Energy Study Institute Task Force, 1991). The concept of sustainable development captures the conservation ethic which has been on central stage at many recent global and national environmental and water conferences. As water conflicts increase, water managers need a broad understanding of the principles of the water cycle and ecology, and they must understand how to make and interpret basic water computations and practical aspects of water science and engineering.

Water meets many problems endangering the water resource sustainability. By the entry of the Czech Republic into EU and implementation of its Acts in the field of the water management, the Czech Republic agreed on the regular and continuous quantitative and chemical groundwater monitoring within the country. In France, in the Czech Republic and everywhere in Europe, the water quality of aquatic environments has deteriorated in recent years. The European Parliament has reacted by adopting the Water Framework Directive in 23 October 2000. It requires member states to achieve good status of all water bodies (rivers, lakes, coastal waters, groundwater) in 2015, e.g. sustainable management of water resources; prevent any deterioration of aquatic ecosystems; ensure adequate supplies of drinking water quality; reduce the pollution of groundwater by hazardous substances.

And so, many cities of the world are currently very actively engaged in actions for the improvement of the environmental conditions. Increase in population coupled with social and economic development decrease the water availability per person at global and national levels. However, the lack of data often complicates a reliable groundwater resources evaluation.

The groundwater supply is generally provided from shallow and deep aquifers. Although shallow aquifers are far more accessible for the exploitation, they often represent only low quality groundwater source as climate changes and various catastrophic events may be immediately reflected in the aquifer properties in terms of quality and quantity. Among the most common catastrophic events in European conditions are severe droughts and floods. Both France and the Czech Republic have already experienced such situations. Shallow aquifers are also inherently

vulnerable to a wide range of human impacts. The development of mechanized pumping technologies in the mid-twentieth century has induced widespread drawdown externalities, including the depletion of the all-important shallow aquifers. All these imperfections make shallow aquifers unsuitable for a sustainable development.
On the other hand, groundwater from deep confined aquifers, well protected from surface processes and influences, represents an important strategic resource that often replaces conventional water supply from shallow reservoirs and/or from crystalline rocks. For that reason it is not surprising, that the exploitation of deep aquifers has significantly increased during the recent decades.

Problems concerning the abstraction of high-quality drinking and thermal water do exist everywhere throughout the world. Pumping areas are often very extensive and influenced by various human activities driving the groundwater - surface water interactions and hence endangering the groundwater quality. Groundwater problems range from simple cases of managing individual wells or small regions to problems covering vast regions, such as the Ogallala Aquifer in the USA (Rosenberg et al., 1999; Fryar et al., 2001), Guarani Aquifer in South America (Sracek and Hirata, 2002; Wendland et al., 2007; Rabelo and Edson, 2009; Gastmans et al., 2010), Nubian Sandstones (Lloyd, 1990; Moneim, 2005) or Great Artesian Basin in Australia (Pestov, 2000; Zhang et al., 2007). Such significant hydrogeological systems demonstrate that due to their strategic, social and economic importance, it is indispensable to make a coordinated use of water resource for drinking supply, agricultural, industrial and geothermal purposes. The surface of European aquifers is generally of smaller scale but of the same importance from the socio-economical point of view and should be therefore the subject of an effective water management.

Apart from the supply of potable water, the investigation of deep aquifers becomes very challenging with the increasing demand for renewable energy sources as well. Geological and hydrogeological properties represent limiting factors determining the effective groundwater geothermal potential. Groundwater and its dynamics radically control the geothermal potential of sedimentary basin.

The sustainability of potable and thermal water resources is the main challenging issue during my Ph.D. studies and stands behind all my investigations presented in this thesis. I focused on two European hydrogeologically significant aquifer systems both dating from the Cretaceous:

- The Bohemian Cretaceous Basin in the Czech Republic
- The Aquitaine Basin in France

They both represent a multi-layered aquifer system suffering from intense groundwater exploitation for numerous purposes. The exploitation in those systems is crucial for the population of both countries demanding a sufficient amount of high-quality water. Although there is not currently any catastrophic situation concerning the water supply in neither of the studied areas, the water quality deterioration and the drop of the groundwater levels has been already registered at many places. Water management authorities have to consider hydrogeological models to propose the most adequate management solution for a sustainable development. However, well developed hydrogeological models should not omit the changeable groundwater dynamics, the factor of groundwater recharge variability and oscillations since the Late Pleistocene that significantly influenced the modern groundwater regime. The detailed knowledge on the palaeorecharge conditions is crucial for the groundwater planning in order to evaluate the present-day aquifer capacity and sustainability and to achieve optimal solutions for groundwater use. But, the accurate information on these criteria is often somewhat missing or not fully understood and is therefore difficult to be included in the proposed models.

As a consequence, the need for the knowledge on the character of groundwater recharge during the Late Pleistocene was challenging for this study aiming at clarifying the regime of groundwaters and the palaeorecharge conditions in the AB and the BCB with an emphasis on the continuity/discontinuity of the recharge processes during the last 40 ka. Applied methodology at each site was selected according to the reconnaissance level and the data density. The isotopic hydrogeology methods were applied in both the BCB and the AB while the investigation on the geothermal sustainability was performed in the BCB only.

Both approaches used in the thesis are introduced in the *Chapter 3* devoted to the presentation of the methodology for four case problems and the procedure of their solution. Although the brief introduction to the used dataset is given in this chapter, all details are developed and described furthermore as a part of the publications making part of *Chapter 4* and *Chapter 5* for isotopic and geothermal studies, respectively.

*Chapter 4* describes techniques of the isotopic study and includes the introduction of three case studies aiming at determining the groundwater recharge pattern and its relation to climatic changes and human activities. The isotopic investigation of the important potable water accumulations was initiated in the Aquitaine Basin (AB) clarifying the recharge history using isotopes of hydrogen, oxygen and carbon. Carbon isotopes were especially useful during the study in the Bohemian Cretaceous Basin (BCB). The basin was studied not only for the estimation of the residence time in aquifers, but also for the assessment of the origin of carbon which is dissolved in groundwater. The results from France and the Czech Republic were put in the European context focusing on the recharge heterogeneity within the European continent as a consequence of a climatic instability during the Late Pleistocene period.

A great part of northern Europe was covered by thick ice sheet during the Late Weichselian period preventing aquifers from the recharge processes. The existence of the recharge gap is closely related to the palaeoenvironmental (permafrost) and palaeoclimatic changes (variations of temperatures, amount of precipitation, change of evaporation conditions and increasing aridity) during the late Weichselian period which finished by the Pleistocene-Holocene transition approximately 10 ka BP. In the Late Pleistocene, the major ice sheets spread rapidly. Although it is considered, that the maximal position – Last Glacial Maximum (LGM) - was reached at ca 18 ka BP (radiocarbon age) or 21 ka BP (calendar age), various scenarii have been proposed according to different studies. The southern Europe (including the AB) was generally free of these palaeoclimatic features, aquifers in the northern and central European aquifers (including the BCB) had suffered from the climatic instability in last 40 ka. The relationship between climate and the mean annual stable isotope contents of precipitation (Dangaard, 1964; Rozanski et al., 1992) provides valuable information about palaeoclimatic conditions. Environmental isotope techniques have been largely used in the whole domain of water resources development and management. The stable isotopes oxygen-18 ($^{18}O$) and deuterium ($^{2}H$) as well as the radioactive isotope tritium ($^{3}H$) are rare components of the water molecule. Together with other isotopes, such as carbon-13 ($^{13}C$) and carbon-14 ($^{14}C$), they offer a broad range of possibilities for studying processes within the water cycle (Clark and Fritz, 1999; Mazor, 2004). Although these isotopes allow us to recognize the palaoclimatic fingerprint in groundwaters, various processes occurring in aquifers tend to erase the recorded climate fluctuations.

*Chapter 5* describes the geothermal methods applied in the BCB which is, apart from being the important drinking water supply reservoir, the most extensive accumulation of thermal water. The area in the northwest of the Czech Republic, particularly the Benešov-Ústí aquifer system (BUAS), with current exploitation of thermal water, is the most promising area for geothermal development in the Czech Republic. However, the uncontrolled exploitation can lead to falling temperatures and changes in the quality of the groundwater resources in the future. That is why the geothermal sustainability assessment of the BCB enriched the isotopic investigation primarily focusing on the sustainability of the potable water resources. Heat energy is generally distributed in two different ways – conduction and convection. Geophysical measurements, i.e. well-logging methods can provide fundamental information useful for geothermal gradient assessment. Notably, well logs represent an excellent tool for illustrating the effect of groundwater dynamics on the geothermal gradients controlling heat transfer. Until now, several heat flux estimations within the whole BCB existed. Anyway, the detailed study provides precise information measured in recently drilled boreholes. More than one hundred of well-logging measurements were used for interpretation and heat flux calculation. In sedimentary formations, convective heat transfer often dominates over the conductive and many actions have to be undertaken to obtain accurate heat flux values. The BUAS system, which is a closed hydrogeological unit including recharge, storage and drainage zones, confirms the close relation between the groundwater dynamics and the geothermal gradients controlled by heat transfer.

As described previously, the work is divided into several parts referring to separate case studies either in France or in the Czech Republic, dealing with isotopes and geothermal gradient. Each case study was more or less focused on a particular problem, but it was shown that the application of both approaches, isotopic and geothermal, was very useful for the clarification of encountered unclear phenomena. Many new questions appear using only one methodology, but they might be answered if both methodologies are considered together, which was the idea of the work.

# 2 STUDY SITES

Two sites have been studied – the Bohemian Cretaceous Basin (later referred as BCB) in the northwest of the Czech Republic and the Aquitaine Basin (later referred as AB) in the southwest of France. Both sedimentary basins have many common features, one of them being very important sedimentary structure of the country exploited for drinking and geothermal purposes. As the basin surface is very extensive, only part of each basin presented subject of matter, namely the north-western part of the Bohemian Cretaceous Basin and the northern part of the Aquitaine Basin.
Managerial control over the groundwater resource development and the protection of sedimentary formations is often poor and leads to uncontrolled aquifer exploitation and contamination. Both study sites represent a great interest for hydrogeological sciences and a key role for the groundwater exploitation which is constantly very intense and therefore challenging for detailed investigations. Then, the choice of the study areas was adapted to the data availability and notably the scientific gaps and uncertainties which are necessary to be clarified in the field of sustainable development and groundwater regime.

Many common points concerning geology, hydrogeology and water use, might be found for the AB and the BCB. The geographical situation of both sites is presented in Fig. 1. Both areas are also exposed to different geographical and climatic conditions, which is important to consider further during the isotopic studies. That is to say, the AB is exposed rather to ocean atmospheric circulation affecting the isotopic composition of precipitation, essential for isotopic studies. The BCB is an example of the aquifer evolution in continental conditions. Basic information concerning both areas is summarized in Fig. 1.

As many of the study site details concerning general, geological and hydrogeological conditions make part of the enclosed publications, the following information on both study sites rather aims to provide an overall idea on the characteristic features for each site and avoids the repetitive character of the thesis.

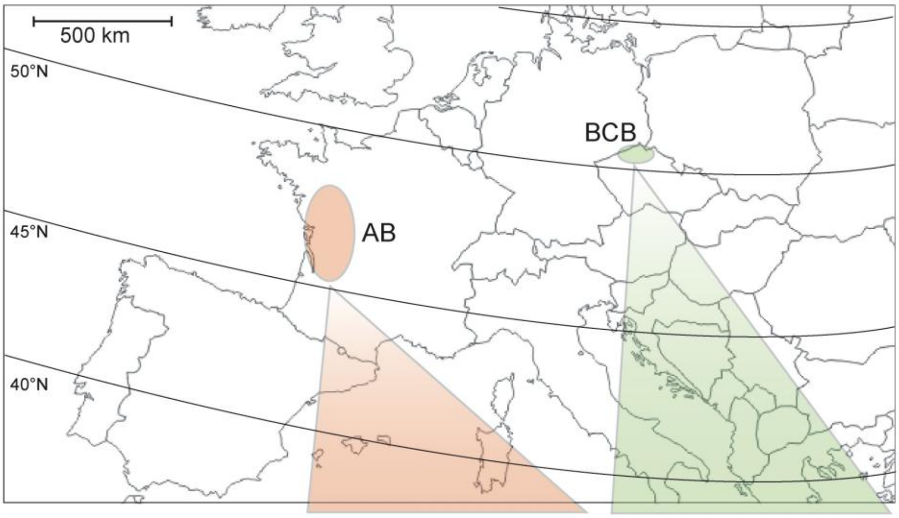


| | | |
|---|---|---|
| Location | SW France | NW Czech Republic |
| Surface of study area | 25 810 km$^2$ | 6 000 km$^2$ |
| Dominant geology of sedimentary sequence | Limestones (+sandstones,claystones) | Sandstones (+marlstones, claystones, carbonated sandstones) |
| Stratigraphy | Jurassic, Cretaceous, Tertiary | Permo-Carboniferous, Cretaceous, Tertiary |
| N$^{O}$ of main aquifers | 7 | 4 |
| Prevailing groundwater use | Drinking supply<br>Geothermal purposes<br>Agriculture | Drinking supply<br>Geothermal purposes<br>Agriculture |
| Geothermal potential | Low temperature | Low temperature |
| Applied methods | Isotopic hydrogeology $^{2}H$, $^{18}O$, $^{13}C$, $^{14}C$, $^{3}H$ | Isotopic hydrogeology $^{2}H$, $^{18}O$, $^{13}C$, $^{14}C$, $^{3}H$<br>Well-logging measurements |

*Fig. 1. Basic information on the study sites.*

## 2.1 Bohemian Cretaceous Basin (BCB)

### 2.1.1 General setting

The BCB is the most extensive continuous sedimentary basin of the platform cover of the Bohemian Massif, as showed in Fig. 2 (the BCB is marked in bright yellow colour). It extends over an area of about 14 600 km$^2$, of which 12 490 km$^2$ lie within the territory of the Czech Republic. The study focuses on its north-western part around Benešov nad Ploučnicí and Ústí nad Labem. The Benešov-Ústí aquifer system (BUAS) is limited unit covering approximately 1 600 km$^2$ which is rather small in comparison with the entire basin structure. The aquifer system is situated in the

Benešov syncline which is a distinct structure intersecting the central zone in a W-E direction. This small unit became the subject of interest for geothermal sustainable development. However, this area was extended up to 6 000 km$^2$ for isotopic groundwater investigations. Hatched part in Fig. 2 outlines the investigated area within the BCB. Study area is limited by borders with Germany and Poland. Its limits generally correspond to mountain ridges which make the study area altitudinal very variable in the range between 100 and more than 700 m a.s.l. The topography is accounted for strongly developed volcanic relief.

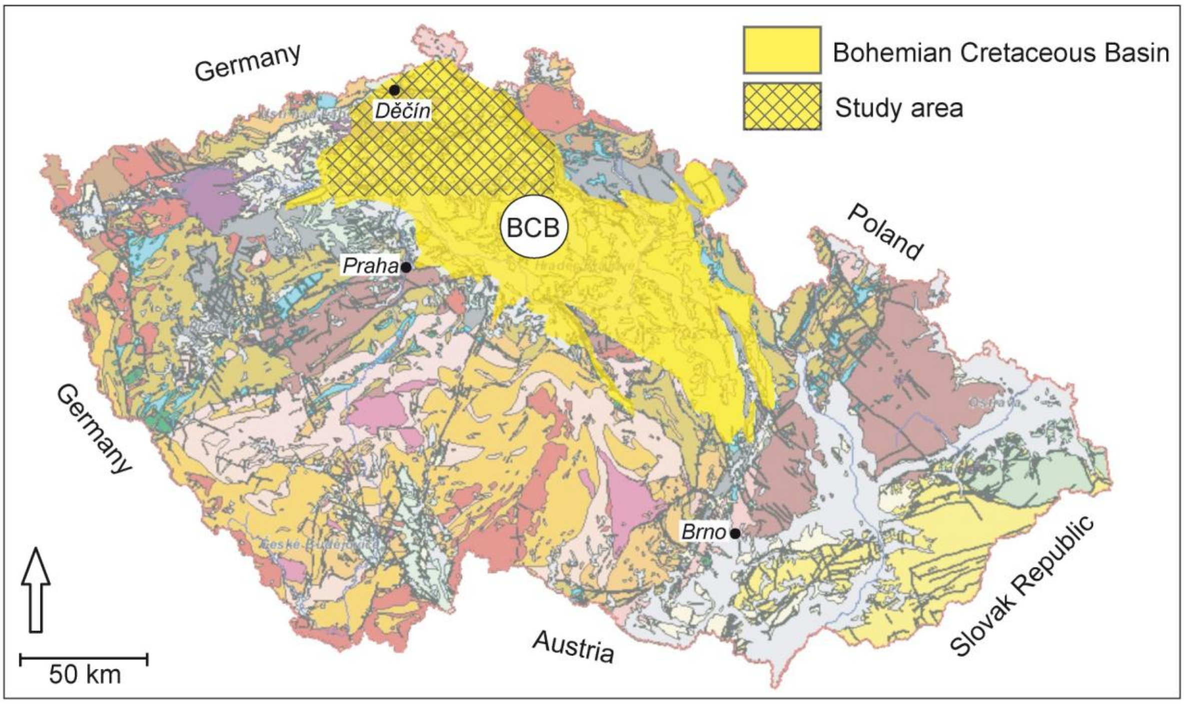


*Fig. 2. Delineation of the Bohemian Cretaceous Basin and the study area within the geologically complex Czech massive.*

### 2.1.2 Geology and hydrogeology

The BCB is very distinct geological unit as it is a largest basin structure of the Upper Cretaceous age in the Bohemian Massif. The study area is considered to be the most complicated portion of the BCB since it is true for its geology, lithology, tectonics and hydrogeology as well.

The simplified schema highlighting main geological units and tectonic features is displayed in Fig. 3.

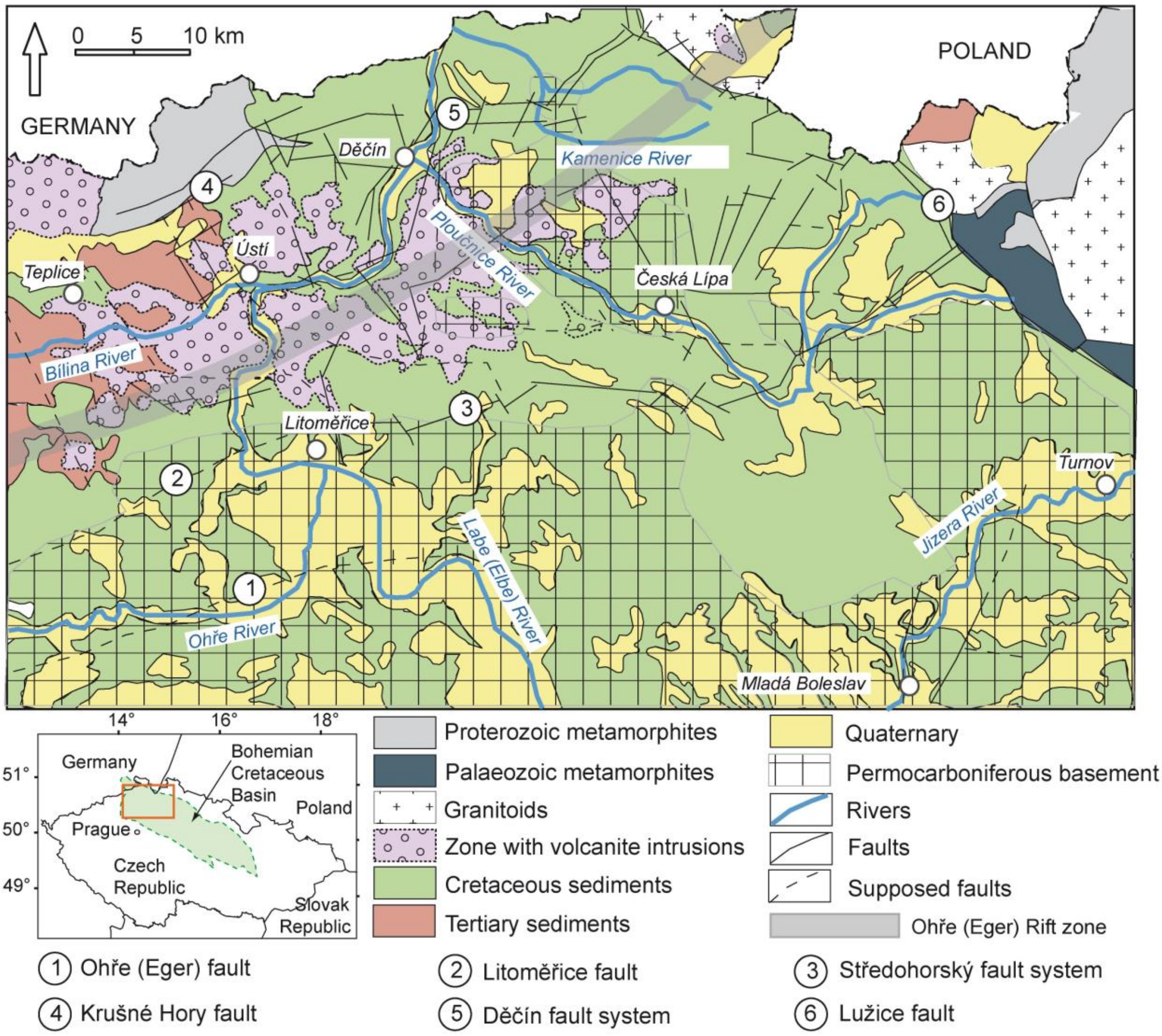


*Fig. 3. Simplified schema of the study area in the Bohemian Cretaceous Basin showing main geological units and fault structures.*

The basement is formed by partially metamorphosed Proterozoic and Palaeozoic rocks, locally pierced by intrusive rocks. The basement is in some places covered with Permo-Carboniferous beds of both sediments and volcanic rocks (Klein, 1979).

The BCB was formed by the reactivation of a fault system in the Variscan basement of the Bohemian Massif during the mid-Cretaceous (Uličný, 1997, 2001). Oldest sediments are of Permo-Carboniferous age, extended primarily throughout the southern and central part of the study area (Krásný, 1973; Fediuk, 1996). They are formed mainly by claystones, siltstones, greywackes, arkoses and conglomerates. During the Mesozoic period, the sediments accumulated from the Early Cenomanian or even from the Late Albian to the Santonian. The Upper Cretaceous sediments in this region show a particular dominance of sandstones, locally very rich in quartz (up to 99%) over other rock types. Nevertheless, detailed evaluation of lithology throughout the study area need to be carried out, notably for thermal conductivity coefficient evaluation (*Chapter 4.11*). Six litho-stratigraphic units can be distinguished, from the oldest to the youngest respectively: Late Albian, Cenomanian (marine deposits), Lower Turonian, Middle Turonian, Upper Turonian, Coniacian and Santonian.

Tertiary sediments and frequent small occurrences of intrusive rocks forming volcanic hills and mountains markedly affect the surface. The occurrence of volcanic rocks is scattered principally throughout the northwestern area.

The sedimentary filling within BUAS typically ranges between 200 – 400 m, but reaches up to 1 200 m in the vicinity of the city of Děčín (Herčík et al., 1999) representing the deepest part of the entire BCB structure.

As a rule, the sediments fill the Benešov syncline which is the most extensive ductile deformation structure in the area. In the central part of the syncline, the Turonian base reaches -650 m, the deepest in the BCB (Herčík et al., 1999).

Tectonics considerably affected the sedimentary succession. The study area is pierced by many faults of local and regional importance. The most important fault structures are displayed in Fig. 3.

The Saxonic block-fault tectonics has substantially influenced the development of the Bohemian Massif after the end of the Variscan orogenesis, when the Bohemian Massif became a rising consolidated block (Malkovský, 1976). The principle directions of displacement zones are SW–NE (Erzgebirge) and NW–SE (Sudetic). Although many faults are not active anymore, they have to be included within any geothermal considerations.

That is to say, that such extinct fault structures do not necessarily indicate direct geothermal effects, but they might be of a great significance in the areas with a developed groundwater dynamics as a groundwater is a dominating medium for the heat transport. Existence of fault structures is often well observed usually on a piezometric map.

Despite the predominance of not active tectonic structures in the study area, the potential active role of Ohře (Eger) Rift is one of the most discussed in the tectonics in the country. According to Kopecký, 1978, the Ohře (Eger) Rift zone was active from Oligocene until Pleistocene. It is the most dominant structure in western Bohemia. The exact position and extension of the Ohře (Eger) Rift is still argued and needs to be clarified. This structure has to be particularly taken into account within any geothermal studies as the surrounding area likely shows elevated geothermal potential. Many distinct volcanic features are identified within the Ohře (Eger) rift, while the volcanic activity in the Labe (Elbe) zone is less obvious. The maximum tectonic vertical movement has been observed along the Krušné Hory fault. The vertical shift is estimated to be about 800–1500 m. Ductile deformations of the Cretaceous sediments (folds) are present across the entire basin with fold structures in W–E direction formed in the initial phases of the Saxonian tectogenesis.

Detailed hydrogeology of the BCB has been summarized in Hydrogeology of the Bohemian Cretaceous Basin (Herčík et al., 1999). This work introduces the division of the BCB area into 10 hydrogeological balance units (bu) as documented in Fig. 4 delineating the study area. The BUAS is included in bu3 although its broader surroundings belong also to bu1, bu2 and bu4. (Fig. 4).

The most investigated structural element has been the bu3 involving a depressed block structure called "Středohorská kra" covering approximately 75% of the bu3 surface area (1 500 km$^2$). Separating the surface into three profoundly different structures, the existence of this tectonic depression has great consequences on the hydrogeological regime.

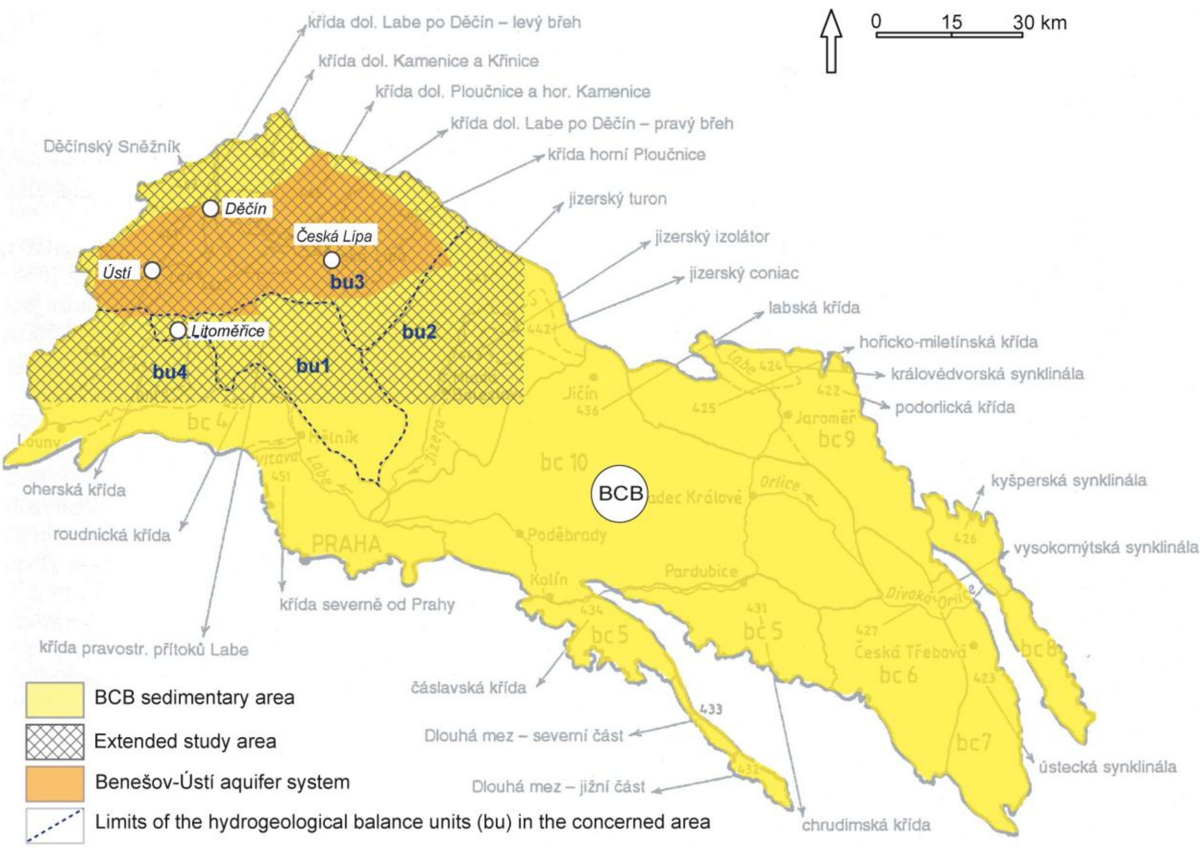


*Fig. 4. Distribution of hydrogeological balance units within the study zone. In Czech – names of hydrogeological departments. Modified from Herčík, 1999.*

The entire aquifer system of Benešov nad Ploučnicí and Ústí nad Labem areas is characterized by subhorizontal aquifer distribution. Aquifers are generally composed of sandstone which predominates in the infiltration zone located in the north eastern part of the aquifer system (see *Chapter 4.11*) near the Lužice fault zone.

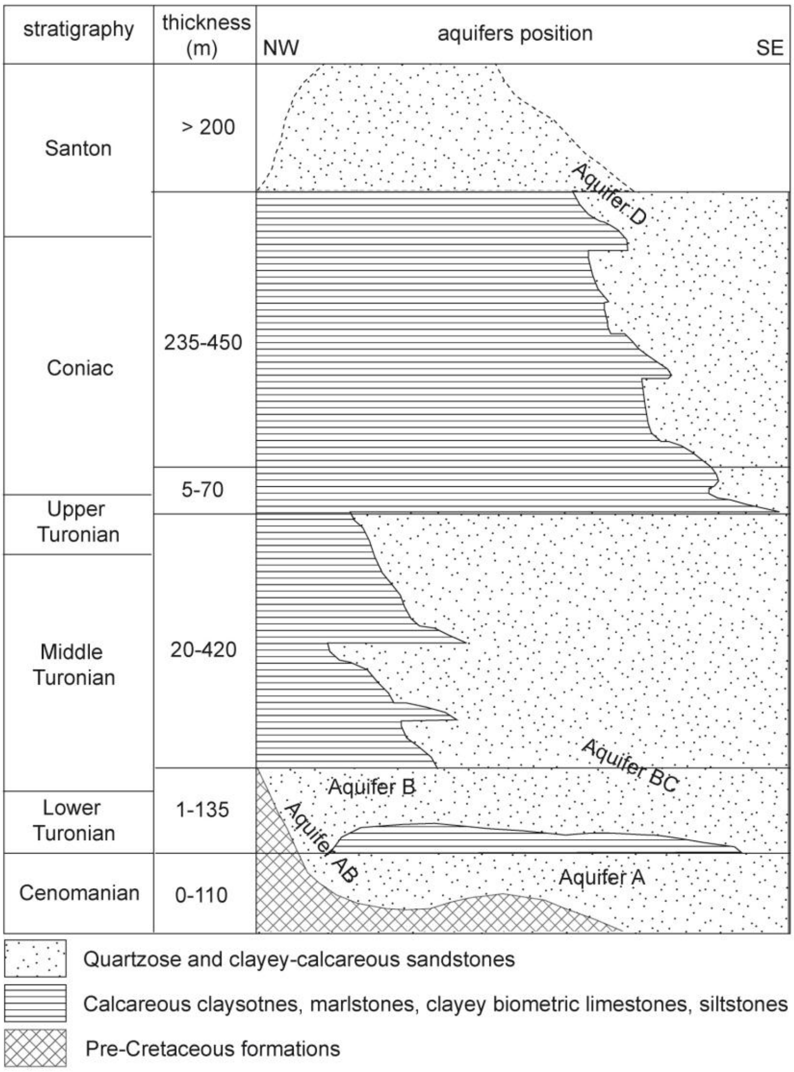


*Fig. 5. Aquifer / aquitard distribution of bu3. Modified from Herčík, 1999.*

Aquitards are generally composed of fine-grained sediments (mostly marlites, siltstones, sandy claystones and claystones) with very low permeability. Aquifer and aquitard distribution of bu3 in the BCB is displayed in Fig. 5. While aquitards are described directly, a system of alphabetical symbols has been developed to facilitate a distinction of aquifers that often communicate together or are formed within several geological layers. The basin in the study area is on the regional scale divided into three main aquifers: (1) A - a basal confined aquifer formed by the Cenomanian sandstone with an intrinsic permeability of $5.10^{-13}$ – $2.10^{-11}$ $m^2$ and a hydraulic gradient of 1-3‰; (2) B,C - middle aquifers in the Turonian sandstone characterised by a free water table, intrinsic permeability of $2.10^{-12}$ – $2.10^{-10}$ $m^2$ and hydraulic gradient of 5-10‰; and (3) D - upper aquifer in the Coniacian–Santonian sediments just below the surface. Values of the hydrogeological parameters stated above are taken from Němeček et al. (1991, 1992). Nevertheless, it is necessary to note that values may locally vary.

The water flow direction is governed by different geological, tectonic and morphological phenomena. The principal drainage axe is formed by the Labe (Elbe) River.

### 2.1.3 Groundwater management and use

Sedimentary area of the BCB together with its geological basement represents one of the most economically promissing regions in the Czech Republic. The importance of its hydrogeological potential is still increasing and will be increasing in the future. Despite very complex geological, lithological and tectonic characteristics, it has very favourable hydrogeological conditions that make the BCB the most extensive reserve of groundwater resources in the Czech Republic. With a growth of groundwater exploitation for various purposes, the BCB stands for the typical example of the groundwater accumulation with elevated vulnerability and questionable sustainability. Extraction of groundwater may intercept water which would be otherwise discharged into a surface water body, and at excessive rates of pumping, water may be drawn directly from the surface water (Sophocleous, 2002). The reconnaissance level of the groundwater reserves and the degree of the real groundwater use is so far rather low. Given the fact that the great part of the western BCB is populated and industrially and agriculturally active, the attention must be paid on the water protection.

Additionally, severe floods have already threatened the basin area along the main water courses. Floods are the most common events affecting the water supply in the Czech conditions. One of the last flood events throughout North Bohemia happened in August 2010 when many households were isolated from drinking water supply for several days. This example demonstrates the vulnerability of water supply which has to be properly evaluated.

Cretaceous sediments create a space for the largest groundwater accumulation in the Czech Republic. The BUAS is shared by Teplice, Ústí nad Labem, Děčín, Česká Lípa, Litoměřice and Liberec districts. Approximate data on the groundwater extraction in each of these districts is schematized in Fig. 6. The authorized groundwater extraction in the entire area reaches 43 734 857 $m^3$/year according to data acquired from the recent survey (Maršálek, unpublished data). This value has been generated from the database of Severočeské Vodovody a Kanalizace (North Bohemian Water Supply and Sewerage Company) excluding industrial demand. Several towns and villages have their proper source of water and the information on the water extraction from such places is not included in the proposed overview in Fig. 6. Considerable part of the mentioned groundwater supply is provided by BUAS.

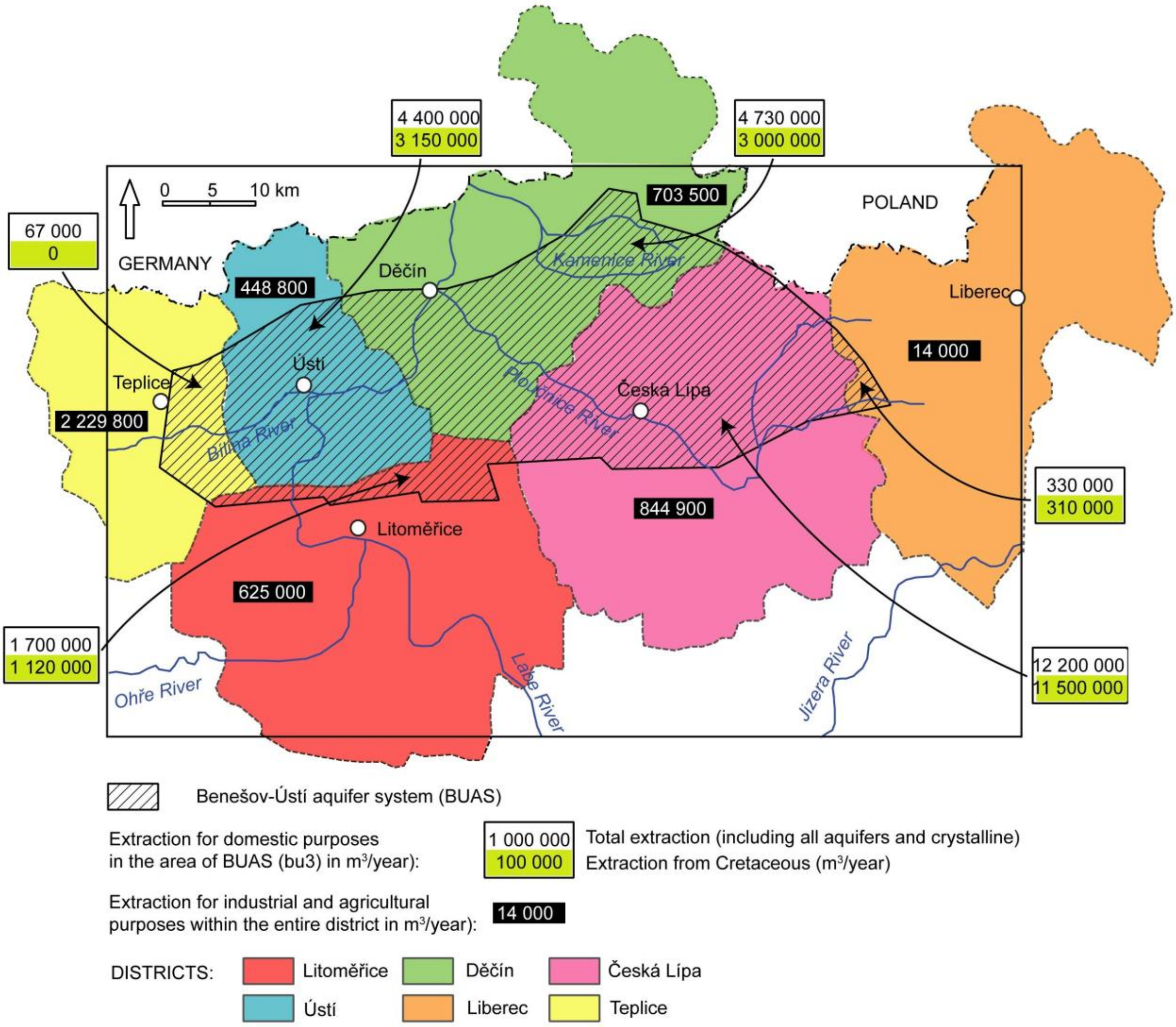


*Fig. 6. District distribution in North Bohemia and values of groundwater extraction. Data acquired from Severočeské Vodovody a Kanalizace (North Bohemian Water Supply and Sewerage Company), unpublished data. Extraction for industrial and agricultural purposes is reported to 2001, extraction for domestic purposes is reported to 2005.*

In areas with increased geothermal gradient, the water has been pumped as a source of thermal energy, especially in Děčín and Ústí nad Labem where exploitation for thermal waters is very frequent. Thermal water occurrence in the Ústí nad Labem sparked off spa constructions in the western Bohemia. Several spa resorts are located in the environs of the study area. Teplice, on the west, is among the most famous and the discovery of its warm springs goes back to 762 AD. The water of Teplice probably originates from Palaeozoic porphyry but is hydraulically connected with the surface water bodies of the Tertiary aquifers. Nowadays, thermal waters are largely used for heating buildings and the thermal swimming pools services.

Groundwater management tasks should consider that thermal waters on a regional scale are closely connected with the fresh water cycle as overexploitation of fresh groundwater sources can significantly influence the properties of the promissing accumulation. Because of the existing conflicts of interest, the detailed hydrogeological study clarifying the groundwater regime not only from geothermal point of view but also from the geochemical and groundwater regime point of view should be carried out. Insight into stable and radioactive isotopic composition would help to specify the potential renewability and vulnerability of the BCB groundwater accumulation.

## 2.2 Aquitaine Basin (AB)

### 2.2.1 General setting

The AB, occupying a large part of the country's south western quadrant and exposed to the Atlantic Ocean, forms the triangular depression limited by the surrounding relief (Fig. 7, marked in bright yellow colour). On the north, the AB is limited by the Armorican Massive; on the east, by the Central Massive and on the south by the Pyrennees mountain range. The AB relief is on the north separated by the vaulted structure called ‘‘Seuil du Poitou” and on the southeast by the ‘‘Seuil de Naurouze” from the Paris Basin and Mediteranean Basin, respectively. After the Paris Basin, it is the second largest Mesozoic and Cenozoic sedimentary basin in France. Its surface area covers 66 000 km$^2$ in total. It was formed on Variscan basement which was peneplained during the Permian and then started subsiding in the early Triassic. The study focused on the Poitou-Charentes area in the AB northernmost part, occupying 25 810 km$^2$. Hatched part in Fig. 7 outlines the investigated area within the AB. It is limited to the west by the oceanic slope of the Atlantic Ocean responsible for the Atlantic climate humidity and instability.


*Fig. 7. Delineation of the Aquitaine Basin and the study area in France.*

### 2.2.2 Geology and hydrogeology

Four major geological entities constitute the Poitou-Charentes region. The granitic and metamorphic “Armorican Massif” on the north and the granitic ”Massif Central”, on the south east of the area. Additionally, two major sedimentary basins of the Mesozoic and the Cenozoic belonging to Alpine orogenic cycle have to be mentioned. The Paris Basin extends from the northernmost part of Poitou-Charentes. The “Seuil du Poitou”, at the intersection of these four entities proves a continuity of the basement between the two ancient massifs, Armorican Massif and Central Massif and communication between the two sedimentary basins (the AB and Paris Basin) via Jurassic seas.

The geology of the region consists of a continuous sedimentary succession from Trias to the Upper Jurassic overlying a Hercynian granite and schist basement. A schematized map of the main sedimentary formations is displayed in Fig. 8.

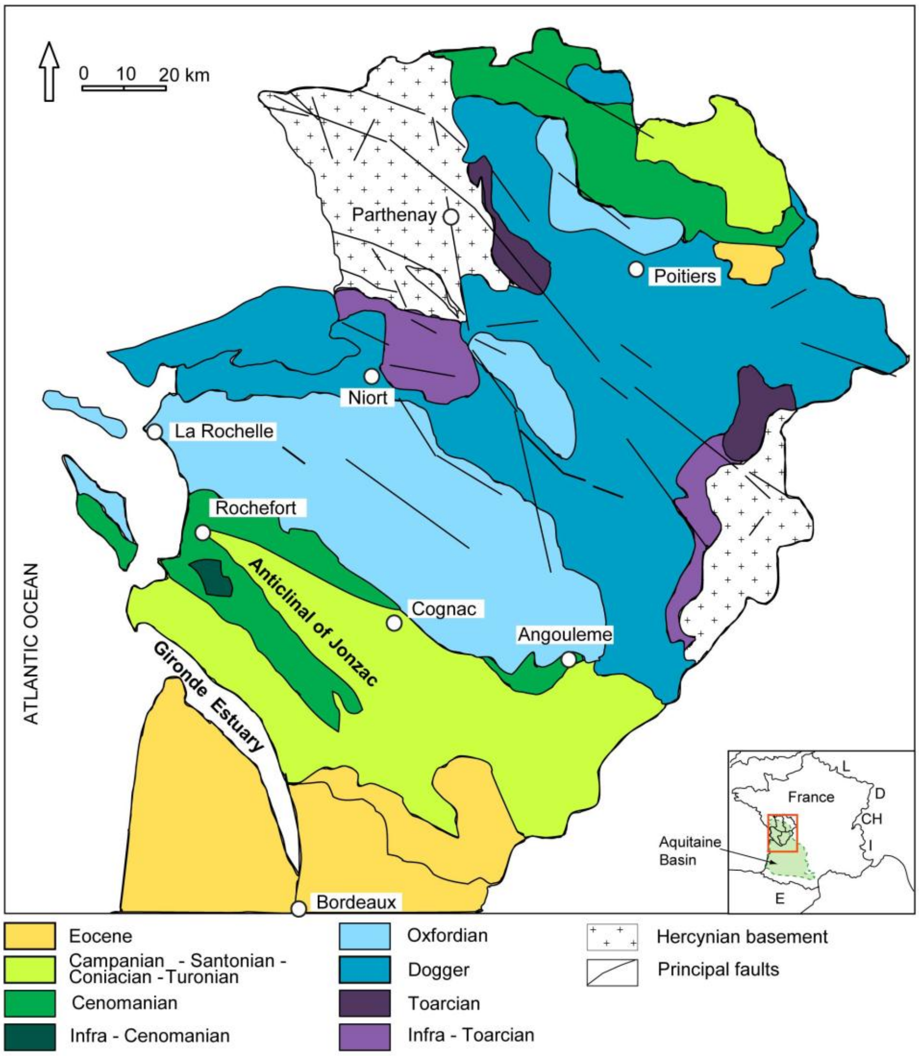


*Fig. 8. Simplified scheme of the study area in the Aquitaine Basin showing the main geological units and the fault structures.*

This extensive multilayered sedimentary formation covers the entire south western part of France and forms several important aquifers. Aquifers of the AB are numerous but often of very limited extension in the Northern part. Bordeaux region and Poitou-Charentes area are of great importance as groundwater is widely pumped for drinking purposes, irrigation and geothermal supplies (in the Jonzac area). Aquifers are often interconnected and abundant upward or downward leakage processes commonly occur as documented in many places (Blavoux et al., 1993; Andre et al., 2002).

The main aquifer systems in the northern part of the basin are the Jurassic, the Upper Cretaceous and the Tertiary layers.

In the **Jurassic**, two hydrogeological units can be distinguished: the Lower and Middle Jurassic confined aquifer (Lias and Dogger) and the Upper Jurassic unconfined aquifer (Oxfordian). The Lias and Dogger aquifers are located between two major impermeable units: the Hercynian basement and the clayey Callovian deposits (Mourier and Gabilly, 1985). Mainly formed of carbonates, they make up together a continuous and deepest aquifer of the studied area. Only in the vicinity of the recharge area, the confining characteristics of the Toarcian horizon could make a distinction between the Lower and Middle Jurassic. Shallow waters in the unconfined Oxfordian carbonate aquifer provide data on modern groundwater recharge.

The multilayered **Cretaceous** formation constitutes the main resource for fresh water and agricultural supply in the south of the Poitou-Charentes area. The Lower Cretaceous is completely missing and the Upper Cretaceous only reaches a thickness of a few hundred meters. The main hydrogeological units were developed in the Cenomanian, the Coniacian-Turonian and the Upper Turonian layer. The Cenomanian is usually sandy and becomes more carbonated towards its top part. The Coniacian–Turonian aquifer, both confined and unconfined, is one of the most exploited hydrogeological unit in the region. The Upper Turonian is considered to be the main aquifer with a high transmissivity coefficient. The permeable succession of the Turonian passes to clayey limestones at the base of the Santonian.

The **Eocene** aquifer, situated mostly in the southernmost part of the studied area (close to the Gironde estuary) and largely exploited towards the south in the Bordeaux region, was developed in fluvial sand and gravels as a multilayered formation covered by clayey deposits.

### 2.2.3 Groundwater management and use

The groundwater resources in the Poitou-Charentes region are relatively abundant, but the coincidence of droughts (periods of very low surface water and groundwater levels) with gradually increasing water supply need (irrigation and notably house use) cause a structural disequilibrium resulting in permanent deficit of the water quantity. Groundwater management issues are regularly updated and are available at the Water Data Partnership Network in the Poitou-Charentes region (RPDE, 2010).

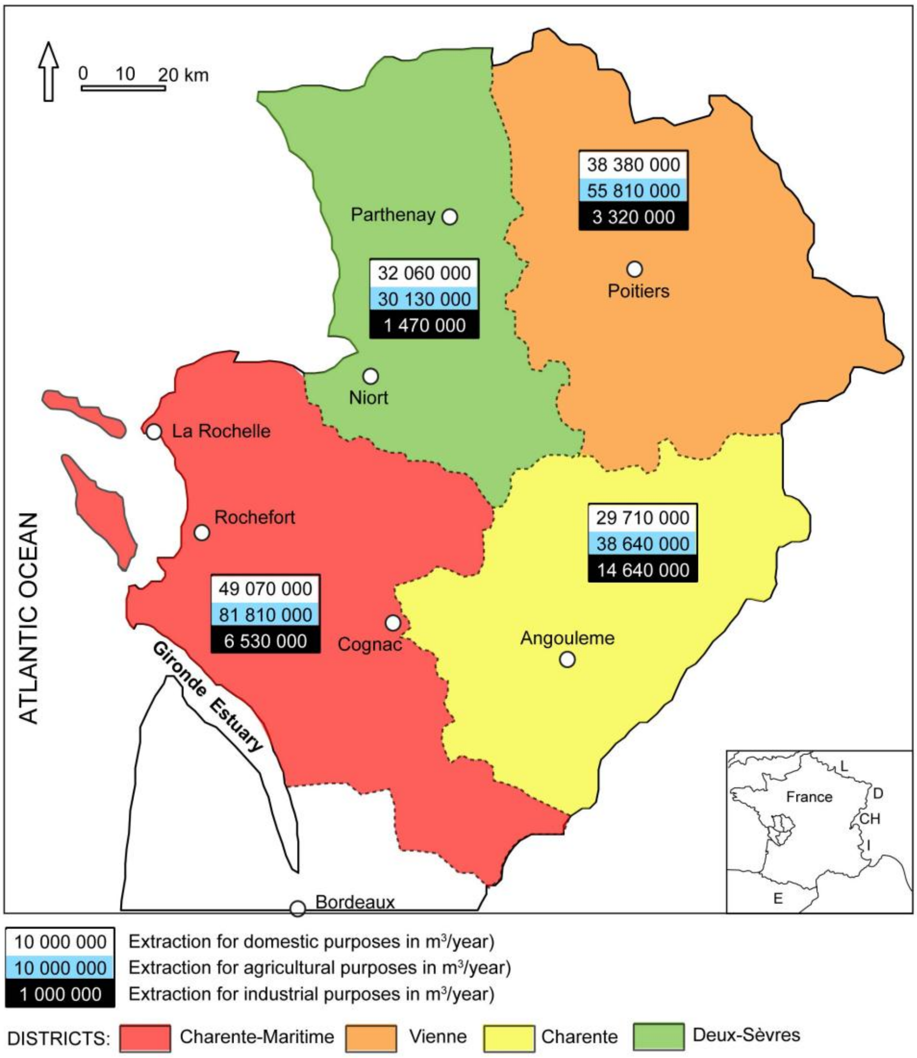


*Fig. 9. District distribution in Poitou-Charentes and values of groundwater extraction (RPDE, 2006).*

Majority of pumping is carried out in the agricultural sector (Fig. 9). Given the fact, that there are many large irrigated areas in the region, the exploitation for such purposes is in great conflict with other water uses like fishery, recreation or drinking water supply. For example, corn monocultures in the Charente Maritime district on the south west of Poitou-Charentes, cover 56 000 hectares. In these 56 000 hectares, 38 000 hectares, which is nearly 70% of corn crops, are irrigated. This represents approximately 80 million cubic meters annually taken from the groundwater reserves mainly. In comparison, domestic use is around 50 million cubic meters for 2006 (Fig. 9).

A return to equilibrium in groundwater use is scheduled for 2017 in the framework of the master planning and water management (SDAGE) developed across the main river basin agencies. By 2017, in the Great Southwest (Adour-Garonne and the region of Poitou-Charentes), 15% of the territories will gradually reduce at least 30% of their exploitation. This reduction could reach up to 50% in some places.

As a consequence of the touristic pressure, the problem concerning the water supply becomes particularly very important the coastal zone,

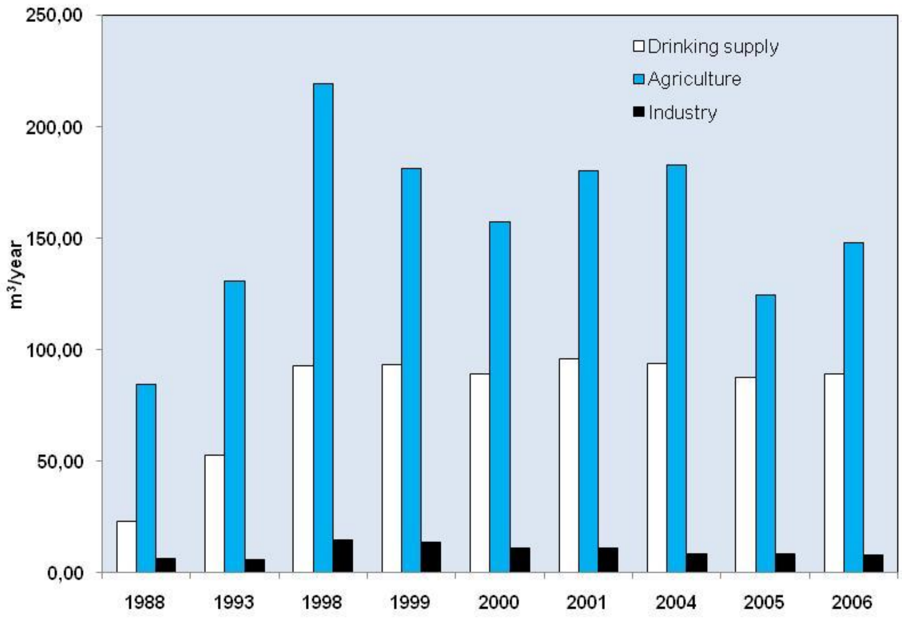


*Fig. 10. Evolution of groundwater extraction between 1988 – 2006 (RPDE, 2006).*

This situation is particularly problematic during some years when winter rains are not heavy enough to allow a sufficient groundwater recharge. Additionally, some local rivers experience severely low water levels and flow rates, thus reducing freshwater inflow in the coastal zone.

Significant needs to compensate an unpredictable amount of precipitation claims for a sustainable water development for the future.

The Poitou-Charentes Region is almost annually affected by water restrictions resulting from severe droughts. In many places, irrigation could be totally forbidden in summer months. The prefecture has already decided to change the calculation methods to evaluate water availability in order to guarantee the continuous water supply during less favourable climatic conditions. Sustainable management and ensuring the resource protection call for a need of improved knowledge and water resources monitoring, although significant progress has already been made.

In the Poitou-Charentes region, the water for drinking purposes is drawn mainly from deep aquifers. This water has to meet certain quality criteria, even before undergoing a purification process.

Moreover, the protection of the groundwater quality in aquifers and rivers presents a major challenge considering the physical, chemical and biological degradation.

This quality deterioration of the groundwater resources results primarily from agricultural and industrial impacts, the latter are usually very local. Nowadays, different pollutants affect water environment and remain in water for a very long time, e.g. nitrates, pesticides and other organic compounds. The quality of coastal waters should be still improved by getting more knowledge about hydrodynamics of water systems and protect them against any kind of pollution.
The quality of drinking water is regulated by Directive 98/83 from 3 November 1998 and decree 2001-1220, which sets the limits and quality standards for drinking water.
In 2003, the Regional Directive (DRIRE) of Aquitaine initiated an action to limit the exploitation permissions and wasting of water.

The AB is the most exploited sedimentary structure for geothermal purposes in France. The geothermy of the AB is valorised by numerous boreholes while most of them have been in operation since more than twenty years. In 2005, about fifteen boreholes were exploited and represented approximately 12 000 TOE of the annual energetic contribution. In the regional scale, such resource allows to reduce $CO_2$ emissions by 25 000 tonnes. The geothermal development in the Aquitaine region is characterised by a great diversity such as heating of households, collective installations, swimming pools, greenhouses, spa industry, fish industry, etc.
There are three main applications of the geothermal energy:

- heat distribution, e.g. Bordeaux region
- heating for the fishery pools, e.g. Arcachon Basin
- energy use for house heating and spa industry, e.g. Dax (more than 15°C/100m; Alezine, 1987).

# 3 METHODOLOGY

## 3.1 General approach

Two different approaches have been selected – isotopic methods and geothermal applications – for the evaluation of the deep aquifers potential. Each of them evaluates the groundwater resources from another point of view:

(i) Interpretation and valorisation of isotopic data is very useful to determine the groundwater recharge pattern, its relation to climatic changes and human activities.

(ii) Geothermal data acquired from boreholes and reflecting true thermal conditions contribute to assess the geothermal potential of aquifers and the flow conditions.

Both approaches should be consequently considered together to propose the optimal solution in groundwater management.

Four case studies were carried out in the scope of this work

(i) palaeorecharge conditions, AB (*Chapter 4.5*)
(ii) carbon origin in groundwater, BCB (*Chapter 4.6*)
(iii) typology of recharge processes in Europe (*Chapter 4.7*)
(iv) geothermal potential of the BCB (*Chapter 4.12*)

Water sampling, analysing and numerous geothermal measurements were not included in the framework of the thesis. The exception concerns the most recent well-logging data in the BCB which have been acquired within the project GACR 205/07/0691 also supporting the current work. Used data are all properly cited and referenced.

*Tab. 1. Comparison of data character AB, BCB and selected European aquifers.*

| | AB | BCB | European aquifers |
|---|---|---|---|
| geographical coordinates | x | x | - |
| stratigraphy | x | x | x |
| temperature from sampling depth | x | x | - |
| major chemistry ($Ca^{2+}$, $Mg^{2+}$,$Na^{+}$,$K^{+}$,$SO_4^{2-}$,$Cl^{-}$,$HCO_3^{-}$,$NO_3^{-}$) | x | x | - |
| pH | x | x | - |
| $^{3}H$ | x | x | - |
| $\delta^{18}O$ | x | x | x |
| $\delta\,^{2}H$ | x | x | x |
| $A\ ^{14}C$ | x | x | x |
| $\delta^{13}C$ | x | x | x |
| temperature records in the well profiles | - | x | - |

Presented work summarizes several research projects with the aim to get more information about the groundwater recharge history, sensitivity of aquifers to climatic changes, different groundwater recharge processes and timing within Europe or to acquire information for the geothermal development in the BCB. Acquired data were analysed, valorised, compared and interpreted.

Yet, several datasets were created. Following chapters introduce the principle approach to each case study while detailed information about each dataset is provided in the fulltext papers furthermore presented either in its published or submitted form.
The comprehensive summary of all used data is given in Tab. 1 providing information on the data characteristics for each study site.

## 3.2 Isotopic investigation – Aquitaine Basin case study

Although aquifers in the AB have been intensely explored and many isotopic measurements were carried out in there previously, it was always with very fragmentary approaches. We set up a comprehensive dataset including 75 groundwater samples with information on the stable isotopes and 59 samples with radiocarbon data including Jurassic, Cretaceous and Eocene. As an insight into groundwater geochemistry, it is necessary to well understand the geochemical processes occurring within aquifers. An extra dataset of chemical data throughout the area was treated. Raw measurement data were taken from Savoye (1993), Le Gal La Salle et al. (1996), Marlin (1996), Marlin et al. (1998), BRGM (1999, 2000, 2001, 2002, 2005) and Mouragues (2000). More details on the type, origin and data treatment is available in the *Chapter 4.5* in the „*Methods and data treatment*“ section. The study of the AB focuses on the palaeorecharge conditions and the recharge continuity. The evaluation of the isotopic data should answer the question if the groundwater recharge occurs continuously or if the recharge was interrupted within the last 40 ka period, namely during Last Glacial Maximum (LGM), which has been ambiguous so far.

### 3.3 Isotopic investigation – the Bohemian Cretaceous Basin case study

Isotopic investigation in the BCB started in the 70$^{th}$ of the 20$^{th}$ century. Many valuable information from the Turonian and the Cenomanian aquifers were collected by Šilar (1976 and personal communication) and Pačes et al. (2008). The dataset of 22 samples with isotope information and 47 chemical analyses is introduced in the *Chapter 4.6* in the „*Database setup and methodology*“ section. The main objective of the BCB isotopic study was to understand the geochemical processes occurring within the aquifers during groundwater flow leading to modifications of the chemical and isotopic composition. Isotopic signature of groundwater, mainly carbon data, helps to identify prevailing geochemical processes in the aquifers. Additionally, these data led to the development of a conceptual model of carbon origin within the system.

### 3.4 Isotopic investigation – Europe

Findings from isotopic investigations in France and in the Czech Republic, in different geographical locations were inspiring to carry out the review study throughout European sedimentary aquifers and compare the recharge conditions in each of them. A very huge dataset comprising 24 European aquifers was used for this review study focusing on the groundwater recharge conditions in Europe. Many research studies on the selected aquifers were collected comprising aquifers from southern to northern Europe in order to distinguish the differences in aquifer recharge behaviour during the Late Pleistocene with the emphasis on the recharge continuity. Data on stable isotopes of groundwater, carbon-13 and radiocarbon activity measurements were taken into consideration. The most valuable information is provided by the combination of stable isotopic data with radiocarbon ages of groundwater established by different correction dating models. Groundwater dating was not in the scope of the current review study; therefore available dating results were generally taken from previous works. Type of data and reference sources are introduced in detail in *Chapter 4.7* in the „*Methodology and dataset*“ section. In order to include as much relevant information as possible, it was necessary to consider palaeoclimatic conditions during the Late Pleistocene and their impact on the groundwater recharge. Such information on palaeoclimate, ice-sheet and permafrost extensions was generally acquired from commonly accepted hypothesis or recent studies. Reference sources and detailed summary on the Wechselian period conditions is available in the *Chapter 4.7* in the „*Weichselian environment in Europe*“ section.

## 3.5 Geothermal application – case study BCB

Many boreholes in the BCB – BUAS region were constructed and measured from the last forty years for various purposes. Measurement records were conserved in different archives (Stavební geologie, Charles University – Faculty of Science, Geoindustrie, Diamo, UP Rynoltice and AQUATEST a.s.). The company AQUATEST a.s. provided very valuable information and interpretation of acquired data. Moreover, AQUATEST a.s. was charged to provide geophysical measurements in recently constructed monitoring wells within deep sedimentary aquifers for the Czech Hydrometeorological Institute (ISPA project funded by the European Union and the Czech Ministry of Environment). Initial database consists of basic identification of borehole - location, depth and continuous temperature records. The temperature records were converted into the geothermal gradient. Furthermore, it was necessary to determine the prevailing lithology allowing the assessment of the heat conductivity coefficient. The latter is necessary for the heat flux calculations. Data processing is described in *Chapter 4.12* in the „*Data set*“ section.

# 4 ISOTOPIC INVESTIGATION

## 4.1 Introduction into isotopic hydrogeology

During the last decades, environmental isotope techniques have been commonly and largely used in the whole domain of the water resources development and management. Isotopic data are routinely used in hydrogeology to complement hydrogeochemical and hydrodynamic data in order to understand patterns of groundwater flow, the origin of water, the residence time and the geochemical processes within aquifers.

The stable isotopes oxygen-18 and deuterium and the radioactive isotope tritium are rare components of the water molecule. Together with other isotopes, such as carbon-13 and carbon-14, they offer a broad range of possibilities for studying processes occurring within the water cycle. These isotopes are therefore important tool not only in groundwater management needs but also in studies related to atmospheric circulation and palaeoclimatic investigations. The relationship between climate and mean annual stable isotope contents of precipitation provides significant insights into palaeoclimatic conditions. Although the isotopic signature of precipitation is archived in groundwater, various processes occurring in aquifers tend to modify the recorded climatic fluctuations. This may also considerably complicate any radiocarbon dating efforts to provide a reliable chronology on the groundwater recharge history.
*Chapters 4.2 - 4.4* briefly introduce the main practical use of isotopes. Individual case studies are then developed in *Chapters 4.5 - 4.7* where more details on the isotope methods are presented.

## 4.2 Stable isotopes of water – tracers of palaeorecharge

Stable isotopes (oxygen-18 and deuterium) allow us to follow the water evolution during its flow path from the infiltration until the drainage processes.
The stable isotopic composition is reported in standard δ notation in ‰ vs. SMOW (Standard Mean of Ocean Water) as follows:

$\delta = (R_{sample} / R_{standard} - 1) * 1000$, where $R_{sample}$ and $R_{standard}$ represent the ratio of heavy to light isotopes of the sample and the standard, respectively. In 1961, Harmon Craig published his finding that $\delta^{18}O$ and $\delta^{2}H$ in fresh waters correlate on a global scale following the "global meteoric water line (GMWL)":

$\delta^{2}H = 8\ \delta^{18}O + 10$ ‰ SMOW (Fig. 11, Craig, 1961).

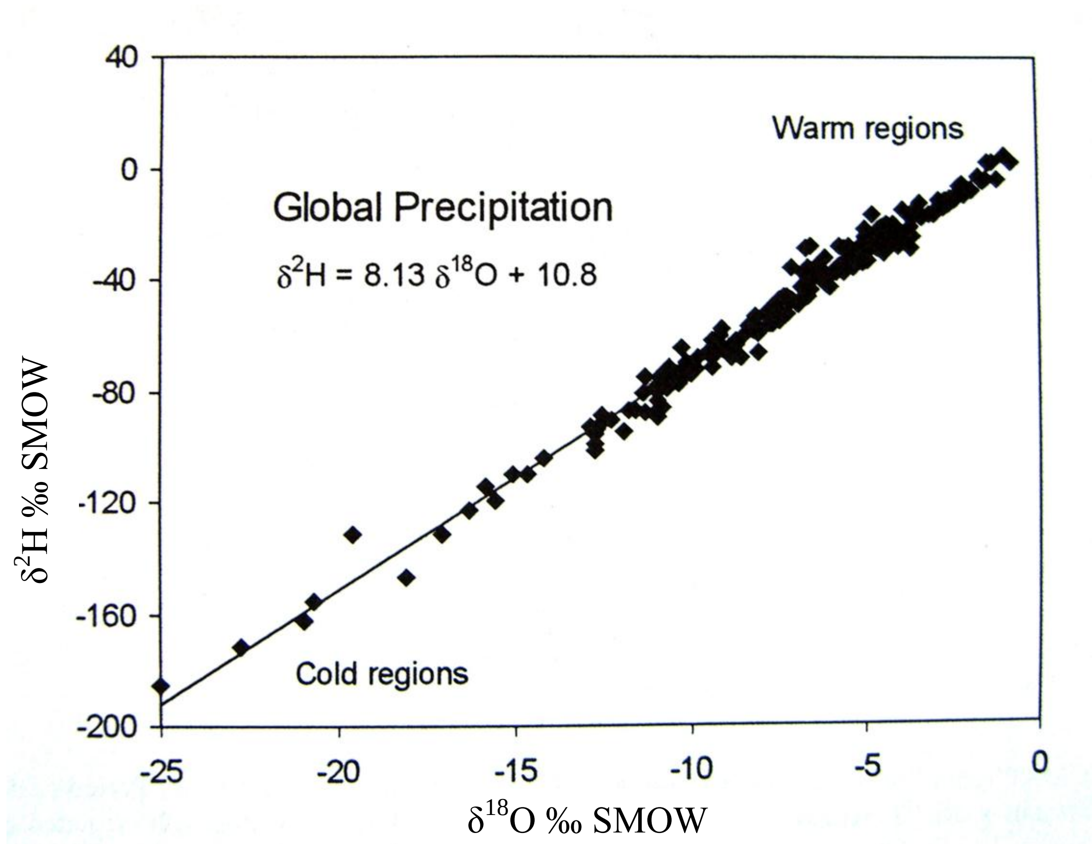


*Fig. 11. The meteoric relationship for $^{18}O$ and $^{2}H$ in precipitation (Clark and Fritz, 1999). Data are weighted average annual values for precipitation monitored at stations in the IAEA global network, compiled in Rozanski et al. (1993).*

On the local scale, the "local meteoric water line" can be slightly deflected from the GMWL. The position of meteoric waters on this line is controlled by a series of temperature-based mechanisms and a number of environmental parameters such as surface air temperature, amount of precipitation, source of moisture and vapour mass trajectories over continents rising over topographic features moving to high latitudes, and seasonal effects (Rozanski, 1985; Clark and Fritz, 1999; Chen et al., 2003; Mazor, 2004). A strong correlation exists between temperature and isotopes in precipitation. Accordingly, the gradients of temperature induce gradients in $\delta^{18}O$ and $\delta^{2}H$. These gradients observable in groundwaters can therefore represent a useful tool in climatological and palaeoclimatological studies.

Some conclusions on palaeoclimatology might be deduced even without precise temperature calculation using the relation proposed by Dansgaard (1964). The position of groundwater samples in respect with the GMWL and with the modern isotopic content of precipitation may propose valuable information. The position of the water samples on the GMWL indicates that the groundwater has not undergone any specific processes such as evaporation or geothermal processes. The shift between the samples and the modern isotopic composition stands for the importance of the climatic changes. This can allow us to detect groups of waters recharged during colder climatic conditions, most often during the LGM. Stable isotopic interpretation should be the first step in any efforts to understand the palaeorecharge processes and needs to be confirmed using groundwater dating methods.

## 4.3 Groundwater dating

Isotopes of carbon and tritium represent a very powerful tool to evaluate the residence time of groundwaters. The most common radioisotopes include carbon-14 and tritium and are routinely employed in hydrogeology to date groundwater.

### 4.3.1 Carbon isotopes

Dating with radiocarbon cannot be done on the water molecule itself but must rely on the dissolved inorganic carbon in the water (DIC) which enter the groundwater from the atmosphere through the soil zone.

Carbon-14 activities are referenced to an international standard and are expressed as a percent of modern carbon (pmC). The main applications of carbon isotope ratios in isotopic and hydrogeochemical studies are used to define chemical reactions, mass balance quantification, and the evaluation of groundwater age.

The simplest approach to radiocarbon dating of groundwater assumes that carbon-14 moves with the water molecules along the flow path and that the main mechanism enabling the modification of the radiocarbon content is a radioactive decay with the half-time of 5 730 years. To proceed to the groundwater age determination, the initial activity of carbon-14 must be determined. However, the isotopic signature is in most situations diluted, particularly by carbon-14 free sources. The complications are enhanced in carbonate environment with a very specific carbon isotope composition or in tectonically active areas. The natural decay thus allows only the determination of the apparent age of the groundwaters. The apparent age has to be corrected in order to approach the real age. It might be determined from various models considering mass balances, isotopic balance or both. The choice of the model should be carried out on the basis of the knowledge concerning the geological environment and occurring geochemical processes. These correction models generally consider the carbon-13 concentration which is reported like other stable isotopes in $\delta$ ratio and is expressed with respect to Pee Dee Belemnite standard (PDB). Carbon-13 is an excellent tracer of carbonate evolution in groundwaters because of the existence of various carbon reservoirs. For that reason it stands for a very useful parameter to accompany the radiocarbon data within any groundwater dating efforts. While carbon-14 activity is independent on the carbon origin, the carbon-13 measurements can help to clarify the original carbon sources. This can solve frequent ambiguous questions whether the low radiocarbon activity is caused by simple radioactive decay or the dilution by dead carbon from the carbonate matrix. Carbon-14 data should be always accompanied by carbon-13 clarifying geochemical processes in deep aquifer systems.

### 4.3.2 Tritium isotopes

Tritium, $^{3}H$, is a short-lived isotope of hydrogen with a half-life of 12.43 years which has been largely produced during the era of thermonuclear bomb testing. Tritium concentrations are expressed in tritium units (TU). Although some measurable amounts of tritium in groundwater may be produced naturally, most often the presence of tritium refers to the modern infiltration after the bomb testing, i.e. 1952 (Clark and Fritz, 1999).

The absence of tritium in groundwater indicates a recharge prior 1952 and radiocarbon methods can be applied to estimate the groundwater residence time up to ca 30-35 ka BP.

## 4.4 Purpose of isotopic investigation

The current work focuses on the delineation of the recharge processes and discusses their continuity, first on the regional scale in France and the Czech Republic and later on the European scale as the different geographical position of the investigated aquifers is responsible for variable climatic conditions which have prevailed since the Late Pleistocene.

As showed earlier, any interactions between rock-groundwater are reflected in the quality and the isotopic composition of water samples. Generally, interactions such as (i) mixing between aquifers, (ii) groundwater - aquifer matrix, (iii) groundwater - surface and irrigation water, (iv) groundwater – deep $CO_2$ sources, (v) groundwater – organic matter, etc. complicate the isotopic studies.
For that reason, a geochemical study should precede any groundwater dating calcualtions in order to assess the geochemical background of the studied aquifer and to propose the optimal method for the groundwater dating. Additionally, the knowledge of water origin is essential to understand the geochemistry and the dynamics of the groundwater system which is fundamental to manage the sustainability of the exploitation of groundwater resources.

Many studies focusing on the delineation of the recharge history have been carried out worldwide and it has been often pointed out, that many difficulties often complicate the dating efforts to provide the accurate recharge chronology. These difficulties remain a point of weakness when hydrogeologists are trying to build models to reproduce the very long term evolution of groundwater flow within deep confined aquifers. The inference about ages of groundwater is important in groundwater resource management as the renewal of groundwater may be very slow. Isotopic data help to validate hydrogeological conceptual models in continental scale aquifers. Very strong uncertainty about the continuous or interrupted recharge of aquifers especially during the transition from Pleistocene to Holocene should be cleared up. Additionally, the groundwater residence time is one of the most important parameters in hydrology. Its knowledge is essential as the input for any prediction for the future development of the resource (Ozyurt and Bayari 2003; Katz et al. 2004).
Continuous recharge indicates favourable recharge conditions through times, while the absence of recharge has been attributed to the existence of more or less continuous permafrost conditions and/or to strong modification in the atmospheric humidity in the peripheral regions of the North European ice cap. Despite numerous research efforts, our knowledge about the precise timing of the LGM and its fingerprint on groundwater remains incomplete and in part controversial.

## 4.5 Palaeorecharge conditions of the deep aquifers of the Northern Aquitaine region (France)

*Published as:*

*Jiráková, H., Huneau, F., Celle-Jeanton, H., Hrkal, Z., Le Coustumer, P., 2009. Palaeorecharge conditions of the deep aquifers of the Northern Aquitaine region (France). Journal of Hydrology, 368, 1-16. [doi:10.1016/j.jhydrol.2009.01.017]*

Journal of Hydrology 368 (2009) 1–16

Contents lists available at ScienceDirect

Journal of Hydrology

journal homepage: www.elsevier.com/locate/jhydrol

# Palaeorecharge conditions of the deep aquifers of the Northern Aquitaine region (France)

Hana Jiráková [a,b,*], Frédéric Huneau [a], Hélène Celle-Jeanton [c], Zbyněk Hrkal [b], Philippe Le Coustumer [a]

[a] *University of Bordeaux-1, GHYMAC Géosciences Hydrosciences, B18 Avenue des Facultés, 33405 Talence Cedex, France*
[b] *Charles University, Institute of Hydrogeology Engineering Geology and Applied Geophysics, Albertov 6, 128 43 Prague 2, Czech Republic*
[c] *University of Clermont-Ferrand, LMV CNRS UMR 6524, 5 rue Kessler, 63038 Clermont-Ferrand, France*

ARTICLE INFO

*Article history:*
Received 7 July 2008
Received in revised form 21 December 2008
Accepted 15 January 2009

This manuscript was handled by L. Charlet, Editor-in-Chief, with the assistance of Bernhard Wehrli, Associate Editor.

*Keywords:*
Confined aquifer
Hydrogeology
Residence time
Stable isotopes
Radiocarbon
Palaeorecharge

SUMMARY

The study was carried out in the northern part of the Aquitaine Basin extending in Southwest France. The basin has been intensively exploited for various purposes for many years. Although the geological context is well known, there are still some gaps in the knowledge about the hydrogeochemical regime, groundwater average residence time and the palaeohydrological conditions prevailing during the recharge period which would help to secure sustainable exploitation of the resources. Environmental isotopes ($^{18}O$, $^{2}H$, $^{3}H$, $^{13}C$) together with radiocarbon were used to evaluate hydrochemical evolution, residence time and palaeorecharge conditions for Jurassic, Cretaceous and Eocene aquifers. Radiocarbon activity in the aquifers varies widely between 0 and 94 pmc. After radiocarbon corrections the ages indicate both modern and old waters sometimes exceeding the limit for $^{14}C$ dating. The Fontes and Garnier model is best adapted to the specificity of the carbonate system. The content in stable isotopes of water is varying between 7.7‰ and 4.9‰ for $\delta^{18}O$ and 52.3‰ to 29.6‰ for $\delta^{2}H$. The wide ranges of stable isotopic values imply variable climatic conditions. A group of isotopically depleted samples was detected, indicating colder climatic conditions during the recharge. Radiocarbon ages calculation, together with isotopic signature, point out that the depletion in stable isotopic values fits the period between 20 and 15 ka B.P. and therefore indicate the Last Glacial Maximum (LGM). According to the correction model, the transition from Pleistocene to Holocene would occur between 15 and 12 ka B.P. Palaeohydrological data from the Northern Aquitaine Basin does not confirm a significant hiatus in the recharge history. The recharge conditions in South Europe seem to have occurred under discontinuous permafrost conditions as documented by many palaeoclimatological archives. This is in favour of an uninterrupted recharge of the confined aquifers of Northern Aquitaine Basin. Such information should be considered by modellers in their attempts to simulate the hydrogeological functioning of large confined aquifers on the very long time range.



## Introduction

During the last decades environmental isotope techniques have been commonly and largely used in the whole domain of water resources development and management. The stable isotopes oxygen-18 ($^{18}O$) and deuterium ($^{2}H$) as well as the radioactive isotope tritium ($^{3}H$) are rare components of the water molecule. Together with other isotopes, such as carbon-13 ($^{13}C$) and carbon-14 ($^{14}C$), they offer a broad range of possibilities for studying processes within the water cycle (Clark and Fritz, 1999; Mazor, 2004). This is the reason why these five isotopes are important tool not only in isotope hydrology, but also in studies related to atmospheric circulation and palaeoclimatic investigations (Araguas-Araguas et al., 2000). The relationship between climate and mean annual stable isotope contents of precipitation (Dangaard, 1964; Rozanski et al., 1992) provides significant insights into palaeoclimatic conditions. The isotopic and elemental composition of groundwater influenced by climate conditions at the time of recharge may serve as indicators of climate change (Chen et al., 2003). However, various processes occurring in aquifers tend to erase recorded climate fluctuations and samples may also be difficult to date accurately because they are either mixed or "contaminated" to some extent by natural subsurface processes. Therefore the isotopic content may either be diluted or enriched (Darling, 2004). Many studies concerning the palaeohydrology of confined reservoirs were carried out throughout the world (Heaton et al., 1986; Phillips et al., 1986; Kimmelmann et al., 1989; Stute and Deak, 1989; Ferronsky

* Corresponding author. Address: University of Bordeaux-1, GHYMAC Géosciences Hydrosciences, B18 Avenue des Facultés, 33405 Talence Cedex, France. Tel.: +33 5 40 00 88 41; fax: +33 5 40 00 31 13.
*E-mail addresses:* hanajirakova@post.cz (H. Jiráková), f.huneau@ghymac.u-bordeaux1.fr (F. Huneau), h.celle-jeanton@opgc.univ-bpclermont.fr (H. Celle-Jeanton), zbynek hrkal@vuv.cz (Z. Hrkal).

0022-1694/$ - see front matter © 2009 Elsevier B.V. All rights reserved.
doi:10.1016/j.jhydrol.2009.01.017

et al., 1991; Love et al., 1994; Huneau et al., 2001; Chen et al., 2003; Edmunds et al., 2006; Zhu et al., 2007). The different authors all pointed out the major importance of palaeorecharge processes to the aquifers and the great difficulty to clearly delineate the chronology and evolution of these mechanisms. This difficulty remains a point of weakness when hydrogeologists are trying to build models able to reproduce the very long term evolution of groundwater flow within such confined aquifers (Jost, 2005; Douez, 2007). They are often confronted to strong uncertainty about the continuous or semi-continuous recharge of aquifers especially during the transition from Pleistocene to Holocene. A few authors have demonstrated that continuous recharge processes have occurred during the last climatic transition and have proved the existence of groundwater of different ages within the aquifers (Zuber et al., 2004; Edmunds et al., 2006; Zhu et al., 2007). Zuber et al. (2004) carried out an extensive multi-tracer study on a limestone aquifer in Poland and identified four age groups of old waters: waters of the glacial-Holocene transition period, transition waters with admixtures of modern water, glacial waters, and glacial waters mixed with older water. Others propose the existence of a recharge gap period at the Pleistocene/Holocene interface. This absence of recharge has been attributed to the existence of more or less continuous permafrost conditions and/or to strong modification in the atmospheric humidity in the peripheral regions of the North European ice cap of the Pleistocene. Several studies in permafrost regions of northern Europe were carried out (Loosli et al., 2001; Beyerle et al. 1998) and they confirmed, that local groundwater recharge was prevented by overlying glaciers. Darling (2004) assumes that more general aridity led to the apparent absence of recharge in most areas for much of the late Devensian. Despite numerous research efforts, our knowledge about the precise timing of the Last Glacial Maximum (LGM) and its fingerprint on groundwater remains incomplete and in part controversial. The Northern Aquitaine area (Southwest France) provides an important dataset with valuable information on groundwater's geochemistry and isotopic composition of different aquifers and thus allows making a new assessment of the palaeohydrological features using environmental isotope techniques.

The Northern Aquitaine Basin is formed of thick sedimentary deposits forming major aquifers, which for more than a century, have been intensively exploited for fresh water, irrigation and geothermal supplies. Approximately 8000 irrigation sites were set up in the region with a majority (about 4000 boreholes) in the southern area of the Charente-Maritime (BRGM, 1999a). Nowadays, the agricultural activities in this region account for about 2/3 of the groundwater abstraction. As previously said the Aquitaine Basin is composed of several water-bearing layers which explain the abundance of groundwater resources. However, part of them are often situated in the very shallow horizons, they are extremely vulnerable to climatic conditions and to surface pollution mostly originating from agricultural activities. The vast majority of the most superficial aquifers are contaminated by nitrate with concentrations often above drinking water standards. There is also evidence that groundwater is being pumped more rapidly than it is being recharged. By 2008, 72% of the measured wells within the unconfined aquifers showed the lower groundwater level to be below the long term average (O.R.E., 2008).

Therefore to guarantee the quality and the volumes of the water pumped, a clear tendency to the development of news boreholes tapping deeper aquifers able to provide pristine waters in great volumes has appeared in the 1990s. But the quality, the origin and the residence time of groundwater may change as the overexploitation increases and as the volume diminishes. Deeper groundwater is now very much in demand and the question of the long term sustainability of such a management of the resource is appearing. This was one of the reasons why numerous fragmentary studies were carried out in the region in recent years. Their goal was to get detailed knowledge of the hydrogeological systems, water quality, water–rock interactions and groundwater average residence time.

These results have never been yet put together in order to define the basin-wide palaeorecharge conditions. The objectives of our work are to consider a selection of geochemical indicators coming from this large dataset to provide an overall understanding of the groundwater evolution in relation with the recharge history and to bring new insight into the palaeohydrogeological conditions in West Europe.

## Study area

### *General setting*

The Poitou-Charentes area occupies an area of 25,810 km$^2$ and extends essentially in the northern part of the Aquitaine Basin and is limited to the west by the oceanic slope of the Atlantic Ocean. As a rule, the climate of the whole Aquitaine Basin is oceanic humid with little differences in temperatures, high humidity and high precipitation amount during the year. Mean annual precipitations in Poitou-Charentes vary between 600 (NE) and 950 mm (SW: littoral of Charente-Maritime), heavy rain periods are frequent all over the year. The average temperature is about 11 °C (Méteo France, 2008) and the most intensive evapotranspiration occurs in summer, from May to September.

### *Geological setting*

From the geological point of view, the particularity of this zone lies in its location (Fig. 1). It is situated between two Hercynian massifs, the Armorican Massif and the Central Massif and two sedimentary basins, the Aquitaine Basin and the Paris Basin. The Northern Aquitaine Basin covers here the whole region going from the Gironde Estuary in the southwest towards the town of Poitiers in the northeast. The Aquitaine Basin and the Paris Basin are separated by the Palaeozoic geological vaulted structure called "Seuil du Poitou". The Aquitaine sedimentary complex has a wide geographical distribution, corresponding to the various physiographic features of deposit conditions. From a general point of view, the geological formations present a decreasing marine influence from west to east and from south to north, corresponding to the decreasing amplitude of the successive marine transgression (Larroque et al., 2008). The Armorican Massif in the northwest and the Central Massif in the east of the studied area are both Palaeozoic formations consisting mainly of granites, volcanic rocks, shales and gneisses. The basin is made up of the large Secondary and Tertiary sedimentation. The Triassic sediments are absent and the region is covered by a continuous succession of strata from the Jurassic period. This is the oldest evidence of sedimentary succession ever located indicating deep sea conditions. It is outcropping in the central part of the region along the "Seuil du Poitou". There are several isolated outcrops of the Lower Jurassic (Lias – Toarcian and Infra-Toarcian) in the central part at the level of the "Seuil du Poitou", but the great part of the area is formed by Middle (Dogger – Callovian and Infra-Callovian) and Upper Jurassic (Oxfordian) sediments. While the Lias and Middle Dogger sediments are formed mainly of pure carbonates, the Callovo-Oxfordian (Upper Dogger and Malm) deposits reveal higher clay content. The partial sea regression at the end of the Jurassic period sparked off the brackish sedimentation. We observe the outcrops of the younger formations, that is to say the Cretaceous sediments outcrop, towards the centre of Aquitaine Basin, namely south and north of

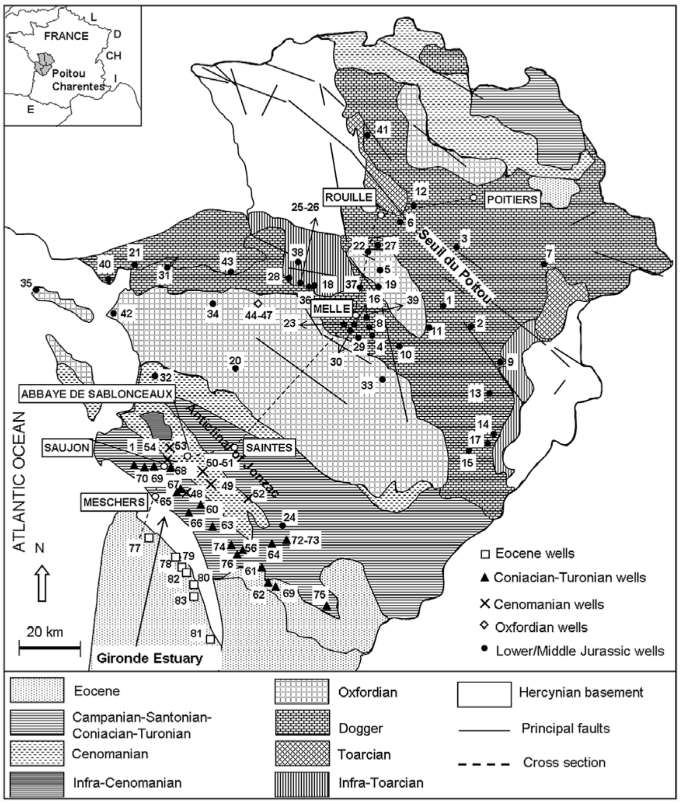


**Fig. 1.** Schematic geological map of the study area. Location of the wells and the cross-section.

Poitou-Charentes. They consist of limestones, sandstones and clays. The Lower Cretaceous occurrence is rare and little known. Several faults which were formed up to the Tertiary period intensely affected the Mesozoic sedimentary cover (Fig. 2), thereby creating the significant anticline structure of Jonzac in the NW–SE direction across the southern part of the investigated area. The Tertiary sedimentary cover, made of sands and gravel carbonates, is mostly developed in the south-eastern part of the studied area with discontinuous isolated outcrops.

*Hydrogeological setting*

There are several important water-bearing formations within the region. On the whole, the Aquitaine Basin is composed of a

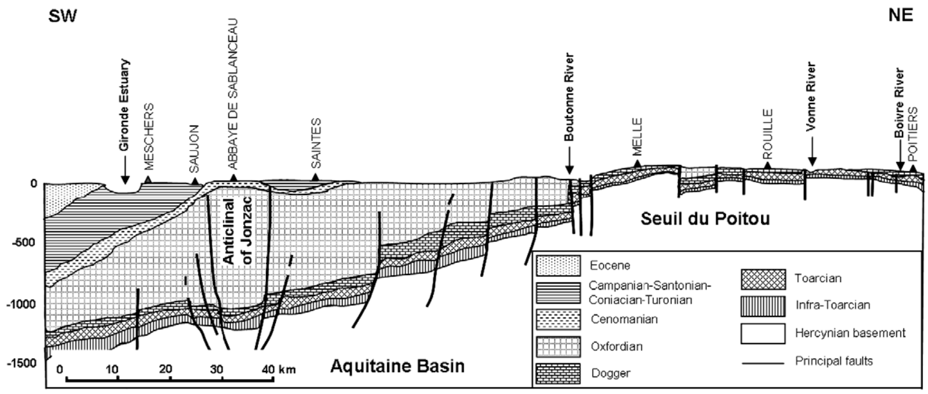


**Fig. 2.** Schematic geological cross-section SW–NE (BRGM, 1999a, modified).

multilayered aquifer system with an alternation of permeable and impermeable interstratified layers (André et al., 2002). Aquifers are mostly fed directly from precipitation and surface runoff in the peripheral outcrop areas of the basin. In depth, exchanges between aquifers like upward or downward leakage can also occur and are documented in many places in the Southern Aquitaine Basin (Blavoux et al., 1993; André et al., 2002). Very little information concerning the northern part of the basin is up to now available. The main aquifer systems are the Jurassic, the Upper Cretaceous and the Tertiary layers. Groundwater is widely pumped from most of these aquifers for drinking purposes, irrigation and geothermal supplies. The distribution of these aquifers in the Poitou-Charentes area is illustrated on the schematic cross-section in Fig. 2. Despite the complex hydrogeological setting, the hydrodynamic conditions are generally characterised by flow through the porous aquifers within the whole studied area. In order to get reliable interpretations about groundwater ages, the study has not been carried out in the karstified or fissured environments.

*Jurassic aquifers*

Lower and Middle Jurassic formations (Lias and Dogger) make up the deepest aquifers of the studied area. These aquifers are located between two major impermeable layers: the Hercynian basement and the clayey Callovian deposits (Mourier and Gabilly, 1985).

The clear distinction between Lias and Dogger, separated by the Toarcian marls, can be established only near the recharge zone. Further away from the recharge zone, only one aquifer should be considered (Mourier and Gabilly, 1985).

The Lias aquifer, generally called *Infra-Toarcian* in our study is formed of sands and quartzite sandstones and becomes more carbonated towards the top where it changes into dolomitic limestones. Sands give the intergranular porosity to the aquifer, while in the carbonated levels fissure porosity is also registered. The Infra-Toarcian groundwater is mostly confined but the thin layers of Toarcian marls and the regional geological organisation facilitate the communication between the overlying sediments, either by the faults or by leakage. The reduced outcrop suggests that the annual direct recharge of the aquifer by rainfall is probably low (Le Gal La Salle et al., 1996). In spite of rare piezometric data in the Lias aquifer, the general flow direction could be specified NE–SW in the northern part and E–W in the southern part of the region. This aquifer is supposed to be recharged by precipitation in the outcrop zones and/or by Dogger contribution through the main faults. The transmissivity varies in the range of $1 \times 10^{-2}$ to $2 \times 10^{-5}$ $m^2/s$ and the storage coefficient from $5 \times 10^{-4}$ to $2 \times 10^{-5}$ (BRGM, 1996). The thickness generally increases from NE to SW.

The overlying *Dogger aquifer* appears as a huge limestone outcropping area in the centre of the study area as well as in the northern part as isolated occurrences. The groundwater level is unconfined in the outcrop areas. Towards the south, this aquifer reaches a few thousands meters below the surface (*Infra-Callovian*). The deep Infra-Callovian is exploited for geothermal purposes (Jonzac, Chantemerle, La Rochelle, Rochefort). The exact flow direction of this aquifer is poorly known. Nevertheless, the measurement realised in 1981 indicated a general NE–SW flow (BRGM, 1996). The productivity is very variable and closely related to the fracture density. The aquifer communicates by fissures and faults with the overlying and underlying formations which together with precipitation contribute to the recharge processes. Some of the wells indicated flow rates higher than 100 $m^3/h$.

*The Upper Jurassic layers* constitute the *Oxfordian aquifer*, by far the most exploited for irrigation. Nevertheless, some wells serve also for the drinking water supply. Due to its position close to the surface, it reflects the interactions with surface water. This aquifer with fissured porosity is composed of alternating limestone and marl layers. Only the very first 25 m from the surface reveal high productivity, because impermeable beds can occur beneath this level. The flow direction is inherited from the relief and the isohypses correspond to the topographical contours. The surface proximity makes thus the aquifer very sensitive to climatic variations and the principle water input is made from meteoric waters. The transmissivity coefficient varies between $4 \times 10^{-3}$ and $7 \times 10^{-2}$ $m^2/s$ (BRGM, 1996).

*Cretaceous aquifers*

The *Cenomanian deposits* consist of bioclastic limestones and sand beds, which form a foremost aquifer. Thus, immense heterogeneity resulting from the lithologic anisotropy has been registered. The multilayered Cretaceous formation constitutes the main resource for fresh water and agricultural supply in the south of the Poitou-Charente area. The Cenomanian aquifer being confined and unconfined in the region appears to be very variable in term of petrography and facies. Beside, it is affected by the folded structure of the anticlinal of Jonzac, in which central part it reaches the surface. The Cenomanian is usually sandy and becomes more carbonated towards its top part. The facies succession differs according to the sector and the multilayered system reaches the thickness of 50–70 m close to the Atlantic coast. Very low transmissivity was calculated ($10^{-4}$ $m^2/s$) in the Cognac region (BRGM, 2006). At the top a marly layer constitutes an overlying confining bed which assures sufficient hydrogeological isolation.

The Coniacian–Turonian aquifer is one of the most exploited in the region. This multilayered aquifer located in the southwestern part of the region, along the Gironde estuary is both confined and unconfined, consistently with its position in the local structure of the anticlinal of Jonzac and synclinal of Saintes. Hence, it is recharged not only from the outcrop zone but also by leakage in its confined part. Moving away from the outcrop zone beneath the Tertiary cover, the fissures and karstic channels become rare. Naturally, the flow rates are very unstable in the fissured environment and sometimes become very significant. The Lower Turonian is composed of marly limestones and forms the impermeable base of the aquifer. The overlying bed is gradually enriched in carbonates and fine sand. The Upper Turonian is considered to be the main aquifer with a coefficient of transmissivity in the order of $10^{-2}$ $m^2/s$. The permeable succession of Turonian passes to clayey limestones at the base of Santonian (BRGM, 2006). This changes the hydraulic parameters, and, as a consequence, coefficient of transmissivity might decrease down to the order of $10^{-5}$ $m^2/s$. The storage coefficient ranges from $10^{-3}$ to $7 \times 10^{-2}$ (BRGM, 2002a).

*Eocene aquifer*

The *Eocene* aquifer, situated mostly in the southernmost part of the studied area (close to the Gironde estuary) and largely exploited towards the south in the Bordeaux region, was developed in fluvial sand and gravels as a multilayered formation covered by clayey deposits. The quality of Eocene groundwater is very variable. Although these levels might be locally quite productive, the overall productivity is low and very susceptible to seasonal fluctuations.

## Methods and data treatment

*Constitution of dataset*

Principle idea of this work was to collect and synthesized data from different studies already carried out in the North Aquitaine region. Origin of the dataset is stated in Table 1. All treated data concern the Poitou-Charentes aquifers which have been intensely

**Table 1**
Localisation of wells in Lambert II geographical system, tapped aquifer, type of aquifer and the reference study.

| No. | X | Y | Aquifer | Aquifer type | References | No. | X | Y | Aquifer | Aquifer type | References |
|---|---|---|---|---|---|---|---|---|---|---|---|
| 1 | 441,900 | 2,136,290 | IT | C | a | 43 | 368,700 | 2,149,520 | D | C | b,c |
| 2 | 449,150 | 2,129,260 | IT | C | a | 44 | 381,000 | 2,142,500 | Ox | U | b,c |
| 3 | 443,830 | 2,158,890 | IT | C | a | 45 | 381,000 | 2,142,500 | Ox | U | b,c |
| 4 | 414,500 | 2,126,650 | IT | C | a | 46 | 381,000 | 2,142,500 | Ox | U | b,c |
| 5 | 417,890 | 2,150,200 | IT | C | a | 47 | 381,000 | 2,142,500 | Ox | U | b,c |
| 6 | 424,600 | 2,170,070 | IT | C | a | 48 | 353,000 | 2,068,000 | C + IC | C | d |
| 7 | 473,429 | 2,153,482 | IT | C | a | 49 | 362,340 | 2,067,880 | C + IC | C | d |
| 8 | 413,847 | 2,129,109 | IT | C | a | 50 | 359,065 | 2,074,450 | C | C | d |
| 9 | 460,960 | 2,117,570 | IT | C | a | 51 | 359,060 | 2,074,400 | C | C | d |
| 10 | 425,300 | 2,122,400 | IT | C | a | 52 | 374,060 | 2,066,590 | C | C | d |
| 11 | 435,250 | 2,127,140 | IT | C | a | 53 | 348,975 | 2,084,315 | C | C | d |
| 12 | 428,800 | 2,173,800 | IT | C | a | 54 | 346,125 | 2,080,200 | C | C | d |
| 13 | 456,120 | 2,106,050 | IT | C | a | 55 | – | – | IC | C | e,f |
| 14 | 458,200 | 2,094,850 | IT | C | a | 56 | – | – | C | C | e,f |
| 15 | 448,425 | 2,087,160 | IT | C | a | 57 | – | – | IC | C | e,f |
| 16 | 409,200 | 2,129,900 | IT | C | a | 58 | 373,610 | 2,046,950 | CoT | C | d |
| 17 | 455,660 | 2,091,310 | IT | C | a | 59 | 384,560 | 2,034,890 | CoT | C | d |
| 18 | 394,860 | 2,144,150 | IT | C | b,c | 60 | 358,900 | 2,063,150 | CoT | U | d |
| 19 | 416,000 | 2,143,800 | IT | C | b,c | 61 | 379,439 | 20,414,605 | CoT | C | d |
| 20 | 370,160 | 2,112,000 | IT | C | b,c | 62 | 381,813 | 2,035,715 | CoT | C | d |
| 21 | 334,700 | 2,150,525 | IT | C | b,c | 63 | 362,700 | 2,052,100 | CoT | U | d |
| 22 | 413,510 | 2,156,780 | IT | C | b,c | 64 | 381,700 | 2,048,833 | CoT | C | d |
| 23 | 406,050 | 2,129,170 | IT | C | b,c | 65 | 351,000 | 2,066,000 | CoT | C | g |
| 24 | 383,712 | 2,051,815 | IT | C | b,c | 66 | 352,450 | 2,062,000 | CoT | C | g |
| 25 | 391,380 | 2,144,860 | IT | C | b,c | 67 | 352,010 | 2,067,890 | CoT | C | g |
| 26 | 391,380 | 2,144,860 | IT | C | b,c | 68 | 348,000 | 2,077,000 | CoT | C | g |
| 27 | 417,390 | 2,157,740 | IT | C | b,c | 69 | 343,000 | 2,076,085 | CoT | C | g |
| 28 | 388,228 | 2,146,710 | IT | C | b,c | 70 | 341,490 | 2,075,850 | CoT | C | g |
| 29 | 409,900 | 2,127,420 | IT | C | b,c | 71 | 337,930 | 2,076,000 | CoT | C | g |
| 30 | 408,230 | 2,128,480 | IT | C | b,c | 72 | 389,400 | 2,049,700 | CoT | C | e,f |
| 31 | 346,520 | 2,150,140 | IT | C | b,c | 73 | 389,375 | 2,049,700 | CoT | C | e,f |
| 32 | 344,400 | 2,110,090 | IT | C | b,c | 74 | 369,000 | 2,048,000 | CoT | C | e,f |
| 33 | 418,250 | 2,107,110 | IT | C | b,c | 75 | 400,000 | 2,027,000 | CoT | C | e,f |
| 34 | 364,930 | 2,137,670 | IT | C | b,c | 76 | 371,000 | 2,046,000 | CoT | C | e,f |
| 35 | 302,430 | 2,142,720 | D + IT | C | b,c | 77 | 351,500 | 2,044,000 | E | C | h,i |
| 36 | 395,180 | 2,144,500 | D + IT | C | b,c | 78 | 352,200 | 2,044,000 | E | C | h,i |
| 37 | 411,000 | 2,144,000 | D + IT | C | b,c | 79 | 352,500 | 2,040,500 | E | C | h,i |
| 38 | 391,000 | 2,153,000 | D + IT | C | b,c | 80 | 356,200 | 2,034,000 | E | C | h,i |
| 39 | 413,000 | 2,131,500 | D + IT | C | b,c | 81 | 361,500 | 2,016,100 | E | C | h,i |
| 40 | 326,600 | 2,147,800 | D + IT | C | d | 82 | 354,000 | 2,038,000 | E | C | h,i |
| 41 | 413,115 | 2,199,880 | D | C | a | 83 | 356,500 | 2,030,000 | E | C | h,i |
| 42 | 330,650 | 2,135,600 | D | C | b,c | | | | | | |

*Aquifer:* IT – Infra-Toarcian, D – Dogger, Ox – Oxfordian, C – Cenomanian, IC – Infra-Cenomanian, CoT – Coniacian–Turonian.
*Aquifer type:* C – confined, U – unconfined.
*References:* (a) BRGM (2002b), (b) Le Gal La Salle et al. (1996), (c) Savoye (1993), (d) Marlin (1996), (e) Mouragues (2000), (f) BRGM (2001), (g) Marlin et al. (1998), (h) BRGM (1999b) and (i) BRGM (2000).

explored but always with very fragmentary approaches from 1991 to 2005. In general, distribution of experimental wells is highly irregular (Fig. 1). The highest density of data appears on the south – close to the Gironde Estuary – and approximately in the central part of Poitou-Charentes. Seventy-five groundwater samples including Jurassic, Cretaceous and Eocene aquifers were analysed for stable isotopes, 59 samples for $^{14}C$ (including $^{13}C$ measurements). Table 1 introduces the entire data set with number of wells, their coordinates (Lambert II system), reached aquifer, and the reference to the original study. Some difficulties were encountered while determining the Jurassic aquifers. The same boreholes corresponding to Infra-Callovian in Le Gal La Salle et al. (1996) are considered as Infra-Toarcian samples in BRGM (2002b). In this study we follow the latter approach and so we deal with the Infra-Toarcian. However, the origin of some samples is clearly defined either as Dogger or mixture of Dogger and Infra-Toarcian which is justified by the well developed communication between these aquifers (Mourier and Gabilly, 1985).

*Analytical tools*

The $^{18}O$ and $^{2}H$ measurements were used to assess the recharge conditions, while $^{13}C$ and $^{14}C$ helped to estimate the residence time in the underground. The stable isotopic composition ($^{18}O$, $^{2}H$ and $^{13}C$) is reported in standard δ notation in which $\delta = (R_{sample}/R_{standard} - 1) \times 1000$, where $R_{sample}$ and $R_{standard}$ represent the ratio of heavy to light isotopes of the sample and standard. The analysis of radiocarbon is reported as pmc (percent of modern carbon). The analytical errors are usually in the range of 0.1–0.2‰ for $\delta^{18}O$, 0.8–2‰ for $\delta^{2}H$, 0.1–1.7‰ for $^{14}C$ and 0.1–0.2‰ for $^{13}C$. The interpretation of radiocarbon dating is affected by mixing with waters of different origin and especially mixing between deep and surface waters. That is why we used also the geochemistry of groundwaters to identify such influences and to provide reliable dating. The main physico-chemical parameters together with isotopic composition are listed in Table 2. Twenty more chemical analyses were randomly chosen from the extensive investigations on Cretaceous aquifer (BRGM, 2005) in order to plot them into a Piper diagram. This allows us to get better idea about the aquifer geochemistry and to determine the sea water intrusion into some wells or the nitrate contamination ("Modern water indicators"). Apart from this, the information on modern water input is in some locations provided by the $^{3}H$ measurement ("Modern water indicators"). To underline the differences between actual and palaeorecharge conditions we discuss the stable isotopic content of groundwaters with respect to modern isotopic content ("Stable

**Table 2**
Physico-chemical parameters, isotopic content of samples, $P_{CO_2}$, degree of openness with respect to $CO_2$ (open (O), close (C) or intermediate (I) system), saturation indexes, initial $^{14}C$ activity ($A_0$) and radiocarbon ages according to the F&G model and error.

| No. | Depth (m) | T (°C) | pH | Alcalinity (meq/L) | Conductivity (µS/cm) | $NO_3$ (mg/l) | $^3H$ (TU) | $\delta^{18}O$ ‰ vs. SMOW | $\delta^2H$ ‰ vs. SMOW | $A^{14}C$ (pmc) | $\delta^{13}C$ (‰ vs. PDB) | $\delta^{13}$ Ceq (‰ vs. PDB) | $\log P_{CO_2}$ | Openness of the system | Saturation indexes: Calcite | Dolomite | Gypsum | Anhydrite | Age: $A_0$ $^{14}C$ | F&G (years BP) | Error |
|---|---|---|---|---|---|---|---|---|---|---|---|---|---|---|---|---|---|---|---|---|---|
| 1 | 152 | 15.5 | 7.8 | 3.60 | 496 | <0.1 | <1 | −7.4 ± 0.1 | −47.0 ± 0.8 | 4.9 ± 0.2 | −9.6 ± 0.1 | −18.1 | −2.44 | I | 0.0 | −0.6 | −2.6 | −2.9 | 45.6 | 18,400 | 430 |
| 2 | 138 | 15.9 | 7.7 | 3.68 | 474 | <0.1 | <1 | −7.3 ± 0.1 | −46.1 ± 0.8 | 5.9 ± 0.4 | −11.3 ± 0.1 | −19.7 | −2.38 | O | 0.0 | −0.5 | −2.6 | −2.8 | 54.7 | 18,400 | 640 |
| 3 | 46 | 13.5 | 7.5 | 4.84 | 637 | <0.1 | <1 | −7.4 ± 0.1 | −48.1 ± 0.8 | 7.6 ± 0.1 | −8.8 ± 0.1 | −17.2 | −2.11 | I | 0.0 | −0.8 | −2.3 | −2.5 | 41.7 | 14,100 | 210 |
| 4 | 111 | 14.4 | 7.2 | 4.30 | 464 | 12.1 | 4 ± 1 | −6.4 ± 0.1 | −38.0 ± 0.8 | – | – | – | −1.80 | – | 0.0 | −1.3 | −2.5 | −2.7 | – | – | – |
| 5 | 114 | 15.0 | 7.0 | – | 535 | 4.0 | 2 ± 1 | −6.1 ± 0.1 | −38.1 ± 0.8 | – | – | – | −1.56 | – | −0.1 | −1.2 | −2.2 | −2.4 | – | – | – |
| 6 | 74 | 14.1 | 7.4 | 5.59 | 700 | <0.1 | <1 | −6.7 ± 0.1 | −41.3 ± 0.8 | 20.3 ± 0.2 | −10.4 ± 0.1 | −18.5 | −1.95 | I | 0.2 | −0.5 | −1.9 | −2.2 | 49.4 | 7400 | 170 |
| 7 | 45 | 15.5 | 7.7 | 4.16 | 839 | <0.1 | <1 | −7.6 ± 0.1 | −48.5 ± 0.8 | 16.7 ± 0.3 | −8.9 ± 0.1 | −17.4 | −2.36 | I | 0.3 | −0.2 | −2.0 | −2.2 | 42.2 | 7700 | 250 |
| 8 | 80 | 14.4 | 7.8 | 4.36 | 457 | 15.2 | 4 ± 1 | −6.4 ± 0.1 | −38.0 ± 0.8 | – | – | – | −2.42 | – | 0.5 | −0.1 | −2.5 | −2.7 | – | – | – |
| 9 | 43 | 12.9 | 7.5 | 5.21 | 581 | 3.6 | 4 ± 1 | −6.2 ± 0.1 | −38.2 ± 0.8 | – | – | – | −2.08 | – | 0.2 | −0.2 | −1.6 | −1.9 | – | – | – |
| 10 | 124 | 12.4 | 7.0 | 4.83 | 510 | 41.3 | 5 ± 2 | −6.5 ± 0.1 | −40.4 ± 0.8 | – | – | – | −1.59 | – | −0.1 | −2.0 | −2.3 | −2.5 | – | – | – |
| 11 | 129 | 13.7 | 7.0 | 6.17 | 541 | <0.1 | <1 | −6.5 ± 0.1 | −39.1 ± 0.8 | 25.6 ± 0.3 | −8.9 ± 0.1 | −15.9 | −1.51 | C | −0.1 | −1.1 | −2.2 | −2.5 | 42.1 | 4100 | 200 |
| 12 | 65 | 14.3 | 7.5 | 5.20 | 628 | <0.1 | <1 | −7.2 ± 0.1 | −46.5 ± 0.8 | 16.3 ± 0.3 | −9.5 ± 0.1 | −17.8 | −2.07 | I | 0.2 | −0.5 | −2.0 | −2.2 | 45.1 | 8400 | 240 |
| 13 | 76 | 13.5 | 7.9 | 3.71 | 382 | 18.8 | 4 ± 1 | −6.4 ± 0.1 | −39.5 ± 0.8 | – | – | – | −2.56 | – | 0.4 | −0.1 | −2.5 | −2.8 | – | – | – |
| 14 | – | 13.7 | 7.1 | 1.55 | 251 | 20.7 | 6 ± 2 | −6.7 ± 0.1 | −40.6 ± 0.8 | – | – | – | −2.16 | – | −0.8 | −2.9 | −2.7 | −3.0 | – | – | – |
| 15 | 355 | 15.3 | 7.4 | – | 398 | 19.9 | 4 ± 1 | −6.2 ± 0.1 | −39.0 ± 0.8 | – | – | – | −2.12 | – | 0.1 | −1.4 | −2.3 | −2.6 | – | – | – |
| 16 | 62 | 12.9 | 7.7 | 5.06 | 458 | <0.1 | 2 ± 1 | −6.3 ± 0.1 | −37.4 ± 0.8 | 25.9 ± 0.2 | −11.3 ± 0.2 | −20.0 | −2.26 | O | 0.4 | 0.0 | −2.1 | −2.4 | 54.7 | 6200 | 140 |
| 17 | 80 | 12.4 | 7.8 | 3.24 | 330 | <0.1 | <1 | −6.2 ± 0.1 | −38.4 ± 0.8 | 19.9 ± 0.2 | −9.0 ± 0.1 | −17.8 | −2.51 | I | 0.2 | −0.5 | −2.2 | −2.4 | 42.7 | 6300 | 180 |
| 18 | 110 | 15.6 | 7.2 | 5.80 | – | <0.5 | – | −5.7 ± 0.2 | −36.0 ± 2.0 | 37.4 ± 0.3 | −8.7 ± 0.2 | −16.3 | −1.75 | I | 0.1 | −0.6 | −1.7 | −2.0 | 41.1 | 800 | 170 |
| 19 | 65 | 14.2 | 7.5 | 4.32 | 433 | 7.4 | 4 ± 1 | −6.4 ± 0.2 | −37.9 ± 2.0 | 35.4 ± 1.6 | −10.2 ± 0.2 | −18.4 | −2.10 | I | 0.0 | −0.7 | −2.3 | −2.5 | 48.3 | 2600 | 460 |
| 20 | 763 | 32.0 | 6.8 | 3.54 | – | <0.5 | – | −6.1 ± 0.2 | −39.8 ± 2.0 | 0.0 ± 1.2 | −3.6 ± 0.2 | −8.8 | −1.52 | C | 0.3 | −0.1 | 0.4 | 0.2 | 14.2 | >30,000 | – |
| 21 | 236 | 19.4 | 7.0 | 3.98 | – | <0.5 | – | −5.9 ± 0.2 | −35.8 ± 2.0 | 0.6 ± 0.6 | −3.1 ± 0.2 | −9.8 | −1.75 | C | 0.3 | −0.2 | 0.3 | 0.1 | – | – | – |
| 22 | 137 | 14.2 | 7.6 | 3.21 | – | <0.5 | – | −6.1 ± 0.2 | −41.6 ± 2.0 | 2.4 ± 0.6 | −9.0 ± 0.2 | −17.5 | −2.38 | I | −0.1 | −1.0 | −2.3 | −2.6 | 42.7 | 23,800 | 2160 |
| 23 | 137 | 16.9 | 7.3 | 4.92 | 568 | <0.5 | 4 ± 1 | −5.8 ± 0.2 | −39.6 ± 2.0 | 25.9 ± 0.3 | −8.6 ± 0.2 | −16.3 | −1.89 | I | 0.0 | −0.7 | −2.2 | −2.4 | 40.6 | 3700 | 200 |
| 24 | 1850 | 64.1 | 6.9 | 4.60 | 10,020 | <0.5 | – | −5.3 ± 0.2 | −34.8 ± 2.0 | 0.9 ± 0.6 | −5.4 ± 0.2 | −8.6 | −1.25 | C | 0.9 | 1.1 | 0.3 | 0.4 | 20.9 | >30,000 | – |
| 25 | 113 | 15.3 | 7.0 | 5.79 | – | <0.5 | – | −5.3 ± 0.2 | −37.6 ± 2.0 | 52.2 ± 0.6 | −11.4 ± 0.2 | −18.4 | −1.56 | I | −0.2 | −1.2 | −1.8 | −2.1 | 54.2 | 300 | 170 |
| 26 | 113 | 15.4 | 7.0 | 6.28 | – | <0.5 | – | −5.8 ± 0.2 | −35.6 ± 2.0 | 58.9 ± 0.5 | −11.1 ± 0.2 | −18.0 | −1.49 | I | −0.1 | −1.1 | −1.7 | −1.9 | 52.8 | Modern | 150 |
| 27 | 117 | 15.0 | 7.4 | 3.60 | 365 | <0.5 | <1 | −6.3 ± 0.2 | −38.3 ± 2.0 | 12.2 ± 0.4 | −8.8 ± 0.2 | −16.8 | −2.12 | I | −0.2 | −1.2 | −2.4 | −2.6 | 41.5 | 10,100 | 370 |
| 28 | 100 | 15.0 | 7.2 | 5.32 | – | 0.6 | – | −6.9 ± 0.2 | −40.0 ± 2.0 | 28.8 ± 0.6 | −8.2 ± 0.2 | −15.8 | −1.77 | C | 0.1 | −0.6 | −1.0 | −1.3 | 38.6 | 2400 | 280 |
| 29 | 136 | 16.2 | 7.3 | 5.16 | – | 39.5 | – | −5.8 ± 0.2 | −38.0 ± 2.0 | 22.2 ± 0.3 | −9.1 ± 0.2 | −16.7 | −1.82 | I | 0.2 | −1.1 | −2.0 | −2.2 | 42.8 | 5400 | 210 |
| 30 | 98 | 15.4 | 6.8 | 4.92 | – | <0.5 | – | −6.1 ± 0.2 | −40.1 ± 2.0 | 24.4 ± 0.5 | −9.1 ± 0.2 | −15.0 | −1.38 | C | −0.6 | −1.9 | −2.1 | −2.4 | 42.6 | 4600 | 270 |
| 31 | 197 | 14.3 | 7.0 | 4.16 | – | 1.0 | – | −6.1 ± 0.2 | −37.4 ± 2.0 | 3.5 ± 1.2 | −2.9 ± 0.2 | −10.0 | −1.76 | C | 0.2 | −0.4 | 0.2 | 0.0 | 13.2 | 10,900 | 3150 |
| 32 | 854 | 42.6 | 7.1 | 3.48 | 6850 | <0.5 | – | −5.6 ± 0.2 | −36.4 ± 2.0 | 0.7 ± 0.6 | −4.7 ± 0.2 | −9.8 | −1.67 | C | 0.6 | 0.6 | 0.4 | 0.3 | – | – | – |
| 33 | 480 | 30.3 | 7.5 | 3.85 | 900 | <0.5 | <1 | −7.6 ± 0.1 | −48.6 ± 0.8 | 3.7 ± 0.2 | −4.4 ± 0.2 | −10.8 | −2.14 | C | 0.4 | 0.3 | −1.2 | −1.4 | 19.0 | 13,500 | 660 |
| 34 | – | 21.5 | 6.9 | 4.00 | – | <0.5 | – | −6.4 ± 0.2 | −40.0 ± 2.0 | 1.1 ± 0.5 | −3.2 ± 0.2 | −9.4 | −1.60 | C | 0.2 | −0.2 | 0.3 | 0.0 | 13.6 | 20,800 | 4060 |
| 35 | 538 | 32.3 | 7.0 | 4.16 | – | <0.5 | – | −4.9 ± 0.2 | −29.6 ± 2.0 | 0.4 ± 0.3 | −5.4 ± 0.2 | −11.1 | −1.62 | C | 0.5 | 0.4 | 0.4 | 0.2 | – | – | – |
| 36 | 90 | 14.2 | 7.3 | 5.02 | – | 42.5 | – | −5.6 ± 0.2 | −39.0 ± 2.0 | 64.7 ± 1.4 | −11.7 ± 0.2 | −19.4 | −1.84 | O | 0.1 | −1.1 | −2.0 | −2.2 | 55.5 | Modern | 250 |
| 37 | 175 | 19.5 | 7.5 | 4.70 | – | <0.5 | – | −7.1 ± 0.2 | −46.7 ± 2.0 | 1.7 ± 0.3 | −4.1 ± 0.2 | −11.9 | −2.11 | C | 0.4 | 0.3 | −0.8 | −1.0 | 18.5 | 19,700 | 1680 |
| 38 | 64 | 14.8 | 7.3 | 5.32 | – | 1.2 | – | −5.8 ± 0.2 | −35.6 ± 2.0 | 19.7 ± 0.6 | −9.2 ± 0.2 | −16.9 | −1.81 | I | 0.0 | −0.8 | −2.2 | −2.4 | 43.4 | 6500 | 350 |
| 39 | – | 14.0 | 7.4 | 5.00 | – | <0.5 | – | −6.4 ± 0.2 | −36.7 ± 2.0 | 25.9 ± 0.6 | −8.8 ± 0.2 | −17.0 | −1.99 | I | 0.0 | −0.6 | −2.2 | −2.5 | 41.7 | 3900 | 290 |

| | | | | | | | | | | | | | | | | | | | | | |
|---|---|---|---|---|---|---|---|---|---|---|---|---|---|---|---|---|---|---|---|---|---|
| 40 | – | 17.1 | 6.9 | 6.90 | 7400 | – | – | −5.6 ± 0.2 | −38.0 ± 2.0 | 2.8 ± 0.3 | −5.6 ± 0.2 | −12.0 | – | C | – | – | – | – | – | – | – |
| 41 | 15 | 12.9 | 7.1 | 5.73 | 667 | 44.5 | 4 ± 1 | −6.4 ± 0.2 | −40.0 ± 0.8 | – | – | – | −1.61 | – | 0.1 | −1.6 | −1.8 | −2.1 | – | – | – |
| 42 | 319 | 28.8 | 6.9 | 4.40 | 7810 | <0.5 | – | −5.5 ± 0.2 | −32.7 ± 2.0 | 1.2 ± 0.5 | −2.6 ± 0.2 | −8.4 | −1.56 | C | 0.4 | 0.2 | 0.3 | 0.1 | – | – | – |
| 43 | 144 | 16.9 | 7.2 | 5.00 | – | <0.5 | – | −6.9 ± 0.2 | −43.5 ± 2.0 | 2.6 ± 0.6 | −1.8 ± 0.2 | −9.3 | −1.81 | C | 0.1 | 0.0 | −0.4 | −0.7 | 7.5 | 8800 | 2460 |
| 44 | 35 | 12.1 | 7.0 | 5.86 | – | 27.3 | – | −5.8 ± 0.2 | −36.0 ± 2.0 | 74.3 ± 1.7 | −12.0 ± 0.2 | −19.1 | −1.54 | O | −0.1 | −1.4 | −1.8 | −2.0 | 57.3 | Modern | 260 |
| 45 | 17 | 12.1 | 7.1 | 5.46 | – | 30.4 | – | −5.8 ± 0.2 | −36.0 ± 2.0 | 83.9 ± 0.6 | −12.4 ± 0.2 | −19.8 | −1.67 | O | 0.0 | −1.5 | −1.7 | −2.0 | 58.8 | Modern | 130 |
| 46 | 16 | 12.7 | 7.2 | 5.32 | – | 37.2 | – | −5.8 ± 0.2 | −35.0 ± 2.0 | 82.6 ± 0.7 | −13.2 ± 0.2 | −20.9 | −1.77 | O | 0.1 | −1.3 | −1.8 | −2.1 | 67.0 | Modern | 130 |
| 47 | 15 | 12.0 | 7.0 | 5.14 | – | 78.7 | – | −5.6 ± 0.2 | −34.8 ± 2.0 | 93.8 ± 2.2 | −14.0 ± 0.2 | −21.1 | −1.59 | O | 0.0 | −2.0 | −1.9 | −2.1 | 71.5 | Modern | 250 |
| 48 | – | 15.1 | 6.7 | 2.62 | 1280 | 0 | – | −5.9 ± 0.2 | −38.3 ± 2.0 | 14.5 ± 0.2 | −11.3 ± 0.2 | −16.9 | – | I | – | – | – | – | 53.5 | 10,800 | 190 |
| 49 | 123 | 15.0 | 7.3 | 4.30 | 618 | 0 | – | −6.6 ± 0.2 | −44.1 ± 2.0 | 13.2 ± 0.3 | −11.3±0.2 | −19.1 | – | O | – | – | – | – | 53.8 | 11,600 | 260 |
| 50 | 168 | 13.7 | 6.9 | 6.31 | 785 | – | <1.7 | −6.3 ± 0.2 | −39.4 ± 2.0 | 64.2 ± 0.5 | −12.6 ± 0.2 | −19.3 | – | O | – | – | – | – | 60.0 | Modern | 130 |
| 51 | 129 | 14.7 | 6.9 | 6.55 | 775 | – | <1.4 | −6.2 ± 0.2 | −38.4 ± 2.0 | 56.7 ± 0.4 | −13.7 ± 0.2 | −20.4 | – | O | – | – | – | – | 67.8 | 1500 | 120 |
| 52 | 79 | 14.9 | 7.4 | 3.80 | 520 | 0 | – | −7.7 ± 0.2 | −52.3 ± 2.0 | 4.5 ± 0.2 | −10.7 ± 0.2 | −18.7 | – | I | – | – | – | – | 50.9 | 20,000 | 450 |
| 53 | 163 | 15.5 | 7.0 | 6.18 | 787 | – | – | −6.3 ± 0.2 | −38.6 ± 2.0 | 27.0 ± 0.3 | −12.6 ± 0.2 | −19.6 | – | O | – | – | – | – | 60.3 | 6600 | 160 |
| 54 | 250 | 17.8 | 6.9 | 4.58 | 770 | 40.0 | – | −6.6 ± 0.2 | −42.4 ± 2.0 | 6.5 ± 0.3 | −10.4 ± 0.2 | −16.8 | – | I | – | – | – | – | 49.2 | 16,700 | 470 |
| 55 | 300 | 17.7 | 7.0 | 6.15 | – | – | 5 ± 1 | – | – | – | −9.2 ± 0.2 | – | – | – | – | – | – | – | – | – | – |
| 56 | 397 | 21.6 | 7.0 | 5.46 | – | – | 6 ± 1 | – | – | – | −12.4 ± 0.2 | – | – | – | – | – | – | – | – | – | – |
| 57 | 47 | 13.0 | 7.3 | 4.67 | – | – | 5 ± 1 | – | – | – | −12.4 ± 0.2 | – | – | – | – | – | – | – | – | – | – |
| 58 | 318 | 21.0 | 7.0 | 5.88 | 739 | – | – | −5.9 ± 0.2 | −34.5 ± 2.0 | 42.8 ± 0.4 | −13.3 ± 0.2 | −20.2 | – | O | – | – | – | – | 66.2 | 3600 | 140 |
| 59 | 468 | 26.2 | 7.0 | 4.56 | 635 | 0 | – | −6.7 ± 0.2 | −41.5 ± 2.0 | 1.5 ± 0.2 | −7.9 ± 0.2 | −14.5 | – | C | – | – | – | – | 36.8 | 26,500 | 1210 |
| 60 | 19 | 13.7 | 7.2 | 5.00 | 679 | – | – | −6.2 ± 0.2 | −40.3 ± 2.0 | 73.3 ± 0.4 | −13.3 ± 0.2 | −21.4 | – | O | – | – | – | – | 69.3 | Modern | 100 |
| 61 | 80 | 13.8 | 7.1 | 5.65 | 709 | 0 | – | −6.0 ± 0.2 | −38.3 ± 2.0 | 11.6 ± 0.3 | −10.4 ± 0.2 | −17.0 | – | I | – | – | – | – | 49.2 | 11,900 | 300 |
| 62 | 268 | 15.8 | 7.5 | 5.72 | 583 | – | – | −7.0 ± 0.2 | −44.0 ± 2.0 | 0.8 ± 0.2 | −7.7 ± 0.2 | −13.9 | – | C | – | – | – | – | 35.6 | >30,000 | 2180 |
| 63 | 5 | 13.8 | 7.1 | 5.23 | 622 | – | – | −6.1 ± 0.2 | −39.3 ± 2.0 | 66.1 ± 0.4 | −13.3 ± 0.2 | −20.9 | – | O | – | – | – | – | 67.7 | 200 | 110 |
| 64 | 100 | 15.8 | 7.2 | 5.81 | 683 | 17.5 | – | −6.0 ± 0.2 | −38.4 ± 2.0 | 61.8 ± 0.5 | −13.7 ± 0.2 | −21.2 | – | O | – | – | – | – | 70.6 | 1100 | 130 |
| 65 | 75 | 15.7 | 7.5 | 4.37 | 764 | <0.5 | – | −5.1 ± 0.2 | −38.6 ± 2.0 | 29.9 ± 0.4 | −10.8 ± 0.2 | −18.9 | −1.99 | I | 0.3 | −0.1 | −2.2 | −2.4 | 51.5 | 4500 | 190 |
| 66 | – | 17.8 | 7.2 | 5.15 | 731 | 39.5 | <1.8 | −5.7 ± 0.2 | −39.3 ± 2.0 | 72.4 ± 0.6 | −13.5 ± 0.2 | −20.9 | −1.70 | O | 0.1 | −1.6 | −2.0 | −2.2 | 68.6 | Modern | 130 |
| 67 | 354 | 20.3 | 7.3 | 3.74 | 785 | 16.0 | – | −5.3 ± 0.2 | −39.3 ± 2.0 | 72.0 ± 0.5 | −12.4 ± 0.2 | −19.9 | – | O | – | – | – | – | 60.2 | Modern | 130 |
| 68 | 342 | 21.9 | 7.3 | 4.29 | 764 | 41.0 | – | −5.4 ± 0.2 | −31.7 ± 2.0 | 87.1 ± 0.6 | −13.8 ± 0.2 | −21.9 | −2.10 | O | 0.4 | −0.8 | −1.9 | −2.2 | 74.5 | Modern | 110 |
| 69 | – | – | 7.1 | – | 847 | 28.0 | – | −5.1 ± 0.2 | −30.8 ± 2.0 | 76.5 ± 0.6 | −12.1 ± 0.2 | −19.4 | −1.73 | O | 0.1 | −0.7 | −2.1 | −2.3 | 58.0 | Modern | 140 |
| 70 | – | – | 7.2 | – | 655 | <0.5 | – | −6.0 ± 0.2 | −46.7 ± 2.0 | 10.9 ± 0.3 | −8.1 ± 0.2 | −15.4 | −1.96 | C | −0.1 | −0.7 | −2.3 | −2.6 | 37.9 | 10,300 | 340 |
| 71 | – | – | 7.1 | – | 613 | <0.5 | – | −5.6 ± 0.2 | −42.1 ± 2.0 | 6.8 ± 0.3 | −6.7 ± 0.2 | −14.0 | −1.95 | C | 0.0 | −0.5 | −2.3 | −2.6 | 30.8 | 12,500 | 500 |
| 72 | – | – | 7.2 | – | 663 | 30.0 | 4 ± 1 | – | – | – | −11.3 ± 0.2 | – | – | – | – | – | – | – | – | – | – |
| 73 | 111 | 17.1 | 7.7 | – | 548 | 2.5 | <1.2 | – | – | – | −11.7 ± 0.2 | – | – | – | – | – | – | – | – | – | – |
| 74 | 104 | 15.9 | 7.5 | – | 788 | 4.5 | 3 ± 1 | – | – | – | −10.9 ± 0.2 | – | – | – | – | – | – | – | – | – | – |
| 75 | 119 | 15.7 | 7.5 | – | 592 | 0 | <1.2 | – | – | – | −6.0 ± 0.2 | – | – | – | – | – | – | – | – | – | – |
| 76 | 155 | 16.9 | 8.2 | – | – | – | <1.8 | – | – | – | −8.5 ± 0.2 | – | – | – | – | – | – | – | – | – | – |
| 77 | – | 17.1 | 7.7 | 6.25 | 7800 | – | <1 | −5.6 ± 0.1 | −33.2 ± 0.8 | – | – | – | −2.25 | – | 0.6 | 0.9 | −1.2 | −1.5 | – | – | – |
| 78 | – | 15.9 | 7.5 | 11.39 | 8200 | 0 | <1 | −5.1 ± 0.1 | −30.3 ± 0.8 | – | – | – | −1.79 | – | 0.7 | 1.0 | −1.1 | −1.4 | – | – | – |
| 79 | – | 15.7 | 7.5 | 7.15 | 8500 | 0 | 3 ± 1 | −5.3 ± 0.1 | −33.6 ± 0.8 | – | – | – | −2.03 | – | 0.6 | 0.9 | −0.8 | −1.0 | – | – | – |
| 80 | – | 16.9 | 8.2 | 3.18 | 391 | 0 | – | | | – | – | – | −2.95 | – | 0.6 | 0.2 | −2.3 | −2.6 | – | – | – |
| 81 | – | 16.0 | 8.0 | 3.87 | 350 | 0 | <1 | −7.5 ± 0.1 | −49.0 ± 0.8 | – | – | – | −2.69 | – | 0.5 | 0.2 | −2.1 | −2.3 | – | – | – |
| 82 | – | – | 6.8 | 21.54 | 30,500 | 0 | – | | | – | – | – | −0.99 | – | 0.2 | 0.0 | −0.5 | −0.8 | – | – | – |
| 83 | – | – | 8.1 | 3.77 | 466 | 1.3 | <1 | −6.0 ± 0.1 | −38.4 ± 0.8 | – | – | – | −2.88 | – | 0.3 | −0.7 | −2.5 | −2.7 | – | – | – |

isotopes of water"). Then, carbon isotopes are employed in the correction model in order to provide reliable residence time of groundwater ("Carbon isotopes and groundwater ages"). The $^{13}C$ content is treated so as to establish the degree of openness with respect to atmospheric $CO_2$; together with $^{14}C$ activity it helps to determine the intensity of isotopic exchange between different phases within the aquifer.

**Results and discussion**

*Physical and chemical data*

Several chemical processes have been identified as being important in controlling the major ion chemistry (Zhang et al., 2000). Proportional content of major elements ($Cl^-$, $HCO_3^-$, $SO_4^-$, $NO_3^-$, $Na^+$, $K^+$, $Ca^{2+}$ and $Mg^{2+}$) was plotted in a Piper diagram so as the main hydrochemical facies could be defined. The waters indicate the variability in the aquifers mineralogy. On the whole, four zones have been detected (Fig. 3):

(A) Ca – $HCO_3$: this zone corresponds to the samples of Cretaceous, Oxfordian and many of Lower to Middle Jurassic aquifer. Three samples from Eocene (80, 81, 83) are of this geochemical type as well.
(B) Na – $HCO_3$: only two sampled waters from Jurassic aquifer (1, 3) indicate this chemical facie.
(C) Ca – $SO_4$: only Middle and Lower Jurassic samples were observed within this zone.
(D) Na – Cl: deeply circulating groundwater and sea invasion account for such a sodium chloride composition in the Jurassic and Eocene (77, 78, 79, 82) aquifers, respectively.

The physical and chemical characteristics of the Jurassic aquifers were already described in detail by Le Gal La Salle et al. (1996). They show important variations according to the increasing depth, to the progressive confinement from NE to SW and to the geological facies variation of the aquifer. This statement suits also the additional Infra-Toarcian samples with high concentration of calcium for most of the samples. The Jurassic aquifer is mainly composed of limestones and dolomites and therefore, the high content in calcium in groundwaters is explained by the intense dissolution of carbonate rocks. Generally speaking, samples originating from deep horizons reveal high ion content. It is demonstrated particularly on deep Jurassic wells (21, 24, 32, 35, 42). These waters are generally rich in $Ca^{2+}$, $SO_4^{2-}$ and $Cl^-$ with $Na^+$. The sulphates originate from gypsum and anhydrite dissolution. The occurence of these sediments is supported by the saturation indexes calculation displayed in Table 2, which show slight over saturation with respect to calcite, dolomite, gypsum and anhydrite. Only 21 shows slight under saturation for dolomite. With respect to the coastal position of some wells (21, 32, 35, 40, 41), there is no doubt about sea water contribution in these aquifer parts. For the well 40, there are no chemical data available and so this sample was not displayed in the Piper diagram and the saturation indexes could not be calculated. Nevertheless, this sample is also very rich in $Ca^{2+}$ and $SO_4^{2-}$, which is the result of gypsum dissolution. The well exploiting the thermal water in Jonzac (24) is located far from the ocean and so its higher chloride and sodium content is unlikely to be caused by sea water mixing. The groundwater sampled from this well comes from the depth of about 1850 m and thus is influenced by strong in depth water–rock interactions and is certainly of different origin than the rest of the wells. It is evident that all waters from Lower to Middle Jurassic aquifers corresponding to the Ca–$SO_4$ and Na–Cl zones originate from the confined aquifer system where the dissolution of evaporitic minerals take place. The Upper Jurassic samples from Oxfordian aquifer do not prove greater chemical variations, and fit the Ca–$HCO_3$ zone. The saturation indexes for Oxfordian waters are mostly negative, which complies with the unconfined structure of the aquifer. There were no chemical analyses available for the samples within the Cretaceous aquifer. Anyway, to get an idea about the chemistry of Cretaceous groundwaters, we used the chemical analyses from the Coniacian–Turonian aquifer within the studied area reported in BRGM (2005). Hence, the samples appearing in the Piper

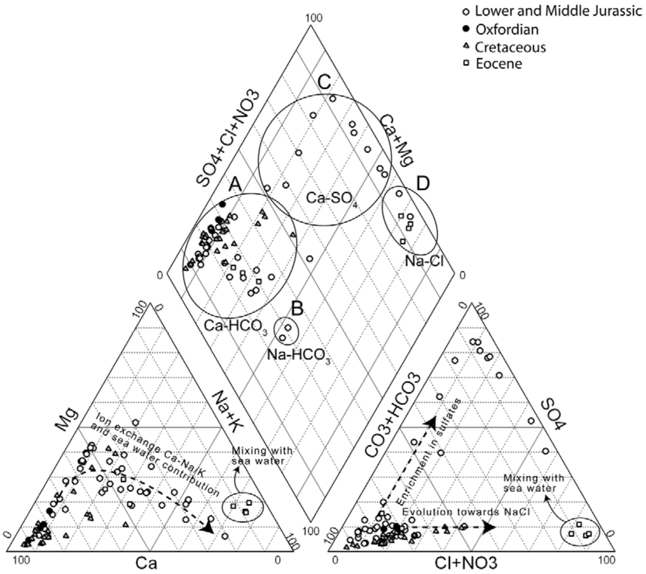


**Fig. 3.** Piper diagram showing the chemical evolution and distribution of the different groundwater facies within main aquifers of Northern Aquitaine.

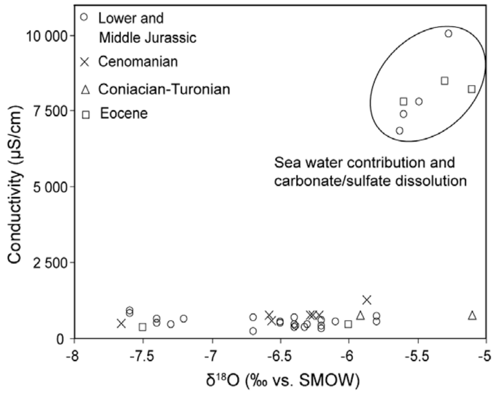


**Fig. 4.** Conductivity plotted versus $\delta^{18}O$. The high values account for mixing of groundwater with sea water and/or for the calcite and sulphate dissolution.

diagram in Fig. 3 represent these samples of Coniacian–Turonian aquifer in the studied region but do not correspond with the investigated and discussed samples within this study. It was observed that the Coniacian–Turonian samples belong mostly to the Ca–$HCO_3$ zone and reveal saturation only with respect to calcite and dolomite. The Eocene waters might be divided into two entirely different chemical groups. One of them corresponds to the Ca–$HCO_3$ zone (80, 81, 83) and the other to the Na–Cl zone (77, 78, 79, 82). The Na–Cl content is clearly caused by sea water contribution into these wells, which might be confirmed by their close position to the Atlantic coast. The Fig. 4 shows the conductivity values for a several wells. Despite the incomplete conductivity record of groundwaters, a group of high conductivity samples was detected. The Eocene samples (77–79) account for sea water mixing, the Jurassic wells 32, 40 and 42 represent the conductivities resulting from both the sea water mixing and carbonate/sulphate dissolution. The value in well 24 mainly results from water–rock interactions in depth. The values for most of the samples range within the span between 250 and 1300 µS/cm, which fits to the carbonated aquifers. Similarly, the pH parameter for most samples is near neutral values ranging between 6.7 and 7.7 which are characteristic for aquifers consisting mostly of carbonate rocks.

The sea water contribution might be additionally proved by the content of $^{18}O$ and $^{2}H$ in the samples, which is generally enriched with respect to the isotopic content of modern precipitation ("Stable isotopes of water"). The samples revealing high Na–Cl content, suggesting the contribution of different water origins, cannot rigorously be used for age interpretation.

*Modern water indicators*

The identification of mixing between modern waters and more confined and isolated waters is essential to give a reasonable age to groundwater. The anthropogenic fingerprint of modern waters can be given by the nitrate content, especially in our study area were agriculture is strongly developed and where high nitrate concentration are often recorded in both surface and groundwater. In addition a few analyses of groundwater tritium content are available and provide us with a good indication about the modern or sub-modern origin of groundwater. Hence noticeable concentration of nitrate is often associated with tritium in a number of wells displayed in Table 2. Significant content of tritium and/or nitrate in groundwater samples will be interpreted as an evidence of young water contribution.

Tritium content was only measured at a few sampling sites (Jurassic 1–17, 19, 23, 27, 33 and 41, Cretaceous 50, 51, 55–57, 66 and 72–76, Eocene 77–79, 81 and 83) and was really detected in 18 samples (4, 5, 8–10, 13–16, 19, 23, 41, 55–57, 72, 74 and 79). Estuary waters reveal the highest content of seven TU (BRGM, 1999b) which is in accordance with young water input. The mixing of estuary and Eocene waters explains three TU in well 79. If the tritium was not detected, the recharge is anterior to the bomb period, i.e. 1952 (Clark and Fritz, 1999). Obviously, a few wells enriched in tritium also show nitrate pollution (e.g. 10, 13, 14, 15, 41, 72). Nevertheless, a clear relationship between nitrate and tritium content was not observed, demonstrating that not all the modern waters are markedly affected by agricultural pollution.

Although at several sites the nitrate content is significantly high, it does not exceed the limit for drinking water (50 mg/l). Only the water sampled from the spring 47 with a value 78.7 mg/l, being situated in the Oxfordian outcrop, is above this limit. The next highest concentration was measured in a spring water as well (41) originating from the Jurassic aquifer (44.5 mg/l). Nitrates were detected in all the investigated aquifers. The samples from the unconfined Oxfordian aquifer are all contaminated by nitrates and the presence of modern water in this aquifer is also attested by the stable isotope content which corresponds to the modern precipitation ("Stable isotopes of water").

To determine the modern water input to the aquifer system, we used both nitrate and tritium records. From Table 2 it is evident, that all the samples with higher nitrate concentration reveal also a few units of tritium if it was measured. This does not work reversely, in other words not all waters with detected $^{3}H$ contain nitrate. It might be either due to the irregular distribution of agricultural activities in the region or the denitrification processes in the aquifers (Landreau et al., 1988; Mariotti, 1994). The consequence resulting from modern water input into the aquifer system is the fact, that this water having the same isotopic content as the modern precipitation can significantly modify the isotopic signature of the palaeowaters. It is not possible to detect all the samples which are influenced by the modern waters, because of a lack of complete $^{3}H$ and nitrate analyses. From the available data, we were able to detect 29 groundwater samples whose isotopic signature is more or less modified. This fact will be considered in the groundwater age determination.

*Stable isotopes of water*

The stable isotope composition in meteoric water reveals a close relation among a number of environmental parameters, such as source of moisture, surface air temperature, amount of precipitation, seasonality and altitude (Rozanski, 1985; Clark and Fritz, 1999; Chen et al., 2003; Mazor, 2004). Within the aquifers, the chemical and isotopic characteristics of water ($\delta^{18}O$, $\delta^{2}H$) vary and show an evolution in the isotopic content. Hence, the $\delta^{2}H$ vs. $\delta^{18}O$ diagram shows the heterogeneity of the recharge conditions (Fig. 5). The figure shows the Local Meteoric Water Line which was plotted on the basis of the isotopic data giving the average weighted values of the isotopic content of rainfall sampled at the Dax, Brest and Orleans between 1996 and 2002 (BRGM, 2004) and then on the basis of rainfall isotopic values calculated from the measurements in lakes and reservoirs close to our experimental area (Petelet-Giraud et al., 2005). The last mentioned values are more depleted than values directly measured in precipitation collected at pluviometric stations and reflect probably the higher altitudes of the lakes. The equation for the Local Meteoric Water Line is $\delta^{2}H = 8.1\delta^{18}O + 10.4$ ($r^2 = 0.97$) which almost precisely fits the Craig's equation (Craig, 1961). The modern recharge is characterised by values of −6.2‰ for $\delta^{18}O$ and −39.2‰ for $\delta^{2}H$. The entire ranges of stable isotope values are from −7.7‰ to −4.9‰ and from

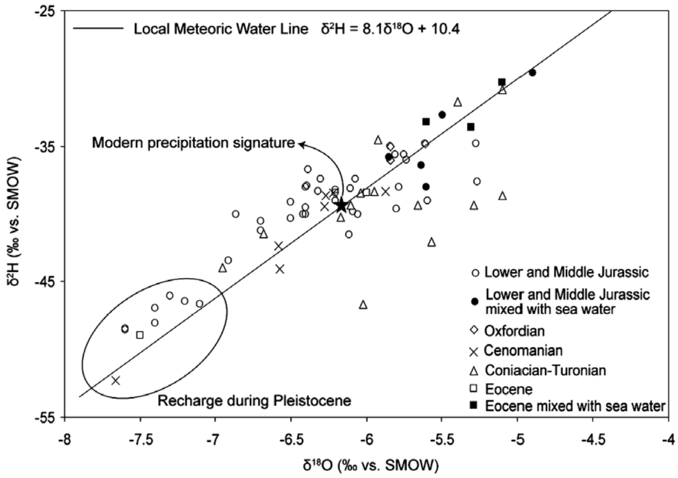


**Fig. 5.** Stable isotope composition of waters in the Aquitaine Basin aquifer system with plot of the Local Meteoric Water Line (BRGM, 1999b, 2004; Petelet-Giraud et al., 2005).

−52.3‰ to −29.6‰, respectively, for $\delta^{18}O$ and $\delta^{2}H$. Two groups of groundwater can be identified (Fig. 5). Low values were measured in several samples suggesting lower temperatures during the recharge period. This group of waters represents the palaeorecharge under cold climatic conditions during the late Pleistocene period and was separated from those of the Holocene (Fig. 5). The isotopic composition of the Pleistocene groundwater samples is on average around −7.4‰ for $\delta^{18}O$ and −48.1‰ for $\delta^{2}H$, which is 1.2‰ lighter in $\delta^{18}O$ and 8.9‰ lighter in $\delta^{2}H$ than that in modern precipitation. They consist of Jurassic samples, one Cenomanian and one Eocene sample. This Eocene sample does not reveal any communication neither with the estuary water nor with the sea water (0.3 $\delta^{18}O$ ‰, 3 $\delta^{2}H$ ‰; BRGM, 1994). The position of this well accounts uniquely for the deep groundwater origin (BRGM, 1999b). In this group of waters only Coniacian–Turonian samples were not identified. However, this fact may be simply due to the lack of data. On the contrary, the higher values concern Jurassic and Eocene samples resulting from mixing processes with isotopically enriched sea water. The rest of the groundwaters are placed along the local meteoric line. All Oxfordian waters indicate a modern origin.

*Carbon isotopes and groundwater ages*

Various correction models were tested in order to provide the most reliable results. Once the recharge conditions and the residence time are determined, the timing of palaeorecharge will be discussed with respect to the LGM and transitional period ("Paleorecharge signature and discussion on groundwater ages").

*Models for radiocarbon dating*

Much of the carbon in groundwater derives from gaseous $CO_2$ in the vadose zone. However, this carbon containing high levels of $^{14}C$ is usually diluted by low $^{14}C$ activity carbon dissolved from minerals during groundwater recharge. The radiocarbon age of groundwater is given by general law of radioactive decay.

In order to calculate the age of groundwater in carbonate aquifers, the initial activity of this radioactive isotope must be determined. It might be determined from various models considering mass balances (TAMERS, 1967), isotope balance (INGERSON and PEARSON, 1964) or both (FONTES and GARNIER, 1979). MOOK (1972, 1976, 1980) consider partial or complete isotopic equilibration between the gaseous phase and all the carbon species. An attempt to simplify the concept of the exchange-mixing model was introduced in a study made by the IAEA (Salem et al., 1980). EVANS's approach (Evans et al., 1979) accounts for the dissolution processes that occur in the presence of an infinite reservoir of carbonate. EICHINGER (1983) introduces a correction for the partial isotope exchange with carbonates of the aquifer matrix. It is important to emphasize that the geochemical models may be reasonable but not always exact correction methods.

For the radiocarbon dating of groundwater it is important to understand the geochemical processes in the unsaturated zone and in the aquifer after the recharge. The DIC and the $^{13}C$ evolution provide an insight into these processes and can help to improve the quality of the age calculation.

*Carbon isotopes*

Many problems have to be solved for a "safe" use of carbon isotopes in groundwater dating especially in the case of carbonate aquifers (Fontes, 1985). The main problem can be met in the case of carbonate saturation, when dissolution proceeds at the same time as precipitation. When this happens, the isotopes are still exchanging between liquid and solid phase while the chemical composition remains constant. This would suggest that chemical effects are often predominant over age effects and that many waters are actually younger than estimated from chemical or isotope models.

In the studied aquifers we have to take into account the carbonate dissolution which is sensitive to the partial pressure of $CO_2$ ($P_{CO_2}$). The higher the $CO_2$ concentration in the soil, the higher the amount of calcite dissolved will be, and the higher the DIC. The dissolution of $CO_2$ and calcite is a possible source of $^{13}C$. The $^{13}C$ content of the biogenic $CO_2$ is considered to be about −21‰ in this study which is characteristic of the natural C-3 vegetation under temperate climate (Deines et al., 1974). This value is within the average value −21.6‰ measured by Emblanch (1997) in carbonated soil of South France and also used by Huneau (2000) in Southeast France. On the other hand, the $^{13}C$ content of carbonated rock is generally considered equal to 0‰ (Clark and Fritz, 1999) with little variations from −2‰ to +2‰. The $^{13}C$ contents for Lower and Middle Jurassic aquifer range widely from −11.7‰ to −1.8‰ vs. PDB. The Oxfordian aquifer reveals a closer relationship to the soil conditions with higher values ranging between −14‰ and −12‰. Concerning the Cretaceous, the $\delta^{13}C$ isotopic content in DIC varies from −13.7‰ to −9.19‰ for the Cenomanian and from −13.8‰ to −6‰ for the Coniacian–Turonian. In order to asses the character of the system in which carbon evolves (open or closed), a calculation of $^{13}$Ceq ($^{13}$C of gaseous phase in equilibrium) is carried out (Le Gal La Salle et al., 1996):

$$\delta^{13}C_{eq} = f_T - (a\varepsilon_{a-g} + b\varepsilon_{b-g} + c\varepsilon_{c-g})/CT$$

where $\delta_T$ is the $^{13}$C content of the TDIC; $a$, $b$, c are the molarities of $H_2CO_3$, $HCO_3^-$ and $CO_3^{2-}$, respectively; $\varepsilon_{a-g}$, $\varepsilon_{b-g}$, $\varepsilon_{c-g}$ are the fractionation factors between the C species (Mook, 1979); CT is the total dissolved inorganic C (mol $l^{-1}$). The calculated 13Ceq (Table 2) varies from −21.9‰ to −8.4‰. Values approaching $^{13}$C in the soil (−21‰) show an open system where the modern recharge dominates. The closer the value is to 0‰, the more the system is closed and the palaeowaters occur. Within our data we have approximately the same number of samples from open (O), closed (C) and intermediate (I) system which indicates a mixture between evolved and less evolved waters. Note, that the Middle and Lower Jurassic deep aquifers are generally enriched in $\delta^{13}C$ with respect to the soil $CO_2$ showing a closed system or gradually closing system, which was already observed by Le Gal La Salle et al. (1996). The measurements on the Oxfordian and Cretaceous aquifer showed values characteristic for open system conditions.

The combination of $P_{CO_2}$, DIC and $\delta^{13}C$ can so provide an indication of recharge conditions as shown in Table 2. The decrease of $P_{CO_2}$ principally indicates dissolution of calcite. The $P_{CO_2}$ of soil was not measured in the region but can be assumed from the modern groundwater samples and is confirmed by André et al. (2005). The average value varies from 0.02 to 0.03 atm or from −1.7 to −1.5 expressed as $\log P_{CO_2}$ and corresponds to the value measured in the south of France by Huneau (2000). The calculated $P_{CO_2}$ for most of the groundwaters is less than that of soil indicating the consumption of $CO_2$ which has been consumed by calcite dissolution. This is confirmed also by calcite saturation or even over saturation for very old groundwaters.

Activities of $^{14}$C vary widely (Table 2) and, in some areas, are very close to 0 pmc, suggesting a very long residence time within the aquifer. In general, the $^{14}$C dating is uncertain for very low values (Zuber et al., 2004). Those values are observed in the Lower and Middle Jurassic aquifer mainly in the western part of the study area (20, 21, 32, 34, 35, 40, 12 and 43). For some of them (21, 32, 35, 40) the old sea water mixing phenomenon is responsible for lower values. Very low values were measured in Jonzac (24) with the activity of 0.9 pmc and in both Cretaceous aquifers (52, 54, 59, 62, 71). On the contrary, high values between 74.3 and 93.8 pmc come from the unconfined Oxfordian aquifer, which indicates a modern contribution to the recharge. The same is registered in the Cretaceous boreholes tapping the unconfined aquifer (e.g. 60, 61) with considerable content in nitrate as a tracer of modern waters. The confined Cretaceous aquifer shows a wide range of activities indicating both very old (62) and more recent (e.g. 68, 69) waters.

The inverse evolution of $^{14}$C and $\delta^{13}C$ downgradient demonstrates that an important loss of $^{14}$C is caused by the geochemical reactions with carbonates in the aquifers (Fig. 6). The carbonate dissolution during the infiltration processes increases DIC and enriches the $\delta^{13}C$ value. After the groundwater reached calcite saturation cation exchange reduces $Ca^{2+}$ concentration and induces again calcite dissolution. This implies an intense isotopic exchange between DIC, and the carbonated matrix through time (Kloppmann et al., 1998; Huneau and Travi, 2008). We observe low content of $^{13}$C in modern waters, whereas palaeowaters are enriched in this isotope. The samples mixed with saline water (21, 32, 35, 40, 42) are located at the bottom of an evolution line (Fig. 6) indicating very low $^{14}$C activities and the enrichment in the $^{13}$C isotope. From this relation we note that samples previously identified as "mixing origin samples" suggest an old sea water intrusion and/or a low ratio of mixing (Clark and Fritz, 1999). Fig. 5 shows, that the sea water participation is minor and therefore the $^{14}$C activity variations are very little.

The observed chemical processes need to be considered within the mixing and exchange model which will be used for the most representative and adequate groundwater age determination.

*The choice of model*

The $^{14}$C content of primary recharge is required for $^{14}$C dating. In addition, the $^{13}$C content in the soil and carbonates has to be identified. The application of a $\delta^{13}C$ value of −21‰ ("Carbon isotopes") for primary recharge and 0‰ for the aquifer carbonate matrix

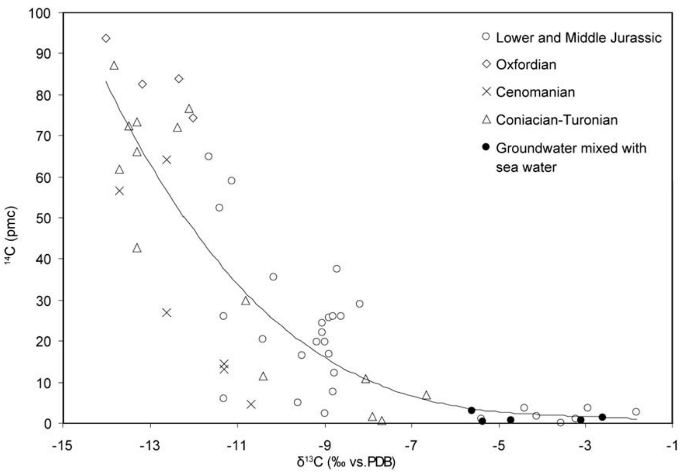


**Fig. 6.** Exponential relationship between carbon isotopes showing the gradual isotopic exchange between solid phase and DIC of groundwater.

(Clark and Fritz, 1999) allowed us to calculate the initial $^{14}C$ activities $A_0$. Only waters clearly showing the absence of mixing with sea water have been considered within the dating. Although none of the studied samples reveal a strong influence of ocean waters, their isotopic composition is certainly influenced by saline waters and the dating would not be reliable.

Seven commonly used models were comparatively assessed in the study. The Mook and IAEA models gave similar results and the Pearson, F&G, Evans and Eichinger models produced results in broad agreement as already observed by Gallagher et al. (2000). Considering the whole geochemistry of the aquifers, the correction introduced in the F&G model seems to match well the geochemical conditions of carbonate aquifers. The rest of models are not convincing because of their inability to correct for solid phase isotopic exchange in aquifers.

*Palaeorecharge signature and discussion on groundwater ages*

The results obtained with the F&G model are displayed in Table 2 and shown on Fig. 7, which plots the groundwater ages vs. stable isotope content. The figure displays the error spans calculated for each sample. For an easy identification of samples, which were determined in "Modern water indicators" as modern due to higher nitrate content, they were highlighted in grey in the picture. It is generally considered, that the relationship of deuterium with age is more reliable than that of oxygen-18, since oxygen-18 is more sensitive to possible evaporation effect during infiltration processes (Clark and Fritz, 1999). Moreover, the deuterium content in water can not be influenced by the geothermic exchanges between water and rock (Rozanski, 1985). Although the deuterium function (Fig. 7a) seems to be indeed more reliable than that of oxygen-18 (Fig. 7b), both graphics show three principle groups of groundwaters which could be determined with respect to different content of heavy isotopes marked by average values of −6.2‰ in $\delta^{18}O$ and −39.3‰ for $\delta^2H$. The first group correlated with the radiocarbon ages from 10 ka B.P. up to the present corresponds to Holocene waters revealing the highest values with on average −6‰ and −38.5‰ for $\delta^{18}O$ and $\delta^2H$, respectively. The average values for the second are −7.4‰ and −48‰ for $\delta^{18}O$ and $\delta^2H$, respectively. This group of samples ranges between 20 and 15 ka B.P. and represents the cold recharge of the LGM. Finally the third group of samples is dated prior to LGM and reveals the average values −6.5‰ and −41.8‰ for $\delta^{18}O$ and $\delta^2H$, respectively. Hence, the observed light isotopic content might be consistent with colder climatic

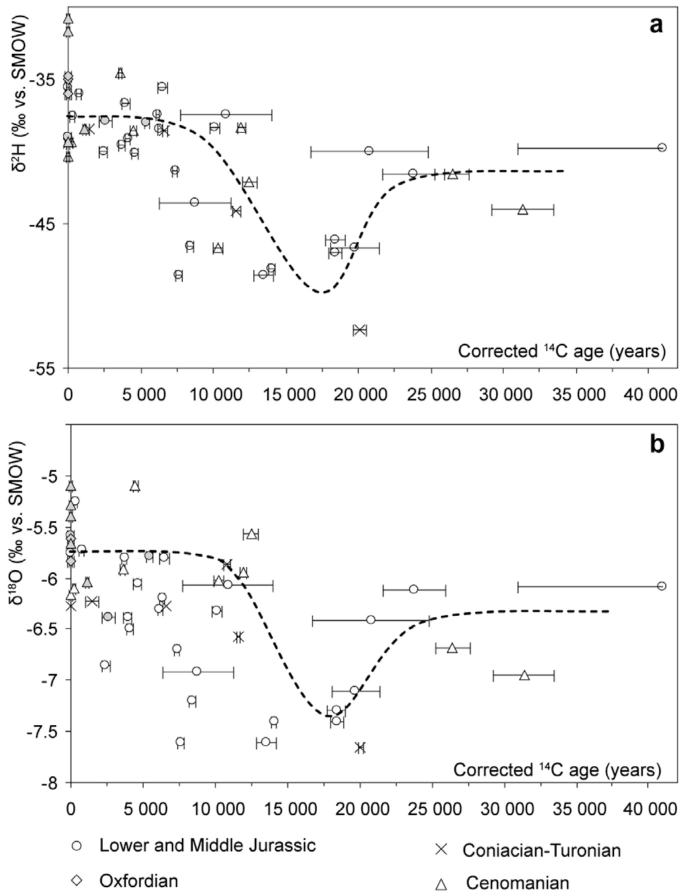


**Fig. 7.** Evolution of deuterium (a) and oxygen-18 (b) in relation to the groundwater ages corrected by the F&G model (1979). Waters containing nitrate are highlighted in grey colour.

conditions of the end of the Pleistocene. The other two groups of waters – prior and post LGM period – reveal enriched values, thus warmer climatic conditions corresponding to the interstadial ages. From the scatter of the points it is evident that the isotopic enrichment prior to LGM is not as high as in the Holocene and therefore the last interglacial occurring in Holocene is warmer than the period to the LGM. The climatic transition Holocene/Pleistocene corresponds to the period between approximately 15–12 ka B.P. In several European sites, the climatic transition was determined around 15–10 ka B.P. Our finding falls within this span and is consistent with findings of other authors who assume that the LGM period took place about 18 ka ago (CLIMAP, 1976; Stute et al., 1992; Castro et al., 2000). Buoncristiani and Campy (2004) studied the expansion and retreat of the Jura ice sheet in Northeast France. They assume that the LGM period took place about 18 ka ago. The same timing was established using $^{4}He$ and $^{14}C$ data in different aquifers in world (Castro et al., 2000). In addition the radiocarbon dating on mammals' bones in the Aquitaine region (Drucker et al., 2003) or the pollen investigations of deciduous trees (Brewer et al., 2002) determine the LGM between 18 and 15 ka B.P.

The F&G model allows us to determine the ages up to 30 ka. In the case of very low $^{14}C$ values of DIC, the age can be calculated but usually exceeds 30–20 ka. According to Fontes (1985), estimations of groundwater "ages" older than 25 ka are risky and the ages over 30 ka B.P. are unacceptable. In our study, we have such samples from the Jurassic aquifer (20, 24). Apart from the Jurassic samples it is evident, that old waters appear also in Coniacian–Turonian aquifer (59, 62). One Cenomanian sample which is extremely depleted in stable isotopes suggests an age around 20 ka B.P. There is some doubt about the continuous precipitation input during the LGM period, namely between 17 and 14 ka B.P. Within this span, we have no direct observation. We have one misrepresentative observation (54) around 16.7 ka B.P. which must be discarded owing to high nitrate content caused by modern surface water contamination. This sample which was not for this reason reported in Fig. 7 comes from the Cenomanian aquifer and the modern water input makes it artificially younger. The rest of the samples containing nitrates were intentionally reported in Fig. 7 in order to demonstrate mixing between modern and more evolved waters occurrences (e.g. 19, 29, 64).

Anyway, our dataset does not clearly show the existence of a recharge hiatus. We can just note the existence of a short period without data around 17 ka B.P. This could be according to Darling (2004) the so called "recharge gap". Nevertheless, the $^{14}C$ dating is a very delicate method and the apparent gap in recharge might be a consequence of the lack of "gap-aged" samples rather than of the absolute absence of recharge. Obviously, the probability to find water of a particular age decreases with lower recharge intensity, which doubtless occurred during LGM. In comparison to the groundwater ages, the gap is not long enough to make it possible to confirm a complete recharge absence. According to Darling (2004) and Douez (2007) the LGM resulted in more or less continuous permafrost conditions which prevented the aquifers from being recharged. Darling (2004) demonstrated significant recharge gaps in several European countries. On the basis of several studies the permafrost occurred mainly in the countries of Northern Europe (Bath et al., 1979; Purtschert et al., 2008), where it is very likely to suppose absence of recharge during the LGM period. However, the recharge gap in Southern European aquifers is more disputable and according to Texier and Bertran (1993), only very discontinuous permafrost can have developed in the Aquitaine Basin, which might have resulted in discontinuous recharge. The Pleistocene period with the minimum temperature established by numerous studies as varying between 5 and 9 °C lower than at present time (Rozanski, 1985; Stute et al., 1995; Thompson et al., 1995; Edmunds et al., 2006; Huneau, 2000; Aeschbach-Hertig et al., 2002; Chen et al., 2003), is unlikely to cause continuous permafrost conditions in this area. As proposed by Darling (2004) the recharge conditions could also have been influenced via the precipitation regime perturbation and lower rainfall amounts in the regions farther away from the ice cover which could have led to lower recharge intensity. The considered recharge gaps in different European sites appear to occur during different time spans, and some observations remain difficult to explain but are certainly related to the methods of dating used. Radiocarbon dating methodology on groundwater can only give an estimation of "groundwater

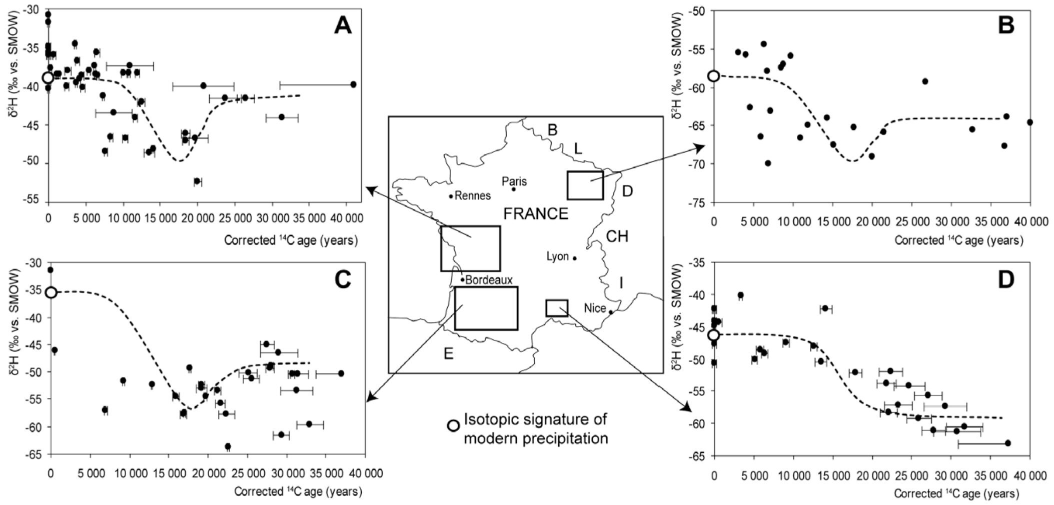


**Fig. 8.** Isotopic contrast registered in different aquifers in France with isotopic signature of modern precipitation: A – this study, B – southern part of Aquitaine Basin (Douez, 2007), C – Lorraine region (Blavoux and Olive, 1981), D – Valréas Basin (Huneau, 2000).

age" and is extremely sensitive to the geochemical and hydrodynamic conditions within the aquifer.

*Groundwater ages in France*

To generalise and interpret our results on a larger scale, we collected data from various large aquifers of France. These allow us observing the differences in recharge signature. Apart from the discussed North Aquitaine Basin the referenced regions are: South Aquitaine Basin (Douez, 2007), Valréas Basin in Southeast France (Huneau, 2000) and the Lorraine region investigated since 1980 (Blavoux and Olive, 1981; Rudolph et al., 1984). Fig. 8 shows the plot of $\delta^2H$ versus corrected groundwater age for each region. Concerning modern waters these graphics clearly show the differences in the isotopic content in particular regions. The main phenomenon which is responsible for these differences is the continental effect. While the average $\delta^2H$ value for the waters in the North Aquitaine Basin discussed in this paper is around −38‰, the inland samples from the Lorraine region show a lighter average value around −63‰. The groundwater from the South Aquitaine Basin reveals slightly higher content in heavy isotopes than the North Aquitaine Basin. This fact accounts for the geographical position of the regions with the distance from the ocean. The precipitation contributing to the aquifers in the Aquitaine Basin are mainly formed above the ocean, which explains the high isotopic values in this area. On the contrary, the Lorraine region is not influenced by the sea proximity, which explains that the values remain depleted.

Regardless of the different isotopic content for selected regions, the same general trend is observed. During the last 20,000 years, the climate has undergone a period of major change from a glacial period with cold atmospheric temperatures between 18 and 15 ka, to an interglacial warm period as was shown in many regions in the world (Clark and Fritz, 1999; Edmunds and Shand, 2008).

The observation in France, particularly in the North Aquitaine Basin, fits this hypothesis.

The incertitude of the dating method is added in the Fig. 8 for the aquifers (with the exception of aquifers in Lorraine, where the data are not available). In the south of the Aquitaine Basin we do not have much information about the waters younger than 10 ka. This dataset shows a large number of samples within the span between 23 and 16 ka. Considering the error bars for each sample, it is not possible to place any recharge gap during the assumed coldest climatic period. The similar observation has been made in the Lorraine region, where – in spite of the lack of data for error bar plotting – the samples show ages ranging from 35 ka up to the present days continuously, without a clear recharge gap. Despite the lower density of water samples revealing the age within the LGM span, the investigation in Valréas Basin brought comparable findings. At least one sample was determined between 18 and 15 ka. In the Aquitaine Basin and in the Lorraine region, the isotopic content oscillated during last 30 ka with high values prior to LGM, low values during LGM and the highest values since the climatic transition at the beginning of the Holocene. The water level changes could have some effect on the isotopic signature of rainfall recharging the aquifers. During the LGM, the level of the Atlantic Ocean was about 120 m below present time situation and the shore was about 100–120 km towards the west. Thus the study area was in a more "continental situation" which can affect the isotopic content towards slightly more depleted values. But this very little change is probably hidden by the stronger paleoclimatic effect.

Over most of Europe, there appear to be little changes in the atmospheric circulation pattern since Late Pleistocene (Rozanski, 1985; Jouzel et al., 2000). Areas most affected by change seem likely to be either in high latitudes (Jouzel et al., 2000) or in zones which oscillate between humid and arid conditions, e.g. in the northern Sahara (Sonntag et al., 1978).

We do not have data from other climate archive on south western France but we can mention that in south-eastern France, during the LGM, the average rainfall amount is estimated, thanks to pollen reconstruction, around 700 and 900 mm/year (Peyron et al., 1998) which is quite in agreement with present time situation. Since atmospheric circulations were more or less identical, we can suspect that rainfall amount was not greatly modified.

From the knowledge of modern isotopic signature and the average isotopic value during the LGM, we are able to estimate the isotopic enrichment since the LGM up to the Holocene period. Even if the isotopic values in different regions are influenced by the continental and altitudinal effects, the average enrichment is around 10–12‰ in $\delta^2H$ as shown on the Fig. 8 and around 2.0–2.2‰ for $\delta^{18}O$ for aquifers of North Aquitaine Basin, Lorraine and the Valréas Basin. The isotopic enrichment in the south of Aquitaine is difficult to estimate because of the lack of modern water samples. The cited values are in good agreement with data from many different European aquifers (Clark and Fritz, 1999).

**Conclusion**

Our investigation of the northern part of the Aquitaine Basin, which provides large and high storage capacity aquifers, made it possible to characterise the recharge evolution in Southwest France. The surveyed aquifers are widely heterogenous from the stratigraphic point of view but they are all made of carbonates which give the main geochemical signature to groundwater. As a consequence the hydrochemistry varies in accordance with the changes in lithological facies but is clearly dominated by carbonate equilibrium. The study of carbon isotopes allowed us to estimate the overall age of groundwater occurring in the main regional aquifers. Very low activities observed at many places suggest that water infiltrated during the end of the Pleistocene and can thus be considered as palaeowater. The palaeoclimatic effect is responsible for the very wide spectrum of stable isotope values encountered. The depletion in $\delta^{18}O$ and $\delta^2H$ values reflects lower average atmospheric temperatures during the LGM period between 20 and 15 ka B.P. The transition from Pleistocene to Holocene is marked by fast enrichment in $\delta^{18}O$ and $\delta^2H$ especially between 15 and 12 ka B.P. The climate in this period changed from cold and dry to warm and humid which is shown by isotopic enrichment during the Holocene period. The recharge chronology does not clearly confirm a significant hiatus during the LGM and the end of the Pleistocene. This information may be useful for future hydrogeological investigation in the Aquitaine Basin and elsewhere in Southern Europe and confirms the interest of groundwater as a palaeoclimate archive. Such information is also essential and should be considered by modellers in their attempts to simulate the hydrogeological functioning of large confined aquifers on the very long time range. It is then of major importance to be able to evaluate if these systems are at present time functioning in permanent or transient conditions from the recharge processes point of view.

**Acknowledgements**

This work was supported by the French Ministry of Foreign Affairs and the Ministry of Education, Youth and Sports of the Czech Republic. Financial support was also granted by the Grant Agency of the Czech Republic (GACR 205/07/0691). We would like to particularly thank the French Embassy in Prague for its help concerning this project.

## References

Aeschbach-Hertig, W., Stute, M., Clark, J.F., Reuter, R.F., Schlosser, P., 2002. A palaeotemperature record derived from dissolved noble gases in groundwater of the aquia aquifer (Maryland, USA). Geochemica et Cosmochemica Acta 5, 797–817.

André, L., Franceschi, M., Pouchan, P., Atteia, O., 2002. Origin and evolution of sulphur in the Molassic sands aquifer from the Aquitaine Basin. C. R. Geoscience 334, 749–756.

André, L., Franceschi, M., Pouchan, P., Atteia, O., 2005. Using geochemical data and modelling to enhance the understanding of groundwater flow in a regional deep aquifer, Aquitaine Basin, south–west of France. Journal of Hydrology 305, 40–62. doi:10.1016/j.jhydrol.2004.08.027.

Araguas-Araguas, L., Fröhlich, K., Rozanski, K., 2000. Deuterium and oxygen-18 composition of precipitation and atmospheric moisture. Hydrological Processes 14, 1341–1355.

Bath, A.H., Edmunds, W.M., Andrews, J.N., 1979. Palaeclimatic trends deduced from the hydrochemistry of a Triassic sandstone aquifer. United Kingdom. Isotope Hydrology 1978, vol. II. IAEA, Vienna, pp. 545–566.

Beyerle, U., Purtschert, R., Aeschbach-Hertig, W., Imboden, D.M., Loosli, H.H., Wieler, R., Kipfer, R., 1998. Climate and groundwater recharge during the last glaciation in an ice-covered region. Science 282, 731–734.

Blavoux, B., Olive, P., 1981. Radiocarbon dating of groundwater of the aquifer confined in the lower Triassic sandstones of the Lorraine region, France. Journal of Hydrology 54, 167–183.

Blavoux, B., Dray, M., Fehri, A., Olive, P., Gröning, M., Sonntag, C., Hauquin, J.P., Pelissier, G., Pouchan, F., 1993. Palaeoclimatic and hydrodynamic approach to the Aquitaine basin deep aquifer (France) by means of environmental isotopes and noble gases. In: Isotope Techniques in the Study of Past and Current Environmental Changes in the Hydrosphere and the Atmosphere. IAEA, Vienna, pp. 93–305.

Brewer, S., Cheddadi, R., Beaulieu, J.L., Reille, M., 2002. The spread of deciduous Quercus throughout Europe since the last glacial period. Forest Ecology and Management 156, 27–48.

BRGM, 1994. Etude du potentiel aquacole des nappes d'eau souterraines salées de la Pointe de Grave en Gironde. R 38074 RS SP 94, 52 p. <http://www.brgm.fr/Rapport?code=RR-38074-FR.pdf> [cited April 2008].

BRGM, 1996. Faisabilité d'un modèle hydrogéologique sur la bordure sud du Marais Poitevin (17–79). R 39301, 51 p. <http://www.brgm.fr/Rapport?code=RR-39301-FR.pdf> [cited April 2008].

BRGM, 1999a. Gestion des eaux souterraines en Poitou-Charentes, Année 2. RP-50107-FR, 108 p. <http://www.brgm.fr/Rapport?code=RP-50107-FR.pdf> [cited April 2008].

BRGM, 1999b. Gestion des eaux souterraines en Aquitaine, Année 3. Opération sectorielle, Relation entre l'estuaire de la Gironde et la nappe de l'Eocène. R-40729, 122 p. <http://www.brgm.fr/Rapport?code=RR-40729-FR.pdf> [cited April 2008].

BRGM, 2000. Gestion des eaux souterraines en Aquitaine, Année 4. Opération sectorielle, Relation entre l'estuaire de la Gironde et la nappe de l'Eocène. R-50467, 2000, 77 p. <http://www.brgm.fr/Rapport?code=RP-50467-FR.pdf> [cited April 2008].

BRGM, 2001. CPER 2000–2006 Année1. Construction d'outils d'aide à la décision, Aquifère du Turonianien. RP-50826-FR, 97 p. <http://www.brgm.fr/Rapport?code=RP-50826-FR.pdf> [cited April 2008].

BRGM, 2002a. CPER 2000–2006 Phase1. Outils d'aide à la décision pour la gestion de l'aquifère du Turonianien-Coniacien. RP-51591-FR, 134 p. <http://www.brgm.fr/result/RAPPORT SP.jsp?pageActive=0&cook=1210599373764> [cited April 2008].

BRGM, 2002b. CPER 2000–2006 Phase1. Outils d'aide à la décision pour la gestion de l'aquifère de l'Infra-Toarcien. Approche des modalités de la recharge de l'aquifère Infra-Toarcien et des communications avec d'autres aquifères par les méthodes isotopiques. Origine et datation des eaux, origine de la minéralisation. RP-51194-FR, 108 p. <http://www.brgm.fr/Rapport?code=RP-51194-FR.pdf> [cited April 2008].

BRGM, 2004. Projet de mise en place d'une banque de données isotopiques. Etat d'avancement année 2003. RP-51092-FR, 68 p. <http://www.brgm.fr/Rapport?code=RP-51092-FR.pdf> [cited April 2008].

BRGM, 2005. CPER 2000–2006 Phase2. Action d'accompagnement pour l'aquifère du Turonianien-Coniacien en Charente. Suivi de la crête piézométrique et du débit des sources et des cours d'eau. RP-53494-FR, 80 p. <http://www.brgm.fr/Rapport?code=RP-53494-FR.pdf> [cited April 2008].

BRGM, 2006. Aquifères & Eaux Souterraines en France, tome1. BRGM editions, Orléans, 479 p.

Buoncristiani, J.F., Campy, M., 2004. Expension and retreat of the Jura Ice sheet (France) during the last glacial maximum. Sedimentary Geology 165, 253–264.

Castro, M.C., Stute, M., Schlosser, P., 2000. Comparison of $^{4}He$ ages and $^{14}C$ ages in simple aquifer systems, implications for groundwater flow chronogies. Applied Geochemistry 15, 1137–1167.

Chen, Z.Y., Qi, J.X., Xu, J.M., Xu, J.M., Ye, H., Nan, Y.J., 2003. Palaeoclimatic interpretation of the past 30 ka from isotopic studies of the deep confined aquifer of the North China plain. Applied Geochemistry 18, 997–1009.

Clark, I.D., Fritz, P., 1999. Environmental Isotopes in Hydrogeology. Lewis Publishers, Boca Raton. 311 p.

CLIMAP Project Members, 1976. The surface of the ice-age earth. Science 191 (4232), 1131–1137.

Craig, H., 1961. Isotopic variations in meteoric waters. Science 133, 1702–1703.

Dangaard, W., 1964. Stable isotopes in precipitation. Tellus 16, 436–468.

Darling, W.G., 2004. Hydrological factors in the interpretation of stable isotopic proxy data present and past: a European perspective. Quaternary Science Reviews 23, 743–770. doi:10.1016/j.quascirev.2003.06.016.

Deines, P., Lagmuir, D., Harmon, R.S., 1974. Stable isotope ratios and existence of gas phase in the evolution of carbonate groundwaters. Geochimica Et Cosmochimica Acta 38, 1147–1164.

Drucker, D.G., Bocherens, H., Billiou, D., 2003. Evidence for shifting environmental conditions in south west France from 33,000 to 15,000 years ago derived from carbon-13 and nitrogen-15 natural abundances in collagen of large herbivores. Earth and Planetary Science Letters 216, 163–173.

Douez, O., 2007. Réponse d'un système multicouche aux variations paléoclimatiques et aux solicitations anthropiques: Approche par modélisation couplée hydrodynamique, thermique et géochimique. Doct. Thesis. Univ. Bordeaux 3, 306 p.

Edmunds, W.M., Shand, P., 2008. Natural Groundwater Quality. Blackwell Publishing, Oxford, UK. 469 p..

Edmunds, W.M., Ma, J.Z., Aeschbach-Hertig, W., Kipfer, R., Darbyshire, D.P.F., 2006. Groundwater recharge history and hydrogeochemical evolution in the Minqin Basin, North West China. Applied Geochemistry 21, 2148–2170. doi:10.1016/j.apgeochem.2006.07.016.

Eichinger, L., 1983. A contribution to the interpretation of $^{14}C$ groundwater ages considering the example of a partially confined sandstone aquifer, In: Stuvier, M., Kra, R.S., (Eds.), Proceedings of the 11th International $^{14}C$ Conference, Radiocarbon, vol. 25(2), pp. 347–356.

Emblanch, C., 1997. Les équilibres chimiques et isotopiques du carbon dans les aquifères karstiques: étude en région méditeranéen de montagne. Doct. Thesis Univ. Avignon, 198 p.

Evans, G.V., Otlet, R.L., Downing, A., Monkhouse, R.A., Rae, G., 1979. Some problems in the interpretation of isotope measurements in United Kingdom aquifers. In: Isotope Hydrology II. IAEA, Vienna, pp. 79–708.

Ferronsky, V.I., Polyakov, V.A., Ferronsky, S.V., 1991. Isotope variations in water in the hydrological cycle as a tool in a climate change mechanism study. In: Isotope Techniques in Water Resources Development. IAEA, Vienna, pp. 67–586.

Fontes, J.C., 1985. Some considerations on ground water dating using environmental isotopes. Hydrogeology in the Service of Man. Memoires of the 18th Congress of the International Association of Hydrogeologists, Cambridge, pp. 188–154.

Fontes, J.C., Garnier, J.M., 1979. Determination of the $^{14}C$ initial activity of total dissolved carbon: a review of the existing models and a new approach. Water Resources Research 15, 399–413.

Gallagher, D., McGee, E.J., Kalin, R.M., Mitchell, P.I., 2000. Performance of Models for Radiocarbon Dating of Groundwater, An Appraisal Using Selected Irish Aquifers. University of Arizona, Department of Geosciences, Tucson, USA, pp. 235–248.

Heaton, T.H.E., Talma, A.S., Vogel, J.C., 1986. Dissolved gas palaeotemperatures and $^{18}O$ variations derived from groundwater near Uitenhage, South Africa. Quaternary Research 25, 79–88.

Huneau, F., 2000. Fonctionnement hydrogéologique et archives palaeoclimatiques d'un aquifère profond mediteranéen. Doct. Thesis. Univ. Avignon, 180 p.

Huneau, F., Travi, Y., 2008. The Miocene aquifer of Valréas, France. In: Edmunds, W.M., Shand, P. (Eds.), NaturalGroundwater Quality. Blackwell Publishing, London, pp. 87–305.

Huneau, F., Blavoux, B., Bellion, Y., 2001. Differences between hydraulic and radiometric velocities of groundwaters in a deep aquifer: example of the Valréas Miocene aquifer (southeastern France). Comptes Rendus de l'Academie de Sciences – Serie IIa: Sciences de la Terre et des Planetes 333 (3), 163–170.

Ingerson, E., Pearson, F.J., 1964. Estimation of age and rate of motion of groundwater by the $^{14}C$-method. In: Recent Researches in the Fields of Hydrosphere, Atmosphere and Nuclear Chemistry. Maruzen Co, Tokyo, pp. 263–283.

Jost, A., 2005. Caractérisation des forçages climatiques et géomorphologiques des cinq derniers millions d'années et modélisation de leurs conséquences sur un système aquifère complexe: le bassin de Paris. Doct. Thesis. Univ. Pierre et Marie Curie, Paris VI, 344 p.

Jouzel, J., Hoffmann, G., Koster, R.D., Masson, V., 2000. Water isotopes in precipitation: data/model comparison for present-day and past climate. Quaternary Science Reviews 19, 363–379.

Kimmelmann, A.A., Reboucas, A.C., Santiago, M.M.F., Gouvea Da Silva, R.B., 1989. Isotopic study of the Boutucatu aquifer system in the Brazilian portion of the Parana Basin. In: Isotope Hydrology Investigations in Latin America, IAEA-TECDOC – 502. IAEA, Vienna, pp. 51–71.

Kloppmann, W., Dever, L., Edmunds, W.M., 1998. Residence time of chalk groundwaters in the Paris Basin and the North German Basin: a geochemical approach. Applied Geochemistry 13 (5), 593–606.

Landreau, A., Mariotti, A., Simon, B., 1988. La dénitrification naturelle dans les eaux souterraines. Hydrogéologie 1, 35–43.

Larroque, F., Treichel, W., Dupuy, A., 2008. Use of unit response functions for management of regional multilayered aquifers: application to the North Aquitaine Tertiary system (France). Hydrogeology Journal 16, 215F–233F. doi:10.1007/s10040-007-0245-2.

Le Gal La Salle, C., Marlin, C., Savoye, S., Fontes, J.C., 1996. Geochemistry and $^{14}C$ dating of groundwaters from Jurassic aquifers of North Aquitaine Basin (France). Applied Geochemistry 11, 433–445.

Loosli, H.H., Aeschbach-Hertig, W., Barbecot, F., Blaser, P., Darling, W.G., Dever, L., Edmunds, W.M., Kipfer, R., Purtschert, R., Walraevens, K., 2001. Isotopic methods and their hydrogeochemical context in the investigation of palaeowaters. In: Edmunds, W.M., Milne, C.J. (Eds.), Palaeowaters in Coastal Europe: Evolution of Groundwater Since the Late Pleistocene. Geological Society of London, Geol. Soc. Special Publication, London, pp. 193–212.

Love, A.J., Herczeg, A.L., Leany, F.W., Stadter, M.F., Dighton, J.C., Armstrong, D., 1994. Groundwater residence time and palaeohydrology in the Otway Basin, South Australia: $^{2}H$, $^{18}O$ and $^{14}C$ data. Journal of Hydrology 153, 157–187.

Mariotti, A., 1994. Dênitrification in situ dans les eaux souterraines, processus naturels ou provoqués. Hydrogéologie 3, 43–68.

Marlin, C., 1996. Estimation du temps de résidence des eaux souterraines des aquifères du Crêtacê et du Jurassique, Coniacien–Turonien, Cênomanien et Infra-Callovien, dêpartement de la Charente-Maritime. Université Paris-Sud, Laboratoire d'Hydrologie et Gêochimie isotopique. Technical Report, 32p.

Marlin, C., Van Exter, S., Raguideau, A., 1998. Estimation du temps de résidence des eaux souterraines des aquifères du Crétacé Supérieur dans le département de Charente-Maritime. Universitê Paris-Sud, Laboratoire d'Hydrologie et Gêochimie isotopique. Technical Report, 18p.

Mazor, E., 2004. Chemical and Isotopic Groundwater Hydrology, third ed. Marcel Dekker, New York. 453 p.

Mêteo France, <http://www.meteofrance.com/FR/climat/index.jsp> [cited Avril 2008].

Mook, W.G., 1972. On the resconstruction of the initial $^{14}C$ content of groundwater from the chemical and isotopic composition. In: Rafter, T.A., Grand Taylor, T. (Eds.), Proceedings of the 8th International $^{14}C$ Conference. Royal Society of New Zealand, Wellington, pp. 342–352.

Mook, W.G., 1976. The dissolution-exchange model for dating groundwater groundwater with $^{14}C$. In: Interpretation of Environmental Isotope and Hydrochemical Data in Groundwater Hydrology. IAEA, Vienna, pp. 13–225.

Mook, W.G., 1979. On the carbon isotope fractionation during precipitation of calcium carbonate. In: Proceedings Symp. AdvisoryGroup Meeting. IAEA, Vienna, pp. 213–225.

Mook, W.G., 1980. Carbon-14 in hydrogeological studies. In: Fritz, P., Fontes, J.C. (Eds.), Handbook of Environmental Isotopes Geochemistry 1. Elsevier, Amsterdam, pp. 50–74.

Mouragues, N., 2000. Caractêrisation et vulnérabilité d'un hydrosystême complexe sub-profond associé à la structure anticlinale de Jonzac. Doc. Thesis. Univ. Bordeaux1, 187 p.

Mourier, J.P., Gabilly, J., 1985. Le Lias et le Dogger au Sud-Est du Seuil du Poitou, tectonique synsédimentaire, paléogéographie. Géologie de la France 3, 293–310.

O.R.E. (Observatoire Rêgional de l'Environnement Poitou-Charentes), Rêseau Piézométrique Régional, <http://www.observatoire-environnement.org/OBSERVATOIRE/piezometre/etat-piezometrique.html> [cited April 2008].

Petelet-Giraud, E., Casanova, J., Chery, L., Nêgrel, P., Bushaert, S., 2005. Attempt of isotopic characterisation ($\delta^{18}O$ and $\delta^{2}H$) of present rainwater signature using lakes and reservoirs. Application to south-western France. La Houille Blanche 2, 57–62.

Peyron, O., Guiot, J., Cheddadi, R., Tarasov, P., Reille, M., De Beaulieu, J.L., Bottema, S., Andrieu, V., 1998. Climatic reconstruction in Europe for 18,000 YR BP from pollen data. Quaternary Research 49, 183–196.

Phillips, F.M., Peeters, L.A., Tansey, M.K., Davis, S.N., 1986. Paleoclimatic inferences from an isotopic investigation of groundwater in the central San Juan Basin, New Mexico. Quaternary Research 26, 179–193.

Purtschert, R., Corcho Alvarado, J.A., Loosli, H.H., 2008. Dating examples in European reference aquifers. In: Edmunds, W.M., Shand, P. (Eds.), Natural Groundwater Quality. Blackwell Publishing, London, pp. 109–130.

Rozanski, K., 1985. Deuterium and oxygen-18 in European groundwaters – links to atmospheric circulation in the past. Chemical Geology 52, 349–363. doi:10.1016/0168-9622(85)90045-4.

Rozanski, K., Araguas-Araguas, L., Gonfiantini, R., 1992. Relation between long-term trends of oxygen-18 isotope composition of precipitation and climates. Science 258, 981–984.

Rudolph, J., Blavoux, B., Dray, M., Olive, P., 1984. Utilisation des gaz rares pour la dêtermination des conditions climatiques lors de la recharge des nappes aquifêres profondes. Cas des grês triasiques de Lorraine. 10ème rêunion annuelle des sciences de la terre, Bordeaux, Soc. Gêol. Fr. Edit. Paris, p. 490.

Salem, O., Visser, J.H., Dray, M., Gonfiantini, R., 1980. Groundwater flow patterns in the western Lybian Arab Jamahiriaya. In: Arid-Zone Hydrology: Investigation with Isotope Techniques. IAEA, Vienna, pp. 165–179.

Savoye, S., 1993. Etude chimique et isotopique des eaux de l'aquifêre Infra-Callovien du Bassin Aquitain. DEA University Paris-Sud, Centre d'Orsay, 100 p.

Sonntag, C., Klitsch, E., Loehnert, P., Munnich, K.O., El Shazly, E.M., Kalinke, C., Thorweihe, U., Weistroffer, K., Swailem, F.M., 1978. Paleoclimatic information from deuterium and oxygen-18 in carbon-14 dated north Saharian groundwaters. In: Groundwater Formation in the Past. Isotope Hydrology. IAEA, Vienna, p. 569 p..

Stute, M., Deak, J., 1989. Environmental isotope study ($^{14}C$, $^{13}C$, $^{18}O$, D, noble gases) on deep groundwater circulation systems in Hungary with reference to palaeoclimate. Radiocarbon 31, 902–918.

Stute, M., Schlosser, P., Clark, J.F., Broecker, W.S., 1992. Paleotemperatures in the Southwestern United States derived from noble gases in ground water. Science 256, 1000–1003.

Stute, M., Forster, M., Frischkorn, H., Serejo, A., Clark, J.F., Schlosser, P., Broecker, W.S., Bonani, G., 1995. Cooling of tropical Brazil during the last glacial maximum. Science 269, 379–383.

Tamers, M.A., 1967. Radiocarbon ages of groundwater in an arid zone unconfined aquifer, In: Isotope Techniques in the Hydrological Cycle. American Geophysical Union Monograph, vol. 11, pp. 143–152.

Texier, J.P., Bertran, P., 1993. Données nouvelles sur la présence d'un pêrgelisol en Aquitaine au cours des dernières glaciations, Permafrost Periglac. Process 4, 183–198.

Thompson, L.G., Mosley-Thompson, E., Davis, M.E., Lin, P.N., Henderson, K.A., Cole-Dai, J., Bolzan, J.F., Liu, K.B., 1995. Late glacial stage and Holocene tropical ice core records from Huascaran, Peru. Science 269, 46–50.

Zhang, Z.H., Shen, Z.L., Xue, Y.Q., Ren, F.H., Shi, D.H., Yin, Z.Z., Zhon, Z.X., Sun, X.H., 2000. Evolution of Groundwater Environment in North China Plain. Geological Publish House, Beijing.

Zhu, G.F., Li, Z.Z., Su, Y.H., Ma, J.Z., Zhang, Y.Y., 2007. Hydrogeochemical and isotope evidence of groundwater evolution and recharge in Minqin Basin, Northwest China. Journal of Hydrology 333, 239–251. doi:10.1016/j-jhydrol.2006.08.013.

Zuber, A., Weise, S.M., Motyka, J., Osenbrück, K., Rozanski, K., 2004. Age and flow pattern of groundwater in Jurassic limestone aquifer and related tertiary sands derived from combined isotope, noble gas and chemical data. Journal of Hydrology 286, 87–112.

## 4.6 Carbon isotopes to constrain the origin and residence time of groundwater in the Cretaceous Basin of Bohemia (Czech Republic)

*Published as:*

*Jiráková, H., Huneau, F., Hrkal, Z., Le Coustumer, P., Celle-Jeanton, H., 2010. Carbon isotopes to constrain the origin and residence time of groundwater in the Cretaceous Basin of Bohemia (Czech Republic). Applied Geochemistry [doi:10.1016/j.apgeochem.2010.05.012]*

Applied Geochemistry 25 (2010) 1265–1279

Contents lists available at ScienceDirect

Applied Geochemistry

journal homepage: www.elsevier.com/locate/apgeochem

# Carbon isotopes to constrain the origin and circulation pattern of groundwater in the north-western part of the Bohemian Cretaceous Basin (Czech Republic)

Hana Jiráková [a,b], Frédéric Huneau [a,*], Zbyněk Hrkal [b,c], Hélène Celle-Jeanton [d,e,f], Philippe Le Coustumer [a]

[a] Université de Bordeaux, GHYMAC Géosciences Hydrosciences, B18 Avenue des Facultés, 33405 Talence, France
[b] Charles University, Institute of Hydrogeology Engineering Geology and Applied Geophysics, Albertov 6, 128 43 Prague 2, Czech Republic
[c] Water Research Institute TGM, Podbabská 30, 160 62 Prague 6, Czech Republic
[d] Clermont Université, Université Blaise Pascal, Laboratoire Magmas et Volcans, BP 10448, 63000 Clermont-Ferrand, France
[e] CNRS, UMR 6524, LMV, 63038 Clermont-Ferrand, France
[f] IRD, R 163, LMV, 63038 Clermont-Ferrand, France

A R T I C L E I N F O

*Article history:*
Received 23 July 2009
Accepted 31 May 2010
Available online 4 June 2010

Editorial handling by W.M. Edmunds

A B S T R A C T

The Bohemian Cretaceous Basin represents a complex hydrogeological system composed of several aquifers with very favourable hydrogeological properties. These aquifers have been exploited for many years. The sustainability of such resources might be guaranteed by well organised water management, which requires a detailed knowledge about the functioning of the hydrogeological system. Although many efforts have previously been made to evaluate groundwater residence time, the many intricate geochemical processes complicate groundwater dating. The current study clarifies the functioning of this complex hydrogeological basin using hydrogeochemical and isotopic investigations. Chemical data and a combination of $^{13}C$ and $^{14}C$ isotopes within the Cenomanian and the Turonian layers indicate groundwater interactions with deep-seated $CO_2$, rock matrix, surface waters and fossil organic matter. Very depleted $\delta^{13}C$ values (average $\delta^{13}C \sim$ 13.4‰) suggest interactions with fossil organic matter, whereas enriched values account for the interaction with deep $CO_2$ gas ascending from the upper mantle via the numerous faults and fractures, and also, to a lesser extent, from calcite dissolution. Geochemical processes that take place in the system cause a clear depletion in $^{14}C$ that greatly complicates groundwater residence time evaluation. Different dilution correction models have been applied considering the different C origins. The stable isotope content, mainly $^{18}O$ values, indicates both the contribution of modern precipitation and the partial infiltration of palaeowaters during colder climatic conditions from the end of the Pleistocene. The apparent $^{14}C$ groundwater ages range from modern to 11.1 ka BP, which suggests some post glacial infiltration from melting ice sheets. Finally, all the acquired information was used to propose a conceptual model of C origin within the basin.



## 1. Introduction

The Bohemian Cretaceous Basin (BCB) is the largest sedimentary complex of the Czech Republic. Because of its favourable hydrogeological conditions, it has been exploited for more than a century, most often for water supply and geothermal purposes. Nowadays, with the increasing exploitation of drinking and thermal waters, a new challenge appears, to protect the BCB groundwater. Groundwater in deep sedimentary formations represents an important strategic resource that often replaces conventional water supply from shallow reservoirs and/or from crystalline rocks following pollution or even catastrophic events in order to prevent disease epidemics and/or to guaranty the access of populations to safe drinking water supply. This was particularly true during the huge floods of 2002 in the whole of Central Europe (Šilar, 2007). Deep aquifers with long residence time waters are also well protected from all negative climatic events leading to the decrease of infiltration (lower amount of precipitation, increase in temperature or/and evapotranspiration rate modification, etc.). Thus groundwater resources from deep sedimentary formations can guarantee the sustainable development of water supply (Raoult et al., 1997, 1998; Edmunds et al., 2002; Jost, 2005; Douez, 2007; Celle-Jeanton et al., 2009); but, in many places, they should be better constrained in order to sustain them.

Environmental isotope techniques have been applied in many regional and local investigations in order to understand the origin of water, the flow paths, the residence time and the geochemical processes within aquifers (Marques et al., 1996; Edmunds and Smedley, 2000; Huneau and Blavoux, 2000; Birkle et al., 2001; Huneau et al., 2001; Edmunds et al., 2003; Edmunds, 2005; Carreira et al., 2008; Edmunds and Shand, 2008; Huneau and Travi, 2008;

* Corresponding author. Tel.: +33 5 40 00 88 41; fax: +33 5 40 00 31 13.
*E-mail address:* frederic.huneau@u-bordeaux1.fr (F. Huneau).

0883-2927/$ - see front matter © 2010 Elsevier Ltd. All rights reserved.
doi:10.1016/j.apgeochem.2010.05.012

Coetsiers and Walraevens, 2009; Celle-Jeanton et al., 2009; Jiráková et al., 2009). Isotopic hydrogeology, with various approaches for groundwater dating notably by using C isotopes, has already been used in the Czech Republic (Šilar, 1976, 1989; Bates et al., 2007; Pačes et al., 2008). The results of these studies showed that the majority of groundwater in the platform sediments of the whole Bohemian Massif are within the limits of radiocarbon dating and that some waters reveal both $^{3}H$ content and very low radiocarbon activity, indicating that complex interaction processes could be involved and could have lead to a modification of the original isotopic signature.

This paper presents a global re-evaluation and synthesis of the data obtained from different studies with special emphasis on the origin of C isotopes in groundwater. At present, the simplest approach to radiocarbon dating of groundwater assumes that $^{14}C$ moves with the water molecules along the flow path and that the main mechanism enabling the change of the $^{14}C$ content is radioactive decay. In most situations this is not the case, because the signature may be diluted, particularly by $^{14}C$-free sources (Carreira et al., 2008). The determination of the main geochemical processes within the aquifers allowed introducing several dating techniques to estimate the apparent radiocarbon groundwater age. Knowledge of water origin is then essential to understand the geochemistry and the dynamics of the groundwater system which is fundamental to manage the sustainability of the exploitation of groundwater resources.

## 2. Study area

### 2.1. General setting

The BCB is the most extensive continuous sedimentary basin of the platform cover of the Bohemian Massif. It extends over an area of about 14,600 $km^2$, of which 12,490 $km^2$ lie within the territory of the Czech Republic (Fig. 1). On the west, the basin crosses the border with Germany and extends towards the Dresden area. The study area covers approximately 6000 $km^2$. The west and the north borders are formed by mountain ridges. The climate is continental humid with mean annual temperatures from 7 °C to 9 °C (data from 1961 to 1990; Czech Hydrometeorological Institute, 2009). The temperatures are controlled mainly by altitude differences which range between 100 and 700 m a.s.l. for the majority of study area. The annual precipitation has a zonal character ranging from 500 mm in the south up to 1000 mm in the north (data from 1961 to 1990; Czech Hydrometeorological Institute, 2009). The recharge of the Cenomanian and Turonian aquifers occurs mainly in the north-eastern part of the study area which corresponds to a mountainous area. The infiltrated water follows the hydraulic gradient and flows towards the Labe River which represents the main drainage axis of the basin.

### 2.2. Geological setting and tectonics

The BCB is an intra-continental basin formed as a seaway between the North Sea Basin and the Tethys Ocean. A simplified geology with major structural characteristics is displayed in Figs. 1 and 2. The basement is formed by partially metamorphosed Proterozoic and Palaeozoic rocks, locally pierced by intrusive rocks. The occurrence of volcanic rocks is very scattered throughout the north-western area. The basement is in some places covered with Permo-Carboniferous beds of both sediments (claystones, siltstones, greywackes, arkoses, conglomerates) and volcanic rocks (Klein, 1979). This geological succession (Fig. 3) extends mainly over the south with a few occurrences in the north (Krásný, 1973; Fediuk, 1996). Some of the Permo-Carboniferous sediments may contain fossil organic matter, particularly black coal deposits identified mainly in the south-eastern part of the study zone, with a maximum thickness of several hundreds of meters SW from Mladá Boleslav (Jetel, 1982). Permo-Carboniferous sediments do not outcrop in the study zone, they are only found to the NE of the study area. During the Variscan, major folding and metamorphic events occurred. The BCB was formed by the reactivation of a fault system in the Variscan basement of the Bohemian Massif during the mid-Cretaceous (Uličný, 1997, 2001). The sediments accumulated from the Early Cenomanian or even from the Late Albian to the Santonian. The Upper Cretaceous sediments in this region show a particular dominance of sandstones, locally very rich in quartz (up to 99%) over other rock types. Six lithostratigraphic units can be distinguished, from the oldest to the youngest respectively: Late Albian, Cenomanian (marine deposits), Lower Turonian, Middle Turonian, Upper Turonian, Coniacian and Santonian. Čech et al. (2005) observed abundant plant debris in the marine Cenomanian beds and Kolářová and Krásný (1972) confirmed the occasional occurrence of carbonized wood and plant detritus within the marine Cenomanian sediments. Similarly, on the basis of well-logging measurements, Datel et al. (2009) identified some sandstone beds within the Cenomanian aquifer containing fossil organic material. According to Pačes et al. (2008), siltstones and clays in the Cenomanian locally contain up to 1% fossil organic C.

The thickness of the sedimentary formation in the BCB typically ranges between 200 and 400 m, but in the vicinity of the city of Děčín reaches up to 1200 m. Tertiary sediments and frequent small occurrences of intrusive rocks forming volcanic hills and mountains markedly affect the surface. The sedimentary succession in this area is considerably affected by fault structures of local and regional importance. The Saxonic block-fault tectonics has substantially influenced the development of the Bohemian Massif after the end of the Variscan orogenesis, when the Bohemian Massif became a rising consolidated block (Malkovský, 1976). Numerous faults are still important. The principle directions of displacement zones are SW–NE (Erzgebirge) and NW–SE (Sudetic). The Ohře (Eger) rift, active from the Oligocene to the Pleistocene (Kopecký, 1978), is the most dominant structure in western Bohemia and strikes the study area only with its marginal faults (Krušné Hory and Litoměřice fault). Many distinct volcanic features are defined within the Ohře (Eger) rift, but the volcanic activity in the Labe (Elbe) zone is less obvious. The intersection of the zone with the Ohře (Eger) rift coincides with the Pliocene neovolcanic event made up of an extrusion of nephelinite basanite to olivine basalt. The maximum tectonic vertical movement took place along the Krušné Hory fault. The total throw is estimated to be about 800–1500 m. Ductile deformation of the Cretaceous sediments (folds) is present across the whole basin with fold structures with a W–E direction formed in the initial phases of the Saxonian tectogenesis and that are not continuous over the whole area. The folds were sometimes displaced by faulting during subsequent deformational phases (Malkovský, 1976; Herčík et al., 1999).

### 2.3. Hydrogeological setting

The BCB has been extensively exploited for water supply since the 1930s as a consequence of the favourable hydraulic parameters and high quality of groundwater. Groundwater has already been investigated by various researchers (Hynie, 1949, 1961; Hercog, 1965; Kliner and Kněžek, 1974; Jetel and Krásný, 1976; Herčík et al., 1999; Bates et al., 2007) confirming that this part of the BCB is one of the most complex hydrogeological structures of the entire basin. Its complexity lies in the laterally and vertically unstable lithofacies evolution of the Cretaceous cover. The whole structure was slightly folded and broken into numerous blocks displaced hundreds of meters inducing a very complicated hydrogeo-

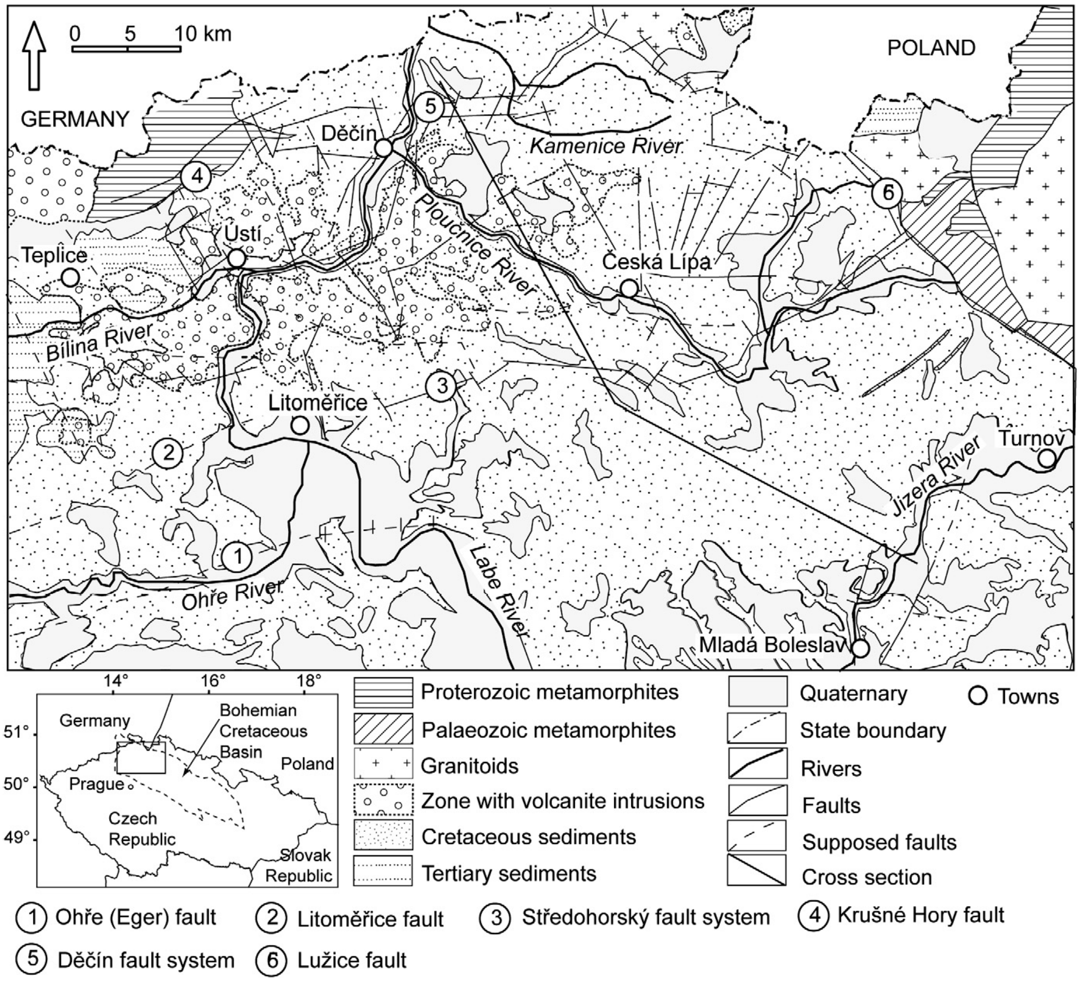


**Fig. 1.** Schematic geological map of the study area with main tectonic features and cross-section.

logical regime. The most significant groundwater resources belong to the central structure which is formed by the lowered block. The organisation of aquifers is mainly subhorizontal and differs according to their position within the study area. Fig. 2 shows the aquifer organisation in a selected cross-section. Within the BCB the following succession of aquifer layers can be found:

(1) Basal Aquifer A in the Cenomanian (occasionally connected to the Lower Turonian forming AB aquifer).
(2) Aquifer B in the Lower Turonian.
(3) Aquifer C in the Middle Turonian.
(4) Aquifer D in the Upper Turonian–Coniacian–Santonian.

The basal Aquifer A is formed by the Cenomanian sandstones and is about 50 m thick, with sporadic claystone layers. It is generally confined and present throughout the whole area. Transmissivity, as a function of the intergranular porosity and numerous fractures (Jetel and Rybářová, 1991) is about 64 $m^2$/day; mean porosity has been determined to be about 20% (Herčík et al., 1999). Aquifer A forms an extended flux field asymmetrically divided by the Labe (Elbe) River into two sections. The dynamics of groundwater circulation in the Cenomanian aquifer are controlled by the piezometric level of the recharge area in the north and the height above sea level of the discharge areas along the drainage of local rivers – Labe (Elbe), Kamenice and Ohře (Eger). The average effective velocity of groundwater flow varies between 0.06 and 0.6 m/a (Jetel and Rybářová, 1991). The Cenomanian aquifer is generally well separated from the overlying aquifer by the marly layer of the Lower Turonian. This impermeable layer is absent only in the south-western part. There, the Cenomanian and the Turonian aquifer form a continuous formation (AB). The Lower–Middle Turonian aquifers (C, BC) with an average thickness of about 150 m are developed mostly of siltstones and sandstones in an area on the right bank of the Labe (Elbe) River, where they host the largest resources of groundwater in the whole Cretaceous Basin. Groundwater of the Turonian aquifer is unconfined over almost the whole

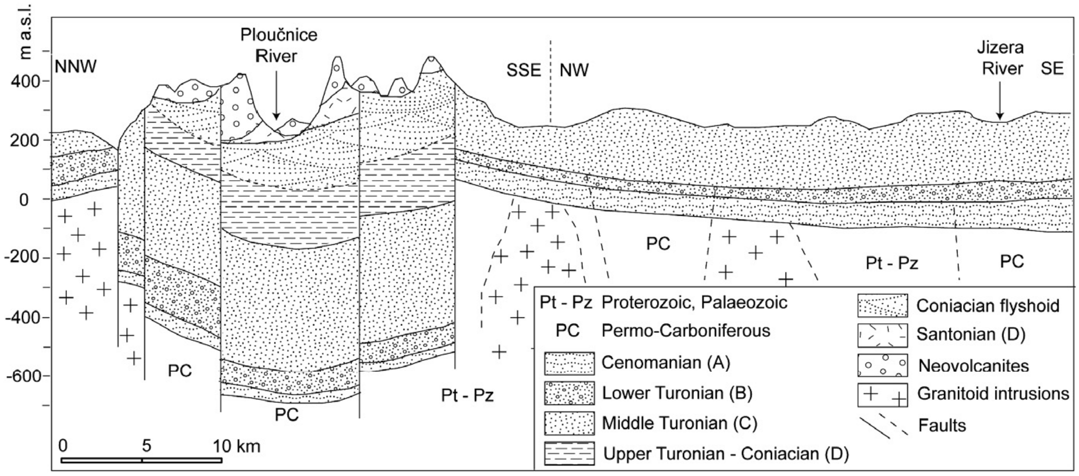


**Fig. 2.** Schematic cross-section with main aquifers (modified from Herčík et al. (1999)).

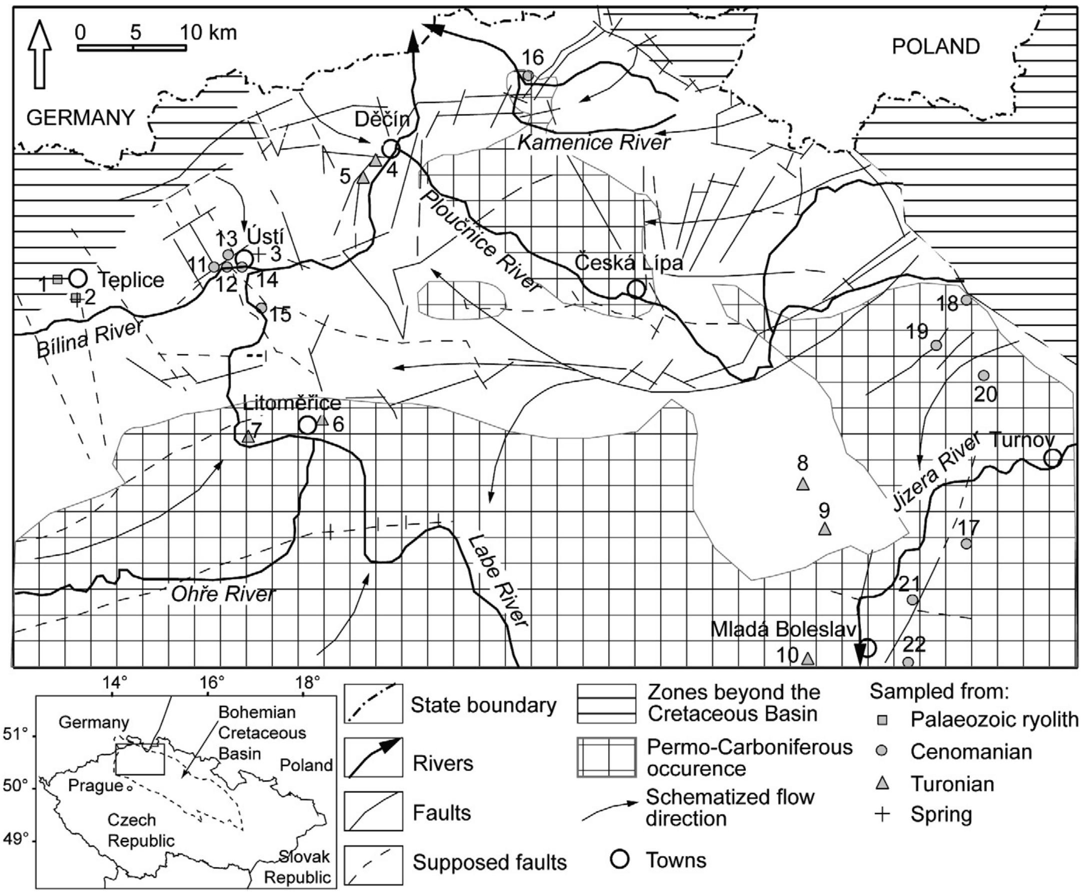


**Fig. 3.** Location of sampling points, flow direction and Permo-Carboniferous occurrence.

western part of the BCB. Confined levels are only found in the area where the Turonian sandstones are overlain by the Upper Turonian aquitard. The permeability is both of intergranular and fissured types and generally decreases towards the SE due to the lithofacies development of the entire Cretaceous complex. The highest average transmissivity coefficient in the aquifer has been documented on the northern margin with a value of 762 $m^2$/day, while the lowest values (about 48 $m^2$/day) were encountered in the southern part (Herčík et al., 1999). On the east, the flow direction is influenced by the drainage effect of the Jizera River. In general, the groundwater of aquifer C (or BC) is drained by the surface watercourses. From the water management point of view, the Turonian aquifer plays the major role with its significant thickness and favourable hydrogeological parameters. The general flow direction in the study area is globally similar for Cenomanian and Turonian aquifer as shown by the piezometric data collected between 1985 and 1987 (Herčík et al., 1999). Although the tectonics has some consequences on the piezometric level, the effect of faults on the regional groundwater flow direction is insignificant (Šilar, 1976; Herčík et al., 1999). The general flow direction is schematized in Fig. 2. The uppermost aquifer in Coniacian–Santonian (D) is composed of sandstones which discontinuously crop out in the central part of the area of interest. The permeability is of combined intergranular and fissured types. Aquifer D is not generally of high hydrogeological significance.

It is relevant to mention, that some spas are located in the study area, or in its environs. Teplice, on the west, is among the most famous and the discovery of its warm springs goes back to 762 AD. The coal mining activities in the region have affected the hydraulic properties of the spring and consequently its flow rate has decreased considerably (Čadek, 1968). The water of Teplice originates from a Palaeozoic porphyry and is hydraulically connected with the surface water bodies of the Tertiary aquifers.

## 3. Database setup and methodology

This paper provides a review of studies carried out in the northwestern part of the BCB (Šilar, 1976, personal communication; Pačes et al., 2008); the dataset of 22 samples is introduced in Table 1. The most extensive isotopic database for the Czech massif has been provided by Šilar (1976), nevertheless only two samples are located within the research area. For these, the Total Dissolved Inorganic C (TDIC) was collected in the field in the form of a precipitate of $BaCO_3$. The samples were analysed in the laboratory of the International Atomic Energy Agency, Vienna, by β counting. Most of the analyses in Table 1 come from an unpublished dataset acquired by the same author during the years 1972–2002 (Silar, personal communication). The majority of the samples belong to the Turonian and the Cenomanian aquifers. Eight more measurements from the eastern part of the study area come from the study of Pačes et al. (2008); including three Turonian and five Cenomanian samples.

Besides the isotopic signature ($^{13}C$, $^{14}C$, $^{3}H$, $^{18}O$, if available), Table 1 gives an information on coordinates (S-JTSK/Křovák coordinate system, adapted for the territory of former Czechoslovakia), depth and reached aquifer. Oxygen-18 content of the water samples are reported in ‰ vs. Standard Mean of Ocean Water (SMOW), radiocarbon as percent of modern C (pmC) and $\delta^{13}C$ is expressed with respect to Pee Dee Belemnite (PDB). The spatial distribution of the investigated 22 wells is displayed in Fig. 3.

The isotopic dataset obtained rarely contains complete information on groundwater geochemistry and this led the authors to set up a new dataset on chemistry. Some chemical analyses have been collected from the studies of Šilar (1976) and Pačes et al. (2008) which accompany the isotopic information described above. To add more information on the chemistry of the different aquifers, analyses were gathered from the archive of the Czech Geological

**Table 1**
Location of the sampling points in the S-JTSK/Křovák coordinate system, main physico-chemical characteristics related to carbonate equilibrium and isotopic content.

| No. | Location | X | Y | Z (m) | Depth (m) | Aquifer | T (°C) | pH | $HCO_3$ (mg/L) | $\delta^{18}O$ (‰ vs. SMOW) | $^3H$ (TU) measured | $^3H$ (TU) corrected for 2009 | $\delta^{13}C$ (‰ vs. PDB) | $^{14}C$ (pmC) | Date | References |
|---|---|---|---|---|---|---|---|---|---|---|---|---|---|---|---|---|
| 1 | Teplice 1 | −776,069 | −976,279 | 222 | 941 | Pal | 41.5 | 6.7 | 546 | −9.4 | 13.5 ± 1.7 | 8.2 | −5.9 | 21.6 ± 3 | 2000 | a |
| 2 | Teplice 2 | −776,050 | −976,460 | 192 | 54 | Pal | 36.0 | 6.5 | 673 | −9.8 | 13.5 ± 1.7 | 8.2 | −5.4 | 21.6 ± 3 | 2000 | a, b |
| 3 | Ústí-spring | −761,512 | −975,582 | 150 | – | Q | – | – | – | – | 12.6 | 6.8 | −14.1 | 89.9 ± 1.5 | 1998 | a |
| 4 | Děčín | −747,600 | −966,100 | 131 | 240 | T | 24.9 | 6.7 | 138 | −11.2 | 8.5 ± 2.5 | 5.1 | −9.3 | 10.9 ± 5 | 2000 | a |
| 5 | Vilsnice | −749,590 | −967,774 | 143 | 175 | T | 21.8 | 6.9 | 236 | −10.9 | 8.5 ± 1.7 | 5.1 | −6.4 | 5.3 ± 1 | 2000 | a |
| 6 | Litoměřice | −756,526 | −990,115 | 246 | 76 | T | 11.8 | 6.8 | 450 | −8.6 | 4.8 | 3.2 | −9.1 | 39.0 ± 3 | 2002 | a |
| 7 | Píšťany | −760,893 | −991,960 | 250 | 125 | T | 12.7 | 6.5 | 764 | −8.9 | 7.9 ± 2.5 | 5.3 | −7.4 | 33.9 ± 3 | 2002 | a |
| 8 | Bělá p. Bezdězem | −707,600 | −997,900 | 300 | 200 | T | – | 7.1 | 287 | – | <1.2 | 0.0 | −12.7 | 73.4 | 2003 | c |
| 9 | Čistá | −707,600 | −10,03,900 | 275 | 201 | T | – | 7.4 | 247 | – | <1.2 | 0.0 | −13.0 | 63.8 | 2003 | c |
| 10 | Mladá Boleslav 1 | −707,900 | −10,12,100 | 235 | 29 | T | – | 7.1 | 311 | – | 8.7 | 5.9 | −12.9 | 78.8 | 2003 | c |
| 11 | Předlice | −763,722 | −976,444 | 144 | 500 | C | 22.7 | 6.7 | 348 | −10.7 | 11.0 ± 1.7 | 6.7 | −6.9 | 9.0 ± 3 | 2000 | a |
| 12 | Klíše 1 | −762,980 | −975,950 | 148 | 457 | C | 30.5 | 7.2 | 512 | – | 4.0 | 2.2 | −5.9 | 12.2 ± 5 | 1998 | a |
| 13 | Klíše 2 | −762,855 | −975,175 | 183 | 511 | C | 33.5 | 6.6 | 380 | −10.1 | 8.5 ± 1.7 | 5.1 | −6.5 | 12.0 ± 5 | 2000 | a |
| 14 | Ústí | −761,402 | −975,927 | 146 | 357 | C | 31.7 | 7.6 | – | – | 4.0 | 2.2 | −4.5 | 6.9 ± 3 | 1998 | a |
| 15 | Brná | −759,538 | −980,147 | 142 | 431 | C | 32.7 | 7.6 | 384 | – | 4.2 | 2.3 | −5.3 | 4.8 ± 3 | 1998 | a |
| 16 | Všemily | −734,667 | −959,938 | 280 | 319 | C | – | – | – | – | 8.0 ± 2 | 1.0 | −10.2 | 9.6 ± 3 | 1972 | a, b |
| 17 | Branžež | −691,600 | −10,02,600 | 252 | 439 | C | 22.7 | 6.6 | 88 | −10.2 | 9.3 ± 1.7 | 5.6 | −16.3 | 24.6 ± 3 | 2000 | a |
| 18 | Český Dub | −691,800 | −983,300 | 325 | 219 | C | – | 7.7 | 253 | – | <1.2 | 0.0 | −8.4 | 16.3 | 2003 | c |
| 19 | Všelibice | −698,300 | −988,400 | 380 | 284 | C | – | 7.9 | 201 | – | <1.2 | 0.0 | −12.0 | 53.8 | 2003 | c |
| 20 | Kobyly | −694,200 | −991,000 | 520 | 411 | C | – | 7.8 | 211 | – | <1.2 | 0.0 | −10.6 | 45.8 | 2003 | c |
| 21 | Kněžmost | −695,500 | −10,04,800 | 242 | 410 | C | – | 7.4 | 125 | – | <1.2 | 0.0 | −14.1 | 24.0 | 2003 | c |
| 22 | Mladá Boleslav 2 | −697,900 | −10,12,900 | 235 | 386 | C | – | 7.6 | 101 | – | <1.2 | 0.0 | −13.0 | 14.2 | 2003 | c |

Pal – Palaeozoic, C – Cenomanian, T – Turonian, Q – Quaternary.
a, Šilar (personal communication); b, Šilar (1976); c, Pačes et al. (2008).

Survey ČGS-Geofond in Prague including local and regional research studies (Žitný, 1970; Čapek, 1979; Brožek, 1987; Skořepa, 1993). In total 47 chemical analyses were considered (Table 2) to construct a Piper diagram displaying the different water types.

The main objective of the study is to understand the geochemical processes occurring within the aquifers during groundwater flow leading to modifications of the chemical and isotopic composition. First, the information on chemistry is considered, to determine or identify the processes occurring between rocks and groundwater. Then, the isotopic signature of waters is considered in order to determine the recharge conditions and to establish groundwater origin. For this purpose, C isotopes are used in particular giving evidences of the different geochemical processes taking place within the aquifers. The second goal of this work is to propose a conceptual model of the hydrogeology of the BCB. Carbon isotopes will be mainly considered as tracers to identify C origin in the groundwater system. In addition, an attempt to date groundwater will be made for most samples.

## 4. Results

### 4.1. Chemistry

The chemistry of groundwater is an indicator of the hydrodynamic and geochemical processes taking place within the aquifers. It reflects the flow conditions of groundwater, the interconnection of individual aquifers and often expresses the hydrodynamic role of tectonics and the dominance of certain geochemical processes in the evolution of the chemistry of fresh and mineral waters (Kolářová and Krásný, 1972).

Generally pH values lie in the range between 6.5 and 7.9 indicating that most of the TDIC occurs in the form of $HCO_3$. The maximum temperature in the Cretaceous formation reaches 33.5 °C in a 511 m deep well (No. 13). The Teplice waters from the Palaeozoic range between 36 °C and 41.5 °C. The mineralisation of these thermal waters slightly exceeds 1000 mg/L. The mean Total Dissolved Solids (TDS) of the Turonian aquifer (371 mg/L) is lower than for

**Table 2**
Main physical and chemical characteristics of BCB groundwaters. Geographical position is given in the S-JTSK/Křovák coordinate system.

| Name | *X* | *Y* | Aquifer | pH | *T* (°C) | $Ca^{2+}$ (mg/L) | $Mg^{2+}$ (mg/L) | $Na^{+}$ (mg/L) | $K^{+}$ (mg/L) | $SO_4^{2}$ (mg/L) | Cl (mg/L) | $HCO_3$ (mg/L) | $NO_3$ (mg/L) |
|---|---|---|---|---|---|---|---|---|---|---|---|---|---|
| SH-10 | −769860.0 | −984150.0 | T | 7.6 | 18.0 | 104.3 | 38.8 | 29.8 | 6.2 | 96.1 | 42.5 | 457.7 | 0.0 |
| J-019,835 | −714469.2 | −963175.8 | T | 7.8 | 10.2 | 54.1 | 1.8 | 24.0 | 2.1 | 16.1 | 23.0 | 196.6 | 0.0 |
| SK-1T | −740956.3 | −969256.0 | T | 7.6 | 28.1 | 52.1 | 1.6 | 2.3 | 2.0 | 12.4 | 1.8 | 155.6 | 0.0 |
| VH-1T | −710843.0 | −974437.0 | T | 7.3 | 6.0 | 35.1 | 1.8 | 2.5 | 0.9 | 6.4 | 2.8 | 106.8 | 2.3 |
| VF-1 | −729513.5 | −973202.6 | T | – | – | 32.1 | 1.9 | 5.4 | 2.2 | 11.9 | 1.8 | 125.1 | 1.0 |
| DP-4 | −721932.6 | −972985.3 | T | 7.2 | – | 62.1 | 1.8 | 1.5 | 1.0 | 1.0 | 2.1 | 194.6 | 1.2 |
| VP7523 | −707600.0 | −997900.0 | T | 7.1 | – | 108.3 | 2.2 | 1.7 | 1.0 | 26.9 | 5.8 | 286.8 | 0.0 |
| VP7152 | −707600.0 | −1003900.0 | T | 7.4 | – | 82.2 | 6.8 | 2.9 | 1.1 | 15.1 | 5.6 | 247.1 | 5.7 |
| VP7524 | −707900.0 | −1012100.0 | T | 7.1 | – | 130.9 | 16.0 | 5.0 | 1.6 | 77.4 | 18.8 | 311.2 | 22.2 |
| DL 2 | −700625.0 | −985940.0 | T | 7.1 | 9.8 | 59.9 | 0.3 | 2.0 | 0.8 | 11.5 | 4.3 | 166.0 | 8.5 |
| Rd 3 | −738325.0 | −998750.0 | T | 7.2 | 10.4 | 117.6 | 7.1 | 7.0 | – | 54.3 | 8.9 | 325.2 | 1.1 |
| PV 9 | −758274.6 | −990041.2 | T | 7.6 | – | 126.0 | 76.0 | 10.0 | 19.0 | 472.0 | 14.8 | 318.4 | 0.0 |
| TS-1 | −732670.0 | −1009850.0 | T | 7.0 | – | 135.5 | 15.0 | 6.6 | 3.2 | 99.9 | 20.2 | 341.7 | 0.3 |
| ZP-5 | −729181.7 | −984129.2 | T | 6.9 | 11.1 | 41.5 | 11.1 | 5.0 | 2.5 | 12.0 | 6.7 | 184.3 | 0.3 |
| Be-1 | −715764.0 | −1000549.0 | T | 6.8 | 9.2 | 55.0 | 0.8 | 2.9 | 1.3 | 13.5 | 3.2 | 164.8 | 1.6 |
| RO-1 | −747234.0 | −1004944.5 | T | 6.6 | 12.1 | 220.4 | 79.0 | 19.2 | 10.8 | 439.0 | 53.2 | 485.0 | 0.4 |
| HP1T | −713017.0 | −980563.0 | T | 7.7 | 17.0 | 69.1 | 6.7 | 1.6 | 1.5 | 14.4 | 3.6 | 22.7 | 2.5 |
| Hr-1 | −754260.0 | −997430.0 | T | 8.3 | 11.5 | 88.5 | 33.7 | 124.0 | 21.6 | 136.0 | 35.1 | 544.0 | 0.3 |
| HSP1T | −709538.6 | −1006743.1 | T | 7.2 | 11.4 | 77.4 | 4.6 | 2.5 | 1.1 | 14.4 | 5.3 | 238.6 | 5.6 |
| KL15 | −705469.8 | −1001356.1 | T | 7.0 | – | 83.0 | 1.7 | 2.5 | – | 15.9 | 2.8 | 240.4 | 1.0 |
| L-IV | −694567.0 | −988872.0 | T | 6.9 | 10.0 | 95.4 | 1.2 | 3.0 | 1.5 | 35.0 | 10.6 | 233.1 | 10.3 |
| HU-1 | −762980.0 | −975950.0 | C | 7.2 | 31.5 | 40.8 | 8.3 | 354.5 | – | 229.1 | 51.4 | 704.8 | 0.1 |
| SK-13T | −750930.6 | −971683.7 | C | 7.4 | 23.0 | 37.1 | 6.7 | 74.9 | 9.4 | 36.0 | 16.0 | 289.8 | 0.6 |
| SK-11C | −734274.7 | −972708.0 | C | 6.9 | 24.0 | 38.3 | 1.8 | 8.9 | 3.6 | 14.4 | 2.8 | 133.0 | 0.5 |
| Lo-15JC | −702259.0 | −975168.0 | C | 6.8 | 14.2 | 30.5 | 3.9 | 3.0 | 1.7 | 8.6 | 2.8 | 107.4 | 0.0 |
| Lo-5JC | −725200.0 | −960010.0 | C | 7.1 | 16.0 | 37.9 | 1.9 | 35.0 | 2.0 | 60.5 | 8.9 | 128.1 | 0.8 |
| SK-10C | −720428.9 | −970522.7 | C | 6.8 | 10.0 | 44.0 | 0.9 | 1.0 | 1.0 | 7.0 | 1.8 | 122.6 | 0.0 |
| SK-9C | −719171.0 | −966160.0 | C | 7.0 | 16.0 | 18.0 | 1.8 | 4.7 | 1.3 | 13.5 | 1.8 | 54.9 | 2.2 |
| TH-10 | −763721.7 | −976443.8 | C | – | 28.0 | 28.9 | 3.8 | 233.7 | 17.5 | 214.8 | 28.0 | 445.4 | 0.0 |
| SK-13C | −750913.0 | −971686.6 | C | 7.4 | 22.8 | 23.3 | 3.9 | 338.0 | 13.1 | 117.2 | 76.6 | 710.9 | 0.1 |
| SK-12C | −748000.4 | −974213.6 | C | 7.7 | 26.6 | 45.0 | 5.4 | 16.0 | 8.1 | 24.0 | 1.6 | 170.8 | 0.0 |
| SK-26 | −748618.3 | −980005.2 | C | 7.7 | 30.6 | 40.3 | 8.9 | 15.0 | 5.3 | 25.0 | 3.3 | 162.3 | 0.2 |
| TH-20 | −771087.4 | −975489.0 | C | – | 27.1 | 31.7 | 3.6 | 231.0 | 14.0 | 172.8 | 28.7 | 474.7 | – |
| Mo-3 | −769560.0 | −992680.0 | C | 7.1 | 9.0 | 120.2 | 31.6 | 16.5 | 6.9 | 176.5 | 22.6 | 378.0 | 5.0 |
| Ho-1 | −743585.0 | −997925.0 | C | 7.3 | – | 126.3 | 13.4 | 9.1 | 6.7 | 70.4 | 22.3 | 353.9 | 31.0 |
| O-10 | −742050.0 | −994166.0 | C | 6.7 | 12.4 | 96.2 | 15.8 | 4.7 | 2.0 | 50.6 | 4.6 | 311.2 | 0.0 |
| VP7502 | −691800.0 | −983300.0 | C | 7.7 | – | 64.5 | 12.9 | 3.6 | 4.4 | 3.1 | 3.0 | 253.2 | 0.9 |
| VP7506 | −698300.0 | −988400.0 | C | 7.9 | – | 59.3 | 5.0 | 1.8 | 1.0 | 0.3 | 1.1 | 201.4 | 0.0 |
| VP7500 | −694200.0 | −991000.0 | C | 7.8 | – | 48.1 | 10.2 | 6.1 | 4.6 | 0.3 | 1.9 | 210.5 | 0.0 |
| VP7515 | −695500.0 | −1004800.0 | C | 7.4 | – | 35.0 | 5.9 | 14.4 | 2.4 | 20.6 | 14.8 | 125.1 | 0.0 |
| VP7517 | −697900.0 | −1012900.0 | C | 7.6 | – | 23.0 | 5.1 | 19.9 | 3.0 | 21.5 | 15.9 | 100.7 | 0.0 |
| HP3C | −704332.0 | −977458.0 | C | 7.5 | 12.0 | 83.6 | 10.9 | 1.5 | 2.1 | 105.8 | 1.6 | 184.3 | 0.0 |
| L2-J | −690742.0 | −985167.0 | C | 6.7 | 12.2 | 16.8 | 0.7 | 9.4 | 2.2 | 11.0 | 7.1 | 69.0 | 2.5 |
| L3-J | −687848.0 | −989159.0 | C | 5.2 | 17.6 | 8.0 | 1.0 | 4.0 | – | 13.5 | 5.3 | 19.5 | 0.0 |
| HSP1C | −709598.8 | −1006727.8 | C | 6.8 | 11.8 | 68.7 | 16.9 | 48.5 | 10.7 | 44.7 | 46.1 | 306.3 | 0.3 |
| Teplice Pravridlo | −776050.0 | −976460.0 | Pal | 6.9 | 41.3 | 25.0 | 7.5 | 223.7 | 16.0 | 132.6 | 51.4 | 551.0 | 0.0 |
| Teplice Horsky | −776000.0 | −976000.0 | Pal | 6.9 | 42.2 | 49.5 | 8.4 | 165.8 | 10.0 | 118.1 | 32.3 | 490.0 | – |

Pal – Palaeozoic, C – Cenomanian, T – Turonian.

Cenomanian samples which are around 500 mg/L (Pačes, 1974). Elevated TDS values in the Turonian aquifer were explained by Kolářová and Krásný (1972) as being the result of significant ion-exchange processes particularly in clayey, poorly permeable Turonian rocks.

The dataset contains two Palaeozoic samples, which correspond to the thermal Teplice water, and 24 Cenomanian and 21 Turonian waters. The analyses are displayed in a Piper diagram (Fig. 4). On the whole, the diagram highlights three waters types: Na–$HCO_3$, Ca–$HCO_3$ and Ca–$SO_4$. However water composition in the aquifers is often in a transient state resulting from various processes operating at different timescales (Andersen et al., 2005). Two Palaeozoic samples representing thermal waters in Teplice ($T \sim 40$ °C) reveal a Na–$HCO_3$ type of water. Considering the crystalline geological context of this area, the significant content of $Na^+$ and $HCO_3^-$ ions may result from the weathering and dissolution of silicates such as feldspar from granitic rocks (Appelo and Postma, 2005).

The majority of the Turonian and Cenomanian samples are of Ca–$HCO_3$ type probably as a consequence of calcite dissolution. They were generally sampled on the right bank of the Labe (Elbe) River. As mentioned, the aquifers do not generally contain carbonate rocks (Herčík et al., 1999), but $Ca^{2+}$ and $HCO_3^-$ ions might be produced by the hydrolysis of the calcite cement of the sandstone (Pačes et al., 2008) or in a very limited way by feldspar dissolution in basement rocks.

Some waters tend to be slightly enriched in $SO_4^{2-}$ and $Cl^-$. The $Cl^-$ and $SO_4^{2-}$ content of the Cenomanian waters reaches up to 77 mg/L and 230 mg/L, respectively (Table 2). This may be due to the influence of a local accumulation of connate waters in the basement of the Permo-Carboniferous sediments underlying the Cenomanian aquifer. This is confirmed by the correlations between $Cl^-$ and $Na^+$ (Jetel, 1970). As a consequence, the Ca–$HCO_3$ water type gradually transforms towards a Na–Ca–$HCO_3$ water type or Na–Ca–$HCO_3$–Cl–$SO_4$ water type. This tendency might be explained by the aquifer freshening theory as already observed by several authors in such a sedimentary context (Appelo and Postma, 2005; Andersen et al., 2005). During the aquifer freshening, the mineralised waters are progressively flushed away from aquifers and replaced by freshly infiltrated waters that, therefore, modify the original chemical signature of the aquifer waters. In some places, the elevated $SO_4^{2-}$ concentrations (up to 472 mg/L) could be caused by gypsum dissolution as proposed by Pačes et al. (2008). Cenomanian waters sampled on the left bank of the Labe (Elbe) River, in the proximity of Děčín, Ústí nad Labem and Teplice, plot in the Na–$HCO_3$ water type zone, with temperatures between 25 °C and 34 °C and a composition similar to the Teplice thermal waters. Here, the fractures of the Palaeozoic and Proterozoic metamorphic rocks, constituting the aquifer basement and outcropping in Teplice, probably enable groundwater interconnection with the Cretaceous sandstone aquifer (Pačes, 1974). Such a link may explain the comparable chemical type of the Cenomanian and the

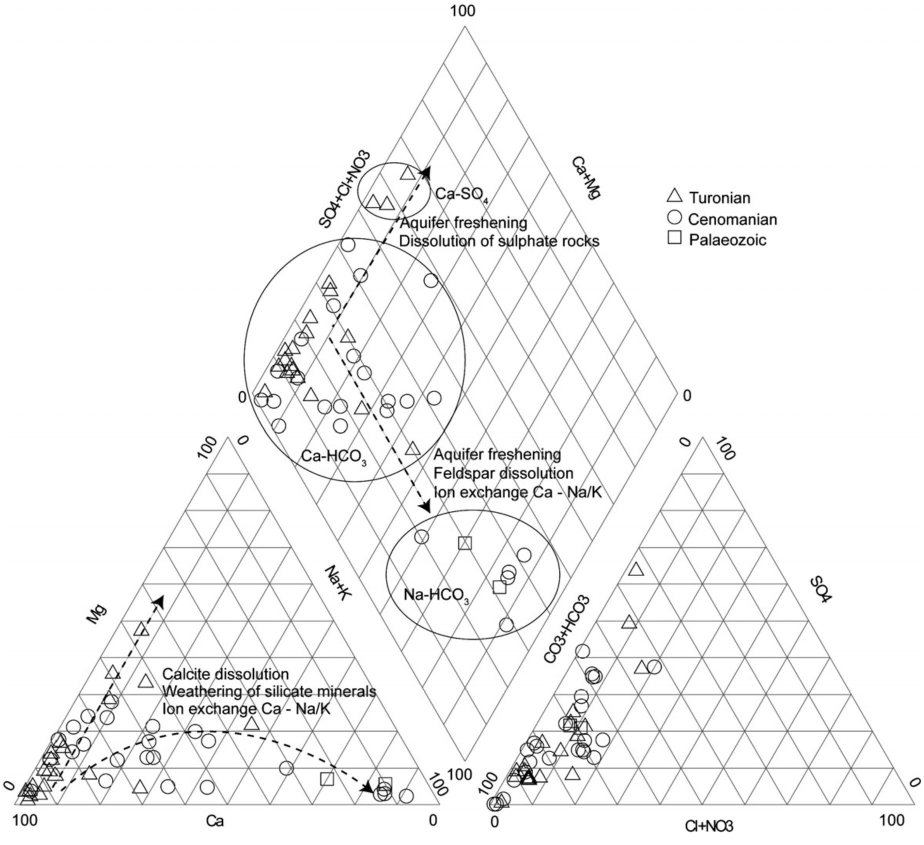


**Fig. 4.** Piper diagram indicating the different groundwater types encountered within the main BCB aquifers.

pre-Cretaceous waters; with a chemical composition mainly influenced by the processes occurring within the aquifer basement. A gradual substitution of $Na^+$ by $Ca^{2+}$ ions occurs along the flow trajectory and may also be caused by aquifer freshening or by isomorphic ion substitution. This exchange could take place by reaction with clay minerals in the matrix of sandstones. Čadek (1968) and Pačes (1974) also suggested that dissolved $CO_2$ from deep sources hydrates and dissociates to $HCO_3^-$ ions which are exchanged for $Na^+$ in feldspars. As also observed by Bates et al. (2007), the Turonian aquifer has lower amounts of $Na^+$ and $SO_4^{2-}$ than the Cenomanian aquifer.

The investigation of the chemical composition of the BCB groundwater confirms an evolution during the groundwater flow. Several geochemical processes might be observed as displayed in Fig. 4. Cenomanian samples reveal two different water types, which are clearly separated by the Labe (Elbe) River. On its left bank, the water is enriched in $Na^+$ ions, while on its right bank (majority of samples) the chemical composition is rather of Ca–$HCO_3$ water type. This phenomenon is probably related to the presence of a deep tectonic structure following the Labe (Elbe) River course. Turonian samples do not reveal important differences according to their geographical location. A few samples seem to be influenced by gypsum dissolution, but most of them are of Ca–$HCO_3$ water type.

### 4.2. Modern water indicators

The identification of a modern water contribution to the aquifer is essential to give a reasonable age to the groundwater (Jiráková et al., 2009). This phenomenon is reliably traced by $NO_3^-$ and $^3H$ concentrations which are the products of modern anthropogenic activities. Nitrates are usually found in the agricultural areas and only in shallow layers, because they easily undergo reduction during their transfer to depth. Nitrate concentration rarely exceeds 5 mg/L. Nevertheless, according Table 2, maximum $NO_3^-$ concentrations of 31 mg/L and 22.2 mg/L were measured in the Cenomanian and the Turonian aquifer, respectively, which is doubtless due to the strongly developed agricultural activities along the Jizera River Valley.

In deep aquifers, $^3H$ appears to be a reliable tracer of modern waters. Most of this radioactive H isotope reached the groundwater system during the period of thermonuclear bomb testing (Clark and Fritz, 1999). Presently, only a small quantity of $^3H$ is observed in precipitation. According to IAEA/WMO (2006), the values recently measured in Vienna range between 5 and 10 TU in modern local precipitation. A certain amount of $^3H$ was observed in the aquifers of the BCB. As the analyses considered in this study were not carried out within the same time span for all the samples, the $^3H$ contents provided are recalculated for the year 2009 (Table 1). Table 1 shows that in some places groundwater in the BCB still contains $^3H$ at the present time. The Quaternary spring of Ústí (No. 3) contains 6.8 TU that confirms the modern origin of water. The recalculated $^3H$ content in most of the Turonian samples for the year 2009 ranges from 3.2 to 5.9 TU. Cenomanian waters generally contain very low quantities of $^3H$, close to 0 TU. Only a few Cenomanian samples have a content around 6 TU (No. 11, No. 13 and No. 17). These values support the hypothesis that groundwater from the BCB may be partially of modern origin, but only to a very limited proportion. Tritium in deep aquifers may be caused by the dense tectonics in the region that may facilitate the diffusion of modern water components towards the deep reservoirs. Additionally, contamination by modern water may be caused by leakage and short circuiting along the well casing and this is particularly likely for old boreholes (Appelo and Postma, 2005). The presence of $^3H$ in waters of presumed deep/confined origin was extensively discussed in Carreira et al. (2008) who described this phenomenon in Portuguese $CO_2$-rich mineral waters. In particular rock environments, small amounts of $^3H$ may be produced naturally, however, the natural production results in measurable but generally very low values which do not exceed 0.1 TU (Clark and Fritz, 1999). The $^3H$ values measured in the BCB aquifers generally exceed this limit.

So, the majority of the Turonian and few Cenomanian samples reveal an influence of modern water infiltration. However, the concentration of $^3H$ for many samples is inconsistent with the low radiocarbon activities measured, suggesting on the contrary a long residence time of groundwater. This inconsistency will be emphasised and discussed later. Nevertheless, the $^3H$ results suggest the mixing of modern water with an older groundwater component and therefore have to be considered during the groundwater dating.

### 4.3. Stable isotopes of water

Stable isotopes of water are commonly used to identify groundwater origin, the recharge areas and the underground flow paths. It was established that groundwater from the sedimentary rocks of the Czech Massif is generally of meteoric origin and that they have not been subjected to surface evaporation (Pačes et al., 2001; Pačes and Šmejkal, 2004; Frape et al., 2007). In the study area, nine determinations of $\delta^{18}O$ have been made which reveal values varying from −11.2‰ to −8.6‰ (Table 1). Two of them (No. 1 and No. 2) originate from the Teplice thermal waters in the Palaeozoic metamorphic rocks and have values of −9.4‰ and −9.8‰, respectively. Although there is no meteorological station in the Czech Republic regularly measuring the isotopic signature of precipitation, the data of the Leipzig station (IAEA/WMO, 2006) has been used, which is close to the study area and has very similar climatic and altitude conditions. The weighted mean annual isotopic content of Leipzig rainwater is −8.63‰ $\delta^{18}O$. This value is consistent with the study of Noseck et al. (2009) carried out in a region very close to the Ruprechtov site. The $\delta^{18}O$ values of groundwaters are depleted compared to meteoric waters. Cenomanian samples No. 11, No. 13 and No. 17 are very depleted in $^{18}O$ (from −10.1‰ to −10.7‰). Samples No. 4 and No. 5, that belong to the Turonian aquifer, are the most depleted of the dataset (−11.2‰ and −10.9‰) but it should be noted that the stratigraphical identification is very ambiguous in this area. In fact, the Cenomanian and Turonian aquifers evidently communicate mainly due to the very active and large Děčín fault system which enables vertical groundwater flows. Therefore samples No. 4 and No. 5 could possibly represent the signature of Cenomanian waters. Only the Turonian samples No. 6 and No. 7 differ significantly from all the Cenomanian samples and reveal values (−8.6‰ and −8.9‰, respectively) close to modern infiltration. The significant depletion in stable isotopes observed for Cenomanian samples may be explained by several phenomena. First, the altitude effect could be responsible for depleted values considering that the recharge area of both aquifers is located close to a mountainous system. Secondly, the Pleistocene continental glaciation could be significant (Šilar, 2007) as the glacial limit of the Fennoscandian Ice Sheet reached the north borders of Czech territory (Ehlers and Gibbard, 2004; Toucanne et al., 2009). Precipitation during the glacial ages was characterised by depleted isotopic values as the result of the low temperature effect (Clark and Fritz, 1999). The depleted values in stable isotopes observed in Cenomanian samples therefore suggest recharge during colder climatic conditions. Nevertheless, several authors have shown that during cold periods, precipitation did not reach the groundwater system (Darling, 2004; Douez, 2007). It is supposed that the periglacial climate and the permafrost conditions were adverse for groundwater recharge and a recharge gap during the Last Glacial Maximum (LGM) has been proposed. As the ice sheet represents an archive of the palaeoglacial climate, their thaw at the end of the Pleistocene period might have led to the infiltration of depleted waters. Indeed, after the LGM, the water from the melted north European glacier was preferentially drained by the existing large basins such as the Wesser, the Ems and the Labe (Elbe) (Toucanne et al., 2009) that were, for that reason, charged by waters with a depleted isotopic signature.

*4.4. Carbon isotopes in the context of the BCB*

As demonstrated by Fontes (1985), Edmunds and Smedley (2000), Carreira et al. (2008), Jiráková et al. (2009), many problems have to be solved for a reliable interpretation of C geochemistry. Numerous difficulties can be met within aquifers exposed to several interactions leading to variations in the C isotopic signature. In the studied aquifers, account has been taken of different potential sources of C. It is, therefore, essential to define the isotopic signature of all potential end members in order to establish their degrees of interaction with the groundwater.

*4.4.1. Geogenic carbon*

First, the isotopic signature of rock calcite should be defined. The $\delta^{13}C$ values of carbonates from Upper Cenomanian and the Turonian formations have been measured in the very similar geological environment of the western BCB in the Dresden area (Voigt and Hilbrecht, 1997). Calcareous sandstones from the Upper Cenomanian show a minimum value of $\delta^{13}C \sim 1.7‰$ which gradually increases and reaches a maximum in the uppermost Cenomanian layer ($\delta^{13}C \sim 4.6‰$) reflecting an enrichment in $\delta^{13}C$ at the Cenomanian–Turonian boundary event (Voigt and Hilbrecht, 1997). In the Lower Turonian, the values steadily decrease. Middle and Upper Turonian show $\delta^{13}C$ values in the range of 1–2.1‰. Upper Turonian values are documented also in Weise et al. (2004) who observed values of the same order. Carbon from Cretaceous carbonate rocks is $^{14}C$ free (Clark and Fritz, 1999).

The second end member with low radiocarbon activities and enriched $^{13}C$ values is the $CO_2$ (gas) of upper mantle origin. Numerous isotopic investigations of gases carried out in the western part of Ohře (Eger) rift have identified $CO_2$ gas from deep-seated sources with $\delta^{13}C$ values ranging between −1.8‰ and −3.2‰ (Pačes, 1974, 1987; Weinlich et al., 1998, 1999, 2003; Pačes et al., 2001; Geissler et al., 2005). The radiocarbon activity for geogenic $CO_2(g)$ is usually around 0 pmC. Near the study area Šilar (1976) measured a value of about 2.4 pmC in the Cheb Basin.

*4.4.2. Atmospheric carbon*

Another input to the system is defined by modern atmospheric $CO_2$, which is generally about 100 pmC for $^{14}C$ (Clark and Fritz, 1999). The quantity of $^{13}C$ in the atmosphere is now decreasing as the result of the industrial revolution and the use of fossil C with depleted $^{13}C$ values (Clark and Fritz, 1999). Studies carried out between 1977 and 1992 (Levin et al., 1995), indicated an atmospheric $CO_2$ signal between −7.8‰ and −8.22‰ as a consequence of atmospheric C dilution, although studies performed by other authors give a mean $\delta^{13}C$ atmospheric value of −7.5‰ (Mook, 2000).

*4.4.3. Soil and vegetation carbon*

Soil atmosphere and vegetation are characterised by a value of 100 pmC for $^{14}C$ (Clark and Fritz, 1999). Since the Czech Republic has C3 cycle characteristics in term of vegetation type. The $\delta^{13}C$ content in plants ranges between −24‰ and −30‰ with an average of about −27‰ (Vogel, 1993). This is in agreement with the finding of Novák et al. (2003) who carried out soil measurements at several European sites and, in the western part of the Czech Republic at Načetín site, recorded a value of $\delta^{13}C$ around −27‰ for the soil organic matter. The $\delta^{13}C$ of soil $CO_2$ in most C3 ecosystems is generally enriched ($\delta^{13}C \sim -23‰$, Deines et al., 1974).

As already mentioned, there is evidence of the presence of fossil organic matter in the Cretaceous sediments of the region. Thus, it is relevant to define the fossil organic C isotopic composition since $CO_2$ can also be produced from the decay of organic matter. The $\delta^{13}C$ of fossil organic matter is usually between −30‰ and −20‰ (Truesdell and Hulston, 1980; Weinlich et al., 1999; Bergfeld et al., 2001). Martínek et al. (2006) carried out a palaeoenvironmental study in the mountainous region of northern Bohemia and most often values obtained were in the range of −25‰ to −27‰ for $\delta^{13}C$ in fossil organic matter from the lower Permian layers. Several measurements have been carried out on coal in Central Europe with $\delta^{13}C$ values being about −23.5‰ for Carboniferous coals from the Polish Silesian Basin, −24.4‰ for the Saar coals and −23.9‰ for the Aachen coals (Rice and Kotarba, 1993). Fossil organic matter is also $^{14}C$ free (Clark and Fritz, 1999).

**5. Discussion**

*5.1. Identification of carbon origins within the BCB*

The study of C isotopes ($^{13}C$ and $^{14}C$) not only provides information about residence time but also information about the C origin. As a consequence, radiocarbon can even be considered in some contexts as a pertinent tracer of groundwater flow and evolution (Rose and Davisson, 1996; Rose et al., 1996). The investigated water samples are reported in a graph showing $^{13}C$ and $^{14}C$ evolution (Fig. 5). It appears, that the points are scattered among the different end members described previously. The $\delta^{13}C$ analyses carried out on the TDIC range from −16.3‰ to −4.5‰ clearly suggesting a mixture of C from different sources. The radiocarbon activities cover the entire interval between radiocarbon free sources and sources of modern origin. To identify the mixing processes within the aquifers, consideration needs to be given not only to the C isotopic signature but also to the overall geochemistry of the aquifers and the geographical position of sampling sites, notably the relationship to the tectonics. Water No. 3 sampled near Ústí nad Labem corresponds to a Quaternary spring ($\delta^{13}C \sim -14.1‰$, $^{14}C \sim 89.89$ pmC) and gives a reasonable idea of the pristine isotopic composition of newly infiltrated waters.

The enriched $\delta^{13}C$ signature of most waters tends to indicate that the majority of samples are variably influenced by $CO_2$ from the upper mantle characterised by a $\delta^{13}C$ signature of about −2.7‰ and deprived of any $^{14}C$. This phenomenon was also noticed along the Ohře (Eger) Rift SW from the study area in the vicinity of the Czech spa region (Weinlich et al., 1998; Geissler et al., 2005). The origin of the $CO_2$ in many of the $CO_2$-rich mineral waters from western Bohemia has been investigated by numerous authors; the $CO_2$ originates from magmatic sources, but the water molecule isotopes always reveal a meteoric origin for the water (Šilar, 1976; Hladíková et al., 1987; Pačes et al., 2001; Pačes and Šmejkal, 2004). Other studies have been carried out in the Poděbrady spa region (Kolářová and Krásný, 1972; Jetel and Rybářová, 1991) located in the eastern proximity of the study area. These studies result in the identification of a $CO_2$-rich mineral water accumulation and suppose that the gas ascends through the deep fault structures.

In the dataset, samples No. 4, No. 5, Nos. 11–18, No. 21 and No. 22 have undergone isotopic exchanges with C from mantle gases. In addition, this is supported by the position of these samples in Fig. 5, which are distinguished by low $^{14}C$ activities and $^{13}C$ values close to the deep $CO_2(g)$ end member. Samples No. 4 and No. 5 ($^{14}C \sim 10.93$ pmC and 5.35 pmC) come from the Turonian layer and interaction with deep $CO_2$ is not very common for this shallow aquifers. Both these samples were taken from the Děčín area where

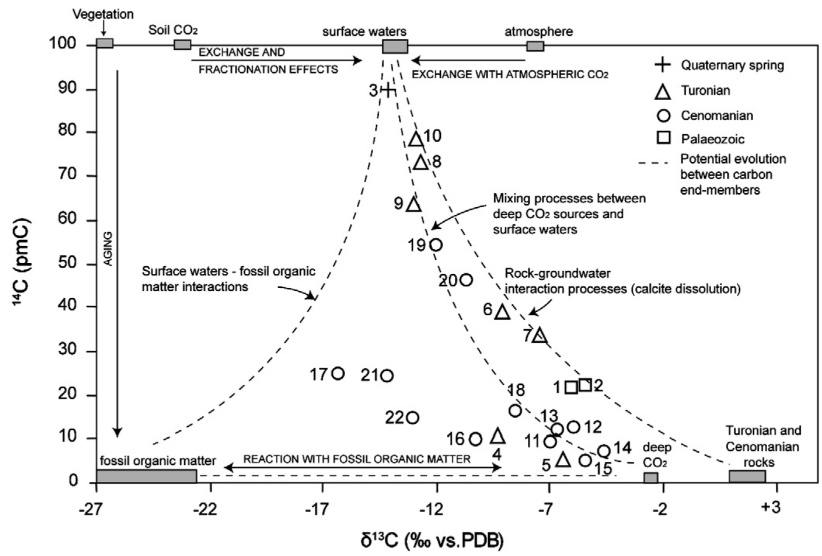


**Fig. 5.** Evolution of C isotopes in BCB groundwaters.

tectonics markedly affects the surface. Moreover, it has already been mentioned, that the stratigraphy is very ambiguous in the west of the BCB as the Turonian layer can only be distinguished with difficulty and is even often missing. Then, the isotopic signature of No. 4 and No. 5 may possibly represent the Cenomanian waters as confirmed by the $\delta^{18}O$‰ depleted value. Waters No. 11 to No. 16 ($^{14}C$ in the range from 4.75 pmC to 12.16 pmC) come from the vicinity of Ústí nad Labem, which is in the north part of the BCB, corresponding to a tectonically rich area so explaining their low radiocarbon content. Cenomanian waters No. 17, No. 18, No. 21 and No. 22 ($^{14}C$ ranges from 14.2 pmC to 24.57 pmC) were sampled in the proximity of the fault on the left bank of the Jizera River and near the Lužice fault, respectively.

Turonian samples No. 6 and No. 7 are located on the fault zone of Litoměřice, but the C isotope record ($^{14}C \sim 33.94$ pmC and 38.95 pmC) does not suggest any evident interaction of Turonian waters with deep $CO_2$. These samples tend to reveal another phenomenon observed from the $\delta^{13}C$–$^{14}C$ scatter in Fig. 5 and accounting for groundwater–rock interactions. In the BCB, aquifers generally have low contents of carbonates, although there are some insignificant calcareous sandstone, siltstone, marlstone and claystone layers within the Turonian strata (Kolářová and Krásný, 1972; Datel et al., 2009), but it should be noted that calcite cement is present in most Cretaceous sandstones in Bohemia. Fig. 6 shows an increase of $HCO_3^-$ values accompanied by an enrichment in $\delta^{13}C$ content, suggesting that some calcite dissolution processes must take place in the aquifers, which is probably due to the hydrolysis of calcite cement (Coetsiers and Walraevens, 2009). However, this relationship is ambiguous, as increasing content in $HCO_3^-$ may be the result of more than one process (e.g. reaction with the organic matter).

Additionally, a third interaction involving mainly samples No. 16, No. 17, No. 21 and No. 22 can be noted in Fig. 5. Having depleted $^{14}C$ activities (from 9.62 pmC to 24.57 pmC), these samples are characterised also by very depleted $^{13}C$ values (from $-16.3$‰ to $-10.2$‰) which can not be explained only by a mantle $CO_2$ contribution or calcite dissolution. Such a tendency is in agreement with reactions with C from fossil organic origin with a $\delta^{13}C$ value comparable to the one of organic C (Van Der Kemp et al., 2000) but with 0 pmC content of radiocarbon. Negative values between $-17.1$‰ and $-25.5$‰ were also measured by Pačes et al. (2001) in some groundwater samples in the mountainous region SW from the study area and they were attributed to $CO_2$ generated by the decomposition of organic matter. As discussed earlier, fossil organic matter occurs within the region mainly in the Permo-Carboniferous layers but to a lesser extent can be also found in the Cenomanian strata (Kolářová and Krásný, 1972; Jetel, 1982; Pačes et al., 2001; Martínek et al., 2006; Datel et al., 2009). The waters most depleted in $\delta^{13}C$ are No. 17, No. 21 and No. 22 sampled on the left bank of the Jizera River and No. 16 originating from the northern area near the Kamenice River. These samples come from the area were the occurrence of Permo-Carboniferous layers is well documented (Krásný, 1973; Malkovský, 1976; Fediuk, 1996). Moreover, the vicinity of the fault zone can facilitate the distribution of groundwater, which had been in contact with the Permo-Carboniferous. It is also relevant to note that the southernmost part of the study area is famous for its very thick Permo-Carboniferous layers rich in coal deposits (Jetel, 1982). Similar results associating depleted $\delta^{13}C$ and low radiocarbon content have already been observed in the nearby region of eastern Bavaria by Weinlich et al. (1999) and Geissler et al. (2005). The radiocarbon content observed in the Shönbrunn mine was around 5.9 pmC associated with very depleted $CO_2(g)$ ($\delta^{13}C \sim -17.4$‰). However, no observed clear and direct interaction between fossil organic matter and surface waters is observed. As shown in Fig. 5, samples which are markedly influenced by reaction with fossil organic matter in the BCB (No. 16, No. 17, No. 21 and No. 22) seem to be in a transitional state. The more the samples are enriched in $^{14}C$, the more they are depleted in $\delta^{13}C$ values. This phenomenon is difficult to explain as several processes are involved.

*5.2. Approach towards groundwater dating*

Several attempts have previously been made to date groundwater in the investigated area using C isotopes. Šilar (1976) dated mainly groundwaters that were not affected by the $CO_2$ of deep ori-

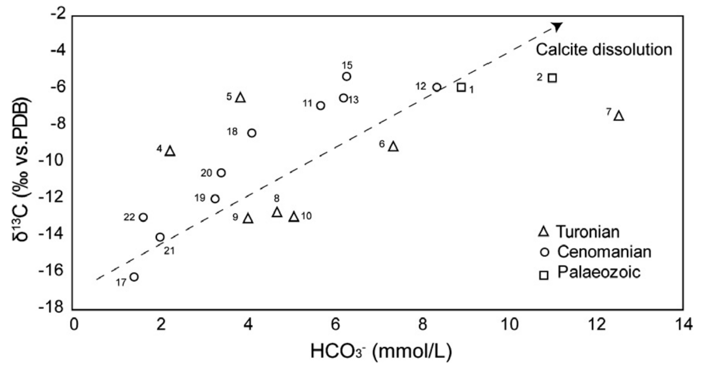


**Fig. 6.** Relationship between $\delta^{13}C$ and $HCO_3$ in BCB groundwaters.

gin. The author considered solely the Vogel approach assuming the initial $^{14}C$ activity equal to 85% of the 0.95 activity of the NBS oxalic acid standard (Vogel, 1970). This model is a simplified approach that does not take into account the different mixing processes and considers only the radioactive decay of $^{14}C$. Some dating results were obtained by Pačes et al. (2008) who considered two different approaches, the Pearson correction model (Ingerson and Pearson, 1964) for the Turonian samples and the geochemical reaction model NETPATH (Plummer et al., 1991) for the Cenomanian samples.

As described earlier, the study area is exposed to numerous geochemical processes that lead to an overestimation of groundwater ages. The majority of the commonly used dating models do not consider dilution by $^{14}C$-free $CO_2$ gas and interaction with organic C. It is proposed to use a $\delta^{13}C$ mixing model based on the dilution factors modified from Clark and Fritz (1999). The dilution correction model attempts to account for the dilution of $^{14}C$ by less active C and for isotopic exchange reaction, which may take place between the different C-bearing chemical species. The results that will be presented for the apparent radiocarbon age of the BCB groundwater are obtained using Eq. (1) (Clark and Fritz, 1999):

$$t = -8267 \cdot \ln\left(a^{14}C_{DIC}/q \cdot a_0{}^{14}C\right) \quad (1)$$

where $a^{14}C_{DIC}$ is the measured activity of $^{14}C$, $a_0{}^{14}C$ corresponds to the $^{14}C$ activity of modern recharge waters (100 pmC), $q$ is the dilution factor. When correcting $^{14}C$ for discrete geochemical processes, a process-specific dilution factor q is determined. The previous discussion on geochemical processes taking place in the aquifer led to proposing three dilution factors for the dilution of recharge waters: (i) by deep $CO_2$ ($q_{CO2(q)}$); (ii) by calcite dissolution ($q_{calcite}$) and (iii) by the processes occurring between the groundwater and the organic matter. While the first two calculations can be applied (Eqs. (2) and (3)), the latter for the organic matter becomes complicated. It is indeed very difficult to trace this process as it is not possible to clearly identify the end members of this interaction and therefore an analogous equation cannot be applied for the dilution factor. Only four samples reveal considerably depleted values in $^{13}C$ (No. 16, No. 17, No. 21 and No. 22), however, it is assumed that the very dominant process within the aquifers is interaction with deep $CO_2(g)$ rather than with organic matter. So the phenomenon of organic matter decomposition was ignored for the four above mentioned samples in the calculation and only dilution by deep $CO_2(g)$ was considered. The following equations for dilution factors are given here (Clark and Fritz, 1999):

$$q_{CO2(g)} = \left(\delta^{13}C_{DICmeasured} - \delta^{13}C_{CO2deep}\right) / \left(\delta^{13}C_{recharge} - \delta^{13}C_{CO2deep}\right) \quad (2)$$

$$q_{calcite} = \left(\delta^{13}C_{DICmeasured} - \delta^{13}C_{calcite}\right) / \left(\delta^{13}C_{recharge} - \delta^{13}C_{calcite}\right) \quad (3)$$

where $\delta^{13}C_{DICmeasured}$ represents the $^{13}C$ content measured in groundwater samples; $\delta^{13}C_{recharge}$ represents the $^{13}C$ content in recharged waters, which for the observed range of pH values corresponds to the $^{13}C$ content in soil ($\delta^{13}C_{recharge} \sim \delta^{13}C_{soil} \sim -23‰$; Clark and Fritz, 1999), $\delta^{13}C_{CO2(q)}$, $\delta^{13}C_{calcite}$ are the average values determined for $CO_2(g)$ of mantle origin (−2.7‰) and calcite (1.5‰), respectively. Dilution factors represent the degree of mixing which may range between 0 and 1. The dilutions factors are then provided in Table 3. It is theoretically possible to consider both dilutions, i.e. with calcite and with $CO_2(g)$, and to calculate the total dilution factor according Eq. (4).

$$q = q_{CO2deep} \cdot q_{calcite} \quad (4)$$

The total dilution factors $q$ obtained from this calculation provide erroneous values ($q > 1$) that are inadmissible, as mentioned above. For this reason, it was decided to calculate only individual dilution factors from Eqs. (2) and (3) regarding the geochemical context of each water sample established earlier. The key tool to identify processes and to decide which dilution factor should be considered for each sample is constituted by the $^{13}C$–$^{14}C$ evolution graph (Fig. 5). It must be stressed, that these simple models may improve the reliability of age estimates, but must be used with caution, and with an understanding of their sensitivity to the input parameters (Clark and Fritz, 1999).

Each sample of the dataset has been considered individually, and the dilution models – considering the dilution by $CO_2(g)$ and by C from calcite dissolution – have been chosen for each situation.

The dilution factors, $q$, of Turonian waters No. 6, No. 7 were determined considering only calcite dissolution ($q = q_{calcite}$). A large dilution by magmatic $CO_2(g)$ within the Turonian aquifer is not considered, because the majority of faults mainly affects the deep formations. Also, for Turonian samples No. 8, No. 9, No. 10 ($q = q_{calcite}$) only dissolution of calcite was considered. These samples were collected in a tectonically relatively calm region; $CO_2$ flux from the upper mantle is then probably not involved. Their radiocarbon activities ($^{14}C \sim 63.8$–$78.8$ pmC) indicate modern waters. It has previously been shown, that calcite dissolution affects the isotopic composition of two Cenomanian samples No. 19 and No. 20 and, therefore, for these waters the $q_{calcite}$ (Eq. (3)) was also used.

The rest of the samples (No. 4, No. 5, Nos. 11–18, No. 21 and No. 22) indicate a dominant interaction with magmatic $CO_2(g)$, therefore, Eq. (2) was used to calculate the dilution factor.

**Table 3**
Dilution factors and dating results obtained from the dilution model.

| No. | Aquifer | Dilution factors | | Radiocarbon apparent ages (BP) | |
|---|---|---|---|---|---|
| | | $q_{calcite}$ | $q_{CO2(g)}$ | Not corrected | Dilution model |
| 1 | Pal | nd | nd | 12,700 | nd |
| 2 | Pal | nd | nd | 12,600 | nd |
| 3 | Q | – | – | 900 | Modern |
| 4 | T | – | 0.325 | 18,300 | 9000 |
| 5 | T | – | 0.181 | 24,200 | 10,100 |
| 6 | T | 0.433 | – | 7800 | Modern |
| 7 | T | 0.363 | – | 8900 | Modern |
| 8 | T | 0.58 | – | 2600 | Modern |
| 9 | T | 0.592 | – | 3700 | Modern |
| 10 | T | 0.588 | – | 2000 | Modern |
| 11 | C | – | 0.207 | 19,900 | 6900 |
| 12 | C | – | 0.158 | 17,400 | 2100 |
| 13 | C | – | 0.189 | 17,500 | 3800 |
| 14 | C | – | 0.089 | 22,100 | 2100 |
| 15 | C | – | 0.128 | 25,200 | 8200 |
| 16 | C | – | 0.369 | 19,400 | 11,100 |
| 17 | C | – | 0.669 | 11,600 | 8300 |
| 18 | C | – | 0.281 | 15,000 | 4500 |
| 19 | C | 0.551 | – | 5100 | 200 |
| 20 | C | 0.494 | – | 6500 | 600 |
| 21 | C | – | 0.562 | 11,800 | 7000 |
| 22 | C | – | 0.507 | 16,100 | 10,500 |

Pal – Palaeozoic, C – Cenomanian, T – Turonian, Q – Quaternary.
$q_{calcite}$ (dilution with calcite), $q_{CO2(g)}$ (dilution with deep $CO_2$(g)).
nd – Palaeozoic samples, dilution model is not adapted.

Teplice samples No. 1 and No. 2 do not originate from sedimentary formations. The absence of calcite in Palaeozoic basement predetermines that the depletion in $^{13}C$ is not the result of calcite dissolution but rather of the interaction with magmatic $CO_2$. This concept leads to negative ages. As expected, the dilution model is well adapted for sedimentary formations, but it failed while applied to the deep crystalline reservoirs.

### *5.3. Groundwater ages in the BCB*

According to the dating approach introduced in Section 5.2, groundwater ages were calculated for most of the samples (Table 3). The age calculation shows that the dilution model provides reliable results only for some samples. Palaeozoic waters (No. 1, No. 2) have to be excluded from the interpretation as the dilution model is not well adapted for crystalline aquifers. Sample No. 3 comes from the Quaternary, thus characterising modern waters. Similarly, Turonian samples No. 6, No. 7, No. 8, No. 9 and No. 10 also reveal modern origin. This result is in agreement with the available $^{18}O$ data which are similar to the modern isotopic content of precipitation. For No. 10, it may be additionally confirmed by the presence of $^{3}H$. With the exception of No. 8 and No. 9, Turonian samples generally contain $^{3}H$ indicating the admixture of waters recharged in the second half of the 20th century (Clark and Fritz, 1999). While some processes (e.g. $^{14}C$-free $CO_2$ gas, organic C, carbonate rocks) artificially "age" groundwater, the contribution of modern water has the opposite effect. The existence of both tendencies may explain the apparent inconsistency frequently encountered between low radiocarbon activity and the presence of $^{3}H$ at the same time.

The Cenomanian waters reveal two groups of groundwater ages. The group of "old" waters is represented by the majority of samples with infiltration from 2.1 to 11.1 ka BP. Waters No. 4 and No. 5 located on the Děčín fault zone reveal ages around 10 ka BP. As mentioned earlier, the stable isotopic content of Cenomanian samples and Turonian samples No. 4 and No. 5 reveal depleted values of $^{18}O$ between −10.1‰ and −11.2‰ vs. SMOW that corroborate the hypothesis of the infiltration of water partially influenced by different climatic conditions. But it should be kept in mind that even limited mixing with modern water (shown by $^{3}H$ content) can strongly modify the original palaeo-signature of groundwater.

As a consequence, the ages, which were calculated using the dilution model, represent only the apparent age of groundwater. Strict radiocarbon ages might be considered for the seven samples without $^{3}H$, i.e. No. 8, No. 9, Nos. 18–22. Samples No. 21 and No. 22 are located on the left bank of the Jizera River in close proximity to the fault zone, they were recharged 7 ka and 10.5 ka BP. The samples No. 18, No. 19 and No. 20 come from the NE part of the study area. In spite of their close geographical location, waters No. 19 and No. 20 have high $^{14}C$ activities and indicate an infiltration 200 and 600 a ago, they represent the group of "recent" Cenomanian waters. Sample No. 18, with an age of 4.5 ka BP, lies on one of the major faults of the study area, the Lužice fault, which might facilitate interactions between aquifers.

### *5.4. Conceptual model of the origin of carbon within the BCB*

It emerged that detailed investigation of the origin of C isotopes can help to determine the several geochemical processes occurring within the aquifers. Although the different chemical reactions affecting the C isotopic signature of TDIC may be adverse for further dating efforts, C isotopes are excellent tracers that help to determine the C origin within the system. Based on the results of several stable and radioactive isotope determinations, different C origins were determined in the BCB allowing the development of a model including all potential C source contributions. The simplified concept is schematized in Fig. 7, which introduces the very complex geological system and which summarizes the geochemical processes discussed (Section 5.1). Special attention has been given to the identification of C origin in the BCB waters. Groundwater is generally drained by rivers, represented in Fig. 7 by the Labe (Elbe) River. Meteoric water with a typical atmospheric stable and radioactive isotopic composition ($\delta^{13}C \sim -8$‰ and elevated $^{14}C$ activity) infiltrated into the reservoir. It is necessary to note, that once the meteoric water reaches the surface, interaction with soil and biogenic C lowers the $\delta^{13}C$ values to approximately −14‰. The biogenic C with values of about $\delta^{13}C \sim -23$‰ can be flushed directly to the reservoirs and may partially influence the shallow horizons. On the other hand, the groundwater reveals low a $^{14}C$, which is accounted for by three phenomena. First, very low radiocarbon activities reveal the ascent of $CO_2$(g) from the upper mantle having itself a very low radiocarbon activity. In addition, the isotopic signature together with the geochemical indicators suggests strong water–rock interactions, which are mainly achieved with the calcite cement in the sandstone layers. The calcite generally has very enriched $^{13}C$ values, for the Cenomanian and Turonian samples in a range from 1‰ to 2.1‰. Therefore, calcite dissolution is partially responsible for the enriched $\delta^{13}C$ values measured in groundwater. Fig. 5 and the evolution of $Ca^{2+}$ and $HCO_3^-$ concentrations suggest that the Turonian samples reveal more intensive water–rock interactions than those of the Cenomanian. This may be due to the fact that the Cenomanian aquifer is considerably influenced by magmatic C, which dominates over the C coming from the calcite dissolution. The last $^{14}C$-free component interfering in this hydrogeological system is the C from fossil organic matter. Organic matter ($\delta^{13}C \sim -20$‰ to −27‰) is distributed irregularly within the BCB. The water can interact directly either with coal-bearing Permo-Carboniferous layers or with fossil organic matter issued from the Cenomanian deposits.

The distribution of all these components within the hydrogeological system is closely linked to the tectonic features of the region. A great part of the area (especially the NW) has been considerably affected by tectonic events which has resulted in numerous faults and fractures. This part was subsequently affected

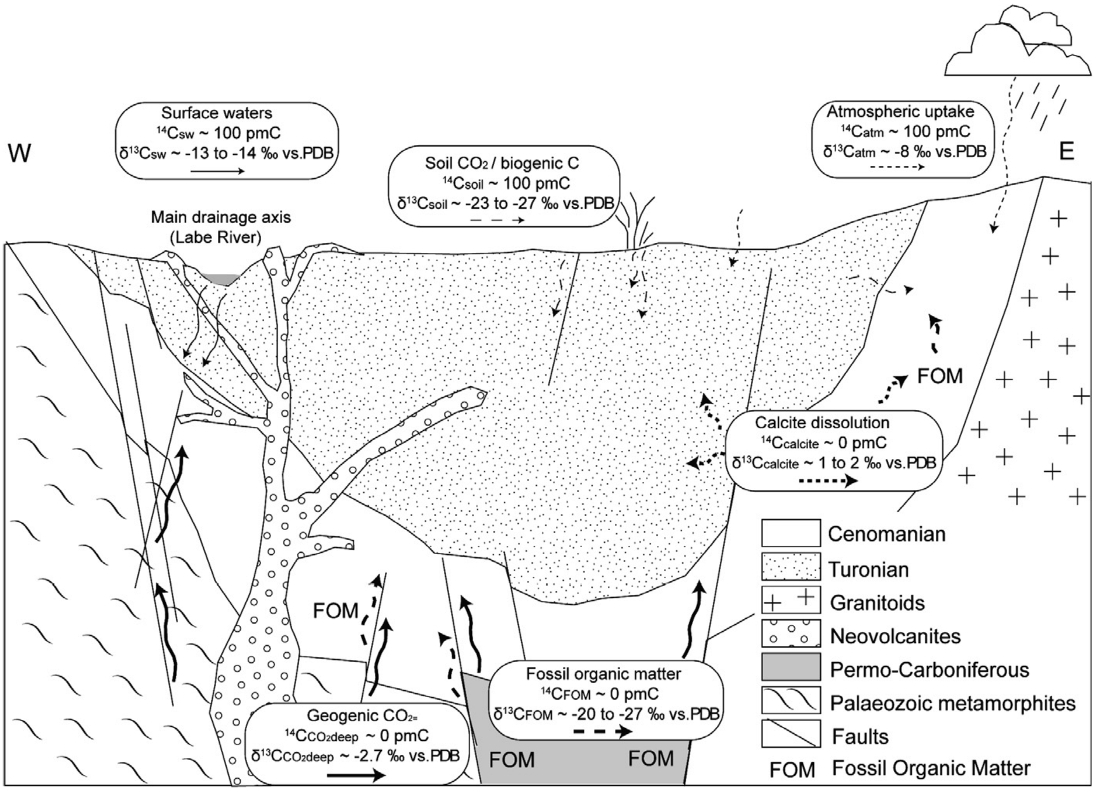


**Fig. 7.** Sketch of the BCB aquifers showing the different C origins.

by numerous magmatic intrusions as schematically shown in Fig. 7. From the dating results introduced in Table 3 and from the location of sampling wells (Fig. 3), it follows that the major fault systems (e.g. Lužice fault, Děčín fault system; Fig. 1) have considerable influence on the groundwater pattern. It was confirmed that the distribution and exchange of isotopes within aquifers happens preferentially in the fault structures as the interaction with deep $CO_2(g)$ appears to be a dominant process in the aquifers of the western part of the BCB. The geometry of the fault structure is the principle feature determining magmatic $CO_2$ distribution. It was shown, that the majority of the Turonian waters are not affected by deep $CO_2(g)$ interactions. However, from the isotopic signature of two samples from the Děčín fault system (No. 4, No. 5) it can be concluded that the faults often intersect both aquifers. Deep faults doubtless represent the main pathway for gas ascent, but in the shallower horizons, the gas might also be distributed by shallower fractures. As observed by Jetel and Rybářová (1991), fracture porosity dominates over the intergranular in the sandstone aquifers, which facilitates gas distribution also within the aquifer itself. Although the faults and fractures do not always affect the direction of groundwater flow (Šilar, 1976; Herčík et al., 1999), they can facilitate interactions between atmosphere, aquifers and upper mantle chemical components.

## 6. Conclusions

Isotopic research, carried out in the very complex aquifer system of the north-western part of the Czech Republic has demonstrated that groundwater evolution is dominated by many kinds of interactions: (i) groundwater–$CO_2$ gas from the upper mantle, (ii) groundwater–rock, (iii) groundwater–fossil organic matter and (iv) groundwater–surface waters. Carbon isotopes ($^{13}C$, $^{14}C$) in such an intricate context behave as powerful tracers of groundwater flow and origin. From the detailed study of the aquifer lithology and tectonic conditions it was possible to present for the first time a simplified conceptual scheme of the basin. Considering the complex flow conditions, a method has been developed to evaluate the apparent residence time of groundwater within the system. The apparent groundwater ages range from modern to 11.1 ka BP. The stable isotopic content, mainly $^{18}O$ values, indicates both the contribution of modern precipitation and the partial infiltration of palaeowaters from the end of the Pleistocene.

Due to this study, it is now possible to focus the investigation on strategic areas such as fault zones, where exchanges between different aquifers along deep discontinuities still need to be clarified and quantified. As a future step, these considerations will help in water management of the area to sustainably develop exploitation of the resource, taking into account its dynamics and renewability.

## Acknowledgements

Financial support for this work was provided by the Grant Agency of the Czech Republic (GACR 205/07/0691). This work was also supported by the French Ministry of Foreign Affairs and the Ministry of Education, Youth and Sports of the Czech Republic. In particular, we thank the French Embassy in Prague for help throughout the project. The authors would like to thank Pr. Benjamin van Wyk de Vries for English language revision.

## References

Andersen, M.S., Jakobsen, V.N.R., Postma, D., 2005. Geochemical processes and solute transport at the seawater/freshwater interface of a sandy aquifer. Geochim. Cosmochim. Acta 69, 3979–3994.

Appelo, C.A.J., Postma, D., 2005. Geochemistry, Groundwater and Pollution. A.A. Balkema Publishers, Leiden.

Bates, B., June, N., Harper, K., Mayo, A.L., Tingey, D., Vilhelm, Z., 2007. Preliminary chemical and isotopic analyses of groundwater systems in the northern Bohemian Cretaceous Basin, Czech Republic. Rocky Mountain Section – 59th Ann. Meeting. Geol. Soc. Am. Abstracts with Programs, vol. 39(5), p. 38.

Bergfeld, D., Goff, F., Janik, C.J., 2001. Carbon isotope systematics and $CO_2$ sources in the Geysers–Clear Lake region, northern California, USA. Geothermics 30, 303–331.

Birkle, P., Merkel, B., Portugal, E., Torres-Alvarado, I.S., 2001. The origin of reservoir fluids in the geothermal field of Los Azufres, Mexiko – isotopical and hydrological indications. Appl. Geochem. 16, 1595–1610.

Brožek, P., 1987. Bukovno-CHMU. Hydrogeological Survey. Report of Stavební Geologie, Prague. GF P059058 (Geofond archive) (in Czech).

Čadek, J., 1968. Hydrogeology of the Teplice and Ústí Thermal Waters. Sborník geologických věd HIG, vol. 6. Ústřední ústav geologický, Prague, pp. 7–207 (in Czech).

Čapek, A., 1979. Mladá Boleslav-Bělá pod Bezdězem: Evaluation of Wells. Report of Vodní Zdroje, Prague. GF P029955 (Geofond archive) (in Czech).

Carreira, P.M., Marques, J.M., Graça, R.C., Aires-Barros, L., 2008. Radiocarbon application in dating complex hot and cold $CO_2$-rich mineral water systems: a review of case studies ascribed to the northern Portugal. Appl. Geochem. 23, 2817–2828.

Čech, S., Hradecká, L., Svobodová, M., Švábenická, L., 2005. Cenomanian and Cenomanian–Turonian boundary in the southern part of the Bohemian Cretaceous Basin, Czech Republic. Bull. Geosci. 80 (4), 321–354.

Celle-Jeanton, H., Huneau, F., Travi, Y., Edmunds, W.M., 2009. Twenty years of groundwater evolution in the Triassic sandstone aquifer of Lorraine: impacts on baseline quality. Appl. Geochem. 24, 1198–1213.

Clark, I.D., Fritz, P., 1999. Environmental Isotopes in Hydrogeology. Lewis Publishers, Boca Raton.

Coetsiers, M., Walraevens, K., 2009. A new correction model for $^{14}C$ ages in aquifers with complex geochemistry – application to the Neogene Aquifer. Belgium Appl. Geochem. 24, 768–776.

Czech Hydrometeorological Institute, 2009. <http://www.chmi.cz/meteo/ok/infklim.html>.

Darling, W.G., 2004. Hydrological factors in the interpretation of stable isotopic proxy data present and past: a European perspective. Quatern. Sci. Rev. 23, 743–770.

Datel, J.V., Kobr, M., Procházka, M., 2009. Well logging methods in groundwater surveys of complicated aquifer systems: Bohemian Cretaceous Basin. Environ. Geol. 57, 1021–1034.

Deines, P., Lagmuir, D., Harmon, R.S., 1974. Stable isotope ratios and existence of gas phase in the evolution of carbonate groundwaters. Geochim. Cosmochim. Acta 38, 1147–1164.

Douez, O., 2007. Réponse d'un système multicouche aux variations paléoclimatiques et aux solicitations anthropiques: Approche par modélisation couplée hydrodynamique, thermique et géochimique. Doct. Thesis. Univ. Bordeaux, p. 3.

Edmunds, W.M., 2005. Groundwater as an archive of climatic and environmental change. In: Aggarwal, P.K., Gat, J., Froehlich, K. (Eds.), Isotopes in the Water Cycle. Past, Present and Future of a Developing Science. Springer, pp. 341–352.

Edmunds, W.M., Shand, P. (Eds.), 2008. Natural Groundwater Quality. Blackwell Publishing, Oxford.

Edmunds, W.M., Smedley, P.L., 2000. Residence time indicators in groundwater: the East Midlands Triassic sandstone aquifer. Appl. Geochem. 15, 737–752.

Edmunds, W.M., Carillo-Rivera, J.J., Cardona, A., 2002. Geochemical evolution of groundwater beneath Mexico City. J. Hydrol. 258 (1–4), 1–24.

Edmunds, W.M., Guendouz, A.H., Mamou, A., Moulla, A., Shand, P., Zouari, K., 2003. Groundwater evolution in the Contitnental Intercalaire aquifer of southern Algeria and Tunisia: trace element and isotopic indicators. Appl. Geochem. 18, 805–822.

Ehlers, J., Gibbard, P.L., 2004. Quaternary Glaciations – Extent and Chronology Part I: Europe. Elsevier, Amsterdam.

Fediuk, F., 1996. Permian ignimbritic rhyolite in Tachov Hill near Doksy, N-Bohemia. Veštník Českého Geologického Ústavu 71 (2), 145–150.

Fontes, J.C., 1985. Some considerations on ground water dating using environmental isotopes. Hydrogeology in the Service of Man. Memoires of the 18th Congress of the International Association of Hydrogeologists, Cambridge, pp. 118–151.

Frape, S.K., Shouakar-Stash, O., Pačes, T., Stotler, R., 2007. Geochemical and isotopical characteristics of the waters from crystalline and sedimentary structures of the Bohemian Massif. In: Bullen, T.D., Wang, Yanxin. (Eds.), Proc. Water–Rock Interaction, vol. 12. Taylor & Francis Group, Balkema, London, pp. 727–733.

Geissler, W.H., Kämpf, H., Kind, R., Bräuer, K., Klinge, K., Plenefish, T., Horálek, J., Zedník, J., Nehybka, V., 2005. Seismic structure and location of a $CO_2$ source in the upper mantle of the western Eger (Ohře) Rift, central Europe. Tectonics 24, TC5001. doi:10.1029/2004TC001672.

Herčík, F., Hermann, Z., Valečka, J., 1999. Hydrogeology of the Bohemian Cretaceous Basin Czech Geological Survey, Prague (in Czech).

Hercog, F., 1965. The Calculation of the Groundwater Reserves in the "Podlažice Depression" Sbor. ref. celostát. Aktivu Využitelné množství podzemních vod, Prague, pp. 47–67 (in Czech).

Hladíková, J., Pačes, T., Šmejkal, V., 1987. The stable isotope study of dissolved components in some mineral and thermal waters in Czechoslovakia. International Symposium on the Use of Isotope Techniques in Water Resource Development. Extended Synopsis, IAEA-SM-299, IAEA, pp. 54–55.

Huneau, F., Blavoux, B., 2000. Isotopic Hydrogeology within the Miocene Basin of Carpentras-Valreas (southeastern France), vol. 262. IAHS-AISH Publication, pp. 433–438.

Huneau, F., Travi, Y., 2008. The Miocene aquifer of Valréas, France. In: Edmunds, W.M., Shand, P. (Eds.), Natural Groundwater Quality. Blackwell Publishing, London, pp. 87–305.

Huneau, F., Blavoux, B., Bellion, Y., 2001. Differences between hydraulic and radiometric velocities of groundwaters in a deep aquifer: example of the Valréas Miocene aquifer (southeastern France). Compt. Rend. Acad. Sci. – Serie IIa: Sciences de la Terre et des Planetes 333 (3), 163–170.

Hynie, O., 1949. The Bohemian Groundwater Reservoirs in the Water Management. Geotechnika, vol. 8. Ústřední ústav geologický, Prague (in Czech).

Hynie, O., 1961. Hydrogelogy of Czechoslovakia I: Fresh Waters. Academia, Prague (in Czech).

IAEA/WMO, 2006. Global Network of Isotopes in Precipitation. The GNIP Database. <http://isohis.iaea.org>.

Ingerson, E., Pearson Jr., F.J., 1964. Estimation of age and rate of motion of groundwater by the $^{14}C$ method. In: Miyake, Y., Koyama, T. (Eds.), Recent Researches in the Fields of Hydrosphere, Atmosphere and Nuclear Geochemistry. Maruzen, Tokyo, pp. 263–283.

Jetel, J., 1970. Hydrogeology of the Permo-Carboniferous and Cretaceous in the Profile Melnik – Jested. Sborník geologických věd HIG, 77-42. Ústřední ústav geologický, Prague (in Czech).

Jetel, J. 1982. Hydrogeology of the Black-Coal Deposits in the Mšeno Basin. Sborník geologických věd HIG, vol. 16. Ústřední ústav geologický, Prague, pp. 33–39 (in Czech).

Jetel, J., Krásný, J., 1976. Approximative Aquifer Character in Regional Hydrogeologic Study, vol. 6. Věstník Ústředního ústavu geologického, pp. 459–461.

Jetel, J., Rybářová, L., 1991. Hydrogeology of the Cenomanian aquifer in the Labe region of the Bohemian Cretaceous Basin. Sborník geologických věd HIG, vol. 19. Ústřední ústav geologický, Prague, pp. 9–63 (in Czech).

Jiráková, H., Huneau, F., Celle-Jeanton, H., Hrkal, Z., Le Coustumer, P., 2009. Palaeorecharge conditions of the deep aquifers of the Northern Aquitaine region (France). J. Hydrol. 368, 1–16.

Jost, A., 2005. Caractérisation des forçages climatiques et géomorphologiques des cinq derniers millions d'années et modélisation de leurs conséquences sur un système aquifère complexe: le bassin de Paris. Doct. Thesis, vol. VI. Univ. Pierre et Marie Curie, Paris.

Klein, V., 1979. The Basement Composition and Morphology of the Cretaceous Basin on the West from Hradce Králové, vol. 53. Věstník Ústředního ústavu geologického, Prague, pp. 357–366.

Kliner, K., Kněžek, M., 1974. Method of Groundwater Flux Separation Using the Water Level Observation, vol. 22(5). Vodohospodářský časopis, Bratislava, pp. 457–466 (in Czech).

Kolářová, M., Krásný, J., 1972. Hydrogeology of the Poděbrady spa Region. Sborník geologických věd HIG, vol. 9. Ústřední ústav geologický, Prague (in Czech).

Kopecký, L., 1978. Neoidic Taphrogenic Evolution and Young Alkaline Volcanism of the Bohemian Massif. Czechoslovakia. Sborník geologických věd GEO, vol. 31. Ústřední ústav geologický, Prague, pp. 91–107 (in Czech).

Krásný, J., 1973. Static Analyses of Hydrogeological Data from the Permo-Carboniferous Basin in the Piedmont of the Krokonoše Mountains. Sborník geologických věd HIG, vol. 13. Ústřední ústav geologický, Prague, pp. 113–152 (in Czech).

Levin, I., Graul, R., Trivett, N.B.A., 1995. Long-term observations of atmospheric $CO_2$ and carbon isotopes at continental sites in Germany. Tellus 47B, 23–34.

Malkovský, M., 1976. Saxonic tectonics of the Bohemian Massif. Int. J. Earth Sci. 65, 127–143 (in German).

Marques, J.M., Aires-Barros, L., Graça, R.C., 1996. The origin and relation among hot and cold $CO_2$-rich mineral waters in Vilarelho da Raia–Pedras Salgadas region, northern Portugal: a geochemical approach. Geotherm. Resour. Council Trans. 20, 363–369.

Martínek, K., Blecha, M., Daněk, V., Franců, J., Hladíková, J., Johnová, R., Uličný, D., 2006. Record of palaeoenvironmental changes in a Lower Permian organic-rich lacustrine succession: integrated sedimentological and geochemical study of the Rudník member, Krkonoše Piedmont Basin, Czech Republic. Palaeogeogr. Palaeoclimatol. Palaeoecol. 230, 85–128.

Mook, W.G., 2000. Environmental Isotopes in the Hydrological Cycle – Principles and Applications. IAEA, UNESCO, Vienna.

Noseck, U., Rozanski, K., Dulinski, M., Havlová, V., Sracek, O., Brasser, T., Hercik, M., Buckau, G., 2009. Carbon chemistry and groundwater dynamics at natural analogue site Ruprechtov, Czech Republic: insights from environmental isotopes. Appl. Geochem. 24, 1765–1776.

Novák, M., Buzek, F., Harisson, A.F., Přechová, E., Jačková, I., Fottová, D., 2003. Similarity between C, N and S stable isotope profiles in European spruce forest soils: implications for the use of $\delta^{34}S$ as a tracer. Appl. Geochem. 18, 765–779.

Pačes, T., 1974. Springs of Carbon-dioxide Waters in Northwestern Bohemia. Field trip guide. Czech Geological Survey, Prague.
Pačes, T., 1987. Hydrochemical evolution of saline waters from crystalline rocks of the Bohemian Massif (Czechoslovakia). In: Fritz, P., Frape, S.K. (Eds.), Saline Water and Gases in Crystalline Rocks. Geol. Assoc. Can. Spec. Paper 33, pp. 145–156.
Pačes, T., Šmejkal, V., 2004. Magmatic and fossil components of thermal and mineral waters in the Eger River continental rift (Bohemian Massif, central Europe). In: Wanty, R.B., Seal, R.R., II (Eds.), Water–Rock Interaction, vol. 11. Balkema Publishers, pp. 161–172.
Pačes, T., Möler, P., Fuganti, A., Morteani, G., Pěček, J., 2001. Sparkling mineral water at western rim of the Doupovské hory Mountains (Czech Republic): genesis by water–rock interaction and deep-seated $CO_2$. Bull. Czech Geol. Surv. 76 (4), 189–202.
Pačes, T., Corcho Alvarado, J.A., Herrmann, Z., Kodeš, V., Mužák, J., Novák, J., Purtschert, R., Remenárová, D., Valečka, J., 2008. The Cenomanian and Turonian Aquifers of the Bohemian Cretaceous Basin, Czech Republic. In: Edmunds, W.M., Shand, P. (Eds.), Natural Groundwater Quality. Blackwell Publishing Ltd., pp. 72–390 (Chapter 17).
Plummer, L.N., Prestemon, E.C., Parkhurst, D.L., 1991. An Interactive Code (NETHPATH) for Modeling Net Geochemical Reactions Along a Flow Path. US Geol. Surv., Water Resour. Invest. Rep. 91-4078.
Raoult, Y., Boulègue, J., Lauverjat, J., Olive, P., 1997. Contribution de la géochimie à la compréhension de l'hydrodynamisme de l'aquifère de l'Albien dans le Bassin de Paris. Compt. Rend. Academie Sci. – Série Iia Sciences de la Terre et des Planetes 325 (6), 419–425.
Raoult, Y., Lauverjat, J., Boulègue, J., Olive, P., Bariac, T., 1998. Étude hydrogéologique d'une ligne d'écoulement de l'aquifère de l'Albien dans le bassin de Paris entre Gien-Auxerre et Paris. Bull. Soc. Géol. France 169, 453–457.
Rice, D.D., Kotarba, M., 1993. Origin of Upper Carboniferous coal bed gases, Lower and Upper Silesian coal beds, Poland. In: Proc. 1993 Int. Coalbed Methane Symp., pp. 649–658.
Rose, T.P., Davisson, M.L., 1996. Radiocarbon in hydrologic systems containing dissolved magmatic carbon dioxide. Science 273, 1367–1370.
Rose, T.P., Davisson, M.L., Criss, R.E., 1996. Isotope hydrology of voluminous cold springs in fractured rock from an active volcanic region, northeastern California. J. Hydrol. 179, 207–236.
Šilar, J., 1976. Radiocarbon Ground-Water Dating in Czechoslovakia – First Results, vol. 51. Věstník Ústředního ústavu geologického, Prague, pp. 209–220.
Šilar, J., 1989. Radiocarbon dating of ground water in Czechoslovakia and paleoclimatic problems of its origin in central Europe. Zeszyty Naukowe Politechniki Slaskiej, Ser. Mat.-Fiz. 61. Geochronometria 6, 133–141.
Šilar, J., 2007. Floods and groundwater resources in emergency situations. In: Vrba, J., Salamat, A.R. (Eds.), Groundwater for Emergency Situations. Proc. Int. Workshop, Tehran, 29–31 October 2006, pp. 15–34.
Skořepa, J., 1993. Roudnice – Hostěraz, Dump of Solid Waste. Report of Aquatest a.s., Prague. GF P079538 (Geofond archive) (in Czech).
Toucanne, S., Zaragosi, S., Bourillet, J.F., Cremer, M., Eynaud, F., Van Vliet-Lanoe, B., Penaud, A., Fontanier, C., Turon, J.L., Cortijo, E., Gibbard, P.L., 2009. Timing of massive 'Fleuve Manche' discharges over the last 350 kyr: insights into the European ice-sheet oscillations and the European drainage network from MIS 10 to 2. Quatern. Sci. Rev. 28, 1238–1256.
Truesdell, A.H., Hulston, J.R., 1980. Isotopic evidence on environments of geothermal systems. In: Fritz, P., Fontes, J.C. (Eds.), Handbook of Environmental Isotope Geochemistry, The Terrestrial Environment, vol. 1. Elsevier, pp. 179–226.
Uličný, D., 1997. Sedimentation in a Reactivated, Intra-Continental Strike-Slip Fault Zone: The Bohemian Cretaceous Basin, Central Europe. Gaea Heidelbergensis, 3, Abstracts, 18th IAS Regional European Meeting, Heidelberg, p. 347.
Uličný, D., 2001. Depositional systems and sequence stratigraphy of coarse-grained deltas in a shallow-marine, strike-slip setting: the Bohemian Cretaceous Basin, Czech Republic. Sedimentology 48, 599–628.
Van Der Kemp, W.J.M., Appelo, C.A.J., Walraevens, K., 2000. Inverse chemical modelling and radiocarbon dating of palaeogroundwaters: the tertiary Ledo-Paniselian aquifer in Flanders, Belgium. Water Resour. Res. 34, 1277–1287.
Vogel, J.C., 1970. Carbon-14 Dating of Groundwater. Isotope Hydrology. IAEA. Vienna, pp. 225–239.
Vogel, J.C., 1993. Variability of carbon isotope fractionation during photosynthesis. In: Ehleringer, J.R., Hall, A.E., Farquhar, G.D. (Eds.), Stable Isotopes and Plant Carbon–Water Relations. Academic Press, San Diego, CA, pp. 29–38.
Voigt, S., Hilbrecht, H., 1997. Late Cretaceous carbon isotope stratigraphy in Europe: correlation and relations with sea level and sediment stability. Palaeogeogr. Palaeoclimatol. Palaeoecol. 134, 39–59.
Weinlich, F.H., Tesař, J., Weise, S.M., Bräuer, K., Kämpf, H., 1998. Gas flux distribution in mineral springs and tectonic structure in the western Eger Rift. J. Czech Geol. Soc. 43 (1–2), 91–110.
Weinlich, F.H., Bräuer, K., Kämpf, H., Strauch, G., Tesař, J., Weise, S.M., 1999. An active subcontinental mantle volatile system in the western Eger Rift, central Europe: gas flux, isotopic (He, C, and N) and compositional fingerprints. Geochim. Cosmochim. Acta 63, 3653–3671.
Weinlich, F.H., Bräuer, K., Kämpf, H., Strauch, G., Tesař, J., Weise, S.M., 2003. Gas flux and tectonic structure in the western Eger Rift, Karlovy Vary – Oberpfalz and Oberfranken, Bavaria. Geolines 15, 181–187.
Weise, F., Čech, S., Ekrt, B., Košťák, M., Mazuch, M., Voigt, S., 2004. The Upper Turonian of the Bohemian Cretaceous Basin (Czech Republic) exemplified by the Úpohlavy working quarry: integrated stratigraphy and palaeoceanography of a gateway to the Tethys. Cretaceous Res. 25, 329–352.
Žitný, L., 1970. Hydrogeological Evaluation. Dolánky in the Český Dub vicinity. Report of Vodní Zdroje, Prague. GF P022249 (Geofond archive) (in Czech).

## 4.7 Insight into palaeorecharge conditions of European deep aquifers

*Accepted for publication as:*

*Jiráková, H., Huneau, F., Celle-Jeanton, H., Hrkal, Z., Le Coustumer, P. Insight into palaeorecharge conditions of European deep aquifers for Hydrogeology Journal.*

# Insight into palaeorecharge conditions of European deep aquifers

Hana Jiráková, Frédéric Huneau, Helène Celle-Jeanton, Zbyněk Hrkal, Philippe. Le Coustumer

**Abstract**

Climatic instability during the Late Pleistocene has been reflected in the pattern of groundwater recharge. This paper summarizes palaeoclimate knowledge during the Late Weichselian period in Europe. The majority of northern Europe was covered by thick ice sheets and permafrost preventing aquifers from recharge processes, the southern Europe was generally free of these palaeoclimatic features. Palaeoclimatic information has been put together with isotope data in order to better understand the palaeorecharge conditions and recharge timing at the scale of the European continent. The $^{18}O$ and $^{2}H$ relationship clearly shows a latitudinal evolution and many distinct climatic influences. Radiocarbon data show that south European aquifers have been generally recharged continuously during the last 40 ka, while north European aquifers often show a recharge gap during the Last Glacial Maximum. Finally, it was possible to distinguish areas with continuous recharge during the whole Late Pleistocene period and areas where aquifers were prevented from recharge during the Last Glacial Maximum. Several examples of melt water recharge or the subglacial recharge have been registered. The identification of such diversity in the groundwater palaeorecharge in Europe is of the great importance for groundwater modellers developing management schemes for groundwater resources.

Keywords
Groundwater, stable isotopes, radiocarbon, permafrost, water resources

## 1. Introduction

The regime of groundwater resources throughout the European continent reveals significant diversity in the terms of aquifer distribution, geometry, chemical and physical properties, geology, tectonic settings, flow dynamics and recharge history. This great diversity in every way should be regarded in the groundwater management measures to ensure efficient groundwater exploration and exploitation for various purposes. More than 2 billion people worldwide depend on groundwater for their daily water supply and proposing efficient plans becomes challenging. Numerous models have been developed for different major deep confined aquifer systems to achieve optimal solutions in groundwater management. Nevertheless, the developed models will be correct and credible only if precise and accurate information on the recharge history is also included as these aquifers might have been affected by different contrasted recharge conditions (Jost, 2005; Douez, 2007; Bense and Person, 2008). The oscillations in the groundwater recharge since the Late Pleistocene considerably influence modern groundwater regime, namely the groundwater flow dynamics which is one of the key parameters to evaluate the aquifer capacity. Detailed chronology of groundwater recharge in Europe is often somewhat missing or not fully understood. Variable recharge conditions have to be considered in every situation as attested by many examples worldwide. Decision makers in the field of water management rely on the credible results from groundwater modeling. The most extensive aquifers generally occur in oversea countries often expending over several countries. The problems of local groundwater development and management are then often constrained by socioeconomic factors. Examples of such huge aquifer formations may be found in the United States - Ogallala aquifer (Rosenberg et al., 1999; Fryar et al., 2001), in South America - Guarani aquifer system (Sracek and Hirata, 2002; Wendland et al., 2007; Rabelo and Edson, 2009; Gastmans et al., 2010), in Australia - Great Artesian Basin (Pestov, 2000; Zhang et al., 2007) or the Africa - Nubian Sandstones (Lloyd, 1990; Moneim, 2005). Such significant hydrogeological systems demonstrate that due to their strategic, social and economic importance, it is indispensable to make a coordinated use of water resource for drinking supply, agriculture, industry and geothermal purposes. The surface of European aquifers is generally of smaller scale, but aquifer formations represent still a strategic importance and should be the subject of effective management to meet the European Union water regulation standards (both qualitative and quantitative ones).

The term “palaeowater” strictly refers to all groundwaters that can be clearly identified in terms of radiocarbon age, or an isotopic or noble gas signature, as originating in colder climatic conditions of the Late Pleistocene (Edmunds and Milne, 2001). Palaeowaters should be in the first step distinguished from those which form part of the present circulation system exposed to different recharge conditions. Anyway, palaeowaters are largely unaffected by natural circulation at the present day as they are remnants of former hydrogeological regimes. This makes them to be considered as an important strategic drinking water resource, especially during catastrophic events (e.g. floods, dry seasons, change of climatic conditions). In addition, old groundwaters make up important archives of past environmental events and provide information on the recharge history which may be accessed on the basis of numerous indicators such as dissolved noble gases, isotopic signature of the water molecule or chloride concentrations (Rozanski, 1985; Rozanski et al., 1992; Araguas-Araguas et al., 2000; Edmunds, 2005). Environmental isotopes generally indicate the climatic conditions during the groundwater recharge and they are usually considered together with radiocarbon data to establish the most probable groundwater recharge period (Vaikmäe et al., 2001a). Radiocarbon method is commonly used for groundwater recharge timing up to 40 ka BP at maximum. This time span covers very significant climate oscillations including several severe cold periods influencing the intensity of recharge processes within Europe.

This paper proposes a synthesis of numerous studies carried out during the last two decades on selected European aquifers with the emphasis on recharge oscillations during the last 40 ka (from the Upper Pleistocene period of the Weichselian to the Holocene). Before recharge characteristics of European aquifers are discussed, the review of the most recent findings on Weichselian period concerning the glaciation chronology and palaeoclimate conditions is proposed. Later on, the relation between the timing of the glacier, the permafrost development across Europe and the groundwater recharge during the Pleistocene period is examined, with focus on the existence of a local palaeorecharge during the Last Glacial Maximum (LGM).

## 2. Weichselian environment in Europe

As the recharge events are very susceptible to reflect principal glacial and interglacial stages, the evolution of groundwater both at the local and at the European scale has been controlled by climate and environmental changes during the Late Pleistocene and the Holocene. We focus on the period within the limits of radiocarbon dating only, i.e. until 40 ka BP. Further details about palaeoclimate within the whole Weichselian period may be found in Vaikmäe et al. (2001a).

**2.1. Chronology of Weichselian (Upper Pleistocene)**

The chronology of European glaciations during the course of the Pleistocene is continuously subject of discussions and precisions (Ehlers, 1996; Ehlers and Gibbard, 2004; Ehlers and Gibbard, 2007). Contrary to the previous glaciations (Elsterian and Saalian), the chronology and the extension of the European ice sheets during the Weichselian (known as Würm in the Alps or Vistulian in northern Central Europe), particularly its last phase (< 40 ka) can be determined with rather high precision as radiocarbon dating can be applied for this time period.

The Weichselian glaciation is the last glaciation known in Europe which start is generally proposed around 116 ka BP (Gibbard and Cohen, 2008). This period is characterised by several changes between glacier advance and retreat. While the general pattern of global cooling and glacier advance was similar, many local differences appear in the ice sheet development within the globe. Weichselian have been divided into five principal stages as follows.

- *Early Glacial (MIS 5, 116 - 72 ka BP)* is the initial phase of Weichselian (Guiter et al., 2003) representing the entrance into the Pleniglacial period and was marked by a succession of alternately short cold and longer temperate periods.
- *Early Pleniglacial (MIS 4, 72 - 60 ka)* is the oldest period of maximum cooling in the Weichselian glaciation. The climatic conditions favoured the appearance of the first Weichselian permafrost in Western Europe, and the formation of large frost wedges (Vandenberghe et al., 1998; Van Vliet-Lanoë, 1998).
- *Middle Pleniglacial (MIS 3, 60 - 29)* was generally less cold than the preceding period with only discontinuous permafrost occurrences and higher amount of precipitation.
- *Upper Pleniglacial, (MIS 2, 29–15 ka)* was the coldest period of the Weichselian including the LGM which is attested by temperature curves derived from ice cores (Jouzel et al., 1999).
- *Late glacial (MIS 1, 15–10 ka $^{14}C$ uncal.)* was marked by a series of oscillations bracketing an abrupt warming when all European glaciers retreat between 15 and 13 ka as a response to an episode of climatic improvement. However, this phase was interrupted by a cold episode, dated around 12 ka BP (referred as Younger Dryas), particularly well recorded in the insect assemblages (Vandenberghe et al., 1998, Alley and Clark, 1999). During the Younger Dryas cooling, the ice sheet retreat almost stopped, ice caps were limited to the mountainous parts of Europe (the Alps etc) and in some areas (e.g. western Norway) local re-advances took place (Benn and Ballantyne, 2005).

A number of studies have focused on the reconstruction of the climate of the LGM and on the following transition toward the Holocene (CLIMAP, 1981, COHMAP, 1988, Lowe and NASP

Members, 1995, Webb and Kutzbach, 1998). The last occurrence of potentially wet and cold conditions before the most severe and driest phase of the LGM was during the interval between ca. 30 and 25 ka BP (Hughes and Woodward, 2008).

The Weichselian ice advances are most often dated to about 15 – 20 ka BP according to thermoluminescence or radiocarbon dating. The major ice sheets spread rapidly and the maximum extent of European glaciation often refers to the LGM. Although it is considered, that the maximal position was reached at ca. 18 ka BP (radiocarbon age) or 21 ka BP (calendar age), various scenarii have been proposed according to different studies.

The ice expanded from northern Sweden across Finland more than thousand kilometres to its maximum LGM position in NW Russia in less than 10 ka (Lunkka et al. 2001) and similarly the ice retreat was completed in less than 10 ka, which indicate great changes in climate systems. In the western Baltic Sea region, the maximum late Weichselian ice cover was reached at ca 22 - 20 ka BP (Wysota et al., 2002; Houmark-Nielsen, 2004), and in the southeastern parts ca 21 - 19 ka BP (Rinterknecht et al., 2006). On the south, the Scandinavian ice sheet reached the northern parts of the British Isles, Germany and Poland, but it never crossed the Elbe River (Ehlers and Gibbard, 2007). Marks (2002) showed that the LGM in Poland occurred at less than 21 ka BP; in Denmark it probably occurred at 22 ka BP (Houmark-Nielsen and Kjær, 2003). In Greece, preliminary uranium dating places the maximal glacial advance to the period prior LGM and suggests that the LGM glaciation was less extensive (Woodward et al., 2004, Allen et al., 2007). Similar evidence has been found by Hughes and Woodward (2008) in Italy where the local glacier maxima probably preceded the global LGM by at least several thousand years. In Mediterranean, glaciers are likely to have advanced and retreated much more quickly and reached their maximum extent in the last cold stage before the large north European ice sheets (Hughes and Woodward, 2008). The Greenland ice core data, the vegetation records, the fossil fauna, and the fossil permafrost features all indicate that the LGM climate was very cold in Europe from 22 ka to at least 16 ka BP (Vaikmäe et al., 2001a). The most substantial change was a drop of global sea-level to about 100–130 m below the present. This regression was combined with a general decline of precipitation and the expansion of the ice sheets.

From ca 20 ka BP, all European ice sheets started to retreat. The approximate glacier extension for 20 ka, 15 ka and 10 ka BP is documented in Fig. 1.

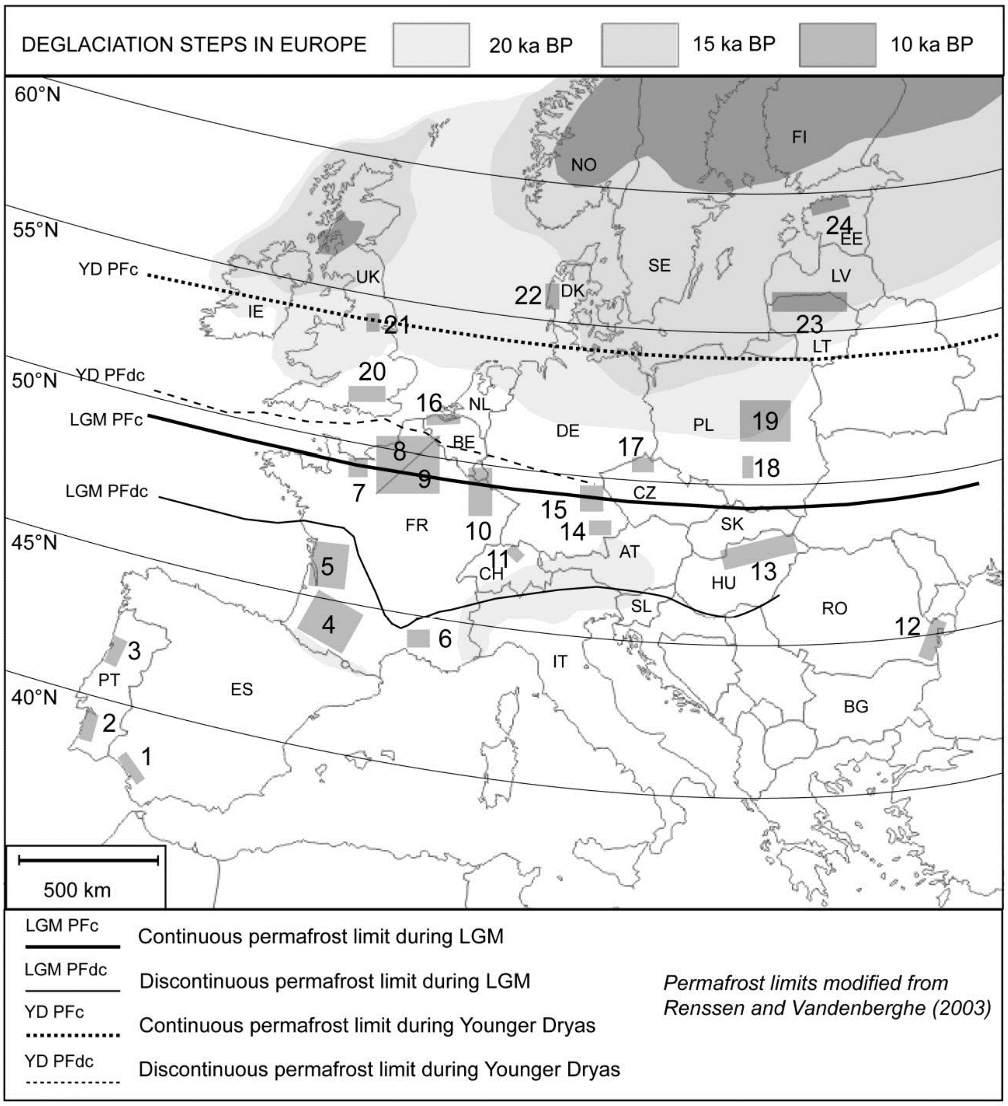


*Fig. 1. Location of studied aquifers, deglaciation steps and permafrost limits. Modified from Labeyrie (2006), Gatto and Carbognin (1981), Delmas et al. (2008), Hughes and Woodward (2008).*

## 2.2. Palaeoclimate and recharge conditions

The existence of a gap during recharge to deep aquifers is closely related to those palaeoenvironmental (permafrost) and palaeoclimatic changes (variations of temperatures, amount of precipitation, change of evaporation conditions and increasing aridity) during the late Weichselian period which finished by the Pleistocene-Holocene transition approximately 10 ka BP.

Temperatures in northern continents ranged below –20°C for most areas north of 30°N and with annual precipitation rate of only 1–2 mm/day (Kutzbach et al., 1998). The ice-free area in the northern high latitudes was covered by polar desert. According to Frenzel (1992), the annual LGM rainfall in western Europe was 500 mm lower than at present. Spruce and oak forests were absent in Europe because of cold, dryness and permafrost. Even the Mediterranean lowlands were treeless (COHMAP, 1988).

The climate situation in Central Europe during the LGM (21–18 ka BP) and the Late Glacial is characterized by high wind activity, especially from the east (Dietrich and Seelos, 2009) and relatively low precipitation (Huijzer and Vandenberghe, 1998).

The ice age climate of southern Europe and the Mediterranean basin was characterized by very low temperatures throughout the year and by very dry conditions. Two relatively homogenous zones appear: (i) A north-western zone above the Pyrenees-Alps line, characterized by very low annual precipitation ($P_{ann}$ of -600/-900 mm, respectively); (ii) A Mediterranean zone drier and colder than today, but less pronounced than the northern-western zone with $P_{ann}$ lower than today (-800 to -100 mm; Peyron et al., 1998). The Mediterranean region was thus relatively wetter than northern Europe during the LGM. Sites from Greece and Italy appear to be intermediate between the southern and northwestern Europe (Peyron et al., 1998). The $P_{ann}$ in the east of Europe was, during the LGM, lower by -50 to -750 mm (Tarasov et al., 1999).

Different approaches have been carried out to evaluate Late Pleistocene temperatures. Peyron et al. (1998) and Tarasov et al. (1999) reconstructed European temperature anomalies (the difference between the temperature today and at the LGM) from fossil pollen ranging from −17°C in Central Europe to −1°C in Arctic Russia. In Europe, reconstructed temperature anomalies, derived from degree-day modelling of palaeo glaciers, can be divided into three main regions: north of the Alps, the Mediterranean Basin, and Eastern Europe. With a precipitation anomaly of -40%, mean temperature anomalies for these three regions are −15±0.3°C, −13±0.8°C, and −10±1°C, respectively (Allen et al., 2007). In the tropics, LGM temperature anomalies, reconstructed from fossil pollen at low elevation, range between –2.5°C and –3°C (Farrera et al., 1999).

According to Lowe and NASP Members (1995) the earliest evidence for sustained warming around 15 ka BP is found in pollen diagrams from south-west Europe. However, the most remarkable evidence for global climatic amelioration dates around 13 ka BP. According to NASP records the thermal maximum of the last glacial-interglacial transition occurred in south-west Europe, lowland Switzerland, the British Isles and the Netherlands between 13 and 12.5 ka BP whereas in southern Scandinavia and Germany it was delayed until 12.5 to 12 ka BP (Walker et al., 1994).

Recharge gap in the Northern Europe is also the consequence of the permafrost extension, estimated through biologic and geologic data such as pollen, lake level oscillations, marine plankton, noble gas and isotopic data, which generally inhibited the aquifer recharge.

The significant advance of British and Scandinavian ice caps until the average latitudes (approximately 53°N) between 30 and 20 ka BP affected the recharge processes at the southern margins of ice sheets within the central and southern Europe (Boulton and Hagdorn, 2006).

There is a common understanding that continuous permafrost occurs at mean annual air temperatures from -6 to -8°C and lower, discontinuous permafrost at -4 to -8°C and sporadic permafrost at temperatures from -1 to -4°C (Brown et al., 1997). At present, permafrost environments occur over 20% of the Earth's land surface; during the LGM an additional 20% may have been affected (French, 1996).

Permafrost occurred mainly during the Early Pleniglacial, Middle Pleniglacial, LGM and Younger Dryas (Renssen and Vandenberghe, 2003). Delineation of the permafrost zone in Europe during the Pleistocene is a controversial issue. Maps of permafrost distributions for various phases have been presented by Huijzer and Isarin (1997), Isarin (1997) and Huijzer and Vandenberghe (1998).

Huijzer and Vandenberghe (1998) made an extensive inventory of the LGM European permafrost relics. Their map shows, that continuous permafrost extended throughout the UK, northern Belgium, the Netherlands and northern Germany and Poland. The boundary with the discontinuous permafrost zone has been put around the Belgian-French border. By contrast, Van Vliet-Lanoë (1998) supposes continuous permafrost also over northern, central and eastern France. Renssen and Vandenberghe (2003) considered the combination of both hypothesis to propose a map of permafrost during the LGM and the Younger Dryas (Fig. 1). This is in consistence with findings of Isarin (1997).

Permafrost limit distribution will be furthermore confronted with isotopic evidences from groundwaters reflecting the palaeoenvironmental conditions.

*Tab. 1. List of studied European aquifers with reference and main isotopic data.*

| No | Country | Site | Aquifer | Dominant lithology | $\delta^{18}O$ (‰ vs. SMOW) | | | $\delta^{2}H$ (‰ vs. SMOW) | | | $\delta^{13}C$ (‰ vs. PDB.) | | | $A^{14}C$ (pmC) | | | References |
|---|---|---|---|---|---|---|---|---|---|---|---|---|---|---|---|---|---|
| | | | | | n | mean | σ | n | mean | σ | n | mean | σ | n | mean | σ | |
| 1 | Spain | Doñana | Plio-Quaternary | clays, sands, silts | 7 | -4,7 | 0,2 | 7 | -27,7 | 2,4 | 7 | -12,8 | 1,2 | 6 | 31,2 | 15,1 | Manzano et al., 2001 |
| 2 | Portugal | Alentejo-Sado Basin | Eocene and Plio-Miocene | conglomerate, limestone, sandstone | 36 | -4,7 | 0,3 | 36 | -29,1 | 2,1 | - | - | - | 14 | 49,0 | 32,7 | Fernandes and Carreira, 2008 |
| 3 | Portugal | Aveiro | Cretaceous | sandstone, clays | 10 | -4,7 | 0,2 | 10 | -26,0 | 1,1 | 10 | -12,1 | 2,3 | 6 | 16,8 | 17,0 | Condesso de Melo et al. (2001) |
| 4 | France | Aquitaine Basin - south | Eocene | sands | 51 | -8,1 | 0,7 | 51 | -52,9 | 4,4 | 24 | -11,1 | 2,6 | 24 | 8,8 | 15,1 | André et al. (2005), Douez (2007) |
| 5 | France | Aquitaine Basin - north | Jurassic+Cretaceous | limestones | 73 | -6,2 | 0,7 | 73 | -39,3 | 4,5 | 59 | -9,3 | 3,3 | 59 | 28,9 | 28,4 | Jiráková et al. (2009) |
| 6 | France | Valréas Basin | Miocene | carbonated sandstones, marlstones | 41 | -7,8 | 0,8 | 41 | -50,3 | 6,2 | 38 | -9,0 | 2,2 | 29 | 23,5 | 29,6 | Huneau (2000), Huneau et al. (2000), Huneau et al. (2001) |
| 7 | France | Normandy | Jurassic | carbonates | 17 | -6,8 | 0,3 | 17 | -44,9 | 1,7 | 17 | -10,5 | 2,5 | 17 | 25,5 | 21,0 | Barbecot et al. (2000) |
| 8 | France | Paris Basin-north | Senonian, Turonian | chalk - fine limestone | 29 | -7,5 | 0,4 | 29 | -50,6 | 4,1 | 29 | -9,3 | 4,0 | 28 | 51,0 | 28,3 | Kloppmann et al. (1998) |
| 9 | France | Paris Basin-south | Albian | sandstone, clays | 55 | -7,9 | 0,6 | 31 | -55,7 | 4,6 | 54 | -11,3 | 3,3 | 51 | 22,3 | 30,9 | Raoult (1999) |
| 10 | France | Lorraine | Triassic | sandstone | 15 | -9,5 | 0,7 | 15 | -64,2 | 4,6 | 16 | -11,2 | 2,0 | 16 | 17,5 | 24,1 | Celle-Jeanton et al. (2009) |
| 11 | Switzerland | Glatt Valley | Quaternary | Glacial deposits, molasse | 8 | -10,7 | 1,0 | 8 | -77,5 | 8,3 | 8 | -11,4 | 2,2 | 8 | 22,8 | 24,5 | Beyerle et al. (1998) |
| 12 | Romania | South Dobrogea | Barremian - Jurassic | limestones | 9 | -11,7 | 0,7 | 8 | -71,9 | 5,5 | 8 | -7,9 | 0,7 | 8 | 41,0 | 29,0 | Tenu et al. (1975) |
| 13 | Hungary | Great Hungarian Plain | Pliocene and Quaternary | sands, clay, gravels | 32 | -10,8 | 1,0 | 32 | -78,3 | 8,8 | 28 | -14,9 | 5,5 | 28 | 16,4 | 19,2 | Stute and Deak (1989) |
| 14 | Germany | Alpine Foreland | Tertiary+Jurassic | various, carbonates | 85 | -11,0 | 1,2 | - | - | - | - | - | - | - | - | - | Bertleff et al. (1993) |
| 15 | Germany | Keuper aquifer | Jurassic | sandstone | 24 | -10,0 | 0,6 | - | - | - | 24 | -14,4 | 2,2 | - | - | - | Geyh et al. (1984) |
| 16 | Belgium | East and West Flanders | Tertiary | clays, sands | 38 | -6,9 | 0,4 | 8 | -52,1 | 4,4 | 38 | -10,0 | 5,4 | 38 | 19,5 | 20,5 | Walraevens (1998), Walraevens et al. (2001) |
| 17 | Czech Republic | Bohemian Cretaceous Basin | Cretaceous | sandstone | 9 | -10,0 | 0,8 | - | - | - | 22 | -9,5 | 3,4 | 22 | 30,5 | 25,4 | Jiráková et al. (2010) |
| 18 | Poland | Cracow region | Jurassic | limestones | 29 | -11,1 | 0,9 | 29 | -78,5 | 5,9 | 22 | -5,8 | 3,8 | 21 | 11,7 | 21,3 | Zuber et al. (2004) |
| 19 | Poland | Warsaw | Oligocene | sands | 35 | -10,2 | 0,3 | 35 | -73,3 | 2,8 | 20 | -11,7 | 1,1 | 20 | 12,9 | 15,9 | Zuber et al. (2000) |
| 20 | England | London and Berkshire Basin | Cretaceous | chalk | 53 | -7,3 | 0,3 | 53 | -50,2 | 2,4 | 35 | -6,4 | 4,2 | 35 | 19,6 | 21,4 | Dennis et al. (1997) |
| | | | | | 44 | -7,4 | 0,3 | 45 | -49,6 | 2,4 | 46 | -6,9 | 4,9 | 31 | 22,8 | 27,5 | Elliot et al. (1999), Darling et al. (1997) |
| 21 | England | Middle-East | Middle Triassic | sandstone | 16 | -8,8 | 0,7 | 16 | -57,0 | 5,1 | 28 | -11,2 | 1,5 | 28 | 32,3 | 23,9 | Bath et al., (1979), Edmunds and Smedley (2000), Darling et al. (1997) |
| 22 | Denmark | Ribe formation | Holocene and Pleistocene | sandstone | 15 | -8,0 | 0,5 | - | - | - | - | - | - | 15 | 30,1 | 19,5 | Hinsby et al. (2001) |
| 23 | Lithuania | north | Devonian | limestones, sandstones | 5 | -10,7 | 0,4 | 5 | -80,8 | 1,6 | - | - | - | - | - | - | Mokrik et al. (2009) |
| 24 | Estonia | north | Cambrian-Vendian | sandstone | 24 | -18,9 | 2,5 | - | - | - | 24 | -14,8 | 3,4 | 24 | 9,1 | 15,1 | Vaikmäe et al. (2001b) |

## 3. Methodology and dataset

In order to characterise the recharge conditions since the Late Pleistocene at the European scale, from Portugal to Estonia, many studies within the European continent have been collected. Some of them were carried out in the scope of the PALAEAUX project integrating state-of-the-art science in the field of hydrogeology, geochemistry and isotopic hydrogeology (Edmunds and Milne, 2001). The current work regards relevant published information about European groundwater evolution.

The 24 studied aquifers are displayed in Fig. 1 and further information about aquifers and data origin, mean values and the standard deviations for $\delta^{18}O$, $\delta^{2}H$, $\delta^{13}C$ and $^{14}C$ activity, may be found in Tab. 1. The most valuable information is provided by the combination of stable isotopic data both with radiocarbon ages established by different correction models. This will be used to evaluate the groundwater recharge timing and to identify major palaeoclimatic changes. The type of data used at each investigated sites can be very different. As follows from Tab. 1, some European aquifers do not provide complete data. However, only information on both stable isotopes and radiocarbon is the most promising to obtain relevant conclusions about the general character of groundwater recharge; the radiocarbon dating on the basis of the proposed data is not in the scope of the current study. We considered only the groundwater ages introduced by the authors in the source documentation (Tab. 1).

## 4. Results and discussion

### 4.1. Stable isotopes in European aquifers

As aquifers conserve the isotopic signature of precipitation and as the content in stable isotopes reflects the climatic conditions such as temperature and humidity, the groundwater forms unique archives of palaeoclimate. Although in many countries the period of precipitation accumulation fits more or less the period of aquifer recharge, it is not necessarily always the case. During cold periods, especially in the north European countries, the precipitation could not be easily infiltrated owing to the permafrost or ice sheets occurrence and was just accumulated in the form of snow and ice. It was only after the ice and permafrost retreat that the aquifers could be recharged again. As a consequence of the previous glaciation, many aquifers could be easily recharged by melt waters considerably depleted in stable isotopes. Nevertheless, such recharge was governed by the past main flows and drainage axis and therefore might be observable in few aquifer systems only. The insight into the stable isotopic signature may suggest the period when the precipitation was formed, but it should be kept in mind that the recharge itself can have occurred much later despite the depleted isotopic signature. This discrepancy may be clarified using radiocarbon dating methods which can provide an idea about the recharge timing as discussed later.

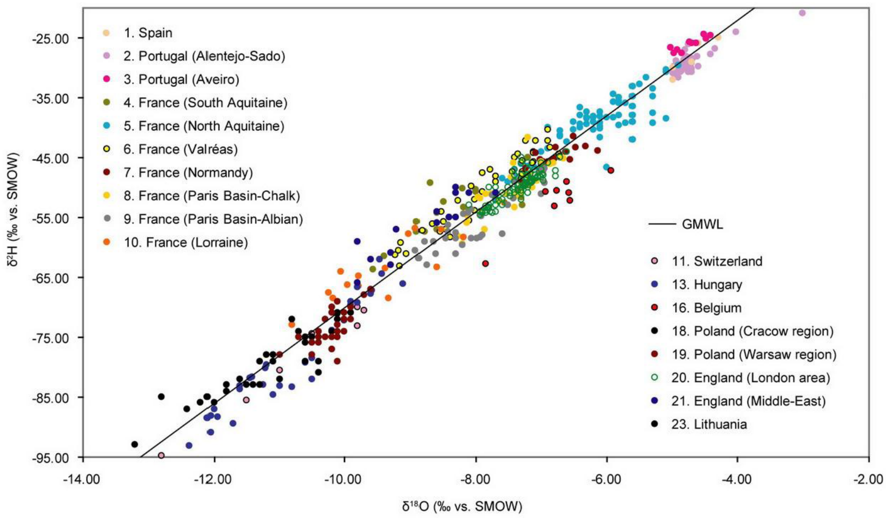


*Fig. 2. $\delta^{18}O$ vs. $\delta^2H$ diagram for European groundwaters. Data comes from references listed in Tab. 1.*

European groundwaters show different effects influencing $^2H$ and $^{18}O$ concentrations. In Fig. 2 groundwaters generally plot along the Global Meteoric Water Line (GMWL) indicating that they were not involved in any considerable specific processes such as evaporation, geothermal activity, etc. Huge span in both stable isotopic values for the European aquifers is the consequence of the different isotopic signature of local precipitation, due both the increase in temperature from northern latitudes to the southern ones, the proximity of the site to oceans and the decrease of temperature with increasing altitude. According to Fig. 2, European groundwaters plot approximately from-25 to – 95 ‰ vs. SMOW for $\delta^2H$ and from -3 to – 13 ‰ vs. SMOW for $\delta^{18}O$ including modern and old waters. The most enriched values are found in Spain and Portugal while the most depleted come from north European countries. These variations are confirmed by Fig. 3 which displays the span of $\delta^{18}O$ values within each aquifer of the dataset. While in the southernmost countries the variance in the isotopic content between old water and modern water is very low, central and northern European countries reveal larger span of values. The stable isotopic content of south European aquifers (N°1-3) reveals enriched values as the consequence of the low latitudes but also because of the ocean vicinity. The most enriched aquifers were found in Portugal. These phenomena are observed even in southern France, where South Aquitaine Basin (N°4) has more depleted values with respect to North Aquitaine Basin (N°5) which was sampled closer to the ocean. On the other hand, in very high latitudes depleted isotopic values are expected, nevertheless the Cambrian-Vendian aquifer in Estonia shows extremely low values for $\delta^{18}O$ ranging between -12 and -22.5 ‰. Depleted values in Switzerland probably reflect the influence of mountainous geomorphology. A huge variability of $\delta^{18}O$ content within one single aquifer often indicates a recharge during very variable climatic conditions.

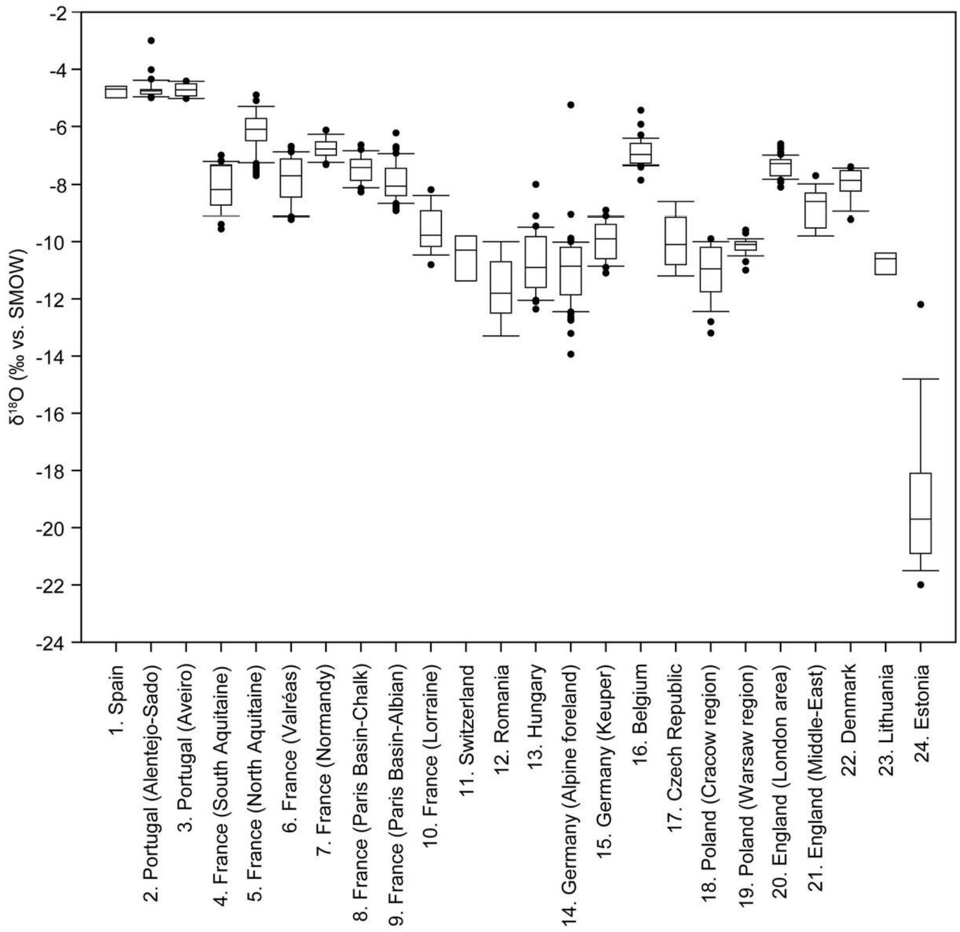


*Fig. 3. Box plot displaying the oxygen-18 content in European groundwaters. Figure shows latitudinal evolution. Enriched values in higher latitudes are often linked to coastal aquifers. Data comes from references listed in Tab. 1.*

In order to well understand the evolution of the groundwater isotopic signature within one aquifer, it is necessary to acquire an idea about the stable isotope content in modern precipitation. European continent is well covered by IAEA-GNIP stations (IAEA/WMO, 2006) despite missing or incomplete records in some countries. A map with an approximate present day $\delta^{18}O$ distribution in western and central Europe has been proposed by Arppe and Karhu (2010). The span of the modern precipitation isotopic signature for studied aquifers ranges from -4.6‰ to -11‰ and from -27‰ to -72‰ for $\delta^{18}O$ and $\delta^{2}H$, respectively (IAEA/WMO, 2006).

Generally, Late Pleistocene groundwaters are depleted in stable isotopes compared to the modern precipitation. The amplitudes of $\delta^{18}O$ and $\delta^{2}H$ values between modern precipitation and the estimated LGM period, i.e. around 18 – 22 ka BP are displayed in Fig. 4 comparing several aquifers in Europe with enough relevant data. Observed amplitudes range from 1.2‰ to 2.7‰ and from 8.2‰ to 20‰ for $\delta^{18}O$ and $\delta^{2}H$ with relatively higher amplitudes in higher latitudes. Nevertheless, the depletion for old groundwaters is not observed in some south European countries. In coastal Portugal the lack of any stable isotope depletion indicates the constancy of the Atlantic air circulation at medium latitudes over the whole Late Pleistocene and Holocene, as well as the proximity to the ocean (Edmunds, 2005; Carreira et al., 1996). The contrast between the Pleistocene and the modern isotopic signature is also documented in Fig. 5 displaying selected European aquifers.

*Tab. 2. Amplitudes of groundwater recharge temperature variation between Pleistocene (>10 ka) and modern air temperature values, inferred from dissolved noble gases concentrations. (NGT = Noble Gases recharge Temperature)*

| Country | ΔNGT (°C) | References |
|---|---|---|
| Portugal | 5-6 | Condesso de Melo et al. (2001) |
| France -south | 5-7 | Huneau (2000), Douez (2007) |
| France - north | 3-9 | Rudolph et al. (1984), Kloppmann et al. (1998), Lavastre et al. (2010) |
| Switzerland | 4-6 | Beyerle et al. (1998) |
| Hungary | 9 | Stute and Deak (1989) |
| Austria | 6 | Andrews et al. (1985) |
| Germany | 5-9 | Bertleff et al. (1993) |
| Belgium | 4-8 | Walraevens (1998) |
| Poland | 4-7 | Zuber et al. (2000), Zuber et al. (2004) |
| England | 4-8 | Bath et al. (1979), Darling et al. (1997), Elliot et al. (1999), Edmunds and Smedley (2000) |
| Estonia | 6 | Vaikmäe et al. (2001b) |

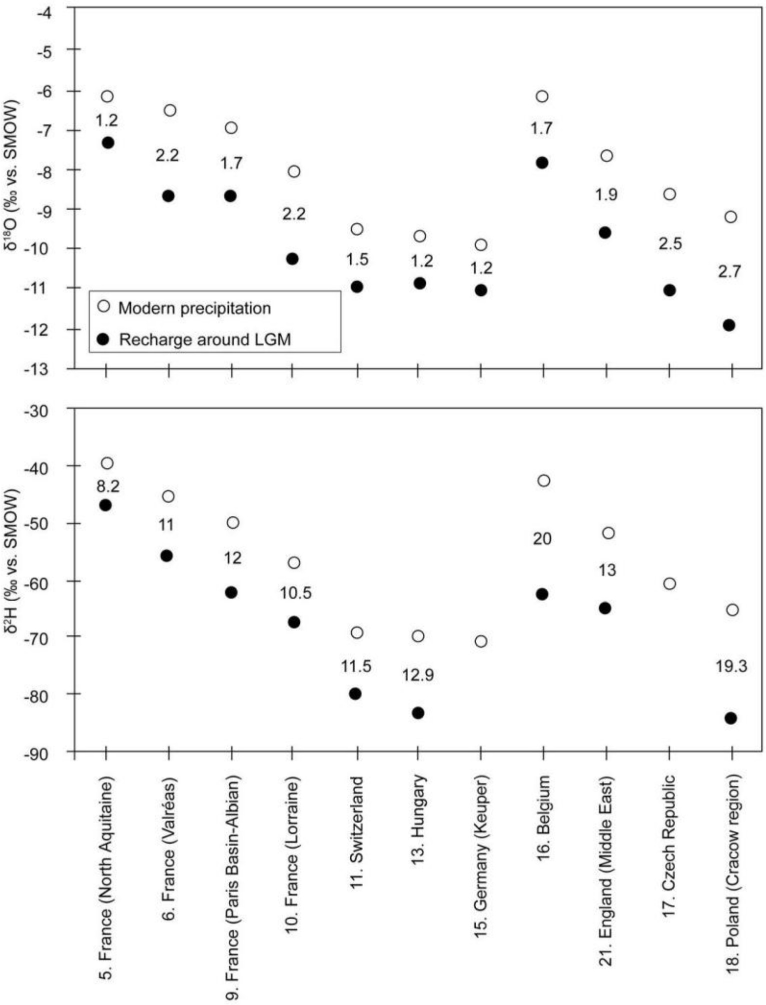


*Fig. 4. Contrasted isotopic content between LGM European groundwaters and modern precipitation indicating the absolute shift in isotopic values between LGM and modern recharge. Data comes from references listed in Tab. 1.*

Further consideration about the isotope shifts exhibited by most palaeogroundwaters requires a palaeoclimatic context in which the recharge temperature is an important element. The temperatures at which recharge waters are equilibrated with air in the unsaturated zone may be determined from the noble gas contents of groundwaters and generally reflect annually averaged values (Stute and Deak, 1989; Aeschbach-Hertig et al., 2000; Aeschbach-Hertig et al., 2002). Tab. 2 summarizes the amplitudes of the temperature variations (ΔNGT) measured on groundwaters between the Late Pleistocene and Holocene periods. Data on ΔNGT are complementary to the stable isotope content information. It is showed, that despite regional differences in the temperature ranges, the overall evolution of temperatures since the Late Pleistocene was throughout Europe quite similar. The ΔNGT values thus confirm previous discussion on stable isotopic content and the existence of palaeorecharge prior to 10 ka BP.

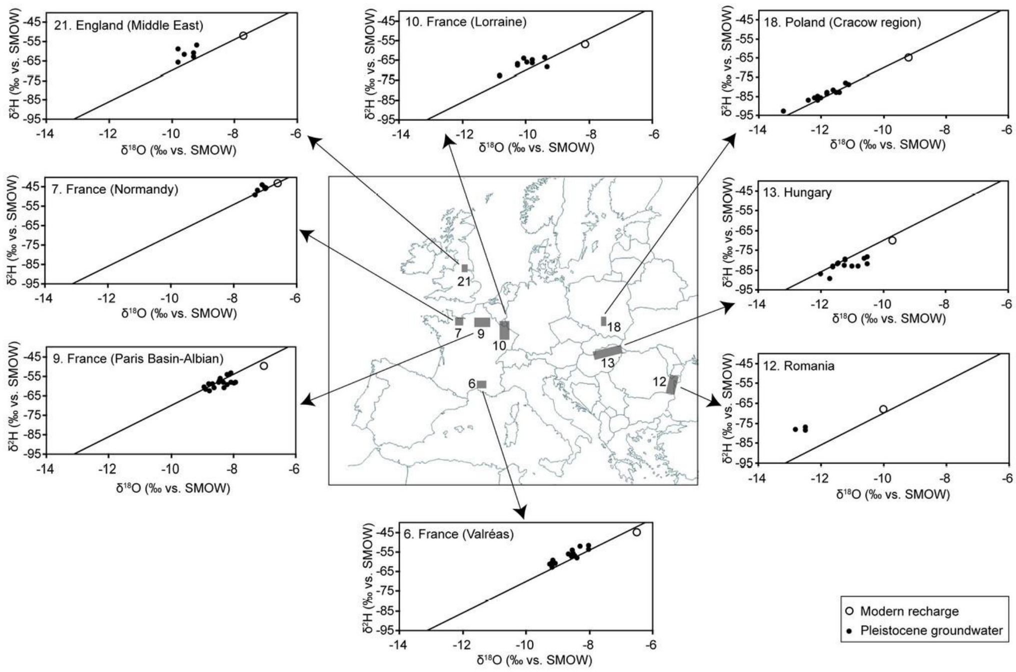


*Fig. 5. The $\delta^2H$ and $\delta^{18}O$ composition of Pleistocene groundwaters in Europe compared with the average of modern local precipitation and the GMWL. Data comes from references listed in Tab. 1.*

Recharge temperatures deduced from noble gases can be confronted with the stable isotope ratios $\delta^{18}O$ and $\delta^2H$ which have long been considered powerful indicators of palaeoclimate. Long-term changes of palaeoclimate might be observed from $\delta^{18}O$/temperature relations. Decreasing temperature drives the rainout process and the precipitation becomes increasingly depleted in stable isotopes. Dansgaard (1964) established a linear relationship between surface air temperatures and $\delta^{18}O$ for mean annual precipitation on a global basis. Later, Rozanski et al. (1992) and Fricke and O'Neil (1999) proposed a $\delta^{18}O$ –temperature coefficient around 0.55‰/°C for long term records covering the Pleistocene period. Following this coefficient and the recharge temperatures derived from ΔNGT (Tab. 2), waters recharged in cold climatic periods should be depleted by approximately 2‰. This calculation is only approximative as the introduced coefficient of 0.55

‰/°C has been averaged from very long-term data set. However, such estimation is in agreement with the studied data introduced in Fig. 4.

**4.2. Recharge conditions in Europe**

Although groundwater presents an excellent archive of recharge conditions, many unclear situations appeared during the recharge condition determination and groundwater dating for European aquifers. The main target of the current work is to investigate the timing of the recharge of the European aquifers in order to clarify the effect of the cold period during the Late Pleistocene on the recharge events. The discussion on palaeorecharge on the global scale in Europe have been already included in the work of Darling (2004) who suggested the existence of the recharge gap for several sandstone aquifers in Europe. However, the recharge gap corresponding to the LGM period is often difficult to identify and some previous studies have confirmed rather uninterrupted recharge during Late Pleistocene and transition into the Holocene (Blavoux and Olive, 1981; Rudolph et al., 1983; Kemp et al., 2000; Jiráková et al, 2009). Our synthesis show variable results indicating different recharge conditions within Europe and very often with certain particularities which will be discussed later on. The LGM is generally considered as a cold period which in some places caused a recharge absence.
After LGM, the retreat of ice sheets and permafrost in the Early Holocene allowed deep percolation of water into the ground establishing the common present-day groundwater table.

Fig. 1 displays a general view on the permafrost and ice sheet extension according to several very recent studies with the location of studied aquifers. All aquifers reveal a Holocene recharge but in only part of them very old groundwater was found. An effective way of comparing the quality of information from selected aquifers is to obtain fingerprint of each of them based on the relationship between $\delta^{18}O$ and radiocarbon ages, or if not available, with radiocarbon activities (Fig. 6).
Commonly, two major groups of aquifers may be distinguished. Besides, a third category has been put apart (involving particular recharge processes):
*(i) Continuous recharge:*
This first group includes groundwater of all ages dating back to 40 ka BP that do not reveal any recharge gap from the Late Pleistocene up to the Holocene.
*(ii) Recharge hiatus around LGM:*
This second group involves aquifers which were prevented from recharge around LGM. Some of these aquifers provide groundwater ages up to 40 ka BP. However, some of these aquifers reveal a

lack of groundwater recharge prior to LGM which is either because of the absence of recharge or a absence of data.

*(iii) Particular situations:*

This third group corresponds to special situations and suggests that the recharge occurred during or shortly after LGM and has been provided by subglacial melted groundwater drainage through tunnel valleys or that aquifers were recharged by melted water from the North European ice sheets driven by the main drainage axes right after the LGM.

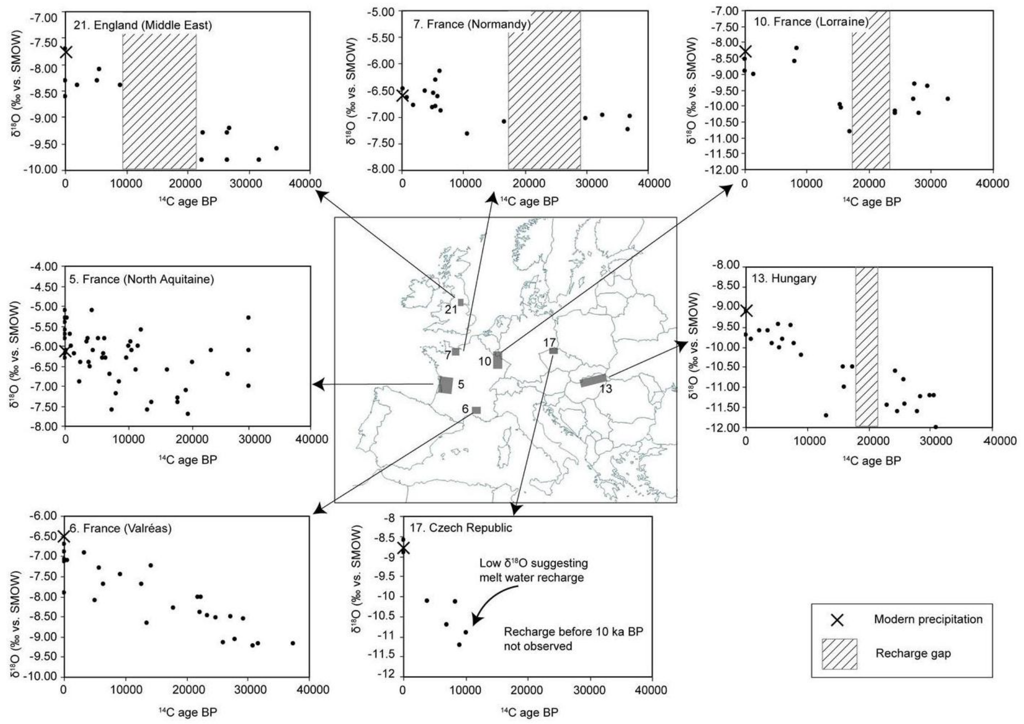


*Fig. 6. $\delta^{18}O$ isotopic signature in European groundwaters during the last 40 ka. 5, 6 – continuous recharge; 7, 10, 13, 21 – recharge gap; 17 – melt water recharge, Pleistocene recharge not observed. Data comes from references listed in Tab. 1.*

**Continuous recharge examples**

Groundwater being recharged continuously during the last 40 ka was identified within the larger part of southern Europe. A strongly depleted stable isotope composition and a low radiocarbon activity are the main indicators of glacial origin of groundwater. It is confirmed by our records from

Portugal, Spain and the southern France, but it is likely that the same trend was followed in the southeastern Europe as documented in groundwaters in eastern Romania. South European aquifers recharge has not been generally affected by the cold climate dominating in northern and central Europe and therefore many records of palaerecharge of deep aquifers do exist. However, it is not the case of the *Doñana aquifer in Spain* (N° 1). This aquifer reveals low content in $^3H$ and the recent component is estimated around 10% at maximum. According to the radiocarbon dating, there are no evidences about recharge prior to 15 ka BP. This could be explained by two hypothesis: a saline water admixture (as saline waters do not reflect palaeoclimatic signature) or the absence of major climatic changes since the LGM, when the weather was humid and warm, not very different from the present climate, as recorded by pollen (Zazo et al., 1996). This statement is supported by the presence of old groundwaters in *Portugal* (N° 2, N° 3) dating about 30 – 40 ka BP (Carreira, 1998) which indicates the continuity of the recharge through LGM.

It is probable, that the *southern France* probably also experienced active recharge during cold periods. The permafrost limit crosses France just in its central part (Fig. 1). The recharge of aquifers in the South Aquitaine (N° 4), North Aquitaine (N° 5) and Valréas Basins (N° 6) has been probably regularly distributed since 40 ka BP up to the Holocene. In South Aquitaine, many samples date from the LGM indicating very favourable recharge conditions. North Aquitaine and Valréas Basin data show the same trend of continuous recharge during LGM, though with rather lower density of information as only a few samples fit the LGM period.

Rather continuous recharge has been documented in the east Romanian aquifers in the South Dobrogea region. Despite a lack of information on the exact extension of the permafrost during LGM in Romania, the Dobrogea region (N° 12) was not considerably affected by this cold stage as also suggested from isotopic investigations.

Continuous recharge in the given examples is the result of favourable and rather stable climatic conditions. Nevertheless, several documentations of continuous recharge exist also from areas of higher latitudes, i.e. areas with possible discontinuous or even continuous permafrost occurrences. This is the case of the confined Albian aquifer (Lower Cretaceous) in Paris basin (N° 9) which does not show any recharge hiatus and has been probably recharged more or less continuously up to 40 ka BP (Raoult, 1999; Jost, 2005). The recharge zone of the Albian aquifer is located on the south-east from Paris but still in the zone of the discontinuous permafrost conditions according to Fig. 1. This supports the hypothesis, that discontinuous permafrost which occupied the northern and the great part of central France may have allowed the recharge processes.

Another example comes from the Keuper aquifer in Germany northward from Nuremberg (N° 15). This area, like central France, has been exposed to transitional conditions between continuous and discontinuous permafrost. Radiocarbon dating does not confirm any recharge gap up to 31.5 ka BP.
Data from southern England in the surroundings of the London Basin (N° 20) suggest similar evolution. This ice-free zone was probably under periglacial and permafrost conditions (Fig. 1). In spite of this, permafrost was possibly not present everywhere or during the entire LGM period, because several studies confirmed continuous palaeorecharge to the Chalk aquifer up to 40 ka BP (Darling et al., 1997; Dennis et al., 1997; Elliot et al., 1999).

**Interrupted recharge examples**

This group assembles aquifers which were recharged up to 40 ka BP but with a hiatus between most often 18 – 22 ka BP as described previously and which corresponds to an ice cover or permafrost extension in the concerned areas. As proposed by Harrar et al. (2001), it is not possible to make any useful general statements about the effects of glaciation and permafrost on aquifers as the relative geometry of the aquifer and glacier are very important.
The recharge gaps observed in such aquifers cover often different spans and vary according the aquifer geographical position. Nevertheless, all registered recharge gaps are consistent with the LGM period. These aquifers generally dominate in the northern part of Europe, however the first records come from latitudes of about 48°. Upward from this latitude, the climatic conditions during the last cold stage were more severe than in the south and are reflected in the groundwater isotopic signature. Several records have been collected from regions where discontinuous permafrost occurred during LGM. It has been found out that the recharge in the majority of the study areas was interrupted, but in some places might have been continuous.
This phenomenon is observable in northwestern France. In *Normandy* (N° 7), the groundwater ages show a recharge dating from the last 40 ka, but data indicate a hiatus from ca 17 to 30 ka BP (Fig. 6). The recharge gap period is difficult to precise as the absence of LGM samples can simply indicate the lack of boreholes and not really a recharge gap. In the nearby *Paris Basin* two different aquifers have been studied. The unconfined Chalk groundwaters indicate mainly a Holocene recharge with a maximal age about 14 ka BP (N° 8). The fact that waters prior to LGM have not been found might be again assigned to lack of samples. The results from $^{14}C$ age modelling in the *Lorraine* region (N° 10) show a palaeorecharge effect up to 33 ka BP. The absence of any ages of between 17 and 24 ka BP may provide evidence for the absence of recharge during or around the LGM (Fig. 6).

Similar recharge history has been registered in *Switzerland* (N° 11). The study of the Glatt Valley in Switzerland indicates that the valley was ice-free before 28 ka BP and after 14.5 ka BP (Schluchter et al., 1987). Radiocarbon dating showed an interrupted recharge between 17 ka and 25 ka which is in agreement with the ice sheet extension.

No groundwater recharge in *Hungary* for both Pliocene and Quaternary aquifer flow systems (N° 13) was registered between 17 and 23 ka BP (Fig. 6). It is consistent with the finding of Kovács et al. (2007) who expects the permafrost and periglacial processes throughout the Pannonian Basin between 18 and 22 ka BP. Old corrected $^{14}C$ ages, which fall within the last global cold period, are also supported by significantly lower temperatures derived from the dissolved noble gas records.

The climate conditions permitted continuous permafrost development in *North Belgium* (N° 16) resulting in great interruptions in the aquifer recharge. In the Tertiary Ledo-Paniselian aquifer the radiocarbon dating determined a recharge absence from 16 to 21 ka BP. The investigation on this aquifer has been developed in Blaser et al. (2010) who used more sophisticated dating methods. Finally, similar results were acquired showing a recharge gap between 14 and 21 ka BP.

The existence of a recharge gap in dating results from several aquifers in the *British Isles* is reinforced by the suggestion first made on the basis of early isotopic studies that there was a hiatus in recharge under glacial and periglacial conditions (Smith et al., 1976; Downing et al., 1977; Bath et al., 1979). Darling et al., 1997 demonstrated that palaeowater signals are better preserved in sandstone than in carbonate aquifers, because in the latter the signals are degraded by mixing resulting from more pronounced dual porosity. Considering sandstone aquifers, a lack of apparent ages between 13 and 17 ka BP for sampled groundwater has been noted for groundwaters from East Midlands (N° 21) (Andrews and Lee, 1979; Bath et al., 1979; Andrews et al., 1984, 1994) (Fig. 6). Fig. 1 shows that ice sheets were probably overlying all the northern part of the British Isles.

The very complex flow pattern in the studied aquifers of *Poland* has complicated the absolute groundwater dating. Isotopic data from the Warsaw region (N° 19), which was during LGM probably situated on the limit with the Fenoscandian ice sheet, indicate an important contribution of water recharged during the end of the last glacial period. This water has an isotopic signature of evaporation prior to recharge which probably means that due to the existence of residual permafrost, the recharge was fulfilled mainly by infiltration from lakes and that the flow pattern was probably more or less continuous since about 14 ka BP (Zuber et al., 2000). Confined aquifers in the Cracow region (south Poland, N° 18) contain several groups of waters including also a mixture of glacial and older waters. Unfortunately, no reliable dating of groundwaters within the whole time span offered by $^{14}C$ method is available for the territory of Poland as there are no sufficiently large non-carbonate aquifers (Zuber et al., 2000). Even if quantitative age estimations for glacial waters seems to be difficult, the mean age of glacial waters in the centre of Cracow can be assumed as equal to 13 ka BP on the basis of dissolved noble gases and stable isotope data.

The fact that the hiatus is of different duration and has been recorded at different moments can be the consequence of different phenomena. The LGM did not occur at the same time within all Europe. The proposed interval from 18 to 22 ka BP represents the most often proposed timing of LGM but in various countries it could occur with slightly different time shifts on a local scale. The weak point of radiocarbon dating lies above all in the radiocarbon activity disturbances due to various geochemical phenomena, notably in the carbonated aquifers. The results therefore present estimations and should be considered rather in relative terms. Addtionally, it has to be kept in mind that LGM waters are more difficult to be identified (due to lower recharge intensity). That is why, the lack of samples does not necessarilly suggest no recharge. Then, as a consequence, waters infiltrated with much lower intensity during colder periods are more difficult to find.

**Particular situations**

The presence of a permanent ice sheet significantly reorganises the groundwater flow, disrupts the alimentation and modifies hydrodynamic and mechanic properties of aquifers.
A first example of special situation comes from Denmark, where the study of a sandy aquifer (Hinsby et al., 2001) allowed distinguishing 2 groups of groundwaters of Holocene and Pleistocene age. The study suggests that the melt water from the southern rim of the Fenoscandian ice sheet at the LGM was drained to the Elbe palaeovalley and its tributaries and afterwards infiltrated into the deep sedimentary formations. Recharge records indicate both old and modern recharges with a hiatus between 11 – 29 ka BP. This is consistent with the theory of ice sheet cover between 15 – 20 ka BP (Fig. 1). For some samples, radiocarbon dating suggests a Holocene age of groundwaters, but noble gas data often indicate very low temperatures (<5°C, Hinsby et al., 2001) corresponding to glacial ages. This was the main reason to take into consideration a possible recharge with melt waters. An analogous situation was detected in the ice-free region of central Europe, particularly in the Czech Cenomanian aquifers (N° 17) (Jiráková et al., 2010). In these cases, groundwater recharge is also linked to the existence of the north European ice sheet from which the melt water was preferentially drained by the existing big rivers such as the Wesser, the Ems and the Labe (Elbe) (Toucanne et al., 2009). This phenomenon is responsible for the post-LGM recharge by very depleted waters. In the Czech Republic, the radiocarbon dating did not confirm the recharge prior 11 ka BP while depleted stable isotopic values suggest an origin in very cold climatic conditions

(Jiráková et al., 2010). The lack of data prior to 11 ka BP is in agreement with the permafrost retreat between 11.8 ka and 11 ka BP (Czudek, 1986).

A very particular situation appears in Estonian aquifers (N° 24). As they are characterised by extremely depleted $\delta^{18}O$ values of groundwater, it is likely that they were recharged by waters of glacial origin. Several hypothesis were framed to explain such a strong depletion. The base of the Fennoscandian ice sheet was during the late Weichselian probably in a molten state for approximately 11 ka (Jõeleht, 1998) which support the hypothesis that the recharge of aquifers could be done by subglacial isotopically depleted melt waters through the tunnel valleys (Vaikmäe et al., 2001b). Mokrik and Mazeika (2002) analysed a model of pre-Late Glacial permafrost environments to explain low $\delta^{18}O$ values and it was concluded that the infiltration took probably place earlier during glaciation between 20-35 ka BP. This is not compatible with Kalm (2006), who supposed that Estonia was ice-free between 22 and 43 ka BP with rather mild climate. Consequently, the most probable explanation for the depleted isotopic content seems to be the recharge of thaw waters from the gradually melting ice sheet base during ice ages. In this case, groundwater infiltrated below glaciers makes difficult to calculate accurate ages as air bubbles in the ice would contain atmospheric $\delta^{13}C$ value (Vaikmäe et al., 2001b).

However, the dating of Mokrik and Mazeika (2002) is in agreement with the investigation of the Middle-Upper Devonian aquifer system in Lithuania (N° 23), where low $^{14}C$ concentrations could also suggest ages around 20ka BP, indicating that the recharge in cold climate conditions may have taken place during the LGM or little prior (Mokrik et al., 2009). Yet, Lithuanian groundwaters do not show such depletion in stable isotopes as in Estonia. For that reason, the recharge in Estonian and Lithuanian aquifers could not occur by the same way or in the same time. On the basis of a great difference in the $\delta^{18}O$ content, it might be thus deduced that Estonian aquifers were charged only from the melting of the ice sheet base. On the other hand, Lithuanian aquifers were recharged by mixture of melt and river waters. The mixture of waters of different origins can explain why the Lithuanian and other north and central European groundwaters are relatively isotopically enriched. Apart from Lithuania, this mixed water recharge was observed in Denmark (N° 22) or in Czech aquifers (N° 17) as described previously.

A subglacial environment is not the particularity of north Europe only. These conditions can also be met in mountainous regions. For example, the groundwater recharge in subglacial environment also likely occurred in south Germany alpine foreland (N° 14) (Bertleff et al., 1993) which was during the Upper Weichselian covered by permafrost and foreland glaciation. The glacier water origin of groundwater is characterised by depleted $\delta^{18}O$ values around -14‰. Some other recharge processes linked with melting glaciers were also observed in other places in alpine regions (e.g. Zuppi and Sacchi, 2004).

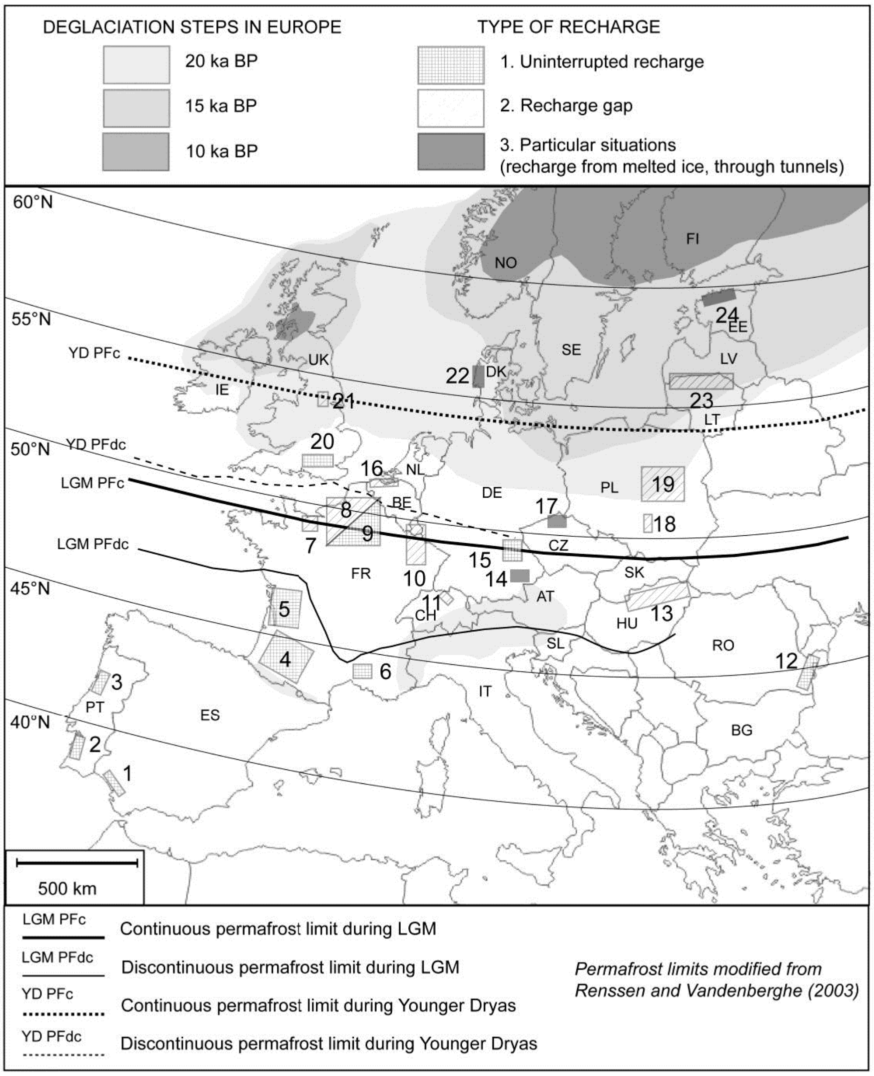


*Fig. 7. Typology of the recharge processes to deep aquifers throughout Europe.*

## 5. Conclusion

This paper introduces an insight into the palaeorecharge conditions prevailing in Europe during the last 40 ka BP (Fig. 7). The most recent findings about permafrost and ice sheet extension have been put together in order to explain some recharge features throughout the European continent. As the groundwater dating was not in the scope of this study, the paper rather aims at understanding the general recharge pattern and show discrepancies in the groundwater recharge processes. The study deals with many European aquifers in very different geological and hydrogeological contexts.

From a very extensive isotopic dataset of 24 different European sites, it has been deduced, that the groundwater recharge over the European continent can be divided into 2 major groups: (i) continuous and (ii) discontinuous recharge conditions. It has been noticed that in ice sheet or permafrost free areas the recharge has probably occurred continuously without any hiatus. This concerns the majority of the southern European as documented by examples in Spain, Portugal, France or Romania. The absence of very old groundwaters prior to LGM, mainly in coastal aquifers, could be explained by saline water intrusions masking the original palaeorecharge signature or constant climatic conditions.

Northwards, the climatic conditions around 20 ka BP were more severe and therefore more complicated recharge or even a lack of recharge is expected as the consequence of ice covered or frozen ground. The recharge hiatus that is notably registered in northern France, England and Hungary, generally corresponds to the LGM period although with slight differences in the hiatus duration or timing within LGM.

Some transitional situation can be observed in areas where more than one type of recharge has been registered. Such cases might be found in southern England, northern France, and Nuremberg area in Germany where groundwater dating suggests continuous recharge despite the fact, that the area was probably covered by permafrost. Though, it follows that in particular situations the existence of permafrost does not always inhibit the infiltration processes. These areas were probably under less severe climatic conditions.

Some recharge types, such as in Estonia and Lithuania, are related to the subglacial environment conditions considering that some areas of the bedrock were unfrozen despite the cold and dry climate. Another particularity have been observed for groundwaters which depleted stable isotopic signature indicated cold climate during recharge period but for which the radiocarbon dating did not confirm the palaeorecharge. The explanation for such cases lies in a post-LGM recharge by depleted melt water. This has been registered in Denmark or the Czech Republic.

Nowadays, all major aquifer formations are used for water supply and need improved knowledge about the history and the renewability of the recharge for a sustainable development of groundwater use. An accurate definition of aquifers recharge timing presents a major interest for groundwater modellers developing management plans for the water resources. Groundwater dynamics can be fully understood only if recharge timing and former environmental conditions are well appreciated. Although the aquifers and groundwater recharge have been since the last two decades intensely investigated throughout Europe and relatively detailed information is known for western and central European aquifers, there are still some gaps in the knowledge of aquifer system functioning in several countries, mainly those of Eastern Europe. Studies about geochemistry and isotopes do exist, but they should be enriched by more investigations focused on groundwater recharge oscillations. The efforts should be therefore made to fill up these gaps and uncertainties to provide continuous information on the recharge chronology of aquifers in order to extend this study.

## Acknowledgements

The authors would like to acknowledge French Ministry of Foreign Affairs and the Ministry of Education, Youth and Sports of the Czech Republic for supporting this study. The work was supported by the French Embassy in Prague and co-funded by the Grant Agency of the Czech Republic (GACR 205/07/0691) and the Specific University Research project (SVV 261 203).

## References

Aeschbach-Hertig, W., Peeters, F., Beyerle, U., Kipfer, R., 2000. Palaeotemperature reconstruction from noble gases in ground water taking into account equilibration with entrapped air. Nature 405 (6790), 1040-1044.

Aeschbach-Hertig, W., Stute, M., Clark, J.F., Reuter, R.F., Schlosser, P., 2002. A palaeotemperature record derived from dissolved noble gases in groundwater of the aquia aquifer (Maryland, USA). Geochemica et Cosmochemica Acta 5, 797–817.

Allen, R.J., Siegert, M.J., and Payne, T., 2007. Reconstructing glacier-based climates of LGM Europe and Russia – Part 3: Comparison with GCM and pollen-based climate reconstructions, Climate of the Past Discussions 3, 1199–1233.

Alley, R.B., Clark, P.U., 1999. The deglaciation of the northern hemisphere: a global perspective, Annual Reviews of Earth and Planetary Sciences 27, 149–182.

André, L., Franceschi, M., Pouchan, P., Atteia, O., 2005. Using geochemical data and modelling to enhance the understanding of groundwater flow in a regional deep aquifer, Aquitaine Basin, south–west of France. Journal of Hydrology 305, 40–62. doi:10.1016/j.jhydrol.2004.08.027.

Andrews, J.N., Lee, D.J., 1979. Inert gases in groundwater from the Bunter Sandstone of England as indicators of age and palaeoclimatic trends. Journal of Hydrology 41, 233-252.

Andrews, J.N., Balderer, W., Bath, A.H., Clausen, H.B., Evans, G.V., Florkowski, T., Goldbrunner, H.E., Ivanovich, M., Loosli, H., Zojer, H., 1984. Environmental isotope studies in two aquifer systems: a comparison of groundwater dating methods. In: Isotope Hydrology 1983, International Atomic Energy Agency, Vienna, 535-576.

Andrews, J.N., Goldbrunner, J.E., Darling, W.G., Hooker, P.J., Wilson, G.B., Youngman, M.J., Eichinger, L., Rauert, W., Stichler, W., 1985. A radiochemical, hydrochemical and dissolved gas study of groundwaters in the Molasse basin of Upper Austria. Earth an Planetary Science Letters 73, 317-332.

Andrews, J.N., Edmunds, W.M., Smedley, P.L., Fontes, J.C., Fifield, L.K., Allan, G.L., 1994. The Late Pleistocene palaeoclimate in southern England deduced from the $^{36}Cl$ content of groundwaters in the East Midlands Triassic Sandstone. Earth Planet Science Letters 122, 159-171.

Araguas-Araguas, L., Fröhlich, K., Rozanski, K., 2000. Deuterium and oxygen-18 composition of precipitation and atmospheric moisture. Hydrological Processes 14, 1341–1355.

Arppe, L., Karhu, J.A., 2010. Oxygen isotope values of precipitation and the thermal climate in Europe during the middle to late Weichselian ice age. Quaternary Science Reviews 29, 1263-1275. doi:10.1016/j.quascirev.2010.02.013.

Barbecot, F., Marlin, C., Gibert, E., Dever, L., 2000. Hydrochemical and isotopic characterisation of the Bathonian and Bajocian coastal aquifer of the Caen area (northern France). Applied Geochemistry 15, 791-805.

Bath, A.H., Edmunds, W.M., Andrews, J.N., 1979. Palaeoclimatic trends deduced from the hydrochemistry of a Triassic sandstone aquifer, United Kingdom. In: Isotope Hydrology, 1978, IAEA, Vienna, 545-568.

Benn, D.I., Ballantyne, C.K., 2005. Palaeoclimatic reconstruction from Loch Lomond Readvance glaciers in the West Drumochter Hills Scotland, Journal of Quaternary Science20, 577–592.

Bense, V.F., Person, M.A., 2008. Transient hydrodynamics within intercratonic sedimentary basins during glacial cycles. Journal of Geophysical Research 113. doi:10.1029/2007JF000969.

Beyerle, U., Purtschert, R., Aeschbach-Hertig, W., Imboden, D., Loosli, H., Wieler, R., Kipfer, R., 1998. Climate and groundwater recharge during the last glaciation in an ice-covered region. Science 282, 731-734.

Bertleff, B., Ellwanger, D., Szenkler, C., Eichinger, L., Trimborn, P., Wolfendale, N., 1993. Interpretation of hydrochemical and hydroisotopical measurements on palaeogroundwaters in Oberschwaben, south German alpine foreland, with focus on quanternary geology. In: Isotope techniques in the study of past and current environmental changes in the hydrosphere and the atmosphere. IAEA-SM-329. IAEA, Vienna, 337-357.

Blaser, P.C., Coetsiers, M., Aeschbach-Hertig, W., Kipfer, R., Van Camp, M., Loosli, H.H., Walraevens, K., 2010. A new groundwater radiocarbon correction approach accounting for palaeoclimate conditions during recharge and hydrochemical evolution: The Ledo-Paniselian Aquifer, Belgium. Applied Geochemistry 25 (3), 437-455. doi:10.1016/j.apgeochem.2009.12.011.

Blavoux, B., Olive, P., 1981. Radiocarbon dating of groundwater of the aquifer confined in the Lower Triassic sandstones of the Lorraine region, France. Journal of Hydrology 54, 167–183.

Boulton, G., Hagdorn, M., 2006. Glaciology of the British Isles Ice Sheet during the last glacial cycle: form, flow, streams and lobes. Quaternary Science Reviews 25 (23-24), 3359-3390. doi:10.1016/j.quascirev.2006.10.013.

Brown, J., Ferrians, O., Heginbottom, J.A., Melnikov, E.S., 1997. Circum-arctic map of permafrost and ground-ice conditions. 1:10,000,000 Map CP-45. Circum-Pacific map series, USGS.

Carreira, P.M., Soares, A.M.M., Marques da Silva, M.A., Araguas, L.A., Stute, M., Rozanski, K., 1996. Response of a coastal aquifer in Portugal to hydroclimatic changes during the last deglaciation period, traced by chemical, isotope and Noble Gas Dta. EOS, Transactions, American Geophysics Union 7 (22), W33.

Carreira, P.M., 1998. Paleoáguas de Aveiro. PhD Thesis, Universidade de Aveiro (Portugal).

Celle-Jeanton, H., Huneau, F., Travi, Y., Edmunds, W.M., 2009. Twenty years of groundwater evolution in the Triassic sandstone aquifer of Lorraine: Impacts on baseline water quality. Applied Geochemistry 24, 1198-1213. doi:10.1016/j.apgeochem.2009.03.005.

CLIMAP, 1981. Seasonal reconstructions of the earth's surface at the last glacial maximum. Geological Society of America, Map Chart Series MC-36.

COHMAP members, 1988. Climatic changes of the last 18,000 years: observations and model simulations. Science 241, 1043-1052.

Condesso De Melo, M.T., Carreira Paquete, P.M.M., Marques Da Silva, M.A., 2001. Evolution of the Aveiro Cretaceous aquifer (NW Portugal) during the Late Pleistocene and present day: evidence from chemical and isotopic data. In: Edmunds, W.M., Milne, C.J. (eds), Palaeowaters in Coastal Europe: evolution of palaeogroundwater since the late Pleistocene. Geological Society, London, Special Publications 189, 139-154. doi:10.1144/GSL.SP.2001.189.01.09.

Czudek, T., 1986. Pleistocene permafrost on the territory of Czechoslovakia (in Czech). Geografický časopis 38 (2-3), 245-252.

Dangaard, W., 1964. Stable isotopes in precipitation. Tellus 16, 436–468.

Darling, W.G., 2004. Hydrological factors in the interpretation of stable isotopic proxy data present and past: a European perspective. Quaternary Science Reviews 23, 743–770. doi:10.1016/j.quascirev.2003.06.016.

Darling, W.G., Edmunds, W.M., Smedley, P.L., 1997. Isotopic evidence for palaeowaters in the British Isles. Applied Geochemistry 12 (6), 813-829. doi:10.1016/S0883-2927(97)00038-3.

Delmas, M., Gunnell, Y., Braucher, R., Calvet, M., Bourlès, D., 2008. Exposure age chronology of the last glaciation in the eastern Pyrenees. Quaternary Research 69, 231– 241. doi:10.1016/j.yqres.2007.11.004.

Dennis, F., Andrews, J.N., Parker, A., Poole, J., Wolf, M., 1997. Isotopic and noble gas study of Chalk groundwater in the London Basin, England. Applied Geochemistry 12, 763-773.

Dietrich, S., Seelos, K., 2009. The reconstruction of paleo wind directions for the Eifel region (Central Europe) during the period 40.3–12.9 ka BP. Climate of the Past Discussions, 5, 2157–2176.

Douez, O., 2007. Réponse d'un système multicouche aux variations paléoclimatiques et aux solicitations anthropiques: Approche par modélisation couplée hydrodynamique, thermique et géochimique. Doct. Thesis. Univ. Bordeaux 3, 306 p.

Downing, R.A., Smith, D.B., Pearson, F.J., Monkhouse, R.A., Otlet, R.L., 1977. The age of groundwater in the Lincolnshire Limestone, England and its relevance to the flow mechanism. Journal of Hydrology 33 (3-4), 201-216.

Edmunds, W.M., 2005. Groundwater as an archive of climatic and environmental change. In: Aggarwal, P.K., Gat, J., Froehlich, K. (eds), Isotopes in the Water Cycle, Past, Present and Future of a Developing Science. Springer, 341–352.

Edmunds, W.M., Smedley, P.L., 2000. Residence time indicators in groundwater: the East Midlands Triassic sandstone aquifer. Applied Geochemistry 15, 737-752.

Edmunds, W.M., Milne, C.J. (eds), 2001. Palaeowaters in Coastal Europe: Evolution of Groundwater Since the Late Pleistocene. Geological Society, London, Special Publications 189.

Ehlers, J., 1996. Quaternary and Glacial Geology. John Wiley and Sons, Chichester, 578 pp.

Ehlers, J., Gibbard, P. L., 2004. Quaternary Glaciations - Extent and Chronology Part I: Europe. Elsevier, Amsterdam, 475 pp.

Ehlers, J., Gibbard, P.L., 2007. The extent and chronology of Cenozoic Global Glaciation. Quaternary International 164-165, 6-20.

Elliot, T., Andrews, J.N., Edmunds, W.M., 1999. Hydrochemical trends, palaeorecharge and groundwater in the fissured Chalk aquifer of the London and Berkshire Basins, UK. Applied Geochemistry 14, 333-363.

Farrera, I., Harrison, S.P., Prentice, I.C., Ramstein, G., Guiot, J., Bartlein, P.J., Bonnefille, R., Bush, M., Cramer, W., von Grafenstein, U., Holmgren, K., Hooghiemstra, H., Hope, G., Jolly, D., Lauritzen, S.E., Ono, Y., Pinot, S., Stute, M., Yu, G., 1999. Tropical climates at the Last Glacial Maximum: A new synthesis of terrestrial palaeoclimate data. I. Vegetation, lake-levels and geochemistry. Climate Dynamics 15 (11), pp. 823-856. doi:10.1007/s003820050317.

Fernandes, P.G., Carreira, P.M., 2008. Isotopic evidence of aquifer recharge during the last ice age in Portugal. Journal of Hydrology 361, 291-308. doi: 10.1016/j.jhydrol.2008.07.046.

French, H.M., 1996. The Periglacial Environment, 2nd edition. Addison Wesley. Longman, London, 341 pp.

Frenzel, B., 1992. Climate in the Northern Hemisphere during the formation of the inland ice masses between about 35 000 to 25 000 BP. Erdkunde 46 (3-4), pp. 165-187.

Fricke, H.C., O'Neil, J.R., 1999. The correlation between $^{18}O/^{16}O$ ratios of meteoric water and surface temperature: its use in investigating terrestrial climate change over geologic time. Earth and Planetary Science Letters 170, 181-196.

Fryar, A.E., Mullican, W.F., Macko, S.A., 2001. Groundwater recharge and chemical evolution in the southern High Plains of Texas, USA. Hydrogeology Journal 9, 522 – 542. doi : 10.1007/s10040-001-161-9.

Gastmans, D., Chang, H.K., Hutcheon, I., 2010. Stable isotopes ($^{2}H$, $^{18}O$ and $^{13}C$) in groundwaters from the northwestern portion of the Guarani Aquifer System (Brazil). Hydrogeology Journal. In press. doi: 10.1007/s10040-010-0612-2.

Gatto, P., Carbognin, L., 1981. The lagoon of Venice : natural environmental trend and man-induced modification. Hydrological Sciences Bulletin 26 (4), 379-391.

Geyh, M.A., Backhaus, G., Andres, G., Rudolph, J. and Rath, H.K., 1984. Isotope study on the Keuper Sandstone Aquifer with a leaky cover layer. In: Proceedings of IAEA-SM-270 Symposium, Vienna, 499–513.

Gibbard, P.L., Cohen, K.M., 2008. Global chronostratigraphical correlation table for the last 2.7 million years. Episodes 31.

Guiter, F., Andrieu-Ponela, V., De Beaulieua, J.L., Cheddadia, R., Calvezb, M., Ponela, P., Reillea, M., Kellera, T., Goeurya, C., 2003. The last climatic cycles in Western Europe: a comparison between long continuous lacustrine sequences from France and other terrestrial records. Quaternary International 111, 59–74.

Harrar, W.G., Williams, A.T., Barker, J.A., Van Camp, M., 2001. Modelling scenarios for the emplacement of palaeowaters in aquifer systems, Geological Society, London, Special Publication 189, 213-229. doi: 10.1144/GSL.SP.2001.189.01.13.

Hinsby, K., Harrar, W.G., Nyegaard, P., Konradi, P.B., Rasmussen, E.S., Bidstrup, T., Gregersen, U., Boaretto, E., 2001. The ribe formation in western Denmark - Holocene and Pleistocene groundwaters in a coastal Miocene sand aquifer. In: Edmunds, W.M., Milne, C.J. (eds), Palaeowaters in Coastal Europe: Evolution of Groundwater Since the Late Pleistocene. Geological Society, London, Special Publications 189, 29-48.

Houmark-Nielsen, M., 2004. The Pleistocene of Denmark: a review of stratigraphy and glaciation history. In: Ehlers, J., Gibbard, P. (Eds.), Quaternary Glaciations - Extent and Chronology Part I: Europe. Elsevier, Amsterdam, 35-46.

Houmark-Nielsen, M., Kjær, K.J., 2003. Southwest Scandinavia, 40–15 kyr BP: Palaeogeography and environmental change, Journal of Quaternary Science 18,. 769–786.

Hughes, P.D., Woodward, J.C., 2008. Timing of glaciation in the Mediterranean mountains during the last cold stage. Journal of Quaternary Science 23 (6-7), 575–588.

Huijzer, A.S., Isarin, R.F.B., 1997. The reconstruction of past climates using multi-proxy evidence: an example of the Weichselian Pleniglacial in northwestern andcentral Europe. Quaternary Science Reviews 16, 513–533.

Huijzer, A.S., Vandenberghe, J., 1998. Climatic reconstruction of the Weichselian Pleniglacial in northwestern andcentral Europe. Journal of Quaternary Science 13, 391–417.

Huneau, F., 2000. Fonctionnement hydrogéologique et archives palaeoclimatiques d'un aquifère profond mediteranéen. Doct. Thesis. Univ. Avignon, 180 p.

Huneau, F., Blavoux B., 2000. Isotopic hydrogeology within the Miocene basin of Carpentras-Valreas (southeastern France). In: Dassargues A. (ed), Tracers and Modelling in Hydrogeology. IAHS-AISH Publication 262, 433-438. ISBN:190150221X.

Huneau, F., Blavoux, B., Bellion Y., 2001. Differences between hydraulic and radiometric velocities of groundwaters in a deep aquifer: example of the Valréas Miocene aquifer (southeastern France). Comptes Rendus de l'Académie des Sciences - Series IIA - Earth and Planetary Science, 333, 163-170. doi:10.1016/S1251-8050(01)01605-6.

IAEA/WMO (2006). Global Network of Isotopes in Precipitation. The GNIP Database. Accessible at: http://www.iaea.org/water

Isarin, R.F.B., 1997. Permafrost distribution and temperatures in Europe during the Younger Dryas. Permafrost and Periglacial Processes 8, 313–333.

Jiráková, H., Huneau, F., Celle-Jeanton, H., Hrkal, Z., Le Coustumer, P., 2009. Palaeorecharge conditions of the deep aquifers of the Northern Aquitaine region (France). Journal of Hydrology 368, 1-16. doi:10.1016/j.jhydrol.2009.01.017.

Jiráková, H., Huneau, F., Hrkal, Z., Celle-Jeanton, H., Le Coustumer, P., in press. Carbon isotopes to constrain the origin and circulation pattern of groundwater in the north-western part of the Bohemian Cretaceous Basin (Czech Republic). Applied Geochemistry 25, 1265-1279. doi:10.1016/j.apgeochem.2010.05.012.

Jõeleht, A., 1998. Geothermal studies of the Precambrian basement and Phanerozoic sedimentary cover in Estonia and in Finland. Doct. Thesis. University of Tartu.

Jost, A., 2005. Caractérisation des forçages climatiques et géomorphologiques des cinq derniers millions d'années et modélisation de leurs conséquences sur un système aquifère complexe: le bassin de Paris. Doct. Thesis. Univ. Pierre et Marie Curie, Paris VI, 344 p.

Jouzel, J., Petit, J.R., Souchez, R., Barkov, N.I., Lipenkov, V.Y., Raynaud, D., Stievenard, M., Vassiliev, N.I., Verbeke, V., Vimeux, F., 1999. More than 200 meters of lake ice above subglacial lake Vostok, Antarctica. Science 10 (286/5447), pp. 2138 – 2141. doi:10.1126/science.286.5447.2138.

Kalm, V., 2006. Pleistocene chronostratigraphy in Estonia, southeastern sector of the Scandinavian glaciation. Quaternary Science Reviews 25 (9-10), 960-975.

Kemp, W.J.M., van der Appelo, C.A.J., Walraevens, K., 2000. Inverse modeling and radiocarbon dating of palaeogroundwaters: the Tertiary Ledo-Paniselian aquifer in Flanders, Belgium. Water Resources Research 28, 1277–1287.

Kloppmann, W., Dever, L., Edmunds, W.M., 1998. Residence time of Chalk groundwaters in the Paris Basin and the North German Basin: a geochemical approach. Applied Geochemistry 13 (5), 593-606.

Kovács, J., Fábián, S.Á., Schweitzer, F., Varga, G., 2007. A relict sand-wedge polygon site in north-central Hungary. Permafrost and Periglacial Processes 18 (4), 379-384.

Kutzbach, J., Gallimore, R., Harrison, S., Behling, P., Selin R., Laarif, F., 1998. Climate and biome simulations for the past 21,000 years, Quaternary Science Reviews 17, 473–506.

Labeyrie, J., 2006. Paleoclimats and climatic mechanisms *(in French)*. C. R. Palevol 5, 27–34. doi:10.1016/j.crpv.2005.09.015.

Lavastre, V.,Le Gal La Salle, C., Michelot, J.L., Giannesini, S., Benedetti, L.,Lancelot, J., Lavielle, B.,Massault, M.,Thomas, B., Gilabert, E., Bourlès, D., Clauer, N., Agrinier, P., 2010. Establishing constraints on groundwater ages with $^{36}Cl$, $^{14}C$, $^{3}H$, and noble gases: A case study in the eastern Paris basin, France. Applied Geochemistry 25, 123–142. 10.1016/j.apgeochem.2009.10.006.

Lloyd, J.W., 1990. Groundwater resources development in the eastern Sahara. Journal of Hydrology 119, 71-87.doi:10.1016/0022-1694(90)90035-V.

Lowe, J.J., NASP Members, 1995. Palaeoclimate of the North Atlantic seaboards during the last glacial/interglacial transition. Quaternary International 28, 51-61.

Lunkka, J.P., Saarnisto, M., Gey, V., Demidov, I., Kiselova, V., 2001. Extent and age of the Last Glacial Maximum in the southeastern sector of the Scandinavian Ice Sheet. Global and Planetary Change 31 (1-4), 407-425. doi:10.1016/S0921-8181(01)00132-1.

Manzano, M., Custodio, E., Loosli, H., Cabrera, M.C., Riera, X., Custodio, J., 2001. Palaeowater in coastal aquifers in Spain. In: Edmunds, W.M., Milne, C.J. (eds), Palaeowaters in Coastal Europe: evolution of palaeogroundwater since the late Pleistocene. Geological Society, London, Special Publication 189, 107-138.

Marks, L., 2002. Last Glacial Maximum in Poland, Quaternary Science Review 21, 103–110.

Mokrik, R., Mazeika, J., 2002. Palaeohydrogeological reconstruction of groundwater recharge during Late Weichselian in the Baltic basin. Geologija 39, 49-57.

Mokrik, R., Mazeika, J., Baublyte, A., Martma, T., 2009. The groundwater age in the Middle-Upper Devonian aquifer system, Lithuania. Hydrogeology Journal 17, 871-889.

Moneim, A.A.A., 2005. Overview of the geomorphological and hydrogeological characteristics of the Eastern Desert of Egypt. Hydrogeology Journal 13 (2), 416-425. doi: 10.1007/s10040-004-0364-y.

Pestov, I., 2000. Thermal Convection in the Great Artesian Basin, Australia. Water Resources Management 14, 391–403.

Peyron, O., Guiot, J., Cheddadi, R., Tarasov, P., Reille, M., de Beaulieu, J.-L., Bottema, S., Andrieu, V., 1998. Climatic reconstruction in Europe for 18 000 yr BP from pollen data, Quaternary Research 49, 183–196.

Rabelo, J.L., Edson W., 2009. Assessment of groundwater recharge and water fluxes of the Guarani Aquifer System, Brazil. Hydrogeology Journal 17, 1733–1748. doi: 10.1007/s10040-009-0462-y.

Raoult, Y., 1999. La nappe de l'Albien dans le bassin de Paris : de nouvelles idees pour de vielles eaux. Doct. Thesis. Univ.Paris VI, 170 p.

Renssen, H., Vandenberghe, J., 2003. Investigation of the relationship between permafrost distribution in NW Europe andextensive winter sea-ice cover in the North Atlantic Ocean during the cold phases of the Last Glaciation. Quaternary Science Reviews 22, 209–223. doi:10.1016/S0277-3791(02)00190-7.

Rinterknecht, V.R., Clark, P.U., Raisbeck, G.M., Yiou, F., Bitinas, A., Brook, E.J., Marks, L., Zelcs, V., Lunkka, J.-P., Pavlovskaya, I.E., Piotrowski, J.A., Raukas, A., 2006. The last deglaciation of the southeastern sector of the Scandinavian ice sheet. Science 311, 1449-1452.

Rosenberg, N.J., Epstein, D.J., Wang, D.,Vail, L., Srinivasan, R., Arnold, J.G, 1999. Possible impacts of global warming on the hydrogeology of the Ogallala aquifer region. Climatic Change 42, 677–692.

Rozanski, K., 1985. Deuterium and oxygen-18 in European groundwaters – links to atmospheric circulation in the past. Chemical Geology 52, 349–363. doi:10.1016/0168-9622(85)90045-4.

Rozanski, K., Araguas-Araguas, L., Gonfiantini, R., 1992. Relation between long-term trends of oxygen-18 isotope composition of precipitation and climates. Science 258, 981–984.

Rudolph, J., Rath, H.K., Sonntag, C., 1983. Noble gases and stable isotopes in 14C dated paleowaters from central Europe and the Sahara, IN: Isotope Hydrology, IAEA, Vienna, 467–477.

Schluchter, C., Wohlfarth-Meyer, B., 1987. Till facies varieties of the Western Swiss Alpine Foreland. Tills and glaciotectonics. Proc. INQUA symposium, Amsterdam, 1986, 67-72.

Smith, D.B., Downing, R.A., Monkhouse, R.A., Otlet, R.L., Pearson, F.J., 1976. The age of groundwater in the Chalk of the London Basin. Water Resources Research 12, 392-404.

Sracek, O., Hirata, R., 2002. Geochemical and stable isotopic evolution of the Guarani Aquifer System in the state of São Paulo, Brazil. Hydrogeology Journal 10, 643-655. doi:10.1007/s10040-002-0222-8.

Stute, M., Deak, J., 1989. Environmental isotop e study ($^{14}C$, $^{13}C$, $^{18}O$, D, Noble Gases) on deep groundwater circulation systems in Hungary with reference to palaeoclimate. Radiocarbon 31 (3), 902-918.

Tarasov, P.E., Peyron, O., Guiot, J., Brewer, S., Volkova, V.S., Bezusko, L.G., Dorofeyuk, N.I., Kvavadze, E.V., Osipova, I.M., Panova, N.K., 1999. Last Glacial Maximum climate of the former Soviet Union and Mongolia reconstructed from pollen and plant macrofossil data, Climate Dynamics 15, 227–240.

Ţenu, A., Noto, P., Cortecci, G., Nuti, S., 1975. Environmental isotopic study of the Barremian-Jurassic aquifer in South Dobrogea (Roumania). Journal of Hydrology 26 (3-4), 185-198.

Toucanne, S., Zaragosi, S., Bourillet, J.F., Gibbard, P.L., Eynaud, F., Giraudeau, J., Turon, J.L., Cremer, M., Cortijo, E., Martinez, P., Rossignol, L., 2009. A 1.2 Ma record of glaciation and fluvial discharge from the West European Atlantic margin. Quaternary Science Reviews 28 (25-26), December 2009, 2974-2981.

Vaikmäe, R., Edmunds, W.M., Manzano, M., 2001a. Weichselian palaeoclimate and palaeoenvironment in Europe: Background for palaeogroundwater formation. In: Edmunds, W.M., Milne, C.J. (eds), Palaeowaters in Coastal Europe: evolution of palaeogroundwater since the late Pleistocene. Geological Society, London, Special Publication 189, 163-191.

Vaikmäe, R., Vallner, L., Loosli, H.H., Blaser, P.C., Juillard-Tardent, M., 2001b. Palaeogroundwater of glacial origin in the Cambrian-Vendian aquifer of northern Estonia. In: Edmunds, W.M., Milne, C.J. (eds), Palaeowaters in Coastal Europe: evolution of palaeogroundwater since the late Pleistocene. Geological Society, London, Special Publication 189, 17-27. doi:10.1144/GSL.SP.2001.189.01.03.

Vandenberghe, J., Huijzer, B., Mücher H., Laan, W., 1998. Short climatic oscillations in a western European loess sequence (Kesselt, Belgium), Journal of Quaternary Science 13, 471–485.

Van Vliet-Lanoë, B., 1998. Pattern ground, hummocks, and Holocene climate changes. Eurasian Soil Science 31 (5), 507–513.

Walker, M.J.C., Bohncke, S.J.P., Coope, G.R., O'Connell, M., Usinger, H., Verbruggen, C., 1994. The Devensian/Weichselian late-glacial in northwest Europe (Ireland, Britain, north Belgium, the Netherlands, northwest Germany), Journal of Quaternary Science 9 (2), 109-118.

Walraevens, K., 1998. Natural isotopes and Noble Gases in Groundwater of the Tertiary Ledo-Paniselian Aquifer in East and West Flanders. Natuurwet. Tijdschr. 78, 246-260.

Walraevens, K., Van Camp, M., Lermytte, J., Van Der Kemp, W.J.M., Loosli, H.H., 2001. Pleistocene and Holocene groundwaters in the freshening Ledo-Paniselian aquifer in Flanders, Belgium. In: Edmunds, W.M., Milne, C.J. (eds), Palaeowaters in Coastal Europe: evolution of palaeogroundwater since the late Pleistocene. Geological Society, London, Special Publication 189, 49-70.

Webb, T., Kutzbach, J.E., 1998. An introduction to Late Quaternary climates: Data syntheses and model experiments. Quaternary Science Reviews 17 (6-7), 465-471. doi:10.1016/S0277-3791(98)00008-0.

Wendland, E., Barreto, C., Gomes, L.H., 2007. Water balance in the Guarani Aquifer outcrop zone based on hydrogeologic monitoring. Journal of Hydrology 342, 261-269. doi:10.1016/j.jhydrol.2007.05.033.

Woodward, J.C., Macklin, M.G., and Smith, G.R., 2004. Pleistocene glaciation in the mountains of Greece. In: Ehlers J., Gibbard, P.L. (eds), Quaternary Glaciations – Extent and Chronology Part I: Europe, 155–174.

Wysota,W., Lankauf, K.R., Szmanda, J., Chruscinska, A., Oczkowski, H.L., Przegietka, K. R., 2002. Chronology of the Vistulian (Weichselian) glacial events in the Lower Vistula Region, Middle-North Poland. Geochronometria 21, 137-142.

Zazo, C., Goy, J.L., Lario, J., Silva, P.G., 1996. Littoral zone and rapid climatic changes during the last 20.000 years: the Iberian study case. Zeitrift für Geomorphologie N.F.Suppl. 102, 119-134.

Zhang, M., Frape, S.K., Love, A.J., Herczeg, A.L., Lehmann, B.E., Beyerle, U., Purtschert, R., 2007. Chlorine stable isotope studies of old groundwater, southwestern Great Artesian Basin, Australia. Applied Geochemistry 22, 557–574. doi:10.1016/j.apgeochem.2006.12.004

Zuber, A., Weise, S.M., Osenbrück, K., Pajnowska, H., Grabczak, J., 2000. Age and recharge pattern of water in the Oligocene of the Mazovian basin (Poland) as indicated by environmental tracers. Journal of Hydrology 233, 174-188.

Zuber, A., Weise, S.M., Motyka, J., Osenbrück, K., Rozanski, K., 2004. Age and flow pattern of groundwater in a Jurassic limestone aquifer and related Tertiary sands derived from combined isotope, noble gas and chemical data. Journal of Hydrology 286, 87-112. doi: 10.1016/j.jhydrol.2003.09.004.

Zuppi, G.M., Sacchi, E., 2004. Hydrogeology as a climate recorder: Sahara-Sahel (North Africa) and the Po Plain (Northern Italy). Global and Planetary Change 40, 79-91.

# GEOTHERMAL APPLICATIONS

## 4.8 Geothermal potential of groundwater

Geothermal energy, produced in the inner geological layers essentially by the disintegration of the radioactive isotopes, slowly reaches the earth surface. The geothermal gradient is being used to quantify the heat flux. The average geothermal gradient for the Earth is about 3°C/100 m which complies with the heat flux of 63 $mW/m^2$.

On the Earth surface, several places reveal much higher geothermal gradient, most often on the continental or oceanic rift zones or on the limits with mountain ranges. Hot rocks near the surface can generate thermal sources or geysers. Outside such particular areas, groundwater generally attains the rock temperature which becomes higher as the depth increases.

The tectonics itself can be viewed for the proper geothermal source but more often, it plays a secondary role for the heat distribution. The role of tectonics should be clarified as it may either facilitate the flow of groundwater which is the medium for the heat transport or on the contrary represent a barrier for the groundwater flow.

Once groundwater reaches deep horizons in sedimentary formation, its contact with hot rocks at several hundred meters below the surface increases the temperature of groundwater. Owing to this geothermal potential, the deep confined aquifers are considered to be one of the most important alternatives of low potential renewable energy resources. As generally considered, groundwater exploitation is involved in the sustainable geothermal development, but it has to be kept in mind that its “renewability” remains somewhat ambiguous. Many sites throughout the world have already experienced the limits of such renewability and the geothermal potential of given areas has to be reconsidered.

The assessment of the geothermal potential of the sedimentary formations is essential for future projects and further steps towards an appropriate geothermal development.

The most expressive parameter is definitely the heat flux reflecting all the processes linked to the heat storage and transport. Heat flux distribution follows an easy equation showing, that the heat flux is the product of the geothermal gradient and the thermal conductivity:

$q = G * \lambda$ ($mW/m^2$),

where q is the heat flux ($W/m^2$), G is geothermal gradient (K/m) and $\lambda$ is thermal conductivity (W/mK).

- The *geothermal gradient* is deduced directly from the well-logging measurements, but great attention has to be paid on different factors affecting the natural conditions. The above mentioned equation is most reliable in the areas without any groundwater flow, i.e. the heat is distributed via conduction only. However, its use in important hydrogeological structures is only approximative. In basin structures, notably in infiltration and discharge zones, the vertical flow considerably disrupts the natural geothermal gradient. Apart from this, the effect of the altitude differences might be also responsible for discrepancies in the heat flow in mountainous areas. To avoid any uncertainties in the heat flow results, the correction for the topography effect should be carried out.

- The *thermal conductivity* has a first-order control on the configuration on the heat flow. This parameter depends on the porosity, lithological and petrographical properties and has to be therefore measured in the particular rock sample. In geologically complex formations, several values should be established according to the different lithologies.

Following the intricate situations concerning the almost omnipresent vertical flow in hydrogeological basins, heat flow calculated using the given equation may be preferentially elevated in the drainage areas while the infiltration areas show rather lower values.

This approach evaluates the existing heat flux reflecting the actual hydrogeological and tectonic conditions.

## 4.9 Geothermal investigation in deep aquifers of the Bohemian Cretaceous Basin

In the Czech Republic, the geothermal energy has been included among the renewable sources of energy in the national energy program for renewable resources. Several geothermal studies in the northern Bohemia have been carried out within the last 30 years. Besides being the largest groundwater resource of potable water in the Czech Republic, the BCB is probably the largest thermal water reservoir in the country with an estimated yield of 300 $Ls^{-1}$ and a present use rate of 200 $Ls^{-1}$ for house heating and pools.

In order to confirm the thermal exceptionality of the BUAS, a research project has been attributed to Charles University to participate in. One of the most important theoretical questions of the project was to evaluate the possible groundwater interaction between the Děčín and the Ústí nad Labem groundwater accumulations. Based on the analysis and interpretation of the available geological and hydrogeological works, a conceptual model of the BUAS has been developed. Detailed studies beyond the scope of this project were simultaneously carried out to propose a groundwater flow model for the water and the heat balance. Preliminary conclusions suggest an existence of two independent subsystems.

Previous studies on the territory of the Czech Republic indicated the geothermal importance of this area indicating an average heat flux around 80 $mW.m^{-2}$ in its axial part (Čermák and Jetel, 1985). Permocarboniferous sediments underneath indicate values close to 100 $mW.m^{-2}$ (Myslil et al., 2005). These data support the fact, that the north eastern sector of the Bohemian Massif is formed of a zone with a relatively weakened Earth's crust.

However, the term “renewable” for geothermal resources is rather ambiguous. In the BCB, the limits of renewability have been already observed as generally increasing intensity of groundwater pumping in drainage zones leads to the temperature decrease in the thermal groundwater accumulations. As a consequence, possible future increase in fresh groundwater extraction in the vicinity of the infiltration areas in the extended BUAS with a great geothermal potential may considerably reduce the thermal water production. As follows, the determination of the upper limit of a long-term geothermal development has become a challenging task in geothermal systems. This can be accomplished by conceptual and subsequently numerical modelling which cannot avoid the development of detailed investigation of the thermal field properties established from the field work measurements. Thermal field data in the upper part of the earth crust are acquired by the temperature well-logging in-situ methods. More details about geothermal research in the BCB is available in *Chapter 4.12*.

## 4.10 Geothermal well-logging

Data on the temperature field in the upper part of the earth's crust are obtained by thermometry, which is one of the commonly used well-logging methods. Most recent deep continuous temperature borehole measurements acquired by Aquatest a.s. were performed by high sensitivity thermometers of 0.01 °C (Fig. 12). It is a unique in-situ method for obtaining depth continuous data on temperature field in the rock environment, which cannot be substituted by any other method providing similar results. Temperature data is the fundamental building block in creating a thermal model of the entire area of interest. Fig. 13 illustrates the field measurement.

*Fig. 12. Photograph of high sensitive probes for temperature measurements.*

*Fig. 13. Illustrative photographs taken during the well-logging measurements.*

## 4.11 Assessment of the lithological properties

Groundwater dynamics and the possible exploitation potential is governed by the ratio between pelitic and psamitic minerals forming the aquifers. Likewise for hydrogeological studies, the lithology is an important parameter also for geothermal investigations and should be evaluated. The BCB has been generally considered to consist of mainly sandstones which are very favourable for underground water flow making the BCB a very exploitable structure. It is true as a whole, but great lithological differences at the local scale were observed in the study area. This can considerably affect the results from the geothermal study and lead to difficulties in proposing accurate thermal conductivity coefficients. That is why the proportion between clayey and sandy rocks must be quantified. Seventy two well-logging records within the whole region were collected (Annexe 1).

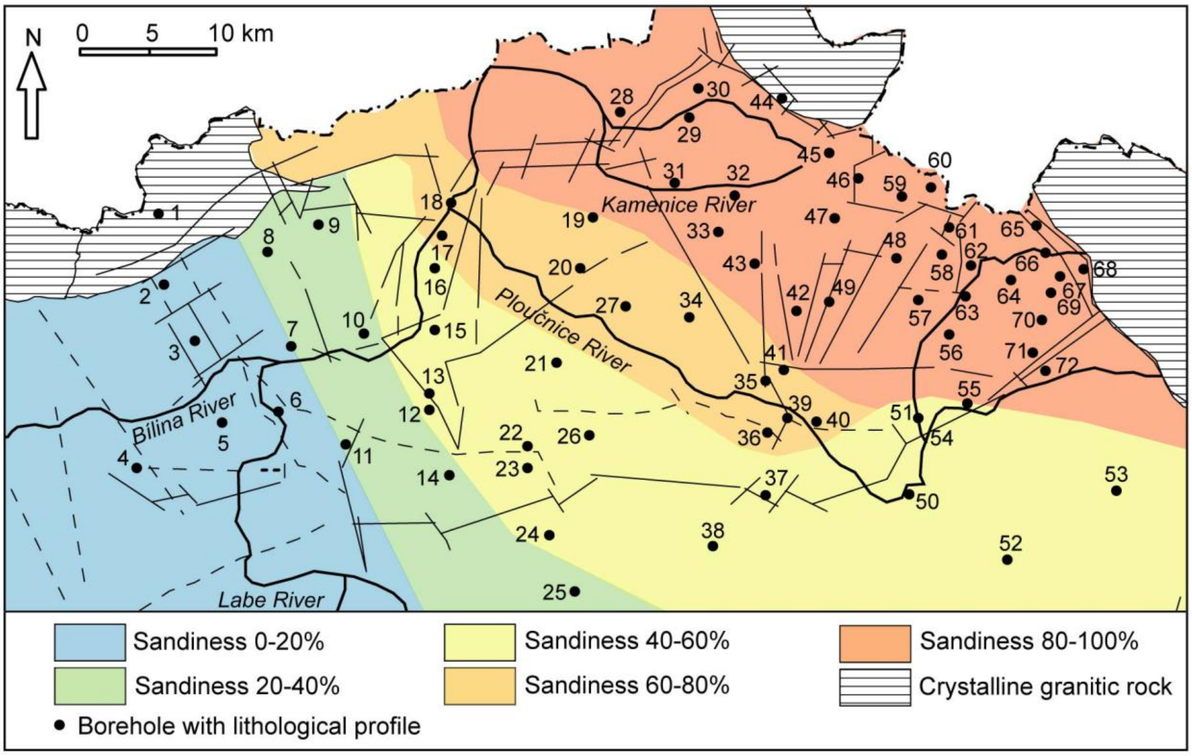


*Fig. 14. Degree of sand ratio in the sedimentary rocks within the study area with indicated gradual transition from high-sandy sediments into clayey sediments from northeast to west. Numbers of boreholes refer to Annexe 1.*

Although a great number of boreholes with identified lithological profile do exist in the study area, only those referring to the whole Cretaceous sequence were considered, that is to say boreholes, that reached the Cretaceous basement (Permo-Carboniferous or crystalline basement). Considered boreholes were analysed for the ratio between sand and clay content through the Cretaceous sequence. Results were categorized into groups with 20% interval of sandiness. Each borehole was thus attributed to a group. The output is schematically displayed in Fig. 14 which shows, that Cretaceous sediments contain indeed a lot of pure sandstone, namely on the north east. Then, pure sandstones reveal a gradual transition into clayey sediments towards the west of the study area. The categorization by the percentage of sand content will be useful for further evaluation of thermal conductivity.

## 4.12 Geothermal assessment of the deep aquifers of the north western part of the Bohemian Basin, Czech Republic

*Paper in press as:*

*Jiráková, H., Procházka, M., Dědeček, P., Kobr, M., Hrkal, Z., Huneau, F., Le Coustumer, P. Geothermal assessment of the deep aquifers of the northwestern part of the Bohemian Cretaceous Basin, Czech Republic. Geothermics.*

# Geothermal Assessment of the Deep Aquifers of the northwestern part of the Bohemian Cretaceous Basin, Czech Republic

Hana Jiráková, Martin Procházka, Petr Dědeček, Miroslav Kobr, Zbyněk Hrkal, Frédéric Huneau, Philippe Le Coustumer

**Abstract**

Groundwater in the Benešov-Ústí aquifer system in the northwestern Bohemian Cretaceous basin has been intensely exploited since the twentieth century. Apart from providing drinking water, it contains the most extensive accumulation of thermal water in the country. However, excessive exploitation can result in temperature declines and changes in the quality of the groundwater in the future. More than a hundred in-situ temperature measurements were used to assess the geothermal gradient and heat flux. However, intense groundwater vertical flow across the well significantly controls the heat flux distribution, resulting in a huge range of values—from less than 50 mW/m$^2$ within infiltration areas to more than 125 mW/m$^2$ in drainage areas. Certain simplifications and corrections considering the vertical flow between different permeable zones were developed, and the correction for topography as well as lithological variability have been applied to improve accuracy of the geothermal gradient assessment. Despite the fact that the Bohemian Cretaceous basin is tectonically very complex, it is concluded that tectonics [with the exception of the Eger (Ohře) rift] has only a secondary effect on the thermal field. Two longitudinal W-E areas in the Benešov-Ústí aquifer system have elevated heat flux values. The calculated heat flux values are useful for heat transfer modelling and the assessment of the sustainable limits of thermal water exploitation.

Keywords

Heat flux, Geothermal gradients, Thermal conductivity, Thermometry, Well logging, Groundwater

## 1. Introduction

The demand for geothermal energy is growing worldwide since it can be both inexpensive and environmentally friendly (Bertani 2005; Lund et al. 2005). The heat flux reflecting the integrated thermal structure is a key element in quantifying the geothermal potential. Well-logging methods are commonly used in obtaining information from well profiles reaching several hundreds or even thousands of meters (e.g. Serban et al., 2001, Demetrescu et al., 2005, Ollinger et al., 2010, Hooijkaas et al., 2010). However, various factors can affect their accuracy and reliability of heat flux quantification. As many authors have observed, heat flux is largely controlled by groundwater flow (Grinbaum, 1962; Mansure and Reiter, 1979; Čermák and Jetel, 1985; Clauser and Villinger, 1990; Kelly and Mareš, 1993; Vasseur and Demongodin, 1995; Štulc, 1998; Lubis et al., 2008). Heat flux assessment within a well in a multilayered aquifer system is often complicated due to vertical flow between aquifers. The vertical flow within the borehole often causes sudden differences between the natural geothermal gradient in the formation and in the well. Precautions are necessary to ensure that the recorded temperature is representative of the rock formation and is not influenced by movement of water in the borehole (Mansure and Reiter, 1979). Groundwater flow often causes up to a 50 % decrease/increase in geothermal gradient in recharge/drainage zones depending on the character and intensity of groundwater flow. Distortions in the geothermal gradient can be used as a tool for determination of recharge/drainage areas (Lubis et al., 2008). Therefore, the phenomenon of natural vertical water flow in boreholes (or a hydraulic short circuit between different aquifers or between fractures with different permeability) has to be taken into consideration in geothermal investigation.

Tracer dilution may be used to identify water movement along or across the borehole and to determine the yield of aquifers. This technique relies on measurement of changes in the physical properties of the fluid in the hole such as resistivity, temperature, radioactivity and transparency after the injection of a tracer into the hole. Variation of these properties as a function of depth in the borehole is used for the assessment of both the hydraulic dynamics and the inflows. Details of these techniques have been described in Chapellier (1992), Kelly and Mareš (1993), Mareš et al. (1994), Kobr et al. (2005). Additionally, permeable zones and sections with vertical movement of water through the well and behind the casing can be identified by the high-resolution temperature logs.

In the Czech Republic, geothermal resources have been studied in detail over the last 10 years. According to the Ministry of Industry and Business, geothermal energy is included in the renewable sources of energy in the national energy program. The history of thermal water exploitation for health resorts and swimming pools dates back several hundred years.

The Bohemian Cretaceous basin (BCB) has been extensively exploited for over 100 years, mostly as a resource for drinking water supply. Favourable hydraulic and geological characteristics have created conditions for extensive thermal water exploitation from the sedimentary basin. In several areas of the BCB, thermal waters have been pumped with generally increasing intensity, thereby affecting the hydrogeological conditions and the water quality. As mentioned above, the aquifer system also has a great fresh groundwater potential. The existing fresh water yield has been estimated at around 9 $m^3/s$ (Herčík et al., 1999). Because of the relatively short period of thermal water exploitation (in geological terms), the real consequences such as changes in temperature and water quality and quantity have yet to be quantified.

Well logging methods in groundwater surveys of complicated aquifer systems in the BCB were described in Datel et al. (2009) focusing on the optimal exploitation of water resources and their protection against contamination. Among various well logging methods (such as measurements of resistivity, conductivity, radioactivity, etc.) available for characterizing the geological and hydrogeological conditions in the study area, thermometry is the only one that can provide a reliable measure of the thermal potential of the formation.

Previous geothermal studies in the territory of the Czech Republic (e.g. Čermák, 1975 and 1979; Čermák and Šafanda, 1982; Hurter and Schellschmidt, 2003; Myslil et al., 2005) indicated the geothermal importance of the western part of the BCB. The most promising areas of the BCB are in its axial part (the deepest part), where the average heat flux exceeds 80 $mW.m^{-2}$. (Tertiary basins in the west have a heat flux higher than 100 $mW.m^{-2}$.) Permocarboniferous basins also show a heat flux of 90 to 100 $mW.m^{-2}$ (Myslil et al., 2005).

This paper presents the result of an investigation aimed at providing detailed information about the temperature, thermal gradient and heat flux on the basis of the interpretation of borehole temperature profiles. The main objective of the study was to evaluate the heat flux distribution within the Benešov-Ústí aquifer system.

The study area is characterised by a well-developed fracture system and relatively thick Cretaceous layers of marly siltstones and sandstones, with generally favourable hydrogeological parameters. As a result, intense groundwater exploitation has occurred which should be optimized for availability in future decades. For this reason, it was decided to carry out a detailed geothermal study based on real measurements in the field. In addition, the work represents a regional study of the northwestern part of the BCB and contributes to the general knowledge of the extent of the present-day geothermal resources. The data can be useful in modelling and simulation of the hydrogeological and geothermal processes to determine the limits of the sustainable development of the geothermal resources.

## 2. Study area

### 2.1. General setting

This study is focused on the Benešov-Ústí aquifer system **(Fig. 1)** which covers approximately 1 600 km$^2$ in the northwestern part of the BCB. This whole aquifer system is bounded by significant tectonics features - the Krušné hory fault, the Středohorský fault system, and the Lužice fault (Fig. 1). Nevertheless, in order to get detailed and representative information about the entire system, the study area has been extended beyond the Benešov-Ústí aquifer synclinal structure. The northern boundary of the study area borders Germany and Poland.

The topography of the investigated area is strongly influenced by volcanism. Relatively young volcanic rocks form cores of hills reaching up to 700 m a.s.l. The surroundings of these hills are usually flat. The ground surface elevation of the wells in the zone of interest is between 130 and 724 m a.s.l.

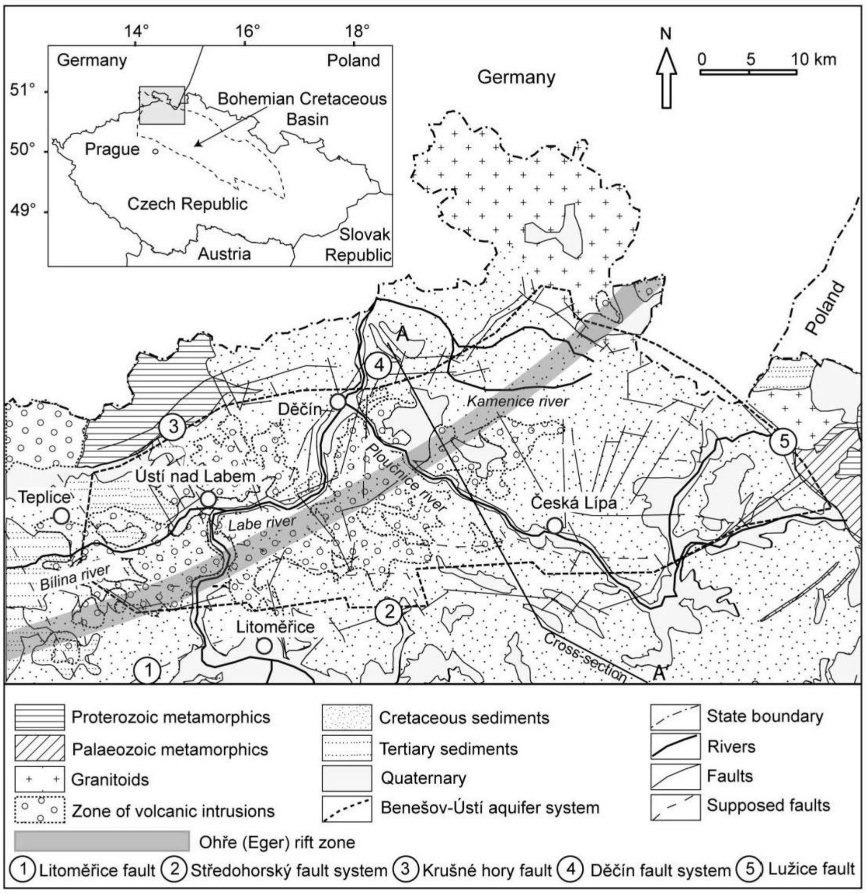


*Fig. 1. Simplified geological map of the study area with main tectonic features. The exact location and extent of Ohře (Eger) rift is unknown so far; the grey zone represents its most probable position and extent.*

### 2.2. Geological, hydrogeological and tectonic setting

The BCB is the most extensive continuous sedimentary basin and the largest basin structure of the Upper Cretaceous age of the Bohemian Massif. The Benešov-Ústí aquifer system is generally considered to be the most complicated tectonic and lithological complex of the whole basin structure. The simplified geology is displayed in Fig. 1. The basement is formed by partially metamorphosed Proterozoic and Palaeozoic rocks, locally pierced by intrusive basaltic rocks and by Palaeozoic granites in the north (Klein, 1979). The basement is partially covered with Permocarboniferous sediments (claystones, siltstones, greywackes, arkoses, conglomerates) and volcanic rocks. During the Variscan period, the region was affected by major folding and metamorphism. The Benešov syncline in the W-E direction is a distinct structure intersecting the central zone. It is filled with sediments typically 200 to 400 m thick, but the thickness reaches as high as 1200 m in the vicinity of the city of Děčín (Herčík et al., 1999). The study area involves the deepest part of the basin. The Cretaceous sediments are generally composed of claystones, marly siltstones, and sandstones (locally very rich in quartz).

Tertiary sedimentary cover and intrusive rocks forming volcanic hills and mountains markedly affect the surface. The sedimentary succession in this area is considerably affected by local and regional fault structures. The precise fault position is often a subject of discussion. The principle directions of displacements zones are SW-NE (Erzgebirge) and NW-SE (Sudetic). Nevertheless, many fold and fault structures are in a W-E direction. The central structure of the study area (Středohorská kra) extending between the Děčín fault zone on the north and the Středohorský fault on the south is the deepest block of the basin, and contains numerous fault systems of different orientation. The Ohře (Eger) rift, active from Oligocene to Pleistocene, is the most dominant structure in the Western Bohemia (Fig. 1). However, the exact position and extension of the Ohře (Eger) rift still needs to be clarified. Moreover, the Ohře (Eger) rift likely enables the ascent of heat from the upper mantle and thus represents the point of interest in our study. The active role of the Ohře (Eger) rift is also documented by $CO_2$ emissions (Geissler et al., 2005) in the western part as discussed later on. Carbon dioxide, which occurs in many groundwaters, migrates along deep-seated dislocation zones and its surface or near-surface appearances are particularly frequent at intersection points of such zones. The $CO_2$ source has been recently discussed in Jiráková et al. (2010), which suggests a mantle origin for the $CO_2$ of local groundwater.

The entire aquifer system of Benešov nad Ploučnicí and Ústí nad Labem areas is characterized by subhorizontal aquifer distribution. The complexity of the study zone is demonstrated in **Fig. 2.** The area is geologically extremely hetergenous as shown in the figure. Most of aquifers are composed of sandstone, which predominates in the infiltration zone located in the northeastern part of the aquifer system near the Lužice fault zone. Aquitards are generally composed of fine-grained sediments (mostly marlites, siltstones, sandy claystones, and claystones) with very low permeability. On the regional scale, the basin is divided into three main aquifers: (1) a basal confined aquifer formed by the Cenomanian sandstone with an intrinsic permeability of $5.10^{-13}$ – $2.10^{-11}$ $m^2$ and a hydraulic gradient of 1-3 ‰; (2) a middle aquifer in the Turonian sandstone characterised by a free water table, intrinsic permeability of $2.10^{-12}$ to $2.10^{-10}$ $m^2$ and hydraulic gradient of 5 to 10‰; and (3) an upper aquifer in the Coniacian–Santonian sediments just below the surface. Values of the hydrogeological parameters are taken from Němeček et al. (1991, 1992). These were obtained from available data from several places in the BCB and local variation at a given site can be expected.

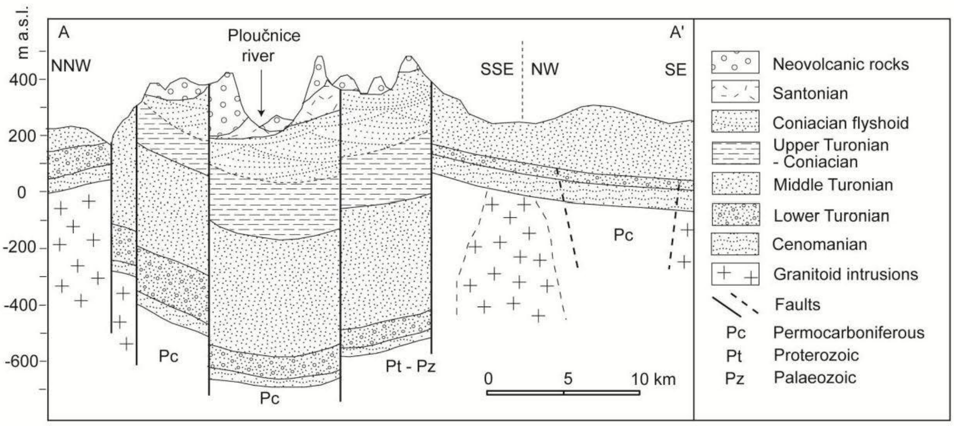


*Fig. 2. Schematic cross-section A-A' (shown in Fig. 1) demonstrating the complex geology of the area (modified from Herčík et al., 1999). Aquifer layers correspond to the Cenomanian (deepest confined aquifer), the Middle Turonian (main aquifer with mostly free water table level; the middle part of the figure shows the confined area) and the Coniacian-Santonian (local interest).*

These three aquifers are separated by regional aquitards of Lower and Upper Turonian marlstones. This general description applies to the central part of the basin cross-section, while the situation might be somewhat different towards either edge of the basin (Datel et al., 2009). The heterogeneity is caused by folding, vertical movements along fault structures, and spatial variation in sedimentation facies.

The water flow direction is governed by an array of different geological, tectonic, and morphological phenomena. The principal drainage axis is formed by the Labe (Elbe) river, but it can change locally depending on the relief. **Fig. 3** displays groundwater contour lines for the Cenomanian and Turonian aquifers in the Benešov-Ústí aquifer system, suggesting the proximity of water level in these systems. General groundwater flow direction is also similar for both aquifers.

The lower and middle aquifers of the Cretaceous Basin in the Děčín and Ústí nad Labem regions have been exploited for thermal waters and represent an example of important thermal accumulations in the Czech Republic. The best known thermal accumulation is in Karlovy Vary, with temperatures exceeding 70°C. Thermal waters on a regional scale are closely connected with the fresh water cycle. Higher water temperatures result from the flow in deep horizons and also from the groundwater residence time. According to Jiráková et al. (2010), apparent groundwater residence time can reach up to 11 ka. The chemical composition of the water can also change during such a long time span.

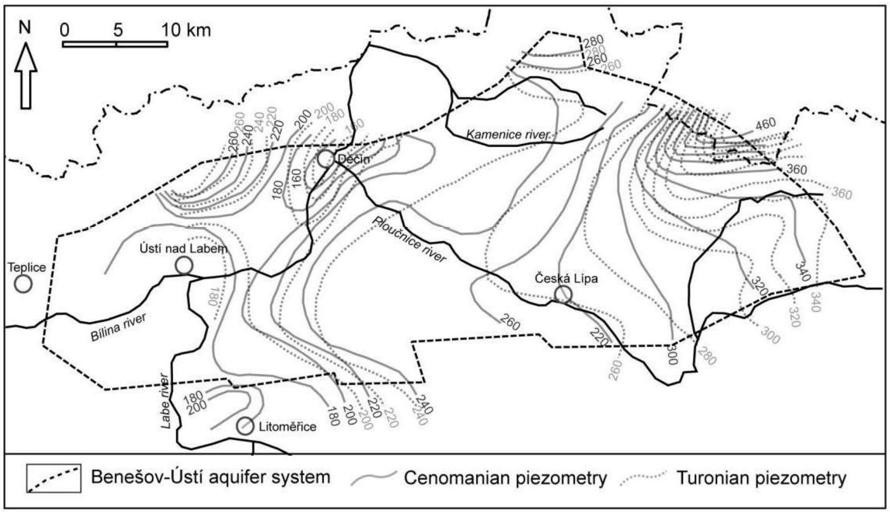


*Fig. 3. Piezometric levels in m a.s.l. for Cenomanian and Turonian aquifers (modified from Herčík et al., 1999) reveal the proximity of water leves and the groundwater flow direction towards the main dariange axis formed by the Labe (Elbe) river in both aquifers.*

In the Ústí nad Labem area, warm water was discovered at the end of the 19$^{th}$ century (when drilling for a freshwater supply) and initiated its industrial use and, to a lesser extent, use for bathing purposes. Currently, thermal waters are largely used for heating buildings and the operation of thermal swimming pools.

## 3. Data set

Many boreholes have been drilled within the Benešov-Ústí aquifer system and its surroundings for various purposes (monitoring, exploration and exploitation of fresh and thermal groundwater, structure boreholes). A large data set of borehole parameters has been collected, due to the borehole exploration in the study area and the long term tradition of well logging measurements in the former Czechoslovakia **(Table 1, Fig. 4).**

*Table 1. List of wells, calculated geothermal gradients, and heat flux values. Thermal conductivity refers to a particular rock type (see Fig. 4).*

| No | Location | Y | X | Z (m a.s.l) | Depth (m) | Corrected gradients(1) (°C/100 m) | Errors(2) | | Thermal conductivity (W/Km) | Heat flux ($mW/m^2$) |
|---|---|---|---|---|---|---|---|---|---|---|
| | | | | | | | $R^2$ | ΔG | | |
| A1 | Předlice | -763721,7 | -976443,8 | 143,7 | 500 | 4,661 | - | 0,116 | 1,8 | 84 |
| A2 | Ústí n.L. | -762980,0 | -975950,0 | 148,0 | 457 | 5,266 | - | 0,117 | 1,8 | 95 |
| A3 | | -761401,5 | -975926,8 | 146,1 | 390 | 5,963 | - | 0,133 | 1,8 | 107 |
| A4 | Brná | -759692,0 | -980021,0 | 144,0 | 431 | 5,562 | - | 0,130 | 1,8 | 100 |
| A5 | | -759538,1 | -980147,0 | 142,1 | 422 | 5,748 | - | 0,131 | 1,8 | 103 |
| A6 | Ústí n.L. | -759327,0 | -975811,0 | 150,0 | 515 | 4,987 | - | 0,103 | 2,1 | 105 |
| A7 | Vilsnice | -750284,1 | -968346,5 | 160,4 | 467 | 4,003 | - | 0,122 | 2,7 | 108 |
| A8 | Děčín | -749348,5 | -968080,0 | 128,6 | 430 | 4,846 | - | 0,116 | 2,7 | 131 |
| A9 | | -748032,7 | -967085,3 | 135,4 | 450 | 4,86 | - | 0,113 | 2,7 | 131 |
| A10 | | -747208,0 | -965000,0 | 128,7 | 335 | 6,22 | - | 0,156 | 2,7 | 168 |
| A11 | | -746873,3 | -965408,1 | 128,9 | 465 | 5,299 | - | 0,137 | 2,7 | 143 |
| A12 | | -746721,0 | -965588,0 | 136,6 | 520 | 4,657 | - | 0,102 | 2,7 | 126 |
| A13 | | -745453,9 | -965880,1 | 142,6 | 540 | 4,231 | - | 0,097 | 2,7 | 114 |
| A14 | Benešov n.Pl. | -740956,3 | -969256,0 | 228,6 | 1136 | 2,971 | - | 0,058 | 2,7 | 80 |
| A15 | Srbská Kamenice | -736467,5 | -962024,9 | 214,4 | 189 | 4,726 | - | 0,309 | 3,0 | 142 |
| A16 | | -736460,6 | -962016,8 | 214,8 | 117 | 6,934 | - | 0,508 | 3,0 | 208 |
| A17 | Dolský Mlýn | -734647,5 | -958344,0 | 200,4 | 187 | 2,005 | - | 0,297 | 3,0 | 60 |
| A18 | Kytlice | -727774,4 | -964056,1 | 382,1 | 78 | 5,57 | - | 0,667 | 3,0 | 167 |
| A19 | Brenná | -719414,0 | -982554,6 | 264,0 | 377 | 3,397 | - | 0,163 | 2,4 | 82 |
| A20 | Velký Valtínov | -710843,0 | -974437,0 | 293,9 | 360 | 0,991 | - | 0,111 | 3,0 | 30 |
| 1 | Cínovec | -778972,4 | -967228,6 | 804,6 | 597 | 2,172 | 0,985 | - | 3,0 | 65 |
| 2 | Světec | -778481,1 | -983368,8 | 202,1 | 122 | 4,278 | 0,996 | - | 2,7 | 115 |
| 3 | Dubí | -778076,5 | -970853,2 | 400,9 | 71 | 3,023 | 0,986 | - | 3,0 | 91 |
| 4 | Teplice | -776068,9 | -976278,7 | 222,1 | 941 | 4,103 | 0,787 | - | 2,7 | 110 |
| 5 | Štěpánov | -775467,0 | -988459,0 | 376,3 | 160 | 5,523 | 0,984 | - | 1,8 | 99 |
| 6 | Teplice | -774269,4 | -976387,8 | 222,3 | 170 | 1,57 | 0,899 | - | 2,7 | 42 |
| 7 | Páleč | -771207,0 | -989312,0 | 420,0 | 140 | 1,492 | 0,897 | - | 1,8 | 27 |

| | | | | | | | | | | |
|---|---|---|---|---|---|---|---|---|---|---|
| 8 | Bořislav | -769860,0 | -984150,0 | 358,3 | 250 | 2,15 | 0,997 | - | 1,8 | 39 |
| 9 | Otovice | -768046,0 | -973692,0 | 178,4 | 133 | 7,455 | 0,969 | - | 1,8 | 134 |
| 10 | Boreč | -766485,0 | -992401,0 | 303,0 | 96 | 1,286 | 0,985 | - | 1,8 | 23 |
| 11 | Klíše | -762855,0 | -975175,0 | 182,9 | 512 | 5,149 | 0,983 | - | 1,8 | 93 |
| 12 | Litoměřice | -758112,4 | -990526,4 | 250,6 | 225 | 3,9 | 0,999 | - | 1,8 | 70 |
| 13 | | -756875,0 | -989748,0 | 191,3 | 115 | 0,704 | 0,996 | - | 1,8 | 13 |
| 14 | Kristin Hrádek | -753119,7 | -959169,8 | 459,3 | 166 | 1,396 | 0,997 | - | 2,4 | 34 |
| 15 | Rýdeč | -752465,1 | -982493,2 | 448,3 | 588 | 3,749 | 0,967 | - | 2,1 | 79 |
| 16 | Prosetín | -750930,6 | -971683,7 | 203,7 | 370 | 4,101 | 0,925 | - | 2,4 | 98 |
| 17 | | -750913,0 | -971686,6 | 202,6 | 465 | 3,992 | 0,946 | - | 2,4 | 96 |
| 18 | Velký Újezd | -750555,0 | -989863,0 | 200,8 | 200 | 4,198 | 0,997 | - | 2,1 | 88 |
| 19 | Vilsnice | -750276,9 | -968339,9 | 160,9 | 202 | 4,524 | 0,998 | - | 2,4 | 109 |
| 20 | Býčkovice | -750072,0 | -987838,0 | 219,1 | 335 | 3,43 | 0,995 | - | 2,1 | 72 |
| 21 | Dobkovice | -749296,7 | -971325,6 | 130,0 | 53 | 1,975 | 0,997 | - | 2,4 | 47 |
| 22 | Maxičky | -748666,0 | -961034,0 | 425,2 | 200 | 4,51 | 0,995 | - | 2,7 | 122 |
| 23 | Zubrnice | -748618,3 | -980005,2 | 342,6 | 812 | 4,951 | 0,973 | - | 2,4 | 119 |
| 24 | Třebušín | -748590,0 | -985024,0 | 316,4 | 456 | 2,143 | 0,996 | - | 2,1 | 45 |
| 25 | Těchlovice | -748022,9 | -974214,5 | 206,5 | 99 | 6,87 | 0,889 | - | 2,4 | 165 |
| 26 | Habřina | -743061,0 | -985878,0 | 278,9 | 469 | 3,749 | 0,837 | - | 2,4 | 90 |
| 27 | | -743047,0 | -985478,2 | 299,4 | 243 | 2,942 | 0,989 | - | 2,4 | 71 |
| 28 | Brusov | -741402,0 | -982805,0 | 331,8 | 670 | 4,317 | 0,98 | - | 2,4 | 104 |
| 29 | | -741275,8 | -982626,8 | 348,3 | 540 | 4,298 | 0,996 | - | 2,4 | 103 |
| 30 | | -741270,1 | -982622,3 | 347,8 | 85 | 4,331 | 0,947 | - | 2,4 | 104 |
| 32 | Růžová | -740651,6 | -959027,8 | 343,6 | 223 | 2,099 | 0,998 | - | 3,0 | 63 |
| 33 | Úštěk, Tetčíněves | -740004,4 | -989146,5 | 216,7 | 130 | 1,397 | 0,999 | - | 3,0 | 42 |
| 34 | Snědovice | -737995,8 | -993265,0 | 246,7 | 225 | 3,778 | 0,987 | - | 3,0 | 113 |
| 35 | Dolní Kamenice | -737082,0 | -956347,0 | 213,5 | 102 | 1,341 | 0,988 | - | 3,0 | 40 |
| 36 | Srbská Kamenice | -736569,0 | -962140,0 | 215,0 | 140 | 6,407 | 0,988 | - | 3,0 | 192 |
| 37 | Jánská | -736438,0 | -962937,0 | 280,3 | 99 | 2,341 | 0,987 | - | 3,0 | 70 |
| 38 | Srbská Kamenice | -735934,0 | -960310,0 | 202,9 | 120 | 3,78 | 0,978 | - | 3,0 | 113 |
| 39 | Veselé | -734896,0 | -966512,0 | 272,7 | 300 | 3,738 | 0,998 | - | 2,7 | 101 |
| 40 | Valteřice | -734697,3 | -977209,7 | 329,1 | 662 | 2,332 | 0,971 | - | 2,4 | 56 |
| 41 | Žandov | -734278,8 | -972697,5 | 293,9 | 762 | 2,667 | 0,998 | - | 2,7 | 72 |
| 42 | | -734275,3 | -972704,6 | 293,8 | 345 | 2,162 | 0,988 | - | 2,7 | 58 |
| 43 | | -734274,7 | -972708,0 | 292,5 | 885 | 2,122 | 0,983 | - | 2,7 | 57 |
| 44 | Vysoká Lípa | -733575,0 | -955353,0 | 276,4 | 107 | 1,548 | 0,994 | - | 3,0 | 46 |
| 45 | | -733544,1 | -955356,3 | 276,6 | 298 | 1,521 | 0,996 | - | 3,0 | 46 |
| 46 | Bliževedly-Hvězda | -733218,0 | -986882,0 | 364,2 | 82 | 1,143 | 0,996 | - | 2,4 | 27 |
| 47 | Všemily | -732760,0 | -955260,0 | 289,4 | 301 | 0,938 | 0,928 | - | 3,0 | 28 |
| 48 | Bořislav | -732171,7 | -958236,5 | 240,6 | 115 | 1,19 | 0,968 | - | 3,0 | 36 |
| 49 | Zadní Doubice | -731380,0 | -950702,0 | 288,8 | 360 | 1,342 | 0,977 | - | 3,0 | 40 |

| | | | | | | | | | | |
|---|---|---|---|---|---|---|---|---|---|---|
| 50 | Cínovec | -729697,7 | -968115,2 | 797,6 | 420 | 1,052 | 0,979 | - | 3,0 | 32 |
| 51 | Drchlava | -728054,8 | -989729,7 | 351,8 | 112 | 0,682 | 0,975 | - | 2,4 | 16 |
| 52 | | -728054,6 | -989722,2 | 351,6 | 215 | 1,568 | 0,996 | - | 2,4 | 38 |
| 53 | Křížový Buk | -726556,0 | -961704,0 | 534,2 | 190 | 1,237 | 0,995 | - | 3,0 | 37 |
| 54 | Sosnová | -725960,0 | -981986,0 | 267,4 | 260 | 0 | 0,989 | - | 2,7 | 61 |
| 55 | Kytlice | -725218,0 | -963791,0 | 425,0 | 70 | 1,242 | 0,989 | - | 3,0 | 37 |
| 56 | Krásné Pole | -725203,6 | -960017,2 | 413,5 | 220 | 1,613 | 0,954 | - | 3,0 | 48 |
| 57 | | -725200,0 | -960010,0 | 412,4 | 645 | 1,719 | 0,969 | - | 3,0 | 52 |
| 58 | Č.Lípa | -724114,7 | -977767,3 | 300,4 | 612 | 1,712 | 0,99 | - | 2,7 | 46 |
| 59 | Jestřebí | -723991,0 | -986397,5 | 254,7 | 272 | 1,649 | 0,987 | - | 2,4 | 40 |
| 60 | Sloup v Čechách | -721932,6 | -972985,3 | 285,7 | 575 | 0,958 | 0,976 | - | 3,0 | 29 |
| 61 | Radvanec | -720428,9 | -970522,7 | 309,0 | 616 | 1,292 | 0,998 | - | 3,0 | 39 |
| 62 | | -720408,0 | -970505,0 | 309,0 | 541 | 1,047 | 0,994 | - | 3,0 | 31 |
| 63 | Jiřetín | -719775,0 | -959850,0 | 573,0 | 120 | 3,743 | 0,992 | - | 3,0 | 112 |
| 64 | Svor. Rousínov | -719171,0 | -966160,6 | 420,9 | 645 | 1,144 | 0,979 | - | 3,0 | 34 |
| 65 | Velenice | -716966,2 | -977245,3 | 287,5 | 370 | 1,961 | 0,988 | - | 3,0 | 59 |
| 66 | | -716966,0 | -977245,3 | 287,7 | 370 | 1,953 | 0,988 | - | 3,0 | 59 |
| 67 | Juliovka | -714282,9 | -964281,1 | 426,6 | 481 | 1,15 | 0,997 | - | 3,0 | 34 |
| 68 | Boreček | -713709,5 | -986093,1 | 278,4 | 211 | 2,426 | 0,965 | - | 2,4 | 58 |
| 69 | | -713700,7 | -986095,8 | 278,2 | 92 | 1,894 | 0,993 | - | 2,4 | 45 |
| 70 | Pertoltice | -712906,7 | -980588,0 | 281,5 | 727 | 3,051 | 0,996 | - | 2,4 | 73 |
| 71 | Heřmanice | -711250,0 | -970250,0 | 333,2 | 265 | 1,63 | 0,975 | - | 3,0 | 49 |
| 72 | Krompach | -710781,0 | -963573,0 | 580,0 | 150 | 0,746 | 0,998 | - | 3,0 | 22 |
| 73 | Skelná Huť | -708876,7 | -988567,6 | 305,7 | 190 | 2,549 | 0,989 | - | 2,4 | 61 |
| 74 | Horní Krupá | -706532,1 | -990920,8 | 359,8 | 336 | 2,316 | 0,972 | - | 2,4 | 56 |
| 75 | Ralsko-Ploužnice | -704761,9 | -987546,1 | 306,4 | 86 | 1,979 | 0,997 | - | 2,4 | 48 |
| 76 | | -704750,2 | -987546,6 | 306,1 | 240 | 4,088 | 0,991 | - | 2,4 | 98 |
| 77 | Žibřidice | -704327,6 | -974758,0 | 335,8 | 400 | 1,348 | 0,984 | - | 3,0 | 40 |
| 78 | Rynoltice | -702674,0 | -969083,0 | 360,0 | 110 | 0,898 | 0,995 | - | 3,0 | 27 |
| 79 | Hrádek nad Nisou | -702180,0 | -960439,0 | 243,0 | 330 | 5,436 | 0,988 | - | 3,0 | 163 |
| 80 | Náhlov | -700248,8 | -984137,5 | 399,9 | 297 | 3,272 | 0,997 | - | 2,4 | 79 |
| 81 | Hlavice | -698629,0 | -985977,3 | 382,3 | 305 | 2,164 | 0,988 | - | 2,4 | 52 |
| 82 | Ještěd | -693390,9 | -977510,7 | 922,1 | 150 | 0,5 | 0,988 | - | 3,0 | 15 |
| 83 | Litoměřice | -754750,7 | -991181,1 | 155,0 | 1800 | 2,4 | 0,994 | - | 3,0 | 71 |

*A1 – A20: Artesian boreholes*

*Coordinate system: JTSK – Křovák (geographical system adapted for former Czechoslovakia*

*([1]) Geothermal gradients were corrected for the effect of topography and the vertical groundwater flow. Well-logging measurements were carried out under stable temperature conditions and intervals with seasonal variation were excluded from the data processing.*

*([2]) R2: correlation coefficient for average gradient compared to measured temperature data, ΔG: Gradient error considering ± 0,5°C surface temperature uncertainty*

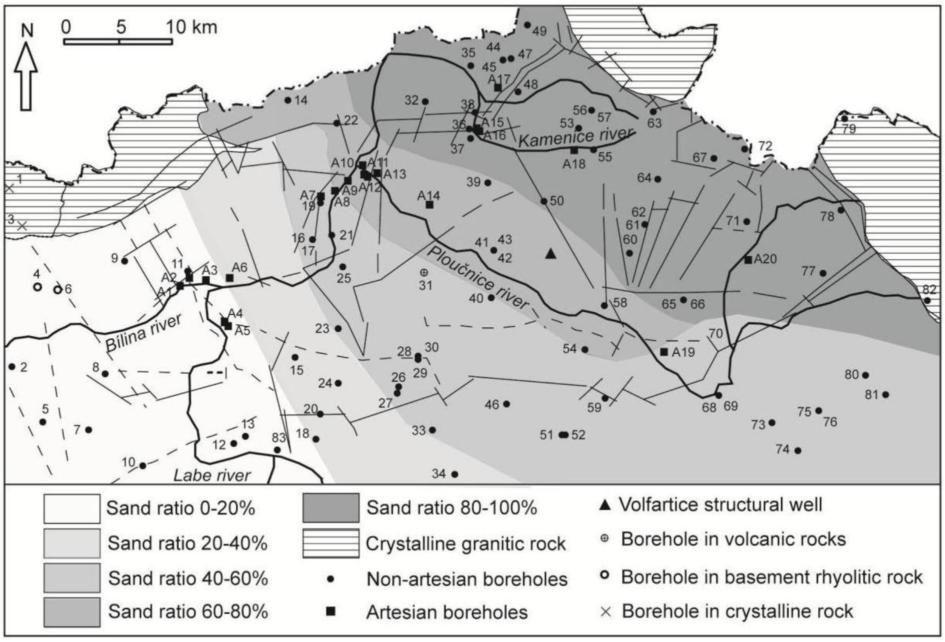


*Fig. 4. Schematic distribution of different lithological types within the study area. The sand content is gradually decreasing from the NE (80-100%) towards the SW (0-20%).*

These boreholes were logged over the last 40 years in the framework of various research programmes. Temperature data are available from the archives of different institutions (Stavební geologie, Charles University—Faculty of Natural Sciences, Geoindustrie, Diamo, UP Rynoltice and AQUATEST a.s.). New well logging measurements were provided for recently constructed monitoring wells within deep sedimentary aquifers for the Czech Hydrometeorological Institute (ISPA project funded by the European Union and the Czech Ministry of Environment). Beside this, a substantial group of boreholes was resurveyed after a long period of time (Procházka, 2004).

Although many borehole measurements provided valuable information on lithology, aquifer characteristics, and hydrodynamic conditions, the temperature profiles which are essential for our study, were not always available. For that reason we considered only a selection of all boreholes with temperature profiles **(Fig. 5).** However, even the existence of a temperature log in a borehole does not always guarantee its applicability for geothermal investigation, as the temperature field can be perturbed by various phenomena. The temperatures in the well and in the surrounding rock environment could be significantly different. A careful evaluation of the temperature measurement quality should precede the thermal data integration into the data set. Strict conditions were applied for the selection of favourable wells so the temperature log would reflect the distribution of natural temperature field in the rock massif. Various phenomena cause severe difficulties in obtaining accurate temperatures: (1) the use of old and inaccurate measuring instruments resulting in inaccurate records, (2) measurement in nonstabilized hydrogeological conditions, (3) measurements in mud filtrate, (4) lithological variability, (5) vertical water flow in a well, and (6) temperature changes in the shallow layers controlled by the seasonal variations. While complications resulting from old measuring instruments occurred only rarely, measurements in non-thermal equilibrium conditions were frequently encountered. Thermal equilibrium conditions are fulfilled after a sufficiently long time has elapsed following well construction; equilibration time depends on borehole geometry, rock properties, and groundwater flow regime. Measurements taken under non-thermal equilibrium conditions in the borehole will always provide unrepresentative temperature values. All measurements used were carried out under thermal and hydrogeological equilibrium conditions between water in the borehole and the surrounding media. Thus, they provide valuable information and are used for the study purposes.

The vertical flow of groundwater occurs as a consequence of the different piezometric levels of two or more aquifers penetrated by a borehole. Therefore, temperature data must be handled carefully if any vertical flow has been observed.

The selected data set comprises 103 wells which are more or less regularly distributed within the study area. Only boreholes generally deeper than 50 m were included, as the near-surface horizons are influenced by seasonal temperature variations. The average depth of the wells is a few hundred meters. Twenty artesian boreholes are identified by “A” before the well number in Fig. 4 and Table 1, which show the exact position and main parameters of the wells used in this study.

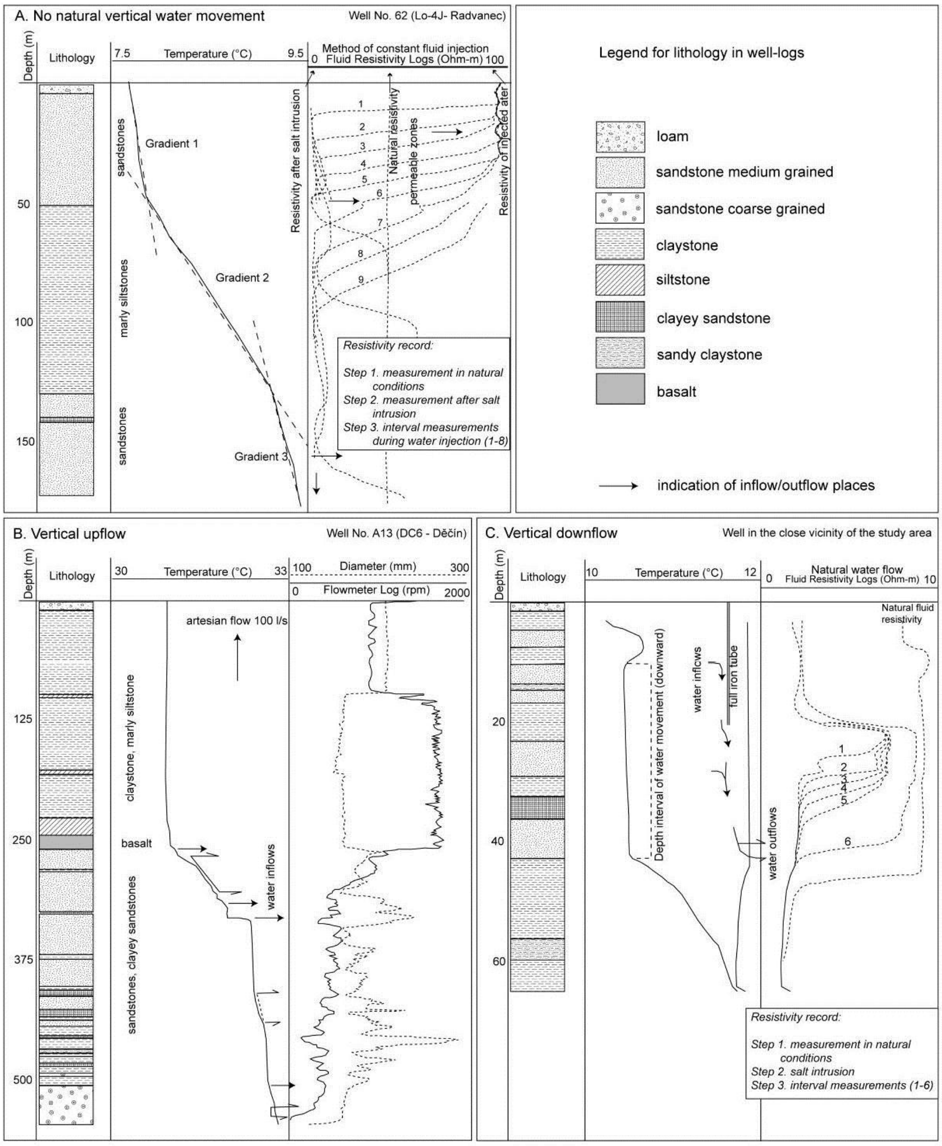


*Fig. 5. Well-logs reflecting contrasted hydrodynamic conditions encountered within the study. The figure shows the registration and measurement heterogeneity in a well without a vertical flow, with an upward vertical flow and downward vertical flow. Inflow locations into a well are indicated by an arrow in the temperature column. (A) No vertical groundwater flow, geothermal gradients controlled by lithological properties, method of constant fluid injection has been used to assess the permeable zones, (B) upward groundwater flow (artesian well) and (C) downward groundwater flow typical for drainage and infiltration areas are reflected in the temperature log. Inflow sites are detected by resistivity measurements under natural conditions.*

## 4. Methods

Continuous temperature logging generally gives a detailed temperature profile with good possibility of detecting perturbing phenomena (Beck, 1977 and 1982; Conaway, 1977; Conaway and Beck, 1977). Temperature-profile measurements were made continuously from the surface to the bottom of the well using a thermometer with a sensitivity of 0.01 ºC, the method's accuracy is then 0.1 ºC.

Using the temperature data, heat flux is calculated with the following formula:
$q = G \times \lambda$ (1)
where $q$ is the heat flux (W/m$^2$), $G$ is geothermal gradient (K/m), and $\lambda$ is thermal conductivity (W/mK).

To calculate the appropriate geothermal gradients in the area, temperature profiles were analyzed considering the vertical flow where applicable. Geothermal gradients determined directly from the temperature profile often reflect variations in the lithology (Fig. 5). Very shallow horizons (to the depth 20 to 25 m) were not used for computing the temperature gradient owing to seasonal effects which can cause quite strong curvatures. A selection of depth versus temperature values was used to calculate the average geothermal gradient for the entire well. Minor variations and deviations in the temperature record were not taken into account.

Fig. 5 illustrates different lithological types and their influence on the geothermal gradient; it also demonstrates three typical examples of groundwater dynamics: (1) no observable vertical flow between aquifers; geothermal gradients are controlled by lithology but are certainly influenced by the groundwater recharge (Fig. 5A, infiltration area); (2) observable upward vertical flow leading to misrepresentation of gradient above the inflow locations (Fig. 5B, drainage area); and (3) observable downward vertical flow leading to misrepresentation of gradients within the permeable zones (Fig. 5C).

The variability in lithology is reflected in geothermal gradients because sand layers reveal rather low thermal gradients, while clay and silty horizons are characterized by high temperature gradients. The situation is best demonstrated in Fig. 5A (no upward flow). Since groundwater circulation is absent in the well, the gradient variability reflects lithologic heterogeneity. In Figs. 5B and 5C, the situation becomes complicated as water circulates in the well. Some measurement techniques to identify the inflow locations and the flow direction and intensity are shown in Fig. 5. The inflow or outflow that often indicates the permeable layers are not easily identified when no natural water circulation is present, since no sudden temperature variations appear on the curve. However, this problem can be resolved by resistivity measurements during the constant fluid injection method illustrated in Fig. 5A (the right part). The first registration reflects natural resistivity. Then the resistivity is artificially modified (by salt admixture) and the pristine water is subsequently injected into the well. Further fluid resistivity measurements in several intervals reflect the water movement along the well. Locations with the most rapid resistivity changes correspond to permeable horizons. The water injection is not necessary if natural groundwater circulation occurs in the well. In this case, the permeable layers can be observed directly by resistivity measurements reflecting the resistivity changes as a function of the inflow intensity (right part of Fig. 5C).

Correction of the upward vertical flow had to be applied for artesian wells (A1 to A20). In artesian boreholes and with vertical upward flow (Fig. 5B), the discharge temperature is controlled by the inflow temperature because the water cannot be cooled down to the ambient rock temperature in the short ascent time from the inflow location. Hence, the difference between discharge and inflow temperatures does not represent the geothermal gradient, and the temperature correction for artesian boreholes is crucial. A similar complication appears in the case of downward vertical flow where the gradient is perturbed in the downward direction down to the permeable layer where the flowing water leaves the well and enters the formation. However, a simplification can be considered to establish geothermal gradient in the case of vertical flow. Only temperature values between the bottom of the well and the lowest inflow location, which is the last point where the measured temperature is not affected by a vertical flow, are considered. Computation of a geothermal gradient needs at least two measurement values, each from a different depth. Therefore, the average surface temperature is introduced for artesian wells. The geothermal gradient is then calculated from the following two temperature points: the measured temperature at an interval below the deepest water inflow, and the average annual surface temperature. This procedure introduces certain errors into gradient calculations, but the elimination of such wells would lead to gross inaccuracies in the computed heat flow. The study area represents a closed unit composed of infiltration area, groundwater transport, warming, and drainage area. Artesian borehole data generally come from drainage zones. The exclusion of these data would mean excluding drainage zones, which is unacceptable for the heat balance of the entire unit.

Surface temperature, $T$, at the well site was calculated using Kubik (1990):

$$T = 10.6 - 4.7 \times 0.001 \times z - 0.33 \times (Lt - 50°) \qquad (2)$$

where $z$ is the altitude at the well site (m a.s.l.) and $Lt$ is latitude in WGS84 coordinate system. This formula provided surface temperature values in the range of 8.5 to 9.7°C within the study area.

As described previously, the correction has been carried out for wells with the downward/upward vertical flow, where only data beyond (below and/or above) the interval of vertical groundwater flow enter the calculation.

Another complication can arise due to the higher altitudes of some wells. This effect, which can modify geothermal gradients within the entire study area, led us to introduce a correction for the topography effect, notably for wells at higher elevations. Serban et al. (2001) studied Transylvanian heat flux in the presence of topography. Their models suggest the topography induces a decrease in heat flux values at the top of the hill and an increase at the bottom of the valley as confirmed also by Šafanda (1987, 1994).
Some authors include palaeoclimatic effect within the corrections (Serban et al., 2001; Majorowicz and Šafanda, 2008). However, these methods cannot be applied to wells considered in this study, as they are not deep enough to provide a reliable correction.

**4.1 Correction for the effect of topography**

Topography of the study area is strongly influenced by the Tertiary volcanism along the Ohře (Eger) rift zone. Due to the large number of boreholes located inside or in a close proximity to the hilly area, it was necessary to calculate topographical corrections of temperature gradients for the majority of the area. For this reason, a 3D model of the study area was compiled using the commercially available COMSOL software, including a digital elevation model (DEM) with a horizontal step of 200 m. At the surface, the mean annual temperature was imposed in accordance with altitude and latitude at the borehole site (Kubik, 1990). The boundary condition on the bottom of the model was set using a heat flow of 75 mW/m$^2$, which implies a temperature gradient of 0.025°K/m, considering a thermal conductivity of 3 W/mK. The steady-state solution of the problem produced a temperature field perturbed by regional topography **(Fig. 6).** The disturbances expressed in percentage were used for corrections of temperature gradients of individual boreholes.

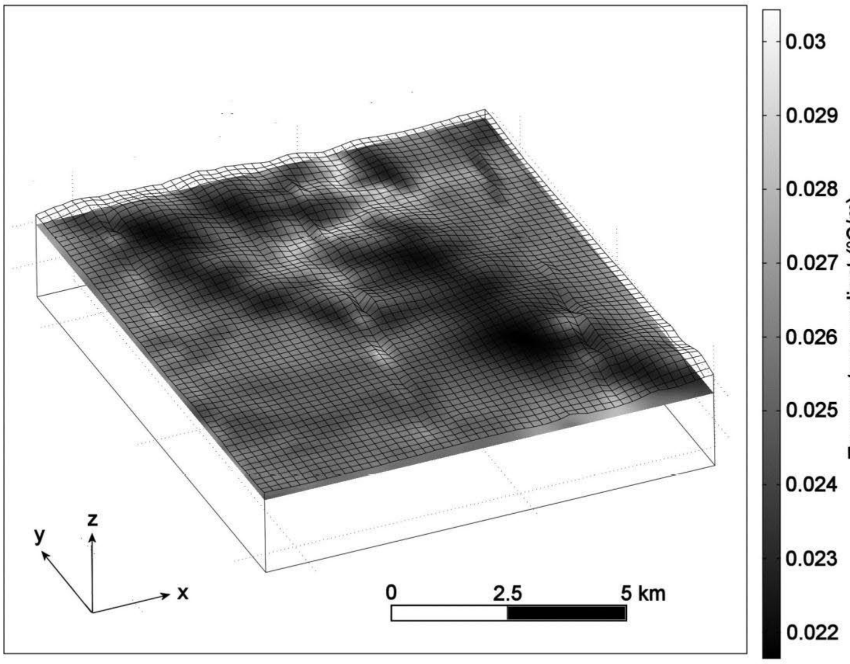


*Fig. 6. Demonstrative 3D model with synthetic temperature gradient in the level of 200 m a.s.l. in a portion of the study area disturbed by the elevation heterogeneity represented by the uppermost layer. The calculations consider the average heat flux of 75 mW/m$^2$ (temperature gradient of 0.025°K/m and thermal conductivity of 3 W/mK).*

## 5. Results

### 5.1. Lithology

Physical properties of rocks such as thermal conductivity are a function of lithological characteristics. This phenomenon has been observed by Štulc (1998) for the study site. For this reason, 71 well logs were collected within the whole region, providing lithological information. Boreholes were divided into five groups according to the overall percentage of sand within the well. Results are displayed in Fig. 4, which shows the gradual transition from pure sandstones in the northeast into clayey sediments in the western part of the study area. Logs used for this interpretation refer to the entire Cretaceous formation; that is to say that the borehole passed through the whole Cretaceous formation (marly siltstones, claystones, sandstones) into either a crystalline basement or Permocarboniferous sediments. As shown in Fig. 4, the sand ratio has been expressed in 20% intervals, which have different on thermal conductivity. The scheme provided in Fig. 4 is only an idealized representation, which is sufficient for the purposes of the current investigation but which can considerably vary from the real situation at the local scale. Lithological profiles of wells from different locations within BCB can be compared in Fig. 5.

**5.2. Thermal conductivity**

Thermal conductivity has a first-order control on the configuration of isotherms and the heat flow in any basin (Onuoha and Ekine, 1999). Despite the lack of core samples from studied boreholes, which could be used to determine the thermal conductivity, this parameter may be established on the basis of previous measurements carried out in the study area and its surroundings on similar rock types (Čermák and Jetel, 1985; Štulc, 1994). Thermal conductivity is about 1.5 to 2.5 W/m.K for the Lower Turonian and 3 to 4 W/m.K for the sandstones of the Cenomanian and Middle Turonian. These thermal conductivity values are in the range for sedimentary formations determined by Čermák (1981), Kobranova (1986), Clauser and Huenges (1995), and Popov et al. (2003). Physical parameters such as porosity and thermal conductivity can also be deduced from a structural borehole in Volfartice situated in the central part of the study area (Fig. 4). A detailed investigation of physical properties was carried out for the entire well depth. Average porosity of sandstones is around 25%. On the basis of this information, approximate values of thermal conductivity might be deduced using the correlation between porosity and thermal conductivity (Popov et al., 2003).

Clearly, thermal conductivity values can vary according to differences in porosity and pore fluid saturation, and vertical variations of the steady-state temperature and the temperature gradient are governed by thermal conductivity, which must be assessed before calculating terrestrial heat flux values at different well locations. Fig. 4 shows that sediments with a dominant occurrence of sandstones in the east gradually turn into clayey and silty sediments with insignificant sand ratio in the southwest. This indicates large differences in thermal conductivity values between rocks on the eastern and western parts of the study area. This finding was used for determining the spatial distribution of thermal conductivity. Five values of thermal conductivity were established for each lithological group according to its sand ratio (Fig. 4): (i) 0 to 20%: 1.8 W/m.K, (ii) 20 to 40%: 2.1 W/m.K, (iii) 40 to 60%: 2.4 W/m.K,

(iv) 60 to 80%: 2.7 W/m.K and (v) 80 to 100%: 3 W/m.K. The value of 3 W/m.K was used for a few wells in the crystalline basement composed of granitic rocks, and the value of 2.68 W/m.K measured by Šafanda et al. (2007) was applied to the rhyolitic rocks, mainly in Teplice region.

**5.3. Result from corrections for topography effect**

As mentioned previously, variations in ground surface elevation are often responsible for discrepancies in gradient and heat flux calculations. For that reason, corrections for the topography effect have been implemented within our investigation area. Values of the correction coefficient range between 0.008 and 0.004 K/m. Thus, corrected gradient values most often deviate by thousandths of K/m from the uncorrected values. The maximum heat flux correction is 12 to 24 mW/m$^2$ considering a thermal conductivity of 3 W/m.K. In the present study, the heat flux was corrected by a maximum of 18 mW/m$^2$.

**5.4. Determination of temperatures and geothermal gradients in the study area**

The groundwater is produced either by artesian flow or pumping. Before discussing its impact on the geothermal gradient, it is useful to consider the aquifer temperature which reflects heterogeneities in geological and tectonic structure of the area. For example, the discharge inside Děčín city reaches 32ºC, while in the western part of Děčín the discharge temperature reaches only 25ºC (both from ca 400 m). In Ústí nad Labem, the discharge temperature (from 400 m) is 32.5ºC and in Česká Lípa it is 13.5ºC (from 250 m). In Teplice, the thermal water has to be pumped from 900 m, where the groundwater temperature reaches 46ºC. However, when the groundwater reaches surface, its temperature is lower by 20ºC.

Temperatures were recorded continuously as a function of depth over the entire well depth. Temperatures representing the natural conditions within a well were determined from the temperature profiles using the methods described previously.
Based on several measurements in the northern part of the BCB, Štulc (1998) concluded that the vertical temperature gradient in the aquiclude and in the lower aquifer was not substantially affected by water flow. Hence the gradients determined from the measured temperatures can be directly used for computing heat flux.

The geothermal gradients listed in Table 1 have been corrected for the effect of topography and represent the averaged values for the well. Errors in geothermal gradients were assessed separately for artesian wells and the rest of the dataset. Uncertainties in non artesian wells are expressed as correlation coefficients for the deviation of average gradients from measured temperature data. In the case of artesian wells, use of surface temperature considerations (Section 4) could introduce considerable error into geothermal gradient; uncertainties for gradients in these cases were calculated for a temperature variation of ± 0,5°C.

Details on stratigraphical variation of temperature gradients were published by Štulc et al. (2000). Middle Turonian sandstones exhibit low gradients of around 3 K/100 m and increase gradually with depth to 5 to 6 K/100m as the high-conductivity sandy component is replaced by low-conductivity clayey and calcareous material. The sharp transition from marlites to sandstones at the Turonian-Cenomanian interface results in a drop in the gradient to 2.5 K/100m. Relatively low values (2.5 to 4 K/100 m) are observed throughout the rest of the Cenomanian sandstones. Our results agree with the trend, showing lower average gradients for the sandy portion of the study area as illustrated in Fig. 4.

The lowest gradient value (0.5 K/100 m) was calculated in the easternmost part of the study area in a mountainous region (N° 82). Such a low value reflects the hydrogeological conditions in the recharge area. Recharge zones (situated mainly in the mountainous region or in the broad vicinity of Česká Lípa) form preferential areas for the meteoric infiltration. Water infiltrates into rocks of high permeability (represented within the study zone by pure sandstones with high effective porosity and high permeability). The depth of infiltration often reaches the Cretaceous basement (100 to 700 m below surface considering the study area) (Procházka, 2008). The infiltration of precipitation water and the snow melt cause the cooling of the whole sedimentary formation and low gradients. Furthermore, low gradients in the eastern and northeastern part reflect the high values of the thermal conductivity of the sandstones.

The highest geothermal gradient of 7.6 K/100m was computed near Ústí nad Labem (N° 9) which corresponds to the drainage area. Such large values of gradient at this site, as well as in other drainage zones (e.g. Děčín and the Kamenice valley), are caused by the gradual ascent of warmed water towards the surface. Clauser and Villinger (1990) reported that drainage zones show a considerable increase in geothermal gradients, leading to a 10 to 90 % rise in heat flux. Geothermal gradients in Ústí nad Labem may also be higher due to its particular lithology characterised by marly siltstones with low values of thermal conductivity. Moreover, the Ústí nad Labem area is located in an active structure of the Ohře (Eger) rift where higher heat flux values are likely to be encountered.

Spatial distribution of averaged thermal gradients is displayed in **Fig. 7** generated by kriging method. Statistical information is provided in **Table 2**.

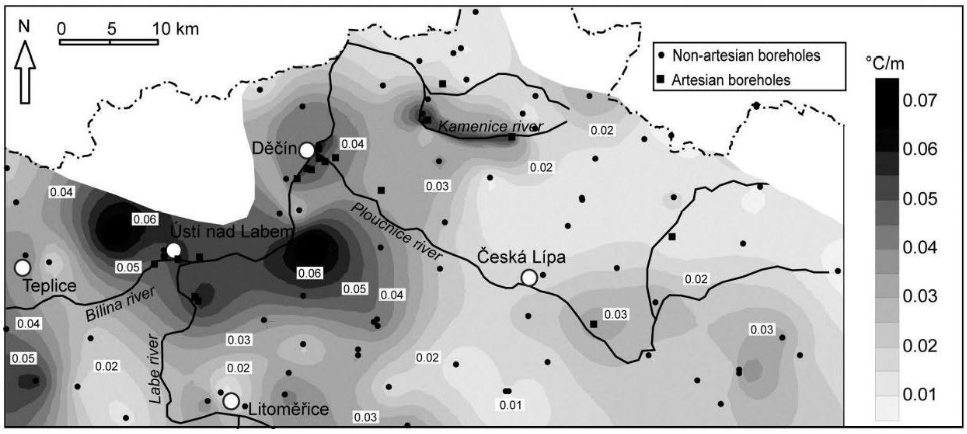


*Fig. 7. Distribution of calculated geothermal gradients in the Benešov–Ústí aquifer system. The gradient calculation involves the careful handling with vertical groundwater flow and the correction for the topography effect.*

*Table 2. Statistical data on temperature gradients and heat flux.*

| | n | minimum | 25th percentile | median | 75th percentile | maximum | δ |
|---|---|---|---|---|---|---|---|
| Temperature gradient (°C/m) | 103 | 15,49 | 46,17 | 63,68 | 92,13 | 181,39 | 30,5 |
| Heat flux (mW/m$^2$) | 103 | 0,0052 | 0,0176 | 0,0261 | 0,0366 | 0,7218 | 0,0125 |

### 5.5. Heat flux results and discussion

The heat flux was calculated using the equation (1) for conductive heat transfer. Corrections were made to consider the effect of topography and variation in thermal conductivity values. These calculations reveal a very large range (Table 2**). Fig. 8** illustrates the spatial distribution of the heat flux within the region. Data from all wells studied were used in this figure for the spatial distribution, including wells with artesian flow. Complete omitting some of these data would lead to an incomplete data set, a lack of measurement points (notably in drainage zones), and therefore a very unreliable thermal field interpretation. Moreover, the data dealing with vertical flow and artesian wells were treated carefully as previously described, and do not contain significant inaccuracies.

As expected, groundwater flow at a given site within the high-productivity aquifers substantially modifies the temperature field. Deep boreholes drilled to the basement of the sedimentary formation (e.g. 2 km) without groundwater flow would allow much more precise heat flux calculation. Owing to the absence of such deep wells, only data from the depths of several hundreds of meters (to the base of the sedimentary basin) were used for computing heat flux. However, from a practical point of view, the proposed map is sufficient.

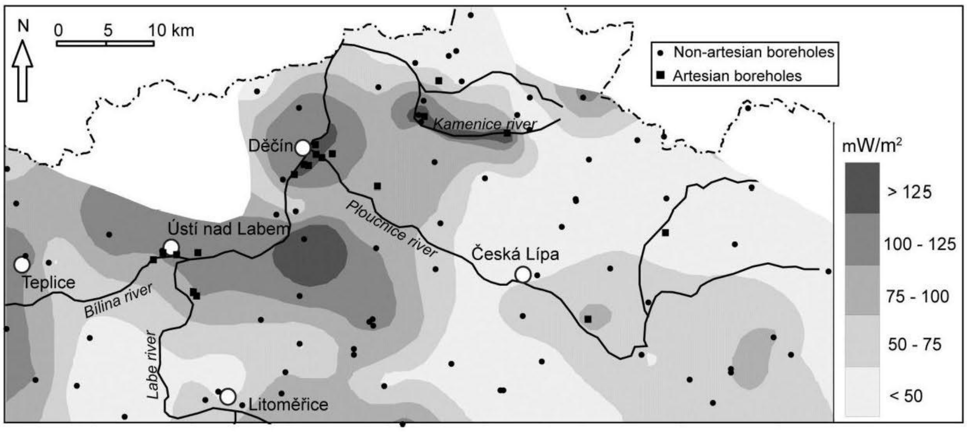


*Fig. 8. Heat flux distribution in the Benešov–Ústí aquifer system as assessed from the geothermal gradients and the thermal conductivities for determined rock types. The map reveals generally higher heat flux in drainage zones in the western part and lower values in infiltration zones in the northeastern part of the study area.*

Anomalies in the thermal field indicated by the elevated heat flux are represented by two longitudinal areas of W-E orientation (Fig. 8). The first crosses Ústí nad Labem with the highest potential near Těchlovice, the second is well developed around Děčín and continues in a northwestern direction towards the Kamenice river, along which a very narrow zone of high heat was identified. Considering detailed geology and tectonics, the heat flux does not only reflect the geothermal gradient at different sites but it also significantly depends on the lithology and thermal conductivity. The heat flux is generally higher in the western part of the study area, confirming the gradual warming of the groundwater during its flow from infiltration areas in the NE towards the drainage zones in the SW of the study area.

Infiltration and/or mountainous zones have lower heat flux values. This is the case in the northeastern part of the study area.

High heat flux values were often observed in artesian wells, which are usually distributed along the main drainage axes. The main drainage axis is formed by the Labe (Elbe) river, which approximately follows the assumed Ohře (Eger) rift structure. Several artesian wells are situated around Ústí and Děčín and then in the valley of Kamenice river. The Kamenice river valley exhibits a very narrow thermal anomaly along the river caused by warmed water drainage from the surrounding rock formation. Similarly, the Děčín valley shows very high heat flux values that are observable only on the right river bank. This phenomenon can be explained by groundwater circulation through numerous tectonic structures. Water infiltrates in the eastern and northern part of the study area, flows westward through sandstone layers, and gradually increases in temperature with depth [mainly in the zone of the Ohře (Eger) rift]. The sandstone formation is covered by a thick layer of impermeable, marly siltstones in the central and western part of the area. Groundwater flows through a tectonically complex area for several thousands of years (Jiráková et al., 2010) before reaching the Labe (Elbe) river.

Generally speaking, groundwater flow significantly affects the geothermal field and plays a key role in heat transfer throughout the whole area of interest. Heat transfer is also influenced by the deep tectonics, such as Ohře (Eger) rift in the study area representing a zone of groundwater warming. Groundwater with dissolved gases (namely $CO_2$) is a heat transport fluid (Bense et al., 2008; Dowgiallo, 2002). Detailed isotopic study carried out by Jiráková et al. (2010) detected mantle-derived carbon ($CO_2$) in groundwater in the vicinity of Ústí nad Labem, Děčín, and around the Kamenice river, which are zones of high heat-flux values. However, a causal relationship between $CO_2$ occurrence and higher heat flux values has yet to be established, and should be investigated further.

Besides the crucial role of deep tectonics in the heat distribution, the most important heat transport mechanism seems to be the meteoric water recharge in the eastern part of the study area. The existence of a fault itself does not always guarantee a heat flow anomaly. Fault structures without any contact with deep parts of the earth crust have a secondary effect on heat flux. They often represent a barrier for the groundwater which might be transported to the particular fault structure (as from a rift zone). This phenomenon is commonly observed in sedimentary rocks as demonstrated in the Děčín fault zone, which is a sealing fault, and causes a great shift in temperatures measured on both river banks. Temperature records from a depth of 500 m on the east of the fault reveal values 7°C higher than on the west of the fault. Similar results about the secondary effect of tectonics on the heat flux were obtained on the south side of the study area, north from Litoměřice.

## 6. Conclusion

The Benešov-Ustí aquifer system is exploited for both drinking water and geothermal heat. A vital condition for the sustainability of thermal water reserves is a sound understanding of the dynamics of the groundwater system in the study area in relation to the complex geology and tectonics. Geothermal investigations in the western part of the Benešov-Ustí aquifer system have enhanced understanding of the thermal field and the groundwater dynamics. Temperature logs in the wells were used to construct a much more detailed heat flux map of the area than those used in the previous studies.

Many phenomena affect the thermal field in the region. Vertical groundwater flow, variations in lithology, and topography lead to a complicated areal distribution of the geothermal gradient and the heat flux. All of these phenomena were integrated in this study and corrections were applied to compute accurate geothermal gradients and heat flux values. Significantly elevated geothermal potential has been identified in two longitudinal areas of W-E orientation in the vicinity of the drainage axes of Labe (Elbe), Ploučnice, and Kamenice rivers.

Although topographic correction would improve the accuracy of the heat flux values, groundwater flow appears to be the dominant mechanism controlling the distribution of the heat flux. This was particularly demonstrated by low and high heat flux values in the recharge ($<50$ mW/m$^2$) and discharge areas ($>75$ mW/m$^2$), respectively. Therefore, this geothermal study also contributed to the delineation of recharge/discharge zones, a matter of interest to hydrogeologists.

The groundwater flows in the westward direction towards the drainage zones, but its path is considerably complicated by fault structure and volcanic intrusions. This study demonstrates that shallow tectonic structures do not directly control the thermal field, but exercise a strong influence on groundwater flow. This is also true for numerous volcanic rocks, which are frequently found inside the study zone and which are related to the Tertiary activity of the Eger (Ohře) rift. Thus, tectonics exerts a secondary effect on the thermal field. Many occurrences of mineral and thermal waters inside and beyond the study area are related to Eger (Ohře) rift. Temperature logs confirmed that groundwater flow occurs within deep confined sandy aquifers. The groundwater flowing towards the Labe (Elbe) river is warmed in the tectonic zone and is enriched in $CO_2$.

This investigation not only provides useful information on the geothermal resources within the region but also presents an important tool for understanding groundwater flow and for constructing realistic hydrogeological models in such a complex geological, tectonical, and geothermal context.

## Acknowledgements

Financial support for this work was provided by the Grant Agency of the Czech Republic N° GACR 205/07/0691 and the University Research project N° SVV 261 203. This work was also supported by the French Ministry of Foreign Affairs and the Ministry of Education, Youth and Sports of the Czech Republic. We would also like to thank AQUATEST a.s. and the Czech Hydrometeorological Institute for provided data. Special acknowledgment is made to Craig Hampson for grammatical and stylistic corrections.

## References

Beck, A.E., 1977. Climatically perturbed temperature gradients and their effect on regional and continental heat-flow means. Tectonophysics 41, 17 – 39.

Beck, A.E., 1982. Precision logging of temperature gradients and the extraction of past climate. Tectonophysics 83 (1-2), 1-11.

Bense, V.F., Person, M.A., Chaudhary, K., You, Y., Cremer, N., Simon, S., 2008. Thermal anomalies indicate preferential flow along faults in unconsolidated sedimentary aquifers. Geophysical Research Letters 35. L24406.

Bertani, R., 2005: World geothermal generation in the period 2001-2005. Geothermics 34 (6), 651-690.

Čermák, V., 1975. Combined heat flow and heat generation measurements in the Bohemian massif. Geothermics 4, 1-4.

Čermák, V., 1979. Geothermal studies and heat-flow map of Czechoslovakia, in: Geodynamic Investigation in Czechoslovakia. Veda, Bratislava, pp. 129-130.

Čermák, V., 1981. Heat flow investigation in Czechoslovakia. in: Zátopek, A. (Ed.). Geophysical Synthesis in Czechoslovakia, Slovak Academy of Science, Bratislava, Slovakia, pp. 427-439.

Čermák, V., Šafanda, J., 1982. Subsurface temperature distribution in Western Czechoslovakia and its mapping for appraising the exploitable resources of geothermal energy, in: Čermák, V., Haenel, R. (Eds.), Geothermics and Geothermal Energy, E. Schweitzerbartsche Verlagsbuchhandlung, Stuttgart, Germany, pp. 6–270.

Čermák, V., Jetel, J., 1985. Heat flow and ground water movement in the Bohemian Cretaceous Basin (Czechoslovakia). Journal of Geodynamics 4, 285-303.

Chapellier, D., 1992. Well Logging in Hydrogeology. A.A.Balkena Publishers. USA.

Clauser, C., Huenges, E., 1995. Thermal conductivity of rocks and minerals, in: Ahrens, T. J. (Ed.), Rock Physics and Phase Relations—A Handbook of Physical Constants, American Geophysical Union Reference Shelf 3, pp. 105-126.

Clauser, C., Villinger, H., 1990. Analysis of conductive and convective heat transfer in a sedimentary basin, demonstrated for the Rhinegraben. Geophysical Journal International 100, 393-414.

Conaway, J., G., 1977. Deconvolution of temperature gradient logs. Tectonophysics 103, 33 - 46.

Conaway, J.G., Beck, A.E., 1977. Continuous logging of temperature gradients. Tectonophysics 41, 1 – 17.

Datel, J.V., Kobr., M., Procházka, M., 2009. Well logging methods in groundwater surveys of complicated aquifer systems: Bohemian Cretaceous basin. Environmental Geology 57, 1021–1034.

Demetrescu, C., Wilhelm, H., Ene, M., Andreescu, M., Polonic, G., Baumann, C., Dobrică, V., Şerban, D.Z. 2005. On the geothermal regime of the foreland of the Eastern Carpathians bend. Journal of Geodynamics 39 (1), 29-50.

Dowgiallo, J., 2002. The Sudetic geothermal region of Poland. Geothermics 31, 343 – 359.

Geissler, W.H., Kämpf, H., Kind, R., Bräuer, K., Klinge K., Plenefish, T., Horálek, J., Zedník, J., Nehybka, V., 2005. Seismic structure and location of a $CO_2$ source in the upper mantle of the western Eger (Ohře) rift, central Europe. Tectonics 24, TC5001, 1-23.

Grinbaum, I.I., 1962. Geophysical Methods for Identification of Filtration Characteristics in a Rock Massif, Nedra, Moscow, Russia (in Russian).

Herčík, F., Hermann, Z., Valečka, J., 1999. Hydrogeology of the Bohemian Cretaceous Basin. Czech Geological Survey, Prague, Czech Republic, 116 pp. (in Czech).

Hooijkaas, G.R., Genter, A., Dezayes, C., 2006. Deep-seated geology of the granite intrusions at the Soultz EGS site based on data from 5 km-deep boreholes. Geothermics 35 (5-6), 484-506.

Hurter, S., Schellschmidt, R., 2003. Atlas of geothermal resources in Europe. Geothermics 32, 779 – 787.

Jiráková, H., Huneau, F., Hrkal, Z., Celle-Jeanton, H., Le Coustumer, P., 2010. Carbon isotopes to constrain the origin and circulation pattern of groundwater in the north-western part of the Bohemian Cretaceous Basin (Czech Republic). Applied Geochemistry 25, 1265-1279.

Kelly, W.E., Mareš, S., 1993. Applied Geophysics in Hydrogeological and Engineering Practice. Elsevier. Amsterdam, Netherlands.

Klein, V., 1979. The basement composition and morphology of the Cretaceous basin on the west from Hradce Králové. Věstník Ústředního Ústavu Geologického 53, 357-366.

Kobr, M., Mareš, S., Paillet, F., 2005. Geophysical well logging, in: Rubin, Y., Hubbard, S. (Eds.) Hydrogeophysics. Springer, Amsterdam, Netherlands, pp. 291 – 331.

Kobranova, V.N., 1986. Petrophysics. Nedra. Moscow, Russia, 392 pp. (in Russian).

Kubik J., 1990. Subsurface temperature field of the Bohemian massif. Studia Geophysica et Geodaetica 34 (2), 110 – 128.

Lubis, R.F., Sakura, Y., Delinom, R., 2008. Groundwater recharge and discharge processes in the Jakarta groundwater basin, Indonesia. Hydrogeology Journal 16, 927-938.

Lund, J.W., Freeston,D.H., Boyd, T.L., 2005. Direct application of geothermal energy: 2005 Worldwide review. Geothermics 34, 691 – 727.

Majorowicz, J., Šafanda, J. 2008. Heat flow variation with depth in Poland: Evidence from equilibrium temperature logs in 2.9-km-deep well Torun-1, International Journal of Earth Sciences 19 (2), 307-315.

Mansure, A.J., Reiter, M., 1979. A vertical groundwater movement correction for heat flow. Journal of Geophysical Research 84 (B7), 3490-3496.

Mareš, S., Zbořil, A., Kelly, W.E., 1994. Logging for determination of aquifer hydraulic properties. The Log Analyst 35 (6), 28-36.

Myslil, V., Stibitz, M., Frydrych, V., 2005. Geothermal energy potential of Czech Republic, in: Proceedings of the World Geothermal Congress, Antalya, Turkey, pp. 1-7.

Němeček, J., Horák, J., Svoboda, M., Urbánek, P., 1991. Hydraulic model of strážský block. Final report, Stavební geologie Aquatest. Prague, Czech Republic, 60 pp. (in Czech).

Němeček, J., Horák, J., Urbánek, P., 1992. The effect of uranium exploitation on surface and subsurface water circulation. Final report, Stavební geologie Aquatest. Prague. Czech Republic, 65 pp. (in Czech).

Ollinger, D., Baujard, C., Kohl, T., Moeck, I., 2010. Distribution of thermal conductivities in the Groß Schönebeck (Germany) test site based on 3D inversion of deep borehole data. Geothermics 39 (1), 46-58.

Onuoha, K.M., Ekine, A.S., 1999. Subsurface temperature variations and heat flow in the Anambra Basin, Nigeria. Journal of African Earth Sciences 26 (3), 641-652.

Popov, Y., Tertychnyi, Romushkevich, R., Korobkov, D., Pohl, J., 2003. Interrelations between thermal conductivity and other physical properties of rocks: Experimental data. Pure Applied Geophysics 160, 1137 – 1161.

Procházka, M., 2004. Controls of technical conditions of old monitoring wells in the frame of reconstruction of monitoring wells state network. AQUATEST a.s., Prague, Czech Republic (in Czech).

Procházka, M., 2008. Control of new monitoring wells in the frame of reconstruction of state network of monitoring wells. AQUATEST a.s., Prague, Czech Republic (in Czech).

Serban, D.Z., Nielsen, S.B., Demetrescu, C., 2001. Transylvanian heat flow in the presence of topography, paleoclimate and groundwater flow. Tectonophysics 335, 331 – 344.

Šafanda, J., Dědeček, P., Krešl, M., Čermák, V., 2007. Report from the Exploration of the Geothermal Borehole GTPVLT-1 in Litoměřice. Geophysical Institute, Academy of Sciences, Prague, Czech Republic, 67 pp. (in Czech).

Šafanda, J., 1987. Some remarks on the estimation of geothermal topocorrections. Studia Geophysica et Geodaetica 31, 284-300.

Šafanda, J., 1994. Effects of topography and climatic changes on the temperature in the borehole GFU-1, Prague. Tectonophysics 239, 187-197.

Štulc, P., 1994. Convective Heat Transfer in the Bohemian Cretaceous Basin. PhD thesis. Faculty of Mathematics and Physics. Charles University, Prague, Czech Republic, 107 pp. (in Czech).

Štulc, P., 1998. Combined effect of topography and hydrogeology on subsurface temperature – implications for aquifer permeability and heat flow. A study from the Bohemian Cretaceous Basin. Tectonophysics 284, 161-174.

Štulc, P., Stoje, V., Kopecký, P., 2000. Dynamics of the subsurface temperature field caused by mining-related groundwater management. Studia Geophysica et Geodaetica 44 (3), 442-459.

Vasseur, G., Demongodin, L., 1995. Convective and conductive heat transfer in sedimentary basins. Basin Research 7 (1), 67-79..

# 5 CONCLUSIONS

## 5.1 Recall of objectives

The main objective of this thesis aimed at improving the present-day knowledge of the groundwater origin and flow conditions using isotopic and geothermal methods in France and the Czech Republic, particularly:

(i) to provide groundwater dating for aquifers in the northern Aquitaine region and the northwestern region of the Czech Republic and to clarify the groundwater flow conditions using also the geothermal gradient and the heat flux in the Benešov-Ústí aquifer system, Czech Republic

(ii) to clarify the palaeorecharge conditions in the Aquitaine and the Bohemian Cretaceous sedimentary Basins during the last 40 ka

This work, concerning the assessment of the aquifer potential for various human needs such as drinking water supply or geothermal use, is based on a huge range of isotopic data (deuterium, oxygen-18, tritium, carbon-13, carbon-14), geochemical data and temperature measurements acquired during the last several decades. So far, introduced data had been interpreted only individually and often without broader environmental consideration. This thesis is the first to combine isotopic and geothermal approaches taking into consideration numerous more or less fragmentary studies throughout Europe with emphasis on the sedimentary formations in southwest France and northwest Czech Republic. This approach makes it possible to introduce global evaluation on the groundwater regimes in deep aquifer systems.

## 5.2 Objective compliance

The origin of groundwater components, the sustainability and the character of groundwater flow in deep aquifer systems has to be fully understood in order to ensure effective groundwater management. The Aquitaine Basin and the Bohemian Cretaceous Basin provide both large and high storage capacity aquifers and represent therefore a good example of highly strategic deep aquifers in contrasted geographical situations.

Various methods in hydrogeology and related scientific branches are being used to answer numerous questions regarding groundwater regime. The presented thesis included a geochemical study which is commonly carried out to identify the origin of groundwater with respect to ambient environment, geological and human processes. While geochemical studies provided us with valuable findings on groundwater origin, quality and recharge timing, the geothermal data offered the possibility to penetrate deeper in the issue of the groundwater flow and dynamics. It was confirmed in the case study of the Bohemian Cretaceous Basin where both data on geochemistry and thermometry were applied.

Various natural processes occurring during the infiltration are reflected in the geochemical and isotopic composition of groundwater. The investigations from this thesis confirm that the groundwater origin and the recharge period are closely related and should be considered together. Different isotopic methods for groundwater dating were tested using radiocarbon data. Radiocarbon dating method was applied for both aquifer systems revealing significant differences in the geological conditions requiring individual dating approaches. Above all, the aquifers in France contain high carbonate percentage seriously affecting the groundwater dating results. Because of that, many different models widely used were tested for particular geochemical conditions. Consideration on carbon-13 and carbon-14 isotopes, geochemistry and geological structure of the study area finally helped to assess the model which best fits the prevailing conditions. The Fontes and Garnier model (Fontes and Garnier, 1979) seems to work very well for carbonated rocks as also indicated by numerous studies elsewhere. Dating results enabled us to identify a group of groundwaters recharged in very different climatic conditions corresponding to the LGM period and therefore contesting any doubts about a recharge gap existence. All dating results suggest continuous groundwater recharge during the whole Late Pleistocene period up to the radiocarbon dating limit, i.e. 30 - 40 ka BP.

The existence or absence of palaeorecharge during LGM has been intensely discussed for a long time. The discussion was furthermore developed in a review study considering many European aquifers. This study summarizes and points out important climatic events which could leave a fingerprint on groundwater inside the aquifers. The detailed overview over ice sheet and permafrost extension helped to accurately interpret isotopic data. Climatic instability during the Late Pleistocene period has been significantly reflected in the groundwater recharge pattern. Groundwater recharge over the European continent was finally divided into two major groups: (i) continuous and (ii) discontinuous recharge conditions. It has been noticed, that the recharge has probably occurred continuously without any hiatus throughout ice sheet or permafrost free areas. This concerns the majority of the southern European territory from western to eastern longitudes as documented by examples in Spain, Portugal, southern France or Romania. Northwards, the climatic conditions around LGM were more severe and are reflected in the current groundwater composition. Recharge gap was observed from northern France towards north European countries. The recharge hiatus duration slightly varies as the most severe climatic conditions did not affect the whole continent at one moment. However, somewhat particular recharge situations were observed in several sites. The BCB aquifers being partially recharged from depleted melt water is considered as one of them. Similar situation were registered in Denmark. Some recharge, such as in Estonia and Lithuania, occurred in subglacial environment conditions if some areas of the bedrock were unfrozen in spite of the cold and dry climatic conditions.

The groundwater regime can be evaluated on the basis of isotopic and geothermal data. This interdisciplinary approach made it possible to compare and reciprocally verify the acquired results from both studies. The groundwater dating required the setting of different dating models due to the variable geological and tectonic organisation of the region. Such intricate situation can be reliably evaluated using carbon isotopes techniques. Carbon-13 and radiocarbon behave as excellent tracers of carbon origin within the aquifer system. Many interaction processes between groundwater and the rock matrix have been identified and had to be taken into account during groundwater dating efforts. Besides often encountered groundwater/rock interactions, processes with mantle $CO_2$ gas and fossil organic matter affect the isotopic composition of the Bohemian groundwaters. The presence of $CO_2$ gas in the BCB was confirmed by the geothermal investigation as well. It has been found, that the gas presence points out the on-going activity at some tectonic structures which is accompanied by elevated temperatures and heat flux. That is to say, the existence of the $CO_2$ gas identified during isotopic study can be later on confirmed by geothermal applications or vice versa which definitely suggests the reciprocity and complementarity of both approaches.
A conceptual model indicating all the potential carbon sources contributions into groundwater was developed on the basis of the isotopic data. The very developed tectonics in the region and the very intense groundwater flow between different aquifers, as showed by temperature measurements, significantly facilitate carbon distribution in aquifers and leads to the mixing of groundwater of different origins. The exposure of groundwaters to numerous geochemical processes often leads to an overestimation of groundwater ages if common methods are applied. That is why the dilution method correction model considering different kinds of interactions involving different types of

carbon origin with groundwater was applied. The apparent groundwater ages do not exceed 11 ka. However, this result is in contrast with the depleted oxygen-18 and deuterium content which would suggest an infiltration in much colder climatic conditions than those prevailing around 11 ka BP in Central Europe. The fact, that very depleted water infiltrated around Pleistocene-Holocene transition and not during the coldest period of LGM indicates, that the north European ice-sheet thaws probably contributed to the groundwater recharge in adjacent areas.

Geothermal gradients clearly delineated the infiltration and drainage zones within the studied area of the BCB which is consistent with the isotopic study indicating the presence of modern and old groundwater. The infiltration zone with the lowest geothermal gradients is situated on the northeast of the study area and might have been therefore recharged from the north by glacial melt water. Although the groundwater dynamics locally and temporarily vary, the dominant groundwater flow is directed towards the main drainage axis formed by the Labe (Elbe) River, i.e. towards west. The recharge of the BCB aquifers in its infiltration zone explains the presence of modern groundwater identified by isotopic methods. The groundwater becomes older along its flowpath. The elevated temperatures of sampled groundwaters reflect the great depths of the groundwater flow but also the long residence time up to 11 ka during which thermal exchanges with the ambient rock take place. On the other hand, modern waters are encountered in the surrounding of the infiltration zone before reaching great depths. The groundwater dynamics in the BCB is very complicated as documented by the intense vertical flow of groundwaters in many wells. This has to be particularly kept in mind if groundwater stratification should be assessed. The groundwater flow and leaching between aquifers cause continual mixing between older and modern waters as confirmed by both geothermal and isotopic investigation.

The detailed geothermal study of the Benešov-Ústí aquifer system in the north western BCB was carried out with the intention to supplement geochemical findings by clarifying the tectonic conditions, direction of groundwater flow, groundwater dynamics and regime. Also, it brought ample knowledge about the prevailing thermal conditions. The BUAS system has been intensively exploited so far and therefore needed to be re-evaluated in terms of the sustainable development not only for drinking water but also as a geothermal resource. Natural geothermal conditions in deep aquifers can be best evidenced by in situ measurements. Ideally, the heat flux could be deduced from deep boreholes reaching the crystalline basement and therefore directly linked to the ascending heat from the inner earth layers. However, the lack of deep crystalline-reaching wells called for alternate solution. In situ thermometry measurements were performed in approximately hundred wells. Very shallow horizons influenced by seasonal temperature variations were not taken into account. Study of temperature profiles provides unique insight into thermal setting inside the well and offers a good possibility of detecting many disturbing phenomena having negative consequences on the final calculation and surface heat flux spatial distribution. The majority of the wells confirmed a vertical flow indicating a high pressure conditions in the lower aquifers. This study presented an excellent example of geothermal field distribution and behaviour within different portions of a closed hydrogeological unit revealing an intense groundwater circulation. The well-logging methods helped to identify the zone of infiltration, storage and drainage which can be distinguished on the basis of thermal data. Infiltration zones, where ifiltration water constantly cools down the rock environment, generally appear colder than drainage areas revealing higher temperatures due to the upward groundwater flow from aquifers towards the drainage axes. It was concluded, that heat fluxes are considerably influenced by the strong groundwater dynamics which disallows the accurate assessment of the heat flux ascending from the upper mantle. Moreover, the variability of the lithology plays a key role in the heat flux determination and was properly considered during calculations.

Despite the intense groundwater flow, the geothermal investigation brought new valuable findings about the geothermal potential for the region and accompanied many results from the isotopic approach. According to the spatial heat flux distribution, the most promising areas occur in the W-E zones along Ústí nad Labem and Děčín. These zones are probably related to the tectonic features in the area and probably indicate the everlasting activity of the most developed and discussed tectonic system crossing the BCB – Ohře (Eger) Rift. Otherwise, compared to the great importance of the dynamics of groundwater which is a dominant factor for the heat transfer, tectonics stands rather for a secondary effect. The conclusions of the geothermal investigation contribute to the greater knowledge of the geological structures and to the determination of the long term exploitable/sustainable amount of groundwater.

## 5.3 Application in practice

The acquired findings from the Czech part of the study – particularly on the geochemistry, mean residence times, infiltration and drainage zone location, etc. provide fundamental data related to the sustainable development and protection of water. These data can be therefore practically used within the on-going project „Rebilance zásob podzemních vod“ (re-balance of groundwater reserves), proposed for years 2010 – 2015 by the Czech Geological Survey in the scope of the Environmental Operational Program. It is supposed to extend the systematic regional hydrogeological surveys performed in the Czech Republic during the period from the 60th to the 90th of the 20th century and geological-hydrogeological activities carried out by the Czech Geological Survey and Water Research Institute in 2005.

Natural groundwater resources are dynamic time changeable component. Existing evaluations of the groundwater resources availability are often older than twenty years and do not consider the strongly influenced groundwater dynamics which can be considerably affected by the climate changes and anthropogenic activities, notably in dry seasons. Long-term hydrological and hydrogeological records show that values acquired in the past do not always correspond to the current state of natural resources, i.e. usable groundwater reserves. Results from past hydrogeological surveys become quickly out-dated and do not often satisfy the demands of modern societies. However, contemporary and future groundwater extraction cannot be based on the old calculations omitting the role of groundwater dynamics and residence time. That is why the calculation reliability and practical use of the current data has to be verified. The realization of this new project will allow a detailed data treatment in selected critical hydrogeological units within the Czech territory.

*Tab. 2. List of activities composing the project concenrnig the re-balance of groundwater reserves. Grey filling highlights activities which are relevant to include results of this work.*

| **ACTIVITIES** |
|---|
| 1. Data search, data analyses, GIS construction |
| 2. Quantitative assessment of the groundwater bodies |
| 3. Field geological survey, geophysics |
| 4. Hydrogeological wells and drilling |
| 5. Conceptual hydrogeological model |
| 6. Hydrological models |
| 7. Hydaulic models |
| 8. Hydrochemical models |
| 9. Groundwater protection related to preserved ecosystems |
| 10. Summary, results, final report |
| 11. Propagation activities, conferences, publications |

The project concerns selected Quaternary, Turonian and Cenomanian aquifers with the highest groundwater accumulations within the country. Being one of the most exploited sedimentary formations in the Czech Republic, the aquifers of the Bohemian Cretaceous Basin are included in the project.The project has been divided into 11 activities as listed in Tab. 2. The highlighted activities in Tab. 2 show those, which could be primarily enriched by the findings on geochemistry, mean residence times and temperature distribution presented in this work. It picks up the threads of an extensive range of the previous research projects including the Project „Optimalization of the use and protection of thermal waters in the BUAS" (205/07/0691) in the framework of which this thesis was elaborated.

## 5.4 Perspectives

The importance of groundwater resources is still growing, especially of those from deep sedimentary aquifers. It has been shown that such groundwater represents very strategic position in the water management as different catastrophic events (e.g. droughts, floods) often threatens shallow aquifers and surface water which can therefore cover only part of the water demand. However, groundwater reserves in deep aquifers are less accessible for the exploitation. Long groundwater residence times suggest also a very limited renewability of the resources and also indicate the existence of fossil waters. The long-term overexploitation of such aquifers can lead to strong aquifer depletion. In order to prevent this scenario, the assessment of pumping limits for a sustainable development requires multi-disciplinary investigation of aquifer systems and reliable groundwater modelling. In the scope of the proposed thesis, temperature data and environmental isotopes together with radiocarbon activities were analysed to acquire more information on deep aquifer systems which allowed significant enrichment and precision of the so far available findings on the groundwater recharge conditions from the Late Pleistocene period at both study sites and on the geothermal field in the north western part of the Czech Republic.

Relevancy of the performed investigations:

- Mean residence time of groundwaters represent very valuable information to be considered during the construction and improvement of conceptual hydrogeological and later on also hydraulic models,

- Determination of carbon origin in groundwaters can help for the conceptual models construction,
- Chemical composition of groundwater drives their potential industrial and domestic use,
- Geothermal gradient and heat flux assessment are primordial for the sustainable geothermal exploitation of sedimentary formations.

# 6 REFERENCES

*Note : Here below provided references refer to the citations in the manuscript text only. Bibliography cited in articles makes part of the article.*


Alezine, T., 1987. Influences de particularités hydrodynamiques et structurales sur la distribution des températures du sous-sol. Application à deux exemples aquitains. Thèse de doctorat, Université de Bordeaux 3, 234 p.

Andre, L., Franceschi, M., Pouchan, P., Atteia, O., 2002. Origin and evolution of sulphur in the Molassic sands aquifer from the Aquitaine Basin. C. R. Geoscience 334, 749–756.

Blavoux, B., Dray, M., Fehri, A., Olive, P., Groning, M., Sonntag, C., Hauquin, J.P., Pelissier, G., Pouchan, F., 1993. Palaeoclimatic and hydrodynamic approach to the Aquitaine basin deep aquifer (France) by means of environmental isotopes and noble gases. In: Isotope Techniques in the Study of Past and Current Environmental Changes in the Hydrosphere and the Atmosphere. IAEA, Vienna, pp. 93–305.

BRGM, 1999. Gestion des eaux souterraines en Aquitaine, Annee 3. Operation sectorielle, Relation entre l'estuaire de la Gironde et la nappe de l'Eocene. R- 40729, 122 p., http://www.brgm.fr/Rapport?code=RR-40729-FR.pdf [cited April 2008].

BRGM, 2000. Gestion des eaux souterraines en Aquitaine, Annee 4. Operation sectorielle, Relation entre l'estuaire de la Gironde et la nappe de l'Eocene. R- 50467, 2000, 77 p., http://www.brgm.fr/Rapport?code=RP-50467-FR.pdf [cited April 2008].

BRGM, 2001. CPER 2000–2006 Annee1. Construction d'outils d'aide a la decision, Aquifere du Turonianien. RP-50826-FR, 97 p., http://www.brgm.fr/Rapport?code=RP-50826-FR.pdf [cited April 2008].

BRGM, 2002. CPER 2000–2006 Phase1. Outils d'aide a la decision pour la gestion de l'aquifere de l'Infra-Toarcien. Approche des modalites de la recharge de l'aquifere Infra-Toarcien et des communications avec d'autres aquiferes par les methodes isotopiques. RP-51194-FR, 108 p., http://www.brgm.fr/Rapport?code=RP-51194-FR.pdf [cited April 2008].

BRGM, 2005. CPER 2000–2006 Phase2. Action d'accompagnement pour l'aquifere du Turonianien-Coniacien en Charente. Suivi de la crete piezometrique et du debit des sources et des cours d'eau. RP-53494-FR, 80 p., http://www.brgm.fr/Rapport?code=RP-53494-FR.pdf [cited April 2008].

Clark, I.D., Fritz, P., 1999. Environmental Isotopes in Hydrogeology. Lewis Publishers, Boca Raton. 311 p.

Čermák, V., Jetel, J., 1985. Heat flow and ground water movement in the Bohemian Cretaceous Basin (Czechoslovakia). Journal of Geodynamics 4, 285-303.

Environmental and Energy Study Institute Task Force, Partnership for Sustainable Development, A New U.S. Agenda for International Development and Environmental Security, Washington D.C., May.1991.

Fryar, A.E., Mullican, W.F., Macko, S.A., 2001. Groundwater recharge and chemical evolution in the southern High Plains of Texas, USA. Hydrogeology Journal 9, 522 – 542.

Fontes, J.C., Garnier, J.M., 1979. Determination of the 14C initial activity of total dissolved carbon: a review of the existing models and a new approach. Water Resources Research 15, 399–413.

Gastmans, D., Chang, H.K., Hutcheon, I., 2010. Stable isotopes ($^{2}H$, $^{18}O$ and $^{13}C$) in groundwaters from the northwestern portion of the Guarani Aquifer System (Brazil). Hydrogeology Journal. In press. doi: 10.1007/s10040-010-0612-2.

Herčík, F., Hermann, Z., Valečka, J., 1999. Hydrogeology of the Bohemian Cretaceous Basin Czech Geological Survey, Prague (in Czech).

Katz B.G., Chelette A.R, Pratt, T.R., 2004. Use of chemical and isotopic tracers to assess nitrate contamination and ground-water age, Woodville karst Plain, USA. Journal of Hydrology 289 (1-4), 36-61. doi:10.1016/j.jhydrol.2003.11.001.

Le Gal La Salle, C., Marlin, C., Savoye, S., Fontes, J.C., 1996. Geochemistry and $^{14}C$ dating of groundwaters from Jurassic aquifers of North Aquitaine Basin (France). Applied Geochemistry 11, 433–445.

Lloyd, J.W., 1990. Groundwater resources development in the eastern Sahara. Journal of Hydrology 119, 71-87. doi:10.1016/0022-1694(90)90035-V.

Marlin, C., 1996. Estimation du temps de residence des eaux souterraines des aquiferes du Cretace et du Jurassique, Coniacien–Turonien, Cenomanien et Infra-Callovien, departement de la Charente-Maritime. Universite Paris-Sud, Laboratoire d'Hydrologie et Geochimie isotopique. Technical Report, 32p.

Marlin, C., Van Exter, S., Raguideau, A., 1998. Estimation du temps de residence des eaux souterraines des aquiferes du Cretace Superieur dans le departement de Charente-Maritime. Universite Paris-Sud, Laboratoire d'Hydrologie et Geochimie isotopique. Technical Report.

Moneim, A.A.A., 2005. Overview of the geomorphological and hydrogeological characteristics of the Eastern Desert of Egypt. Hydrogeology Journal 13 (2), 416-425. doi: 10.1007/s10040-004-0364-y.

Mouragues, N., 2000. Caracterisation et vulnerabilite d'un hydrosysteme komplexe sub-profond associe a la structure anticlinale de Jonzac. Doc. Thesis. Univ. Bordeaux1, 187 p.

Mourier J. P. and Gabilly J. (1985) Le Lias et le Dogger au Sud-Est du seuil du poitou, tectonique syns&iimentaire, paléogéographie, Géologie de la France 3, 293-310.

Myslil, V., Stibitz, M., Frydrych, V., 2005. Geothermal Energy Potential of Czech Republic. Proceedings World Geothermal Congress 2005. Antalya, Turkey.

Ozyurt, N.N, Bayari, C.S., 2003. Lumped: a Visual Basic code of lumped-parameter models for mean residence time analyses of groundwater systems. Computer and Geosciences 29, 79-90.

Pestov, I., 2000. Thermal Convection in the Great Artesian Basin, Australia. Water Resources Management 14, 391–403.

Rabelo, J.L., Edson W., 2009. Assessment of groundwater recharge and water fluxes of the Guarani Aquifer System, Brazil. Hydrogeology Journal 17, 1733–1748. doi: 10.1007/s10040-009-0462-y.

Rosenberg, N.J., Epstein, D.J., Wang, D.,Vail, L., Srinivasan, R., Arnold, J.G, 1999. Possible impacts of global warming on the hydrogeology of the Ogallala aquifer region. Climatic Change 42, 677–692.

Rozanski, K., Araguás-Araguás, L., Gonfiantini, R., 1993. Isotopic patterns in modern global precipitation. In: Continental Isotope Indicators of Climate, American Geophysical Union Monograph.

RPDE (Réseau Partenarial des Données sur l'Eau). http://www.eau-poitou-charentes.org/ 2010.

Savoye, S., 1993. Etude chimique et isotopique des eaux de l'aquifere Infra-Callovien du Bassin Aquitain. DEA University Paris-Sud, Centre d'Orsay, 100 p.

Sophocleous, M., 2002. Interactions between groundwater and surface water: the state of the science. Hydrogeology Journal 10. doi:10.1007/s10040-001-0170-8.

Sracek, O., Hirata, R., 2002. Geochemical and stable isotopic evolution of the Guarani Aquifer System in the state of São Paulo, Brazil. Hydrogeology Journal 10, 643-655. doi: 10.1007/s10040-002-0222-8.

Wendland, E., Barreto, C., Gomes, L.H., 2007. Water balance in the Guarani Aquifer outcrop zone based on hydrogeologic monitoring. Journal of Hydrology 342, 261-269. doi:10.1016/j.jhydrol.2007.05.033.

Zhang, M., Frape, S.K., Love, A.J., Herczeg, A.L., Lehmann, B.E., Beyerle, U., Purtschert, R., 2007. Chlorine stable isotope studies of old groundwater, southwestern Great Artesian Basin, Australia. Applied Geochemistry 22, 557–574. doi:10.1016/j.apgeochem.2006.12.004.

# ANNEXES

# Annexe 1

Proportion of sandy and clayey rocks in the selected wells within the BCB. Grey-highlighted wells were chosen to illustrate a particular lithological group according to a sand ratio (Annexe 2)

| No | Name | Coordinates (JTSK) | | | Location | Depth (m) | Basement | sand content (%) | clay content (%) | sand ratio | | | | |
|---|---|---|---|---|---|---|---|---|---|---|---|---|---|---|
| | | Y | X | Z | | | | | | 0-20 % | 20-40% | 40 - 60% | 60- 80% | 80- 100% |
| **1** | J-880311 | -768451,00 | -966435,00 | 745,00 | Adolfov | 430,0 | xx | 7 | 93 | x | | | | |
| **2** | RPZ-39A | -767808,68 | -971100,87 | 239,57 | Chlumec-Ústí | 640,0 | - | 8 | 92 | x | | | | |
| **3** | RPZ38 | -765564,61 | -975065,42 | 158,34 | Hrbovice | 373,0 | xx | 15 | 85 | x | | | | |
| **4** | SH-10 | -769860,00 | -984150,00 | 358,28 | Bořislav | 489,0 | PC | 16 | 84 | x | | | | |
| **5** | RPZ-37 | -763561,27 | -980936,13 | 410,77 | Stebno | 714,8 | xx | 28 | 72 | | x | | | |
| **6** | HB1 | -759538,10 | -980147,00 | 142,08 | Brná | 422,0 | xx | 3 | 97 | x | | | | |
| **7** | J820394 | -758617,09 | -975307,86 | 163,96 | Krásné Březno | 533,0 | xx | 19 | 81 | x | | | | |
| **8** | J798259 | -760407,01 | -968596,92 | 391,63 | Velke Chvojno | 417,0 | xx | 27 | 76 | | x | | | |
| **9** | J716262 | -756826,88 | -966589,70 | 372,73 | Černá | 413,0 | xx | 43 | 57 | | | x | | |
| **10** | J720423 | -753475,11 | -974547,83 | 359,72 | Mašovice | 665,0 | xx | 33 | 67 | | x | | | |
| **11** | J-807556 | -754739,28 | -982497,04 | 461,70 | Tašov | 548,0 | xx | 31 | 69 | | x | | | |
| **12** | SK-26 | -748618,30 | -980005,20 | 342,61 | Zubrnice | 812,0 | P | 65 | 35 | | | | x | |
| **13** | J-666542 | -748534,69 | -978895,96 | 292,96 | Zubrnice | 710,0 | xx | 54 | 46 | | | x | | |
| **14** | J-686661 | -747080,68 | -984769,25 | 421,69 | Chlumec-Ústí | 580,4 | xx | 28 | 72 | | x | | | |
| **15** | SK-12C | -748000,40 | -974213,60 | 207,71 | Těchlovice | 598,4 | - | 52 | 48 | | | x | | |
| **16** | J-582380 | -748059,35 | -969801,35 | 284,93 | Děčín | 736,2 | xx | 53 | 47 | | | x | | |
| **17** | J-557339 | -747682,67 | -967406,43 | 181,46 | Děčín | 597,7 | xx | 64 | 36 | | | | x | |
| **18** | J-527303 | -747049,86 | -965051,33 | 128,83 | Děčín | 499,6 | xx | 81 | 19 | | | | | x |
| **19** | J-343402 | -736661,79 | -965960,99 | 259,17 | Markvartice-Děčín | 758,0 | P | 60 | 40 | | | | x | |
| **20** | J389460 | -737586,94 | -969554,90 | 311,03 | Horni Habartice | 1016,0 | P | 60 | 40 | | | | x | |
| **21** | J480573A | -739446,48 | -976540,99 | 429,78 | Merboltice | 845,0 | xx | 40 | 60 | | | x | | |
| **22** | LO-1 | -741402,62 | -982805,06 | 331,86 | Úštěk-Brusov | 679,0 | P | 55 | 45 | | | x | | |
| **23** | J-580700 | -741431,51 | -984396,30 | 296,84 | Úštěk | 654,1 | P | 42 | 58 | | | x | | |
| **24** | VP8216N | -740004,40 | -989146,52 | 216,70 | Úštěk, Tetčíněves | 130,0 | xx | 64 | 36 | | | | x | |
| **25** | 2H113 | -737995,82 | -993264,98 | 246,73 | Snědovice | 225,0 | xx | 37 | 63 | | x | | | |

| No | Name | Coordinates (JTSK) | | | Location | Depth (m) | Basement | sand content (%) | clay content (%) | sand ratio | | | | |
|---|---|---|---|---|---|---|---|---|---|---|---|---|---|---|
| | | Y | X | Z | | | | | | 0-20 % | 20-40% | 40 - 60% | 60- 80% | 80- 100% |
| **26** | J478690 | -736953,35 | -981846,05 | 300,16 | Janovice | 477,0 | xx | 60 | 40 | | | | x | |
| **27** | SK-11C | -734274,70 | -972708,00 | 292,47 | Žandov | 885,1 | P | 49 | 51 | | | x | | |
| **28** | 2H305 | -734647,46 | -958344,04 | 200,40 | Dolský Mlýn. Všemily | 187,0 | xx | 53 | 47 | | | x | | |
| **29** | J160333 | -729719,96 | -959077,61 | 375,92 | Studený | 623,0 | P | 97 | 3 | | | | | x |
| **30** | J129296 | -729061,29 | -956743,08 | 333,13 | Jetřichovice | 505,0 | xx | 95 | 5 | | | | | x |
| **31** | J-213406 | -730643,71 | -963480,43 | 367,16 | Česká Kamenice | 644,0 | P | 81 | 90 | | | | | x |
| **32** | J-143455 | -726463,58 | -964284,52 | 415,03 | Kytlice | 736,0 | P | 85 | 5 | | | | | x |
| **33** | J-186495 | -727627,94 | -966997,62 | 511,28 | Prysk | 794,4 | - | 82 | 8 | | | | | x |
| **34** | VF-1 | -729513,49 | -973202,58 | 284,29 | Volfartice | 1587,2 | P,xx | 49 | 51 | | | x | | |
| **35** | VP8450N | -724114,68 | -977767,34 | 300,38 | Č.Lípa | 612,0 | P | 76 | 24 | | | | x | |
| **36** | 706447 | -723958,34 | -981458,90 | 261,23 | Česká Lípa | 420,0 | - | 72 | 28 | | | | x | |
| **37** | 2H234 | -723990,95 | -986397,53 | 254,67 | Jestřebí | 272,0 | xx | 68 | 32 | | | | x | |
| **38** | 2H095 | -728054,56 | -989722,20 | 351,59 | Drchlava (Hradiště) | 215,0 | xx | 47 | 53 | | | x | | |
| **39** | 642447 | -722613,57 | -980518,76 | 263,92 | Česká Lípa | 473,1 | xx | 85 | 15 | | | | | x |
| **40** | 578383 | -720417,22 | -980932,13 | 268,59 | Česká Lípa | 478,0 | xx | 78 | 22 | | | | x | |
| **41** | 568559 | -722694,72 | -977150,15 | 279,04 | Písečná | 476,0 | xx | 82 | 18 | | | | | x |
| **42** | DP-4 | -721932,60 | -972985,30 | 285,72 | Sloup v Čechách | 575,4 | | 83 | 17 | | | | | x |
| **43** | J157558 | -724980,60 | -969289,49 | 387,05 | Okrouhlá | 930,0 | P | 90 | 10 | | | | | x |
| **44** | J-022356 | -722935,28 | -957333,06 | 466,86 | Horní Podluží | 832,0 | xx | 96 | 4 | | | | | x |
| **45** | 01001021A | -719625,43 | -961064,11 | 539,22 | Jiřetín p.Jedlovou | 840,0 | - | 78 | 22 | | | | x | |
| **46** | 74903 | -717365,33 | -963092,07 | 521,56 | Mařenice | 698,7 | - | 94 | 6 | | | | | x |
| **47** | SK-9C | -719171,00 | -966160,60 | 420,91 | Svor | 645,0 | xx | 95 | 5 | | | | | x |
| **48** | 116643 | -714575,31 | -969025,09 | 339,27 | Kunratice | 620,0 | xx | 90 | 10 | | | | | x |
| **49** | 354651 | -719573,68 | -972248,70 | 319,16 | Sloup v Čechách | 660,0 | xx | 85 | 15 | | | | | x |
| **50** | 2H250 | -713709,54 | -986093,07 | 278,36 | Boreček | 211,0 | xx | 54 | 16 | | | x | | |

| No | Name | Coordinates (JTSK) | | | Location | Depth (m) | Basement | sand content (%) | clay content (%) | sand ratio | | | | |
|---|---|---|---|---|---|---|---|---|---|---|---|---|---|---|
| | | Y | X | Z | | | | | | 0-20 % | 20-40% | 40 - 60% | 60- 80% | 80- 100% |
| **51** | 2H247 | -712906,74 | -980588,03 | 281,52 | Pertoltice | 727,0 | xx | 40 | 60 | | | x | | |
| **52** | 2H023 | -706532,08 | -990920,79 | 359,78 | Horní Krupá | 336,0 | P | 55 | 45 | | | x | | |
| **53** | 2H013 | -698629,00 | -985977,30 | 382,27 | Hlavice (Hrubý Lesnov) | 305,0 | xx | 50 | 50 | | | x | | |
| **54** | 324219 | -712847,10 | -980703,78 | 281,09 | Pertoltice | 673,0 | xx | 58 | 42 | | | x | | |
| **55** | 184187 | -709522,67 | -979410,39 | 393,06 | Noviny p.Ralskem | 821,1 | xx | 62 | 38 | | | | x | |
| **56** | VH-1T | -710843,00 | -974437,00 | 293,93 | Velký Valtínov | 360,0 | - | 98 | 2 | | | | | x |
| **57** | 130511 | -712992,37 | -971940,48 | 356,58 | Kunratice u Cvikova | 743,5 | xx | 89 | 11 | | | | | x |
| **58** | 01583 | -711322,03 | -968602,89 | 393,52 | Lvová | 575,0 | xx | 94 | 6 | | | | | x |
| **59** | 2H236 | -714282,92 | -964281,10 | 426,60 | Juliovka | 481,0 | xx | 84 | 16 | | | | | x |
| **60** | 87763 | -712107,20 | -963686,63 | 491,61 | Krompach | 556,0 | xx | 98 | 2 | | | | | x |
| **61** | 59633 | -710804,42 | -966750,72 | 411,73 | Heřmanice | 575,0 | xx | 96 | 4 | | | | | x |
| **62** | 59509 | -709068,75 | -969288,59 | 360,82 | Jablonné v Podještědí | 665,1 | xx | 98 | 2 | | | | | x |
| **63** | 4445 | -709473,92 | -971510,52 | 314,63 | Jablonné v Podještědí | 606,1 | xx | 78 | 22 | | | | x | |
| **64** | 125413 | -706322,77 | -970324,35 | 363,13 | Jablonné v Podještědí | 503,7 | xx | 94 | 6 | | | | | x |
| **65** | 269499 | -704587,79 | -966570,36 | 491,34 | Hrádek n.N. | 521,2 | xx | 95 | 5 | | | | | x |
| **66** | 249415 | -703784,09 | -968549,70 | 373,85 | Polesí | 340,0 | xx | 90 | 10 | | | | | x |
| **67** | 245333 | -702739,72 | -970294,66 | 365,45 | Rynoltice | 360,1 | xx | 92 | 8 | | | | | x |
| **68** | 323313 | -700854,30 | -969621,87 | 453,71 | Rynoltice | 482,0 | xx | 74 | 26 | | | | x | |
| **69** | 203315 | -703351,33 | -971244,23 | 392,55 | Janovice v Podještědí | 422,3 | xx | 89 | 11 | | | | | x |
| **70** | 133261 | -704006,19 | -973373,68 | 383,98 | Křižany | 508,3 | xx | 92 | 8 | | | | | x |
| **71** | 59201 | -704670,47 | -975653,91 | 326,28 | Dubnice | 589,1 | xx | 82 | 18 | | | | | x |
| **72** | 57135 | -703823,83 | -977041,40 | 408,68 | Hamr na Jezeře | 669,6 | xx | 83 | 17 | | | | | x |

# Annexe 2

Complete well-logging records including information on lithology

(wells 2H113, 2H095, VP8450, 2H236)

# Borehole
# 2H113

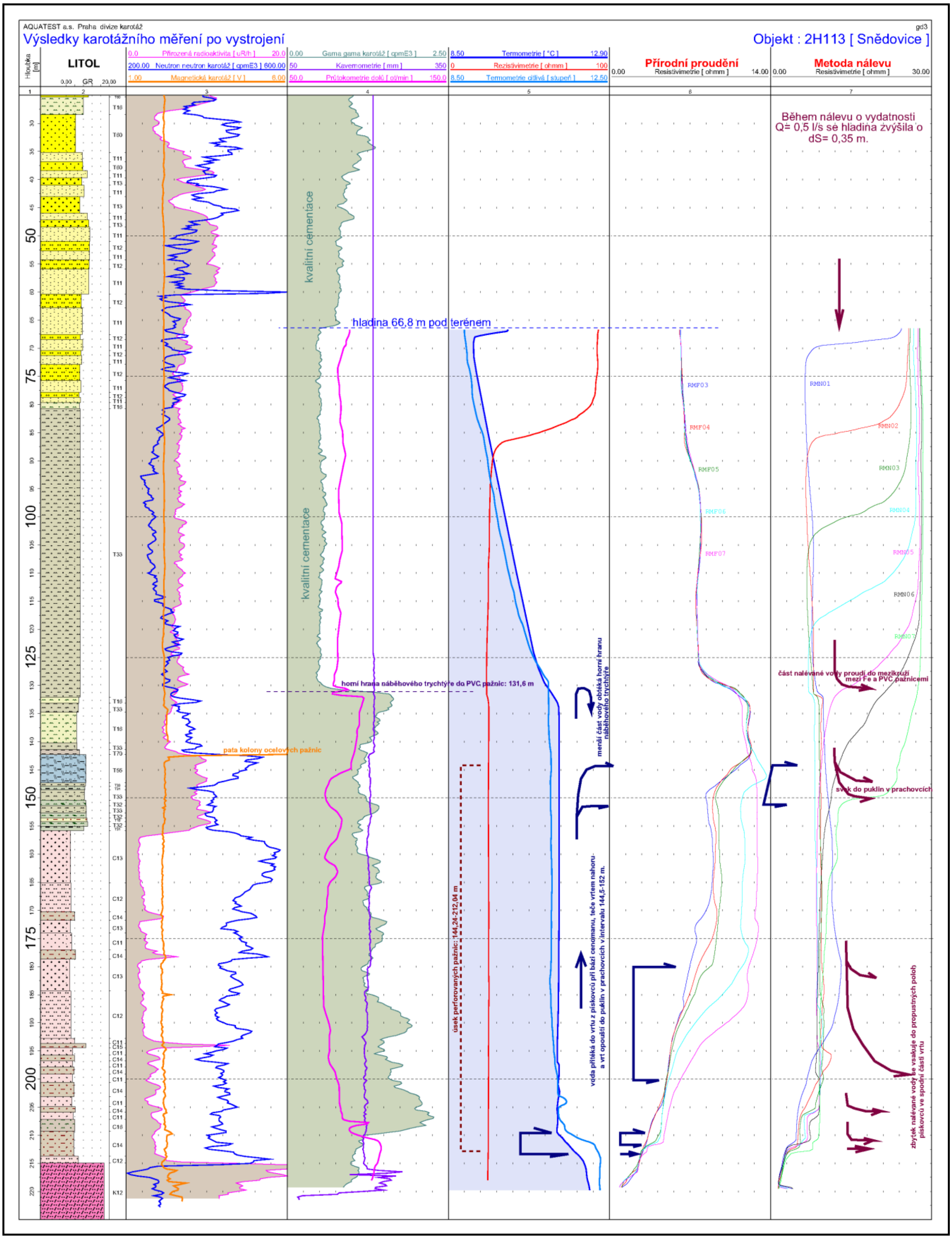
AQUATEST a.s. Praha divize karotáž
gd3
Výsledky karotážního měření po vystrojení
Objekt : 2H113 [ Snědovice ]
LITOL
Přirozená radioaktivita [ uR/h ]
Neutron neutron karotáž [ cpmE3 ]
Magnetická karotáž [ V ]
Gama gama karotáž [ cpmE3 ]
Kavernometrie [ mm ]
Průtokometrie dolů [ ot/min ]
Termometrie [ °C ]
Rezistivimetrie [ ohmm ]
Termometrie difivá [ stupeň ]
Přírodní proudění
Resistivimetrie [ ohmm ]
Metoda nálevu
Resistivimetrie [ ohmm ]
kvalitní cementace
hladina 66,8 m pod terénem
Během nálevu o vydatnosti Q= 0,5 l/s se hladina zvýšila o dS= 0,35 m.
horní hrana náběhového trychtýře do PVC pažnic: 131,6 m
pata kolony ocelových pažnic
úsek perforovaných pažnic: 144,24-212,04 m
část nalévané vody proudí do mezikruží mezi Fe a PVC pažnicemi
svek do puklin v prachovcích
zbytek nalévané vody se vsakuje do propustných poloh pískovců ve spodní části vrtu
voda přitéká do vrtu z pískovců při bázi cenomanu, teče vrtem nahoru a vrt opouští do puklin v prachovcích v intervalu 144,5-152 m.
menší část vody obtéká horní hranu náběhového trychtýře

# Borehole 2H095

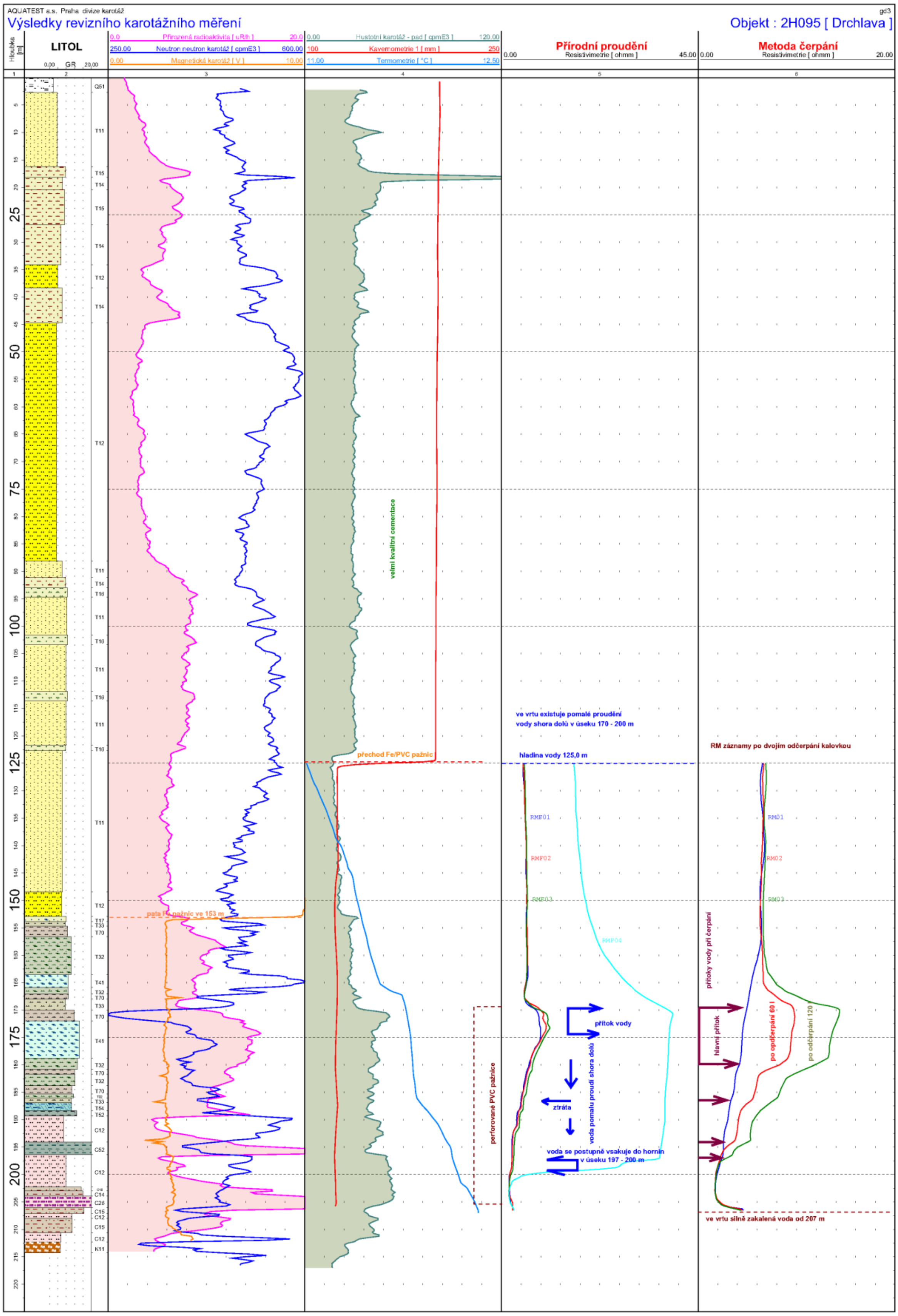

AQUATEST a.s. Praha divize karotáž
Výsledky revizního karotážního měření
Objekt : 2H095 [ Drchlava ]
LITOL
GR
Přirozená radioaktivita [ uR/h ]
Neutron neutron karotáž [ cpmE3 ]
Magnetická karotáž [ V ]
Hustotní karotáž - pad [ cpmE3 ]
Kavernometrie 1 [ mm ]
Termometrie [ °C ]
Přírodní proudění
Resistivimetrie [ ohmm ]
Metoda čerpání
Resistivimetrie [ ohmm ]
velmi kvalitní cementace
přechod Fe/PVC pažnic
pata Fe pažnic ve 153 m
perforované PVC pažnice
ve vrtu existuje pomalé proudění
vody shora dolů v úseku 170 - 200 m
hladina vody 125,0 m
přítok vody
ztráta
voda pomalu proudí shora dolů
voda se postupně vsakuje do hornin
v úseku 197 - 200 m
RM záznamy po dvojím odčerpání kalovkou
přítoky vody při čerpání
hlavní přítok
po odčerpání 60 l
po odčerpání 120 l
ve vrtu silně zakalená voda od 207 m

**Borehole**

**VP8450**

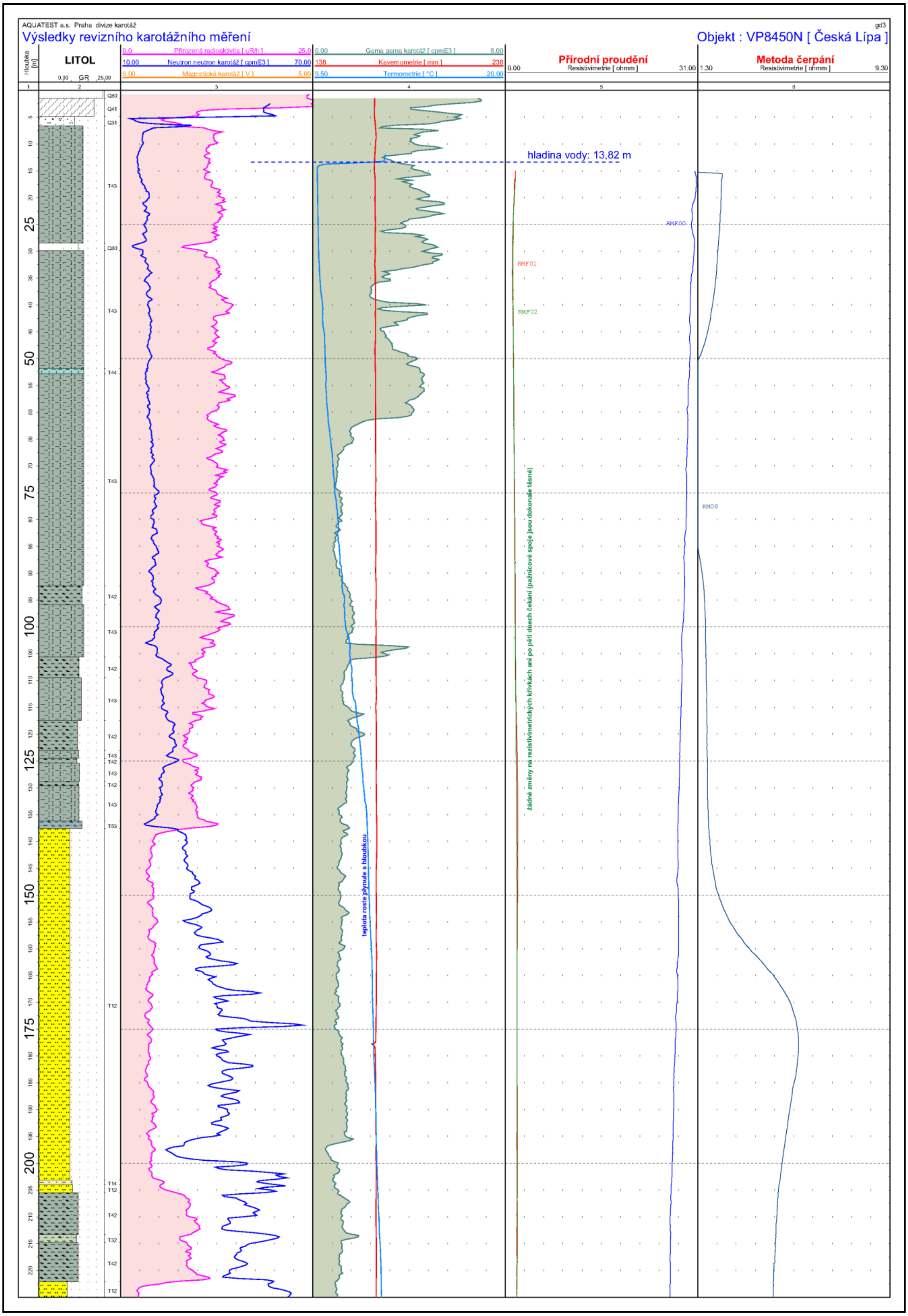

AQUATEST a.s. Praha divize karotáž
gd3
Výsledky revizního karotážního měření
Objekt : VP8450N [ Česká Lípa ]
Hloubka [m]
LITOL
0,00 GR 25,00
0.0 Přirozená radioaktivita [ uR/h ] 25.0
10.00 Neutron neutron karotáž [ cpmE3 ] 70.00
0.00 Magnetická karotáž [ V ] 5.00
0.00 Gama gama karotáž [ cpmE3 ] 8.00
138 Kavernometrie [ mm ] 238
9.50 Termometrie [ °C ] 20.00
Přírodní proudění
0.00 Resistivimetrie [ ohmm ] 31.00
Metoda čerpání
1.30 Resistivimetrie [ ohmm ] 9.30
hladina vody: 13,82 m
RMF00
RMF01
RMF02
RM08
žádné změny na rezistivimetrických křivkách ani po pěti dnech čekání (pažnicové spoje jsou dokonale těsné)
teplota roste plynule s hloubkou

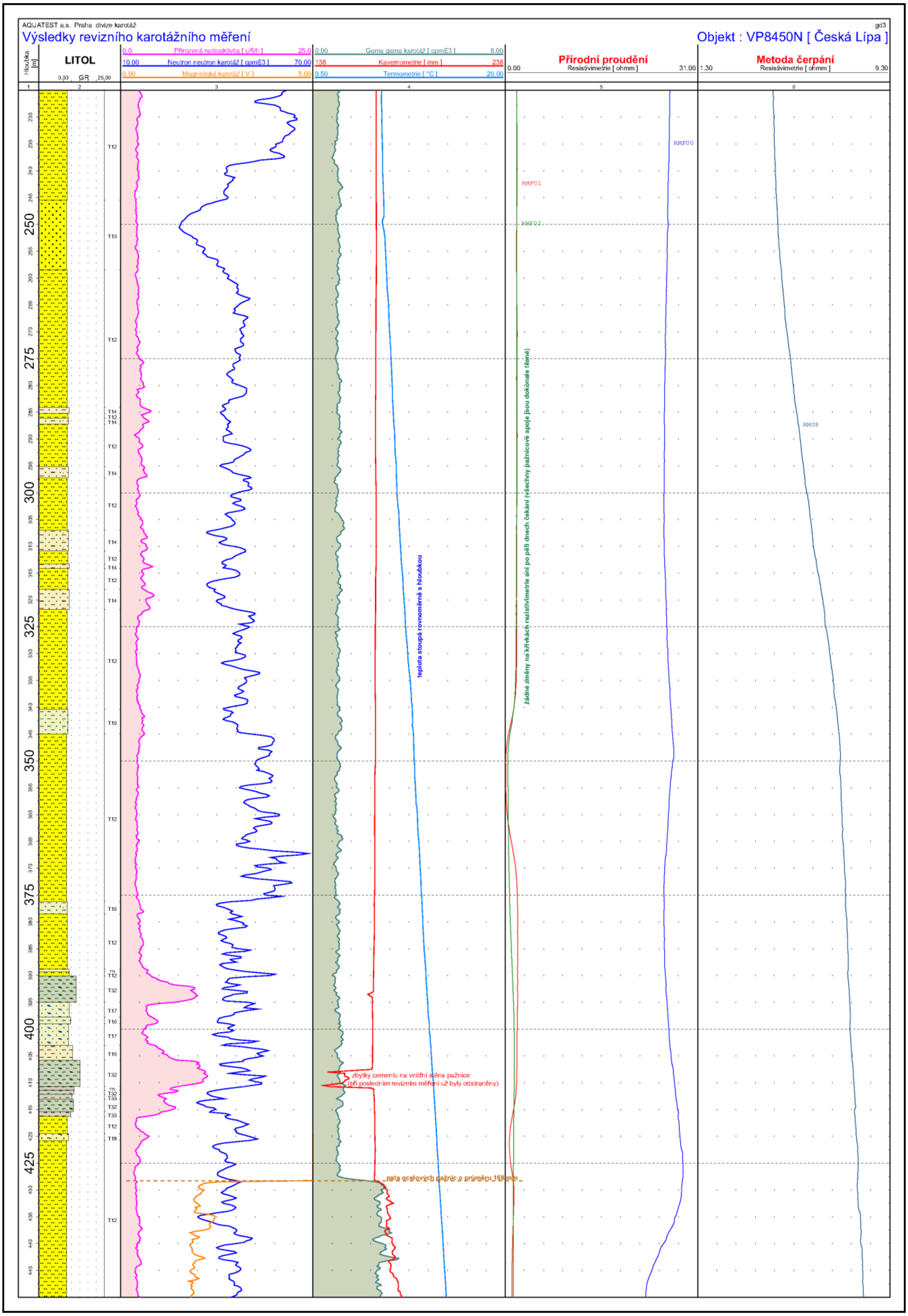
AQUATEST a.s. Praha divize karotáž
gd3
Výsledky revizního karotážního měření
Objekt : VP8450N [ Česká Lípa ]
Hloubka [m]
LITOL
GR
Přirozená radioaktivita [ uR/h ]
Neutron neutron karotáž [ cpmE3 ]
Magnetická karotáž [ V ]
Gama gama karotáž [ cpmE3 ]
Kavernometrie [ mm ]
Termometrie [ °C ]
Přírodní proudění
Resistivimetrie [ ohmm ]
Metoda čerpání
Resistivimetrie [ ohmm ]
250
275
300
325
350
375
400
425
teplota stoupá rovnoměrně s hloubkou
žádné změny na křivkách rezistivimetrie ani po pěti dnech čekání (všechny pažnicové spoje jsou dokonale těsné)
zbytky cementu na vnitřní stěna pažnice
(při posledním revizním měření už byly odstraněny)
pata ocelových pažnic o průměru 168 mm
RMF00
RMF01
RMF02
RM08

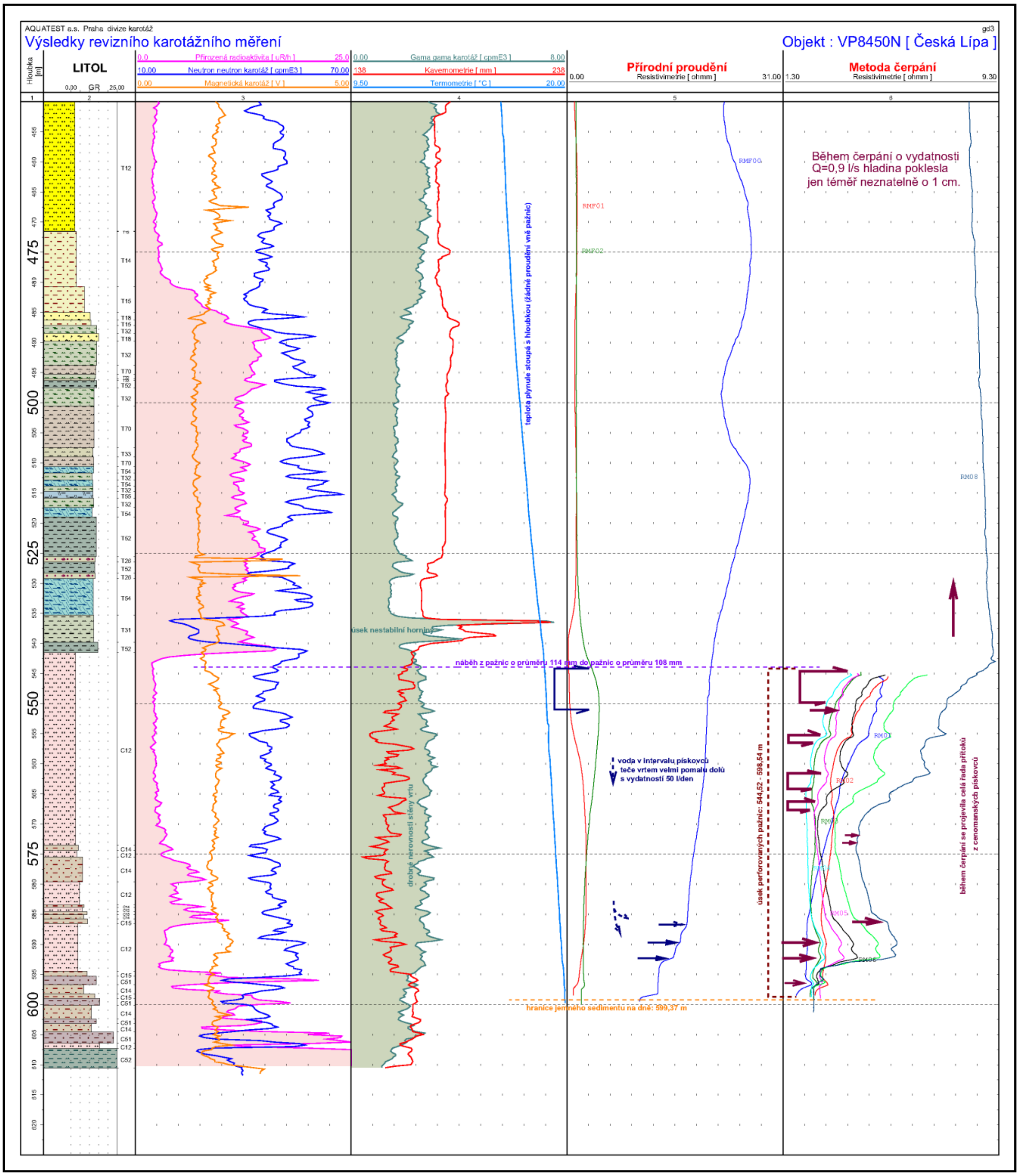
AQUATEST a.s. Praha divize karotáž
gd3
Výsledky revizního karotážního měření
Objekt : VP8450N [ Česká Lípa ]
Hloubka [m]
LITOL
GR
Přirozená radioaktivita [ uR/h ]
Neutron neutron karotáž [ cpmE3 ]
Magnetická karotáž [ V ]
Gama gama karotáž [ cpmE3 ]
Kavernometrie [ mm ]
Termometrie [ °C ]
Přírodní proudění
Resistivimetrie [ ohmm ]
Metoda čerpání
Resistivimetrie [ ohmm ]
Během čerpání o vydatnosti
Q=0,9 l/s hladina poklesla
jen téměř neznatelně o 1 cm.
teplota plynule stoupá s hloubkou (žádné proudění vně pažnic)
úsek nestabilní horniny
náběh z pažnic o průměru 114 mm do pažnic o průměru 108 mm
voda v intervalu pískovců
teče vrtem velmi pomalu dolů
s vydatností 50 l/den
úsek perforovaných pažnic: 544,52 - 598,54 m
drobné nerovnosti stěny vrtu
během čerpání se projevila celá řada přítoků
z cenomanských pískovců
hranice jemného sedimentu na dně: 599,37 m

**Borehole**

**2H236**

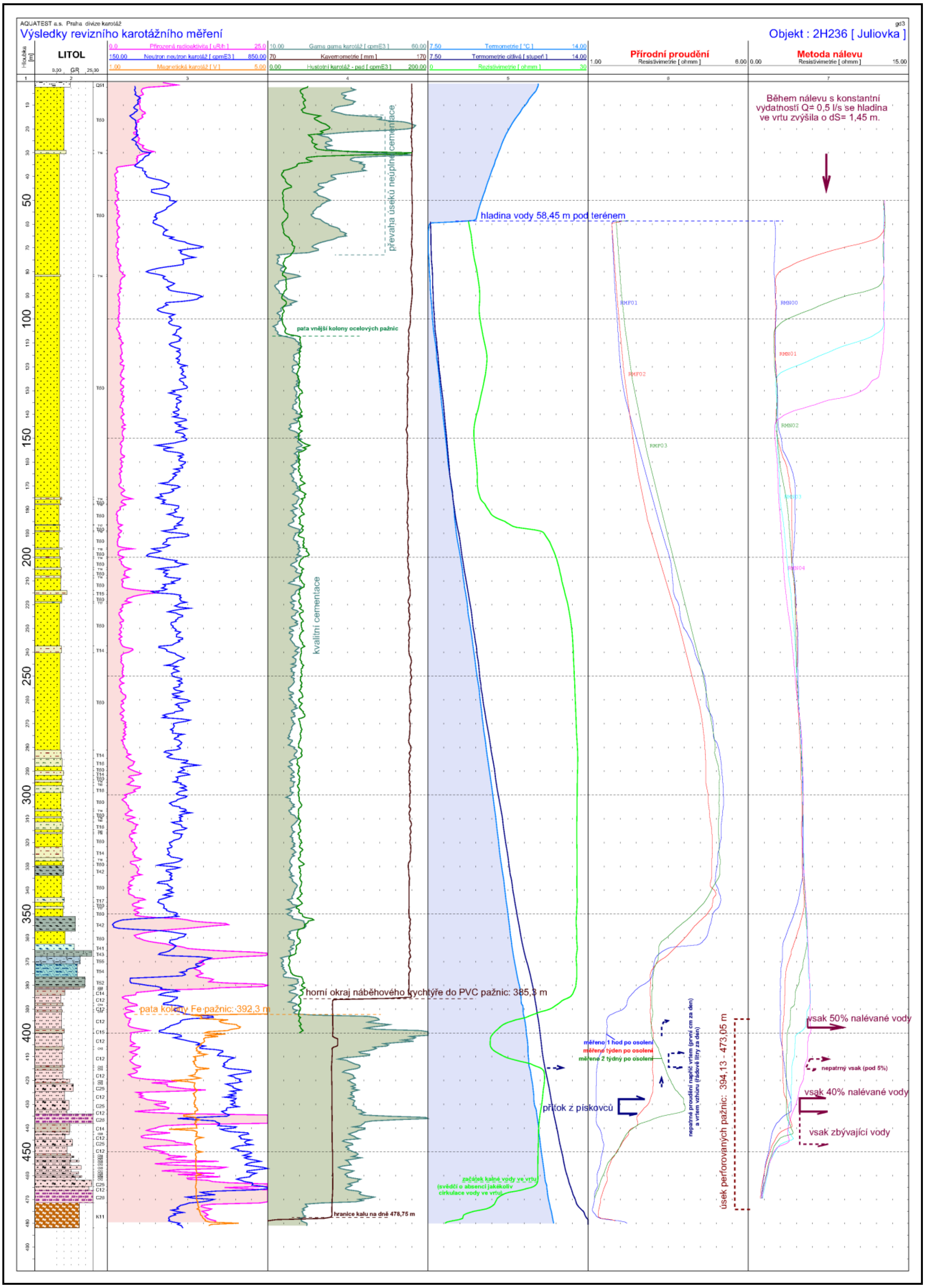

AQUATEST a.s. Praha divize karotáž
Výsledky revizního karotážního měření
Objekt : 2H236 [ Juliovka ]
LITOL
Přirozená radioaktivita
Neutron neutron karotáž
Magnetická karotáž
Gama gama karotáž
Kavernometrie [ mm ]
Hustotní karotáž
Termometrie [ °C ]
Termometrie citlivá
Rezistivimetrie [ ohmm ]
Přírodní proudění
Metoda nálevu
převaha úseků neúplné cementace
pata vnější kolony ocelových pažnic
kvalitní cementace
hladina vody 58,45 m pod terénem
Během nálevu s konstantní vydatností Q= 0,5 l/s se hladina ve vrtu zvýšila o dS= 1,45 m.
horní okraj náběhového trychtýře do PVC pažnic: 385,3 m
pata kolony Fe pažnic: 392,3 m
přítok z pískovců
úsek perforovaných pažnic: 394,13 - 473,05 m
vsak 50% nalévané vody
vsak 40% nalévané vody
vsak zbývající vody
hranice kalu na dně 478,75 m

# LEGEND – LIST OF LITHOLOGICAL SYMBOLS

**Quaternary**

| | |
|---|---|
| Q 31 | sand |
| Q 41 | sandy clay – clayey sand |
| Q 51 | not specified |

**Turonian**

| | |
|---|---|
| T 11 | sandstone fine grained |
| T 12 | sandstone medium grained |
| T 13 | sandstone coarse grained |
| T 14 | sandstone with slight clay content |
| T 15 | clayey sandstone |
| T 16 | silty sandstone |
| T 17 | marly sandstone |
| T 18 | sandstone with an organic compound |
| T 31 | clayey siltstone |
| T 32 | marly siltstone |
| T 33 | sandy siltstone |
| T 41 | sandy marlstone |
| T 42 | marlstone |
| T 43 | clayey marlstone |
| T 44 | cabonatic marlstone |
| T 52 | silty claystone |
| T 53 | coal claystone |
| T 54 | carbonatic claystone |
| T 55 | carbonatic marlstone – limestone |
| T 60 | sandstone |
| T 70 | siltstone |

**Cenomanian**

| | |
|---|---|
| C 11 | sandstone fine grained |
| C 12 | sandstone medium grained |
| C 13 | sandstone coarse grained |
| C 14 | sandstone with slight clay content |
| C 15 | clayey sandstone |
| C 25 | sandstone with an organic compoun |
| C 26 | sandstone with uranium minerals |
| C 51 | sandy claystone |
| C 52 | silty claystone |

**Basement**

| | |
|---|---|
| K 11 | crystalline basement |
| K 12 | permo-carboniferous |